THE UNIVERSITY *of* EDINBURGH

The Role of C-Terminal Phosphorylation in the Regulation of the Tumour Suppressor IRF-1

Fiona M. M. Russell

Thesis submitted for the degree of Doctor of Philosophy

of the University of Edinburgh

August 2012

Declaration

I hereby certify that this thesis has been written by me, is the record of original research carried out by me and has not been submitted (in part or in whole) in application for any other degree or qualification.

Fiona Russell Date:

Acknowledgements

This thesis would not have been possible without a number of people. First, many thanks to Kathryn for being an excellent supervisor who gave much guidance and support while still allowing me to choose the path the project took.

Thanks also to all members of the Hupp and Ball labs - past and current - for creating such a friendly place to work, and for the tradition of cakes. Particular thanks are due to Vikram for always knowing the answer to technical questions, and for his meticulous proof-reading of this thesis.

Finally, thanks to my family and friends, and especially Alex, for being there with constant encouragement, cups of tea and occasional escapes to the lochs and mountains.

Abstract

The transcription factor Interferon Regulatory Factor-1 (IRF-1) has been demonstrated to suppress tumour growth through the regulation of many anti-oncogenic genes. Pro- and anti-apoptotic factors, cell cycle control genes, DNA damage response genes and pro-metastatic factors are all under the control of IRF-1, which effects both transcriptional activation and repression. In addition to these cell autonomous tumour suppressor activities, IRF-1 is also a key regulator of the immune system and, as such, mediates immune surveillance of tumours. Numerous studies have confirmed that loss or mis-regulation of IRF-1 is a key factor in several different types of cancer.

Despite strong evidence for the crucial role of IRF-1 in cancer, and frequent assertions that this protein warrants further investigation as a drug target, very little is known about its regulation. Furthermore, since recent studies have linked upregulation of IRF-1 to the development of autoimmune diseases, it is particularly important that drugs be able to decouple autoimmune and anti-cancer functions of IRF-1 to avoid harmful side effects.

This thesis describes how phosphorylation of IRF-1 in its regulatory C-terminal Mf1 domain modulates transactivatory and tumour suppressor activity. Phosphospecific antibodies were developed as tools to study the C-terminal phosphorylation. Using these, it was shown that treatment of cells with Interferon-γ (IFN-γ) not only causes accumulation of IRF-1 protein, but also results in phosphorylation of IRF-1 at two sites in the C-terminal Mf1 domain.

Phosphomimetic mutants demonstrated that these phosphorylations enhanced the transactivatory activity of IRF-1 at various promoters, but did not affect repressor activity. Gel shift assays revealed that dual phosphorylation of IRF-1 (IRF-1 D/D) promoted DNA-binding and suggested this was through increased interaction with the cofactor/histone acetylase p300 which induces a conformational change in IRF-1, favouring DNA-binding. Acetylation by p300 appears to be important although it is not yet clear whether this directly or indirectly affects IRF-1 activity.

Since the tumour suppressor activity of IRF-1 is of particular interest, the effect of phosphorylation was examined in clonogenic and invasion assays. IRF-1 D/D more efficiently suppressed colony formation in both anchorage dependent and independent assays, and may improve inhibition of invasion in Transwell assays. Thus, cell treatment with the therapeutic agent IFN-γ induces phosphorylation of IRF-1, resulting in enhanced DNA binding of IRF-1 through improved p300 binding. In cells the outcome is more effective tumour suppression and inhibition of metastasis.

Abbreviations

aa	Amino acids
APS	Ammonium Persulphate
ATP	Adenosine Triphosphate
BSA	Bovine Serum Antigen
dNTPs	deoxyribonucleotide triphosphates
DMSO	Dimethyl sulphoxide
DNA	Deoxyribonucleic acid
DTT	Dithiothreitol
ECL	Enhanced chemiluminescence
EDTA	Ethylenediaminetetraacetic acid
ELISA	Enzyme-linked immunosorbant assay
EMSA	Electromobility shift assay
FBS	Foetal bovine serum
GST	Glutathione S-transferase
HEPES	4-(2-hydorxyethyl)-1-piperazineethanesulphonic acid
IEF	Isoelectric Focusing
IPG	Immobilised pH gradient
IRF	Interferon Regulatory Factor
LB	Luria Bertani
MOPS	3-(N-morpholino)propanesulfonic acid
OD_{600}	Optical Density (Absorbance) at 600nm
PBS	Phosphate Buffered Saline
PCR	Polymerase Chain Reaction
P/S	Penicillin/Streptomycin
RCF	Relative centrifugal force
rpm	Revolutions per minute
SDS-PAGE	Sodium dodecyl sulphate-polyacrylamide gel electrophoresis
TBE	Tris-borate-EDTA buffer
Tris	2-amino-2-hydroxymethyl-propane-1,3-diol

Contents

List of Figures

Chapter 1

Introduction

1.1 IRF-1

Interferon Regulatory Factor-1 (IRF-1) is a transcription factor that acts as a tumour suppressor through the regulation of genes in many anti-oncogenic pathways. Although much is known about the function of IRF-1, very little is known about its post-translational regulation. This thesis describes how phosphorylation of IRF-1 regulates its transactivatory activity and presents evidence that phosphorylation enhances IRF-1's tumour suppressor function.

IRF-1 was first identified as an inducer of the interferon-β (IFN-β) gene [1]. Subsequent investigation revealed that the DNA recognition sequence of IRF-1 is found not only in the IFN-α and IFN-β promoters, but also in interferon-inducible genes such as the MHC class I gene [2]. Comparison of the consensus IRF-1 recognition sequence, the IRF-E, with the IFN stimulated response element (ISRE) indicated that the IRF-E matched all ISREs studied; thus, IFN-activated genes are also IRF-1 inducible [3].

Subsequently, IRF-1 has been shown to activate or repress genes involved in many anti-viral, immunomodulatory and anti-oncogenic pathways and has been recognised as a tumour suppressor. This introduction will outline the role of IRF-1 in tumour suppression, the mechanisms of its induction, the current understanding of its regulation by

post-translational modification and co-factor interaction.

1.2 IRF-1 in cancer

The role of IRF-1 in cancer was first recognised in 1993 when it was mapped to a chromosomal locus commonly deleted in leukaemia or myelodysplasia [4]. At the same time, the overexpression of IRF-2 (an antagonist of IRF-1) was shown to transform cells, while concomitant overexpression of IRF-1 was able to suppress the transformation [5]. This provided context for previous observations of growth suppression/terminal differentiation by IRF-1 in myeloid [6] and lymphoid cells [7].

Since then, loss of heterozygosity at the IRF-1 locus has been reported in gastric [8], oesophageal [9], non-small cell lung [10], pulmonary large cell neuroendocrine [11] and breast [12] [13] carcinomas.

In addition to deletion of the chromosomal locus, IRF-1 activity can be inhibited in cancers by point mutation [14], expression of an inhibitor NPM [15] and expression of the HPV oncoprotein E7 [16]. Aberrant splicing and exon skipping can produce attenuated or inactive forms of IRF-1 [17] [18] and even dominant negative forms of IRF-1 [19].

1.3 IRF-1 as a tumour suppressor

Since loss or inactivation of IRF-1 is critical to so many different types of cancer, its tumour suppressor capabilities were studied in some detail. As mentioned above, IRF-1 was shown to reverse the transformation of cells overexpressing IRF-2 [5]. Following this, it was demonstrated that IRF-1 can suppress the transformation induced by other, unrelated, oncogenes, namely *c-myc* and *fos-B* [20]. In addition, in IRF-$1^{-/-}$ cells, expression of a single oncogene, for example, c-Ha-*ras* is sufficient to transform cells, and the transformation can be reversed by expression of IRF-1 [21]. Normally at least two oncogenes are required for transformation. Thus, IRF-1 was firmly estabilished as a tumour suppressor.

Interestingly, however, it was later observed that in mice, loss of IRF-1 alone had very little impact on the frequency of spontaneous tumour development. In contrast, in the background of c-Ha-*ras* expression or p53 knock-out, IRF-1 deficiency resulted in increased frequency of tumour development. Furthermore, in $p53^{-/-}$IRF-$1^{-/-}$ mice, death due to tumour occured much earlier, multiple tumour frequency increased and the spectrum of tumours was altered relative to $p53^{-/-}$ mice [22]. Thus, IRF-1 could be characterised as a tumour susceptibility gene rather than a *bona fide* tumour suppressor.

Despite this, the activity of IRF-1 in cancer is clearly important: Introduction of dominant negative (dn)IRF-1 into human breast cancer cells (which quite likely exhibit a background of other oncogenic mutations) functions to enhance proliferation. Moreover, IRF-1 expression varied with the agressiveness of the cell line; "highly invasive and metastatic" cell lines exhibit lowest IRF-1 expression while "tumourigenic but non-metastatic" cell lines express intermediate levels of IRF-1 compared to normal cells [23].

1.4 Mechanisms of tumour suppression by IRF-1

IRF-1 has been shown to upregulate or suppress genes involved in several anti-oncogenic pathways (Fig 1.1). These will be discussed below.

1.4.1 Apoptosis and Autophagy

Apoptosis is the programmed death of a cell in a controlled manner. In the context of cancer, it enables cells with irreparably damaged DNA to be safely removed before they become neoplastic. It is also the mechanism by which immune cells trigger death of cells displaying tumour associated antigens.

Apoptosis can be induced by two pathways: the extrinsic pathway and the intrinsic pathway (Fig 1.2). This is reviewed in [47]. Briefly, the extrinsic pathway is triggered by the activation of death receptors by death ligands. This induces the recruitment of various factors to the receptor and the formation of a death-inducing signalling complex (DISC).

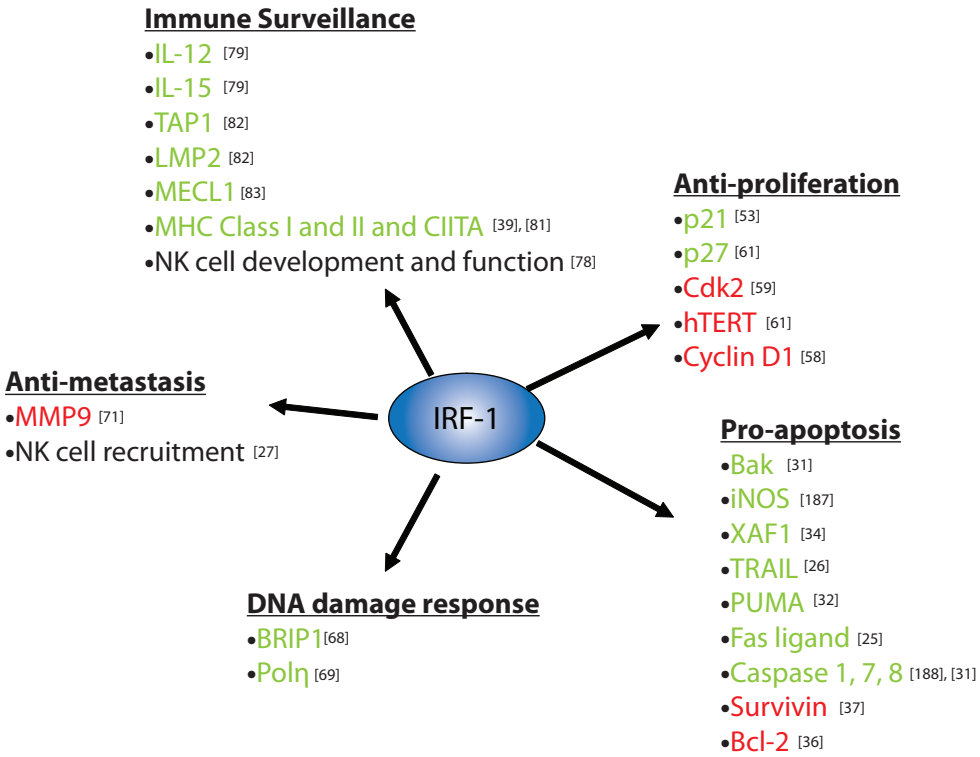

Figure 1.1: IRF-1 regulates gene expression of proteins involved in all aspects of anti-oncogenesis including: immune surveillance ([24],[25],[26],[27],[28],[29]); anti-proliferation ([30],[31],[32],[33]); pro-apoptosis ([34],[35],[36],[37],[38],[39],[40],[41],[42]); DNA damage response ([43],[44]); and anti-metastasis ([45],[46]). Upregulated genes are green, downregulated genes are red.

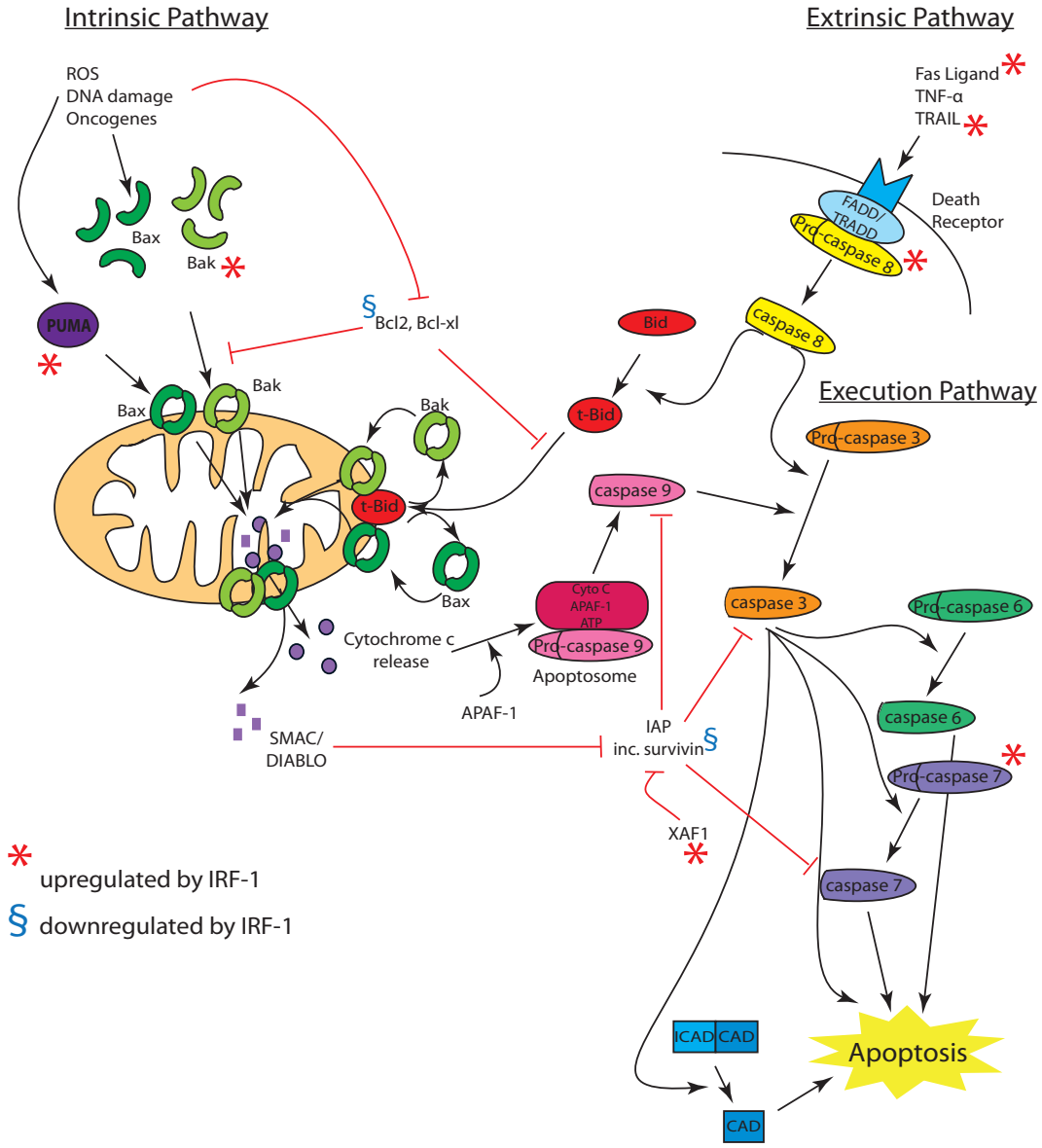

Figure 1.2: IRF-1 regulates the intrinsic and extrinsic pathways of apoptosis. Proteins upregulated by IRF-1 are indicated by $*$, proteins downregulated by IRF-1 are indicated by §. The intrinsic pathway of apoptosis is initiated by intracellular signals such as ROS, DNA damage and oncogenes. These cause upregulation of Bax, Bak* [34] and PUMA* [38], which facilitates activation of Bak. Active Bax and Bak form homodimers and, after insertion into the mitochondrial membrane, induce release of apoptotic factors SMAC/DIABLO and cytochrome c. The activation of Bax and Bak is inhibited by Bcl2§ [42] and Bcl-xl. SMAC/DIABLO and also XAF-1* [36] inhibits the inhibitor of apoptosis proteins (IAPs), which inhibit caspases 3,7* [34] and 9 while cytochrome c associates with APAF-1 to form the apoptosome which catalyses cleavage of pro-caspase-9 to caspase-9. Survivin§ [41], an atypical IAP, is down-regulated by IRF-1. Activated caspase-9 cleaves pro-caspase-3 to caspase-3 at the start of the execution pathway. At this point the intrinsic and extrinsic pathways converge. The extrinsic pathway of apoptosis is initiated by binding of death ligands (Fas ligand* [39], TNF-α and TRAIL* [37],[46]) to the death receptor. Binding activates the death receptor and triggers assembly of various factors into the DISC which catalyses cleavage of pro-caspase-8* into active caspase-8. Caspase-8 cleaves pro-caspase-3 to active caspase-3 at the start of the execution pathway. In some cases, it also converts Bid to t-Bid and recruits the mitochondrial factors to amplify the apoptotic signal. The execution pathway is a cascade of caspase cleavages culminating in the activation of the factors responsible for apoptosis.

Assembly of this complex results in activation of procaspase-8 to caspase-8. Caspase-8 is an initiator caspase which catalyses the activation of effector caspases. The result is a cascade of cleavage events culminating in apoptosis through both the direct action of caspases, and the activation of other pro-apoptotic molecules.

The intrinsic pathway is triggered by events within the cell, for example, DNA damage. This results in the activation of the pro-apoptotic factors Bax and Bak, which form homodimers. PUMA (p53 Upregulated Modulator of Apoptosis) mediates the activation of Bax. The homodimers insert into the mitochondrial membrane and cause the release of cytochrome c and second mitochondria activator of caspases (SMAC). Cytochrome C interacts with apoptotic protease activating factor-1 (APAF-1) and ATP to recruit pro-caspase-9 and form the apoptosome. Cleavage of pro-caspase-9 to caspase-9 ensues, and caspase-9 activates caspase-3 from which point apoptosis proceeds in the same way as for the extrinsic pathway (reviewed in [47]).

Apoptosis can be inhibited by the action of various factors. Bcl2 and Bcl-xl inhibit the activation of Bak, Bax, and Bid. When the intrinsic pathway is activated, the action of Bcl2 and Bcl-xl is itself inhibited. Inhibitor of Apoptosis Proteins (IAPs) can inhibit the activity of caspases 3,7 and 9. Again, pro-apoptotic factors can inhibit these anti-apoptotic factors. SMAC is released from the mitochondria along with cytochrome c and inhibits the action of IAPs as do other proteins e.g. XAF1 (XIAP associated factor 1) [47].

IRF-1 is involved in the regulation of apoptosis at many points in both the intrinsic and extrinsic pathways. It upregulates proteins which initiate apoptosis such as Fas ligand [39] and TRAIL [37], [46], both of which can be used by cytotoxic T cells to induce apoptosis in tumour cells [48], [49] or, in the case of TRAIL, tumour cell auto/paracrine apoptosis [50]. IRF-1 also upregulates mediators of apoptosis such as caspases-7 and -8 [34]. Bak [34] is responsible for release of apoptotic factors from mitochondria [47] and PUMA [38] mediates apoptosis by recruiting Bax to the mitochondrial membrane [51]. Inhibitors of apoptosis are also modulated by IRF-1: XAF-1 [36] sensitises cells to apoptosis through antagonism of the inhibition of caspase-3 and -9 by XIAP [52] and is upregulated by IRF-1. Correspondingly, both Bcl-2 [42], which inhibits Bak activation

and survivin [41], an IAP which inhibits caspase-8 are downregulated by IRF-1. Survivin has been found to be the fourth highest upregulated transcriptome in a number of cancers [53]. The process of apoptosis and the role of IRF-1 is summarised in (Fig 1.2).

The upregulation of MHC Class I molecules by IRF-1 is also of relevance here, as it sensitises tumour cells to apoptosis induced by T cells [27].

The mechanism by which IRF-1 activates apoptosis appears to be cell type dependent, for example, TRAIL upregulation is important in bladder cancer cells [37], and paracrine death of Jurkat T cells [50] whereas in MDA-MB-468 cells, IRF-1 mediates a ligand independent apoptogenic action [54].

The ability of IRF-1 to induce apoptosis in cells was first noticed by Tanaka *et. al.* when investigating the function of IRF-1 as a tumour suppressor. They observed that IRF-1 WT embryonic fibroblasts undergo apoptosis after the expression of the c-Ha-*ras* oncogene, while IRF-$1^{-/-}$ cells do not [21]. The relevance of IRF-1's proapoptotic activity in cancer has since been demonstrated both *in vitro* and *in vivo* in a number of cancers [34], [55], [54], [41].

This apoptotic activity has been intensively studied in breast cancer where IRF-1 has been shown to be responsible for apoptosis in response to treatments such as antioestrogens. Antioestrogens are a highly effective treatment for breast cancer. They compete with oestrogens for oestrogen receptors and, in breast tissue, this results in reduced incidence and burden of cancer but unfortunately, resistance to these compounds is common [56]. Thus, investigating factors that mediate the antioestrogen response, such as IRF-1, is important, as they might give insights into how to reverse this resistance.

IRF-1 is induced by antioestrogens, for example, Faslodex, and mediates their apoptotic action. In Faslodex resistant cells, IRF-1 expression is downregulated and cannot be induced by antioestrogens. Expression of the IRF-1 inhibitor protein NPM is upregulated [57]. It is tempting to speculate that interventions that restore IRF-1 signalling in resistant cells might re-establish sensitivity to antioestrogens. Indeed, induction of IRF-1 by IFN-γ treatment is sufficient to restore antioestrogen sensitivity to apoptosis [58]. This suggests that combination therapy of IRF-1 activating agents with antioestrogen could be

effective against resistance.

Recently, a similar phenomenon has been observed in gastric cancers where IRF-1 overexpression sensitises cells to 5-fluorouracil (the most commonly used chemotherapeutic for this cancer) through enhanced apoptosis [59]. Likewise, in melanoma cells, IFN- induced IRF-1 results in enhanced apoptotic cell death when combined with the chemotherapeutic vinblastine [60].

In vivo studies have confirmed the efficacy of IRF-1 upregulation in tumour suppression. In a mouse xenograft model, adenoviral (Ad)-IRF-1 inhibited tumour growth and the resected tumours showed a downregulation of the antiapoptotic factor survivin [41]. Overexpression of IRF-1 in MCF7 cells significantly reduced the establishment of tumours when these cells were injected into nude mice. IRF-1 was shown to enhance apoptosis of these cells *in vitro* [23]. Ad-IRF-1 moderately suppressed tumour growth in a murine model of oesophageal adenocarcinoma, and again, *in vitro*, apoptosis was enhanced [61].

A particularly interesting aspect of the apoptotic activity of IRF-1 is that it can be selective for transformed cells. As Tanaka *et. al.* observed, the expression of c-Ha-*ras* was required for IRF-1 to initiate apoptosis [21]. Kirchhoff and Hauser confirmed this selective effect when they demonstrated that IRF-1 will not induce apoptosis in non-transformed NIH3T3 cells, but when HER2 and IRF-1 are simultaneously activated in NIH3T3 cells, apoptosis occurs [62]. Similar selectivity has been observed with leukaemic vs normal CD4+ cells although in this case, IRF-1 induced TRAIL expression in SK-BR-3 cells which was secreted and resulted in only leukaemic T cell apoptosis [50]. This selectivity makes IRF-1 an attractive anti-cancer drug target as it should result in fewer side effects.

IRF-1 has also been shown to induce autophagic cell death in human hepatocellular carcinoma cells [63]. This could be another example of its tumour suppressor capabilities, however, autophagy can also protect cells from the environmental stresses of some antineoplastic drugs [64]. In contrast, in immune cells, IRF-1 seems to negatively regulate autophagy, and promotes the apoptotic pathway. In this context, it may actually

contribute to mortality by enhancing apoptosis in response to LPS (lipopolysaccharide, an endotoxin) thus leading to sepsis-induced immunosuppression [65].

Therefore, although IRF-1 generally activates apoptosis, this can be dependent on the environment and cell death by autophagy due to IRF-1 activity has been observed [63], as well as simply cell cycle arrest. In most cases, the activation of apoptosis is advantageous as it removes potentially/actively tumourigenic cells without providing them a potential respite from anti-cancer drugs. In the context of the immune system, however, excessive apoptosis in response to LPS stimulation can lead to sepsis-induced immunodeficiency [65]. IRF-1 KO mice are resistant to the lethal cytokinase cascade triggered by LPS injection [66]. Clearly the effects of IRF-1 expression are not all beneficial (see also its role in autoimmune responses below) and the positive (tumour suppression/immune function) functions come at the cost of a propensity to septic shock and autoimmune disorders.

1.4.2 Cell Cycle Arrest

The role of IRF-1 in cell cycle arrest was first addressed by Tanaka *et. al.* as a follow-up to their earlier observations that IRF-1 suppresses ras-induced transformation [30], [21]. They showed that IRF-1 is a mediator of DNA-damage-induced cell cycle arrest and upregulates the cyclin dependent kinase (Cdk) inhibitor p21 in cooperation with p53 in embryonic fibroblasts (EFs) [30]. Dornan *et. al.* later showed that this cooperation was independent of the DNA-binding activity of IRF-1 but involved IRF-1 binding to and stabilising a DNA-p53-p300 complex. This facilitates acetylation of p53, which results in p53 being clamped to the p21 promoter DNA thus enhancing p21 expression [67]. IRF-1 can also, however, upregulate p21 independetly of p53 [30], [68]. p21 arrests the cell cycle through two mechanisms: It binds and inhibits cyclin-Cdk complexes which oversee progression through the cell cycle, and inhibits DNA replication through interaction with Proliferating Cell Nuclear Antigen (PCNA), a subunit of DNA polymerase δ [69]. siRNA knockdown of p21 blocks cell cycle arrest by IRF-1 in H1299 cells [68].

In addition to upregulation of the cyclin-Cdk inhibitor (CdkI) p21, IRF-1 transcrip-

tionally regulates components of the Cyclin-Cdk complexes. The actions of Cyclin/Cdk complexes are essential for progression of cells through the cell cycle. Cyclins D and E, and Cdks 2 and 4 have been shown to be downregulated in MDA-MB-468 cells by IRF-1 [68], [70], [33]. IRF-1 represses the Cdk2 promoter by interfering with SP1 activation [32]. A specific element in the C-terminus of IRF-1 has been shown to be required for repression of the Cdk2 promoter and loss of this region has a significant impact on the ability of IRF-1 to act as a tumour suppressor [70].

The Cyclin D/Cdk4 complex phosphorylates and inactivates pRb thereby releasing a check on the cell cycle [71]. Work by Kroger *et. al.* has indicated that in myc/ras transformed NIH3T3 cells, inhibition of cyclin D expression mediates IRF-1's tumour-suppressive activities [33]. Interestingly, in the ras/mycNIH3T3 cells, expression of cyclin E and Cdk4 is not affected by IRF-1 expression [33] indicating that the function of IRF-1 is cell type specific.

IRF-1 also upregulates p27 which, besides its traditional role as a CdkI (similar to p21), also mediates IRF-1's downregulation of human telomerase reverse transcriptase (hTERT) [31]. As active telomerase is thought to be necessary for tumourigenesis [72], this could play a large role in IRF-1's tumour suppressor capabilities.

The role of IRF-1 in cell cycle control is still, however, unclear. Work by other authors has observed that IRF-1 does not affect cell cycle: In MCF7 and T47D cells, dnIRF-1 enhanced proliferation and apoptosis but had no effect on cell cycle profile [23] [57], while in Capan 1 pancreatic cells, IFN-γ upregulated IRF-1, showed antiproliferative and tumour suppressive effects but did not affect the cell cycle profile [73]. Similarly, Kirchoff *et. al.* noticed that inhibition of proliferation of C243 cells by IRF-1 was not mediated by cell cycle arrest [74]. The effects of IRF-1 on cell cycle could be cell line dependent - requiring cofactors that are only present in certain cells/after activation by certain stimuli. Alternatively, the activating stimulus could dictate whether cell cycle arrest occurs; perhaps when IRF-1 is overexpressed without stimulus, post-translational regulatory events or activation of cooperating factors is missing. Kroger *et. al.* also observed differences between non-transformed NIH3T3 cells and transformed cells. IRF-1 had very little effect on the cell cycle profile of the non-transformed cells. After transformation, however,

a high proportion of cells were in S phase, and expression of IRF-1 caused G1/S cell cycle arrest, resulting in a reversion of the cell cycle profile to non-transformed proportions [75].

The above suggests that IRF-1 is part of a complex regulatory network that controls cell cycle arrest. Many factors, activated as a result of transformation, or DNA damage, or IFN-γ etc. may cooperate to activate cell cycle arrest, and in certain cell lines, or after certain stimuli, a sufficient combination of factors (including IRF-1) will be upregulated/activated and cell cycle arrest will ensue. In some cases, where overexpression of IRF-1 results in arrest, IRF-1 is the limiting factor, in other cases, where IRF-1 does not cause arrest, other factors are limiting.

1.4.3 DNA Damage Response

As well as being involved in inducing cell cycle arrest in response to DNA damage, IRF-1 upregulates various factors involved in DNA repair. The induction of IRF-1 itself after IR (ionising radiation) or etoposide mediated DNA damage involves an ATM kinase signalling pathway resulting in enhanced IRF-1 mRNA levels and a prolonged half-life of IRF-1 protein [76].

Hepatocytes lacking IRF-1 are deficient in their ability to repair DNA [77] and in cooperation with the loss of p53, loss of IRF-1 results in increased susceptibility to mutation, implying that IRF-1 may be involved in maintaining genetic stability [22].

Recently, some of the proteins responsible for the DNA repair activity of IRF-1 have been identified. BRIP1 is a Fanconi Anaemia protein involved in Interstrand Crosslink Repair (ICR) which has been shown to be under the regulation of IRF-1. siIRF-1 treatment confers hypersensitivity to the DNA crosslinking agent mephalan to cells (a hallmark of a defective ICL repair pathway). Other DNA repair pathway genes were shown to be regulated by IRF-1 in the same ChIP-chip study that identified *BRIP1*, however, these have not been studied in as much detail [43].

DNA polymerase η (Polη) is especially important for error-free bypass of pyrimi-

dine dimers introduced by UV. As it has a low fidelity, it must be carefully regulated to minimise the introduction of mutations into the genome. IRF-1 transactivates Polη in response to a chemical carcinogen MNNG [44] and, although this is perhaps an undesirable event leading to the accumulation of mutations after exposure to the carcinogen, it may indicate IRF-1 could have a genuine role in the appropriate regulation of Polη for example in response to UV damage. In support of this, cells lacking IRF-1 show impaired DNA repair after UV damage [77]. Finally, IRF-1 upregulates PCNA [43], which also forms part of the UV-induced DNA damage repair machinery, along with Polη [44].

1.4.4 Inhibition of Metastasis

Downregulation of IRF-1 has been linked with increased metastatic potential of tumours, for example, there was a correlation between loss of IRF-1 and lymph node metastasis in oesophageal cancer [42] and an invasive phenotype in breast cancer [23]. Furthermore, immunotherapy can result in regression of melanoma metastasis; this was linked to upregulation of IRF-1 and genes involved in antigen presentation [78].

Thus, two mechanisms are possible for IRF-1's suppression of metastasis: The metastatic potential of the cell could be suppressed, and/or the immune recognition of metastatic cells could be enhanced. Relevant to the first mechanism, IRF-1 suppresses the Matrix Metalloprotease-9 (*MMP9*) promoter through competition for binding with the activator NF-κB [45]. Suppression occurs in both tumour cells (Ewing's sarcoma derived)[45] and stromal cells (monocytes) [79]. MMP9 has been shown to be secreted by tumour cells (e.g. MDA-MB-231 breast cancer cells [80]) and additionally, macrophages co-cultured with breast cancer cells released TNF-alpha-induced MMP-9, resulting in increased invasiveness of the MCF-7 and SK-BR-3 cells [81]. Elsewhere, the presence of inflammatory cells in cancer stroma has been linked to poor prognosis, despite being indicative of a defense reaction against the tumour [82].

IRF-1 is also involved in enhancing the immune recognition of metastatic cells. Immunotherapy can result in regression of melanoma metastasis [83], a property which has been linked to the activation of IRF-1 and subsequent upregulation of genes involved in

antigen presentation [78].

The role of IRF-1 in the suppression of metastasis in a mouse model has been studied in some detail by Ksienzyk *et. al.*. They show that IRF-1 enhances Natural Killer (NK) cell recruitment to, and NK cell mediated cell death of, infiltrating tumour cells by a number of coordinately functioning receptor-ligand interactions. The expression of IRF-1 by metastatic cells has effects on both tumour and NK cell receptor/ligand gene expression [46].

1.4.5 Immune Surveillance

The immune system has a role in tumour suppression and can act to reject tumours. IRF-1 impinges on this both through its immunomodulatory function, and through its effects on gene expression.

IRF-1 is required for the development and function of the immune system (reviewed in [29]). It also regulates the recruitment of the immune system to potentially tumourigenic cells, and is involved in the apoptotic death of these cells.

The immune-mediated effects of IRF-1 tumour suppression have been observed *in vivo*. IRF-1 WT mice were protected from death due to lymphoid neoplasia induced by chemical carcinogen compared to IRF-$1^{-/-}$ mice. It was shown that IRF-$1^{-/-}$ mice were unable to upregulate cytokines involved in immune surveillance and that replacement of IL-12, one of the cytokines regulated by IRF-1, was able to somewhat restore the protective effects of IRF-1 [24]. IL-12 had previously been shown to inhibit tumour formation in mouse models through immune mediated rejection [84].

IRF-1 controls the expression of MHC Class I and II genes [28], and genes encoding proteins involved in antigen processing i.e. immunoproteasome subunits LMP2 [25] and MECL1 [26] and antigen transporter TAP1 [25]. CD40L (CD40 ligand) is involved in the processing and expression of tumour antigens to T cells. It is currently in clinical trials as a cancer therapeutic. IRF-1 has been shown to be responsible for the upregulation of antigen transporters and immunoproteasome subunits associated with the CD40 response.

Engagement of the CD40 ligand activates NF-κB dependent upregulation of IRF-1 [85].

In Hepatocellular Carcinoma (HCC), MHC Class I genes were upregulated by IRF-1, and T cell memory was induced. IRF-1 expressing tumour cells were subjected to specific Cytotoxic T Lymphocyte (CTL) killing *in vivo* resulting in suppression of a highly tumourigenic HCC cell line *in vivo* [86]. Similarly, expression of IRF-1 in a non-immunogenic sarcoma cell line resulted in enhanced MHC Class I expression, and reduced tumour growth. Tumour growth was more strongly impeded in immunocompetent mice than immunodeficient mice [27].

As discussed in the previous section, IRF-1 has a role in apoptosis induced by immune cell signals. It is evident from the diverse mechanisms of tumour suppression mentioned above that IRF-1 is a very powerful antioncogenic agent. Its pleiotropic functions mean that expression of IRF-1 can effect tumour suppression not merely when replacing lost IRF-1, but across a range of unrelated cancer types.

There is, however, a caveat. Enhanced expression of IRF-1 could be advantageous for the treatment of cancer but it has been linked to autoimmune disorders. It was noted that in myelodysplasia patients, low expression of IRF-1 confers some protection against autoimmune manifestations [87]. IRF-$1^{-/-}$ mice have reduced susceptibility to antigen-induced autoimmune diseases type II collagen-induced arthritis and experimental allergic encephalomyelitis (an animal model for multiple sclerosis [88] [89]. Thus, instead of non-specifically activating IRF-1 activity, it is important to understand the regulation of this protein in order to allow the development of therapeutics which can selectively exploit the desired attributes.

1.5 Regulation of IRF-1

1.5.1 Regulation at the Promoter Level

IRF-1 is constitutively expressed at low levels, and its half life is rapid - around 30 mins [111], [112]. Thus, upregulation of *IRF-1* gene expression is an important method of

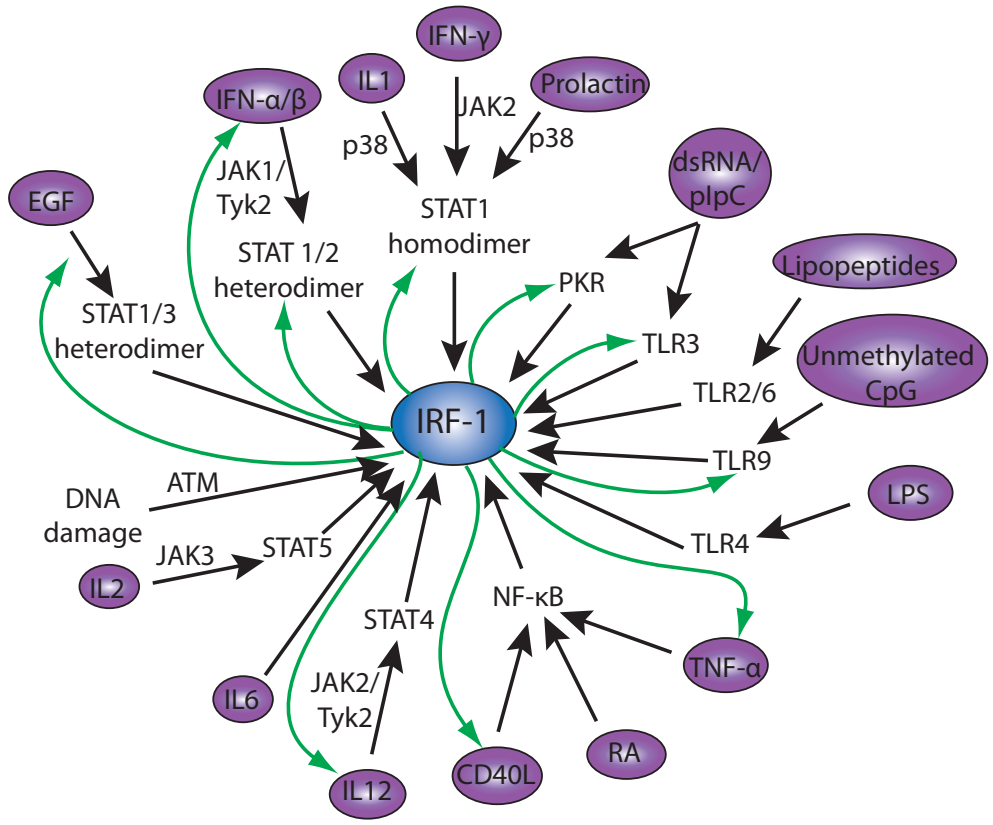

Figure 1.3: IRF-1 is transcriptionally upregulated by a wide variety of stimuli. Black arrows indicate activation of IRF-1, green arrows indicate positive feedback where IRF-1 upregulates factors involved in its postive regulation. [90],[91],[92],[93],[94],[95],[96],[97],[98],[99],[100],[101],[85],[102],[103],[104],[105],[106], [107],[108],[76],[109],[110].

control. IRF-1 can be induced by a wide varitey of stimuli. These are depicted in detail in Fig 1.3 but include interferons, other cytokines and bacterial/viral antigens through Toll Like Receptors (TLRs). The signalling pathways governing *IRF-1* upregulation are not known in all cases, but the GAS (gamma activated sequence) element in the IRF-1 promoter responds to various STAT (Signal Transduction and Activator of Transcription) combinations, depending on the activating signal [113], [114], [110], [115], [31], [108], [104]. A NF-κB site can mediate the upregulation of IRF-1 in response to alternative signals such as [116], [85], [117]. The combination of response elements in the IRF-1 promoter allows cooperative upregulation of IRF-1 as a result of a combination of signals, for example, TNF-α (Tumour Necrosis Factor-α) and IFN-γ together result in higher levels of IRF-1 than is possible with individual stimuli [118].

1.5.2 Post-translational regulation

Although the accumulation of IRF-1 protein is clearly crucial, post-translational modifications are also important for the regulation of IRF-1 activity. This was first evident in a paper by Watanabe *et. al.* who observed that induction of IRF-1 by IFN-β or TNF-α or even a combination of the two was not sufficient for activation of an IRF-E (IRF-1 response element)-dependent reporter construct in L929 cells. In the presence of a virus, IRF-1 was both induced and activated. When IRF-1 is pre-accumulated, activation of the IRF-E can occur even in the presence of cycloheximide, arguing that a post-translational modification is the missing activatory signal since protein synthesis is not required. As this activation is blocked by a broad spectrum kinase inhibitor, phosphorylation is a likely candidate [112].

Casein kinase II (CKII) is known to phosphorylate IRF-1 in the C-terminus. This phosphorylation is required for transactivation activity. The exact role for CKII phosphoryation is unknown but it is suggested that it may be important for the activation of IRF-1 by cytokines [119]. PKC might also phosphorylate IRF-1 as, in the presence of a dominant negative PKC isoform, a 2D gel shows IRF-1 with fewer acidic residues, and the presence of constitutively active (CA)-PKC enhances the IRF-1 mediated transactivation

of the *CIITA* (MHC class II Transactivator) promoter [120].

After DNA damage, the rate of proteasomal degradation of IRF-1 is reduced resulting in accumulation of protein (in combination with elevated mRNA levels). It is thought that ATM kinase might be involved in this regulation as in $ATM^{-/-}$ cells, DNA damage does not affect IRF-1 half life [76]. Whether ATM directly phosphorylates IRF-1 is not known.

The TLR adaptor protein MyD88 may facilitate phosphorylation of IRF-1. In dendritic cells (DCs), TLR2/6/9 activation cannot induce IRF-1 but it does enhance the activity of IRF-1 induced by IFN-γ. It is suggested that the effect of MyD88 is to increase the rate of nuclear translocation of IRF-1 and, as co-expression of IRF-1 and MyD88 results in additional acidic charges on IRF-1 it is likely that phosphorylation is responsible for this [96].

Work in the Ball laboratory has demonstrated that IRF-1 is a phosphoprotein. Dr Sarah Meek has shown that IRF-1 exists as various phosphoisoforms on a 2D gel, and can be collapsed to a small number of spots by a phosphatase (Fig 1.4A). In addition, treatment with the phosphatase inhibitor okadaic acid results in hyperphosphorylation of IRF-1, visualised as a retarded migration on SDS-PAGE (Fig 1.4B).

Since the work for this PhD was started, it has been shown in the Ball laboratory that phosphorylation of the IRF-1 C-terminus regulates the binding to the chaperone Hsp70. This is particularly interesting since Hsp70 has been shown to cooperate with Hsp90 to regulate IRF-1 activity, stability and localisation (Vikram Narayan, unpublished observations, and [121]). The significance of this regulation is considered in more detail in the discussion.

Ubiquitination of a protein can target it for degradation, or modify its activity. IRF-1 is degraded by the 26S proteasome in response to its polyubiquitination. The C-terminal region of the protein is found to determine its stability [122] but is not itself ubiquitinated [123] and it has been suggested that phosphorylation in this region may signal for ubiquitination; this mechanism has been shown to operate for IRF-3 [122].

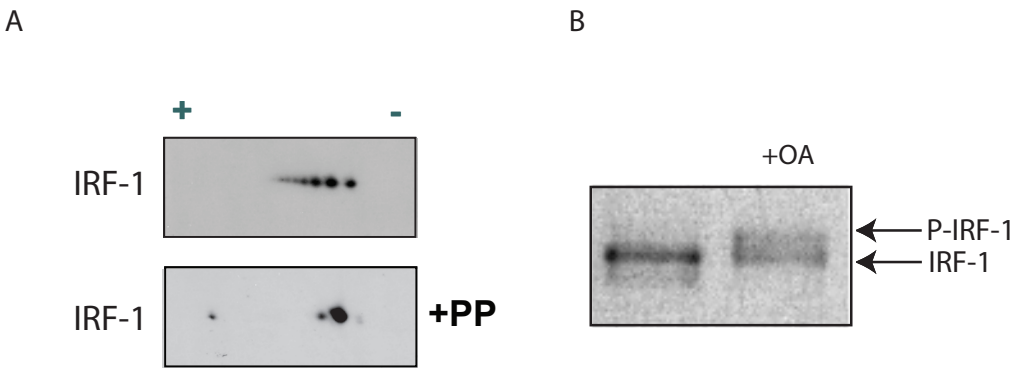

Figure 1.4: IRF-1 is a phosphoprotein. (A) Nuclear fraction was extracted from HCT116 cells, treated +/- lambda phosphatase (400U, 30mins, 30°C) and analysed by 2D gel electrophoresis/immunoblot using anti-IRF-1 antibody (BD biosciences). Phosphatase treatment results in collapse of acidic isoforms of IRF-1 to a single spot, implying IRF-1 exists as a phosphoprotein in cells. (B) IRF-1 expressed in insect cells was treated +/- the phosphatase inhibitor okadaic acid (OA) and analysed by SDS-PAGE/immunoblot using anti-IRF-1 (BD biosciences). Treatment results in the retardation of IRF-1; the lower mobility isoform likely represents hyperphosphorylated IRF-1 (P-IRF-1) (experiments performed by Sarah Meek).

SUMOylation or covalent attachment of "Small Ubiquitin-like MOdifier" to proteins can also affect activity. PIAS3 (Protein Inhibitor of Activated STAT-3), a SUMO ligase, and Ubc9 (Ubiquitin Conjugating Enzyme-9), an E2 conjugating enzyme, were found to elevate levels of SUMOylated IRF-1 with the result of suppression of transactivational activity [124]. Elevated levels of SUMOylated IRF-1 in tumour cells result in accumulation of the protein as SUMOylation possibly competes with ubiquitination for lysine residues. Since SUMOylated IRF-1 is unable to activate apoptosis, this may contribute to the uncontrolled growth of these cells [125].

Acetylation of IRF-1 by p300 has been observed *in vitro* [126]. In NIH3T3 cells, PCAF (p300/CBP Associated Factor) binds IRF-1 and enhances its activity at the ISRE. The Histone Acetyl Transferase (HAT) region of PCAF is required for this increase in IRF-1 activity [127]. The acetylation of IRF-1 in the DNA binding domain by CBP in response to MNNG treatment stabilises the IRF-1 protein and leads to its accumulation in the absence of any change in mRNA levels [44].

1.5.3 Co-factor Binding

As well as acetylation of transcription factors, CBP/p300 and PCAF can acetylate histone proteins to "activate" chromatin, making it accessible to transcription factors [128]. There are a number of cases where IRF-1 binds a HAT protein but direct acetylation has not been investigated or has been ruled out [129] [130], [131]. In these cases, IRF-1 could cooperate in the recruitment of the HAT to modify the chromatin, modify itself, or to modify another co-factor such as NF-κB [131] or p53 [67]. It is likely that future work will demonstrate further the importance of IRF-1 in recruitment of HATs as the HPV E7 oncoprotein functions to inactivate IRF-1 by recruiting HDACs to the IRF-1-bound promoter [16]. This implies that acetylation of substrates by IRF-1-recruited HATs is a common activatory mechanism.

IRF-1 binds a variety of other co-factors to carry out its transactivatory activity. The enhanceosome which synergystically activates the /em IFN-beta promoter is composed of IRF-1, NF-κB, ATF2/cJun and p300. These factors cooperate to generate much higher levels of transcription than is achieved by the sum of their individual contributions [130]. IRF-1 and NF-κ-B interact at several other promoters. For example, at the *iNOS* promoter in macrophages stimulated with IFN-γ and TNF-α, IRF-1 and NF-κB physically interact and cause bending of the promoter DNA. The combination of signals produces synergistic activation of *iNOS* [132].

STAT1 homodimers can activate IRF-1 expression in response to interferon and other stimuli [113], [115], [31]. However, as a monomer STAT1 can cooperate with IRF-1 at a series of promoters. At the *gbp2* promoter, both IRF-1 and STAT1 are required for maximal transcription [133]. Interaction between IRF-1 and STAT1 seems to enhance binding to the *LMP2* promoter [134] and again, both factors are required for transcription [25]. IRF-1 and STAT1 participate in a positive feedback loop as they cooperate to activate the *STAT1* promoter [135].

In contrast to the recruitment of HATs by IRF-1 mentioned above, the chromatin remodelling enzyme BRG1 (Brahma-related gene 1) is required to recruit IRF-1 to the promoter of the antiviral E3 ligase *TRIM22* [136].

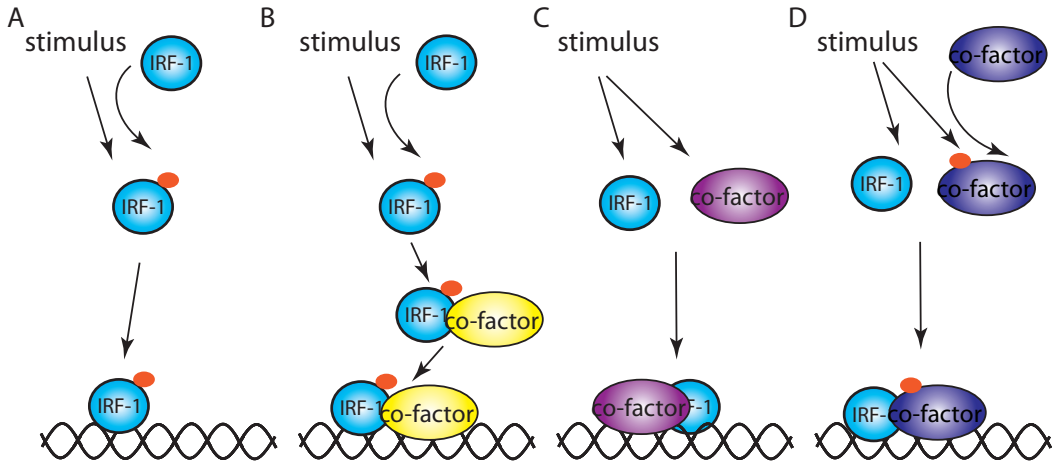

Figure 1.5: Various mechanisms exist to regulate promoter selection of IRF-1. A particular stimulus, such as IFN-γ could direct IRF-1 to a particular subset of promoters through a variety of mechanisms. Any one or a combination of these mechanisms could operate in response to a particular stimulus. (A) Stimulus induces phosphorylation of IRF-1; phosphorylation directs IRF-1 to promoters by causing a specific conformational change in the protein. (B) Stimulus induces phosphorylation of IRF-1; phosphorylation creates a binding site for a cofactor which directs IRF-1 to a particular promoter and could modulate its activity. (C) Stimulus upregulates IRF-1 and a cofactor; enhanced intracellular concentrations of these factors promotes their interaction and the cofactor directs IRF-1 to a particular promoter. (D) Stimulus induces phosphorylation of a cofactor; phosphorylated cofactor binds IRF-1 and directs it to a particular promoter.

1.5.4 Regulation by Other Factors

IRF-1 can also be negatively regulated. Binding of NPM (nucleophosmin) inhibits its DNA binding and transcriptional activity [15] and LPA (Lysophosphatidic Acid) can also block the binding of IRF-1 to DNA [137]. The nuclear translocation of IRF-1 is mediated by importin-α1[138].

In summary, there is a wide repertoire of mechanisms existing in the cell to regulate IRF-1 activity. This is not surprising since so many signals converge on IRF-1 and it upregulates a diverse set genes. Complex regulation allows specific IRF-1 dependent genes to be upregulated in response to a particular stimulus. This can be achieved through post-translational modifications altering DNA and co-factor binding. Alternatively, or in addition, IRF-1 co-factors can be upregulated or modified in response to the same signal, thereby directing IRF-1 activity to particular promoters. This is illustrated in Fig 1.5.

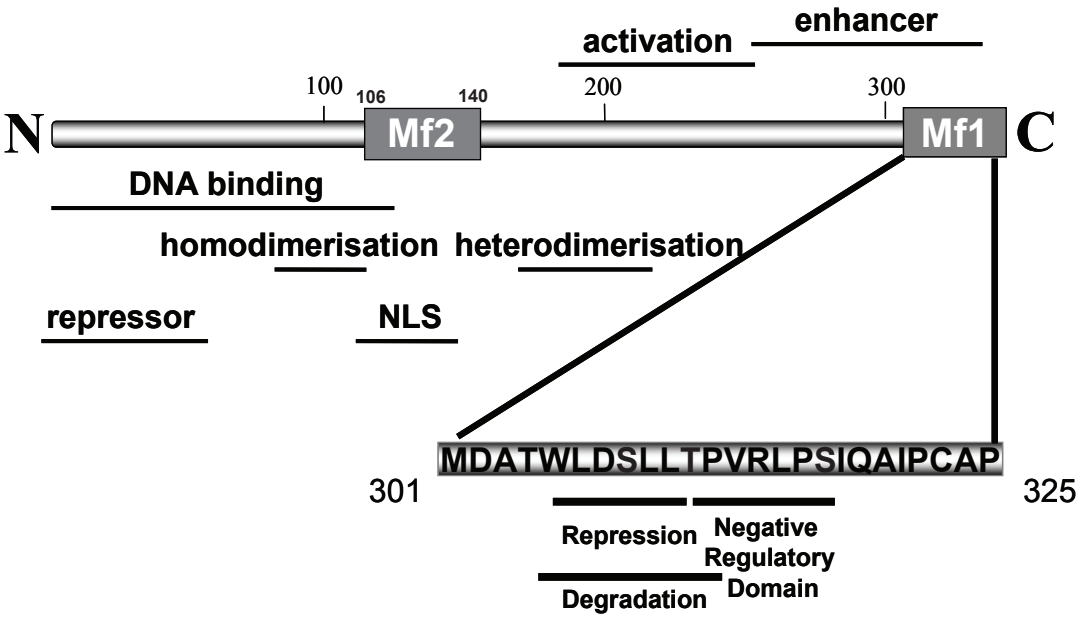

Figure 1.6: Domain organisation of IRF-1. IRF-1 activity is regulated by many overlapping domains whose position is indicated here. Of particular interest to this thesis is the C-terminal multifunctional multiprotein binding interface Mf1 which has been shown to regulate both transcriptional activity (activatory and repressive) and steady state levels of IRF-1.

1.6 IRF-1 Structure and Function

IRF-1 is a multi-domain protein; its domain structure is illustrated in Fig 1.6. The N terminal 120 amino acids comprise the DNA binding domain [139]. This region, which contains a tryptophan cluster, is arranged in a helix-turn-helix motif and is conserved across the IRF family [140]. The first 60 amino acids of IRF-1 also contain a repressor domain which inhibits the transactivatory activity of the protein [141].

Adjacent to the DNA binding domain, between 117-141, are two potential NLS sequences. Deletion of these sequences forces IRF-1 to remain in the cytoplasm, while expression of this region as a fusion protein with GFP localises it to the nucleus [142]. IRF-1 has also been shown to interact with importin-1α; this protein may mediate the nuclear translocation of IRF-1 [138].

Towards the centre of the primary structure are homodimerisation [143], heterodimerisation [142] and a highly disordered multifunctional protein binding (Mf2) domain [144]. A variety of positive and negative interacting factors target this region: IRF-8 [142], NPM

[144] and YB-1 [144] binding inhibit IRF-1 activity, while CHIP binding facilitates ubiquitination of IRF-1 after certain stresses [145].

A transcriptional activation domain resides between 185-256, and an enhancer domain between 257-329 [141]. Thus the C-terminus of IRF-1 is particularly important for its transcriptional activity. Work by Eckert *et. al.* has suggested that the enhancer domain in fact comprises residues 257-300 while the final 25 residues (of the human protein) constitute another repressor domain (at least for the IFN-β promoter).

The Ball laboratory has been particularly interested in these final 25 amino acids of IRF-1, termed the Mf1 domain (Fig 1.6). It has been shown that residues 301-314 are required for repression of Cdk2, and this activity is pivotal for growth suppression, but does not impinge on the transcriptional activatory potential of IRF-1. A co-regulator binding motif (LXXLL) also resides within this region. This may indicate that assembly of a repressor complex at the *Cdk2* promoter is orchestrated by IRF-1 [70]. The LXXLL motif is also recognised by the co-factor p300 and the IRF-1-p300 complex has been shown to enhance transcription of the *p21* promoter through cooperation with p53 [67].

The region 301-311 has been suggested to contain a degradation motif which is recognised by components of the proteasome machinery after IRF-1 has been polyubiquitinated [123]. Hsp70 interacts with the LXXLL motif of IRF-1 and, together with Hsp90, positively regulates IRF-1. Notably, inhibition of Hsp90 results in the Hsp70-dependent degradation of IRF-1 while overexpression of Hsp90 causes nuclear accumulation of IRF-1. Interestingly, IRF-1 activity is regulated by Hsp90 independently of the effects on steady-state protein levels [121].

Transactivatory activity of IRF-1 is regulated by a number of different motifs within the Mf1 domain. A C-terminal point mutation (P325A) is sufficient to dramatically change the half life of IRF-1 from around 30mins to less than 15mins (Fig 1.7A). Interestingly, when protein levels were normalised, this mutant is also more active in a dual luciferase reporter assay at the *TLR3* promoter (Fig 1.7B) [146]. Previous work by Eckert *et. al.* has also shown that deletion of a negative regulatory domain within the Mf1 domain leads to transcriptional activation [70].

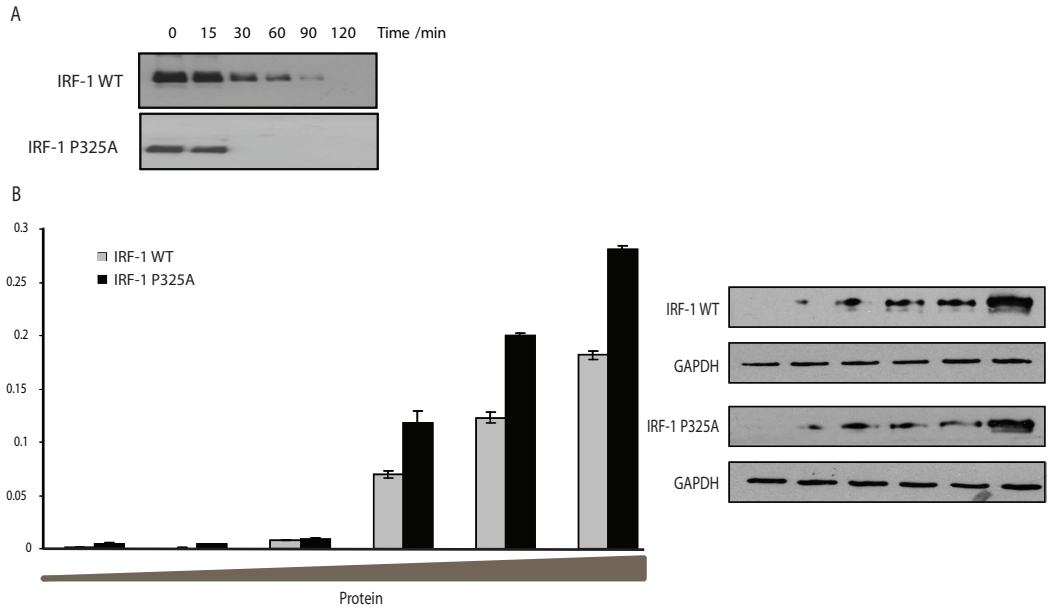

Figure 1.7: A single point mutation of the last residue (P325) of IRF-1 increases both turnover and activity of the protein. (A) IRF-1 P325A has accelerated turnover. HeLa cells were transfected with 0.5μg IRF-1 WT or IRF-1 P325A. After 24h, they were treated with 30μg/ml cycloheximide and harvested after the intervals indicated. Cells were lysed and lysate subjected to SDS-PAGE/immunoblot using anti-IRF-1 (BD Biosciences) (experiment performed by Emma Pion). (B) IRF-1 P325A has enhanced transactivatory activity. Left panel: HeLa cells were transfected with a titration of 0-0.25μg IRF-1WT or 0-0.5μg IRF-1P325A (giving normalised IRF-1 protein levels), 120ng *TLR-3*-luc reporter plasmid and 60ng control CMV-Renilla-luc. Reporter gene activity was measured in relative light units (RLU) and normalised to CMV-Renilla-luc activity. Results are given as mean +/- half the range. Right panel: Expressed protein levels were visualised by SDS-PAGE/immunoblot using anti-IRF-1 (BD Biosciences) and anti-GAPDH (Abcam) as a gel loading control (experiment performed by Angeli Moeller)[146].

Finally, exogenous manipulation of the Mf1 domain can alter IRF-1 activity. Treatment of HeLa cells with an intracellular antibody which recognises an epitope spanning 310-317 results in activation of endogenous IRF-1 activity at a number of promoters without change in IRF-1 levels (Fig 1.8) [146]. It is tempting to speculate that here, the antibody may mimic the effects of a post-translational modification.

The presence of internal regulatory elements within the IRF-1 structure argues strongly that post-translational modifications will modulate the activity of IRF-1 by altering the contribution of each element to the overall activity.

Thus, given the very limited information available on the post-translational regulation of IRF-1, coupled with the growing body of evidence that post-translational events in the Mf1 domain critically regulate IRF-1 function, it is clear that there is a need for dedicated investigation into this topic. This thesis advances the current understanding of IRF-1 post-translational modifications by presenting evidence that phosphorylation at specific sites in the Mf1 domain is induced by IRF-1 activating stimuli. Such phosphorylation activates IRF-1 activity at specific promoters and enhances its capacity as a tumour suppressor, both through suppression of colony formation and inhibition of metastasis.

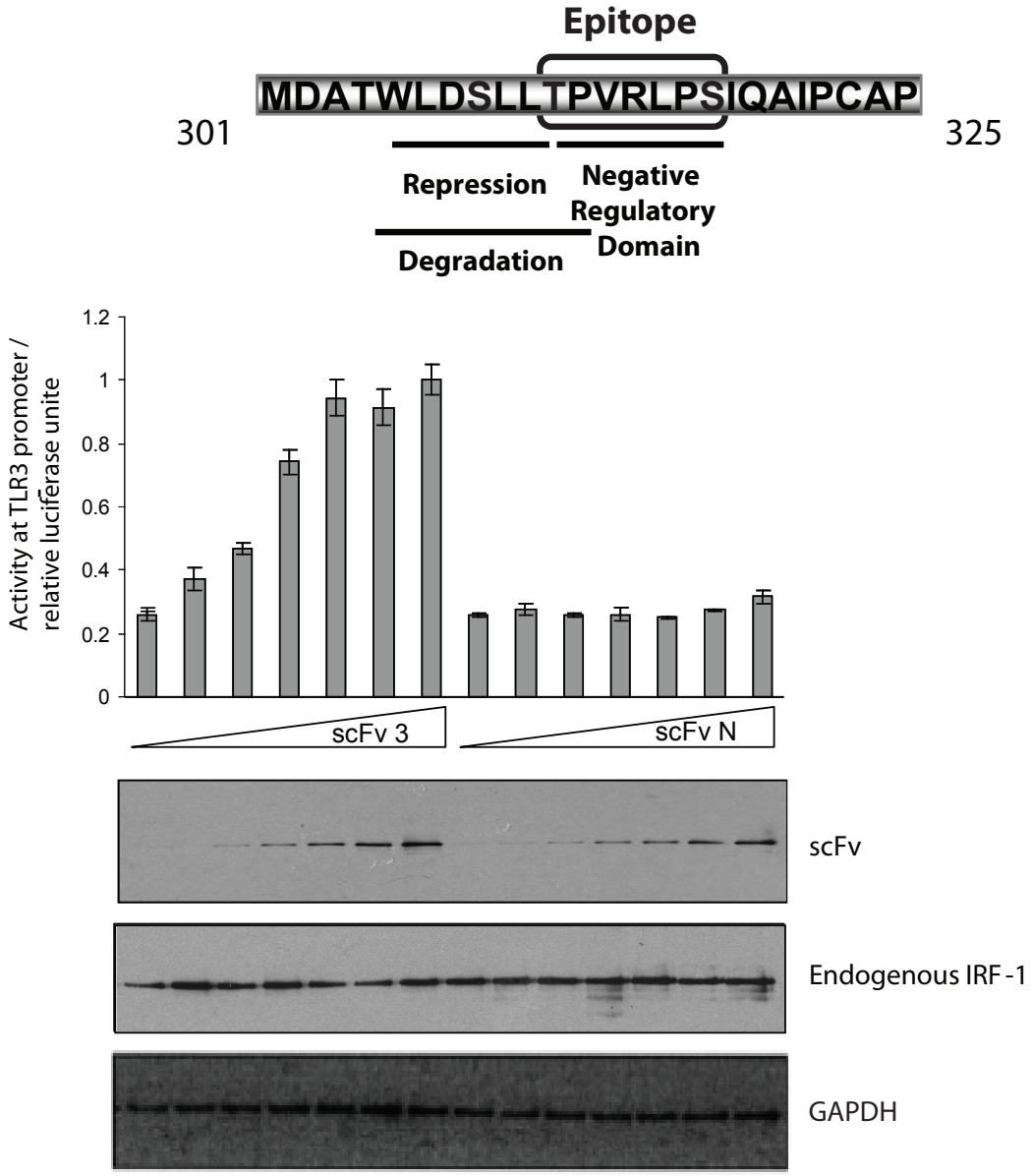

Figure 1.8: Intracellular nanobodies to IRF-1 C-terminus can activate IRF-1 without altering protein levels. Epitope of intracellular nanobody targeting IRF-1 Mf1 domain is indicated. HeLa cells were transfected with a titration of 0-250ng EGFP-scFv3 (Mf1 domain epitope) or EGFP-scFvN (N-terminal epitope), 120ng TLR3-Luc reporter plasmid and 60ng control CMV-Renilla-luc. Reporter gene activity was measured in relative light units (RLU) and normalised to CMV-Renilla-luc activity. Results are given as mean +/- half the range. Expressed protein levels visualised by SDS-PAGE/immunoblot using anti-GFP (Living Colours), anti-IRF-1 (BD Biosciences) and anti-GAPDH (Abcam) as a gel loading control (experiment performed by Angeli Moeller)[146].

Chapter 2

Materials and Methods

2.1 Chemicals and Reagents

All general chemicals were purchased from Sigma unless otherwise stated. Peptides were from Chiron Mimotopes and were N-terminal biotin tagged with an SGSG spacer.

2.2 Antibodies

Protein Target	Source	Supplier (product code)	Dilution
IRF-1	mouse (monoclonal)	BD biosciences (20/IRF-1)	1:1000
IRF-1	rabbit (polyclonal)	Santa Cruz (C-20)	1:1000
IRF-3	rabbit (polyclonal)	NEB (43025)	1:1000
GAPDH	mouse (monoclonal)	Abcam (9484)	1:25000
GFP	mouse (monoclonal)	Living Colours (JL-8)	1:1000
p300	rabbit (polyclonal)	Santa-Cruz (N-15)	1:1000
Hsp70	rabbit (polyclonal)	Stressgen (SPA-812)	1:1000
Hsp90	rabbit (polyclonal)	Stressgen (SPS-771)	1:1000
AMPK	rabbit (polyclonal)	Millipore (07-250)	1:500
IRF-2	mouse (monoclonal)	Abcam	1:500

Table 2.1: Primary Antibodies

Secondary antibodies rabbit anti-mouse (260) and swine anti-rabbit (217) were pur-

chased from Dako.

2.3 DNA constructs

pcDNA3.1:	IRF-1 WT[1], IRF-1 S317A[1], IRF-1 S317D[1] IRF-1 W11R[4]
pDEST14:	IRF-1 WT[2]
pDEST15:	coIRF-1 WT[3]
pTrcHis B:	IRF-1 1-124[2], IRF-1 118-256[2]
pCold(His):	coIRF-1 WT[3]
p*x* luc:	pIRF-E luc[5], pTLR3 luc[6], pIL7 luc[7], pIFN-β luc[8], pCDK2 luc[9], pMMP9 luc[10]
pCMV:	p300[11]

[1] From Dr. Mijram Eckert

[2] From Dr. Angeli Moeller

[3] From Dr. Vikram Narayan

[4] From Dr. Emma Pion

[5] From Panomics Solutions

[6] [147]

[7] [95]

[8] Gift from Dr. T. Fujita (Kyoto University)

[9] Gift from Dr. van Wijnen (University of Massachusetts)

[10] Gift from Ju-Ming Wang (National Cheng Kung University, Taiwan)

[11] From Mauro Giacca (ICGEB, Italy)

co - codon optimised

2.4 Cloning

2.4.1 Site Directed Mutagenesis

Mutagenesis was performed by mixing template, primers and Pfu master mix according to instructions below, then subjecting to the PCR programme described. Template DNA was then digested by Dpn1, leaving only the mutated product . This was transformed into competent DH5α cells (see below) and plated on LB-Agar with ampicillin. A single colony was picked, grown in LB broth with ampicillin and plasmid DNA was purified from the bacteria using QIAGEN mini-prep kit. The mutated plasmid was sequenced by Source Biosciences (Cambridge) before use.

Reaction Mix

12.5μl	Pfu Master Mix
0.13μl	100μM forward primer
0.13μl	100μM reverse primer
50 ng	template
25μl	

PCR Programme

95°C 1min

95°C 50s
55°C 1min
68°C 12mins
} 15 cycles

68°C 30mins

Mutagenic Primers

Altered codons are underlined. Sequence is $5'$ to $3'$.

IRF-1 WT $\rightarrow$ IRF-1 T311A

for mammalian expression vectors

Forward:ACAGCCTGCTGGCACCAGTCC

Reverse:GGACTGGTGCCAGCAGGCTGT

IRF-1 WT → IRF-1 T311D

for mammalian expression vectors

Forward:ACAGCCTGCTGGACCCAGTCC

Reverse:GGACTGGGTCCAGCAGGCTGT

for codon optimised E. Coli expression vectors

Forward:ATAGCCTGCTGGATCCGGTGC

Reverse:GCACCGGATCCAGCAGGCTAT

IRF-1 WT → IRF-1 S317D

for codon optimised E. Coli expression vectors

Forward:TGCGTCTGCCGGATATTCAGG

Reverse:CCTGAATATCCGGCAGACGCA

IRF-1 WT → IRF-1 W11R

for codon optimised E. Coli expression vectors

Forward:TATGCGTCCGCGGCTGGAAATG

Reverse:CATTTCCAGCCGCGGACGCATA

Dpn1 Digestion of Amplification Products

To digest methylated template DNA, Dpn1 was added at 0.4U/μl to amplification products (0.5μl of 20U/μl per 25μl reaction). Reaction was incubated at 37°C for 1 hour, then transformed into DH5α *E. Coli* cells.

2.4.2 Heatshock Transformation

50μl of competent bacterial cells (see below for method of preparation of competent cells) was mixed gently with 1μl of Dpn1-digested amplification product. Mixture was incubated on ice for 30mins then heatshocked at 42°C for 1min. Cells were returned to ice for 2mins and finally added to 0.5ml of LB broth.

Cells were grown in LB broth for 2 hours at 37°C with shaking (225rpm) then plated on LB Agar/50μg/ml ampicillin plates. Plates were incubated at 37°C overnight.

LB (Luria Bertani) Broth

1%(w/v)	Tryptone
0.5%(w/v)	Yeast Extract
1%(w/v)	NaCl

Sterilised in autoclave at 121°C, 20 mins.

LB (Luria Bertani) Agar

1%(w/v)	Tryptone
0.5%(w/v)	Yeast Extract
1%(w/v)	Agar

Sterilised in autoclave at 121°C, 20 mins.

2.4.3 Generation of Competent Cells: Heatshock Method

E. Coli (DH5α or BL21-AI) were inoculated into 3ml LB broth (without antibiotic) and grown overnight at 37°C with shaking (220rpm). 250μl of this starter culture was added to 50ml LB broth (without antibiotic) and incubated again until the OD_{600} reached 0.4. The bacterial cells were pelleted by centrifugation at 4000RCF (relative centrifugal force), 15mins, 4°C. The pellet was resuspended in 16ml ice cold Buffer I and incubated for 10mins on ice. Cells were pelleted as before, and pellet resuspended in 2ml ice cold Buffer II, incubated on ice for 10mins then 50μl aliquots were placed into chilled, sterile tubes. Aliquots were snap-frozen and kept at -80°C.

Buffer I

60mM	CH_3COOK
100mM	RbCl
10mM	$CaCl_2.2H_2O$
40mM	$MgCl_2.6H_2O$
15%(v/v)	Glycerol

Adjusted to pH 5.8 using CH_3COOH then sterilised by filtration

Buffer II

10mM	MOPS
10mM	RbCl
75mM	$CaCl_2$
15%(v/v)	Glycerol

Adjusted to pH 6.5 using NaOH then sterilised by fitration

2.4.4 DNA preparation

QIAGEN miniprep and maxiprep kits were used as directed in manufacturer's handbook.

2.4.5 Sequencing Reaction

The sequencing reaction was performed by mixing template, a single primer and Big Dye buffer and Big Dye Mix (contains dNTPs, polymerase and terminating, dye-linked nucleotides) according to instructions below, then subjecting to the thermal cycling programme described. Dye-terminated extension products were subsequently cleaned up by ethanol/EDTA precipitation as detailed below before sending to Source Biosciences (Cambridge) for DNA Sequencing.

Reaction Mix

0.5μl	3.2μM primer (see below for sequences)
1μl	100 ng/μl DNA
2μl	Big Dye Buffer (5x)
1μl	Big Dye Mix (contains dNPTs, polymerase and terminating, dye-linked nucleotides)
5.5μl	nuclease-free water
10μl	

Thermal Cycling Programme

96°C 1min

96°C 10s
50°C 5s
60°C 4mins
} 25 cycles

Sequencing Primers

For mammalian sequence 5′ to 3′.

IRF-1 S1 (Forward, binds at base 209)

GGAGCCAGATCCCAAGACGTG

IRF-1 S2 (Forward, binds at base 499)

CAGGCTACATGCAGGACTTGGAG

IRF-1 S6 (Reverse, binds at base 891)

GGTGGCATCCATGTTCTTCAG

IRF-1 S7 (Reverse, binds at base 380)

CTCTTAGCATCTCGGCTGG

For codon coptimised E. Coli sequence 5′ to 3′.
IRF-1co S2 (Forward, binds at base 500)
CGGGCTATATGCAGGATCTGGAA
IRF-1co S6 (Reverse, binds at base 892)
GGTCGCATCCATGTTTTTCAG
IRF-1 S7 (Reverse, binds at base 380)
CTTTTCGCATCGCGGCTGC

For IRF-1 domains in pTrcHis vector.
Primers bind at 5′ (f) or 3′ (r) ends of multiple cloning site
Forward:GAGGTATATATTAATGTATCG
Reverse:GATTTAATCTGTATCAGG

Extension product clean-up

Extension products were centrifuged briefly to collect liquid at bottom of tube.
2.5μl 125mM EDTA was added.
30μl 100% ethanol was added.
Tube was vortexed and incubated at room temperature for 15mins.
Mixture was centrifuged at 16000RCF for 20mins to pellet precipitated DNA.
Ethanol was removed.
Tube was spun at 16000RCF for 2mins.
Residual ethanol was removed.
DNA was washed with 30μl 70% ethanol.
Mixture was spun at 16000RCF for 2 mins.
Ethanol was removed.
Tube was spun at 16000RCF for 2 mins.
Residual ethanol was removed.
DNA was allowed to air-dry before being posted to Source Biosciences (Cambridge) at ambient temprerature.

2.5 Protein Expression and Purification

2.5.1 *In vitro* Protein Expression using TNT-coupled lysate systems

IRF-1 WT, T311D, S317D and T311D/S317D and p300 were expressed from pcDNA3.1 plasmid in Promega TNT reticulocyte or wheatgerm lysate according to manufacturer's instructions.

2.5.2 *In vitro* Protein Expression and Purification using the *E. Coli*-based PURExpress *in vitro* protein synthesis kit (NEB)

Untagged IRF-1 was expressed and purified from the PURExpress *in vitro* protein synthesis kit. 250ng pDEST14 IRF-1 was used as the template. Protein is expressed in the cell-free system, then the His-tagged transcription/translation machinery is removed using Ni-agarose beads leaving the purified protein. Protocol was as per manufacturer's instructions.

2.5.3 *E. Coli* Protein Expression and Purification

Protein Expression

BL21-AI cells (for pDEST15 or pTrcHisB vectors) or BL21-DE3 cells (for pCold vector) were transformed (see above) with appropriate vector. The following day, a single colony was picked and used to inoculate a starter culture (50ml) in LB with ampicillin (50μg/ml). The starter culture was grown overnight at 37°C with shaking (220rpm) then inoculated into 2 litres LB with ampicillin and grown under the same conditions until the OD_{600} reached 0.6. Expression of protein was induced using arabinose(0.2%(w/v)) for BL21-AI cells or 0.5nM IPTG for-DE3 cells. For expression of proteins from pDEST15 or pTrcHis vectors, cultures were incubated for 3 hours at room temperature with shaking (220rpm) before collection of bacterial cell pellet by centrifugation at 6000RCF, 20mins, 4°C. For

expression of proteins from pCold vector, cells were acclimitised at 15°C for 15mins prior to induction with IPTG. Following addition of IPTG, cells were incubated for 15mins at 15°C with shaking (220rpm) and pellet was collected as above.

Protein Purification: His-tagged proteins

IRF-1 Domain Purification

The bacterial cell pellet from 2L of culture was resuspended in 10ml lysis buffer (see below). The lysate was subjected to freeze-thaw in liquid nitrogen and sonicated followed by clarification by centrifugation at 12000RCF, 15mins, 4°C. Clarified lysate was filtered through a 0.45μm filter to remove debris, then mixed with 1ml of pre-equilibrated Ni-NTA agarose bead slurry (Qiagen). Lysate and beads were incubated at 4°C for 1 hour on a rotating table. The beads were collected by centrifugation at 400RCF , 5mins, 4°C and the flowthrough was removed. The beads were washed with 3x10ml wash buffer, 1x10ml wash buffer with detergent and 2x10ml wash buffer. 3ml of elution buffer was then added to the beads and incubated for 30mins at 4°C on a rotating table. The beads were pelleted by centrifugation as above and the eluate collected. Purified domains were stored at -80 °C. The presence of purified IRF-1 domains was detected by SDS-PAGE followed by immunoblot or Coomassie Staining (see below).

His Purification Lysis Buffer (for IRF-1-domain purification)

0.5M	NaCl
50mM	Tris pH8
1%	Triton X-100
10mM	Imidazole
1mg/ml	Lysozyme
1mM	DTT
1X	Protease Inhibitor Mix (PIM)

(1X PIM: 20μg/ml leupeptin, 1μg/ml aprotinin, 2μg/ml pepstatin, 1mM benzamidine, 10μg/ml soybean trypsin inhibitor, 2M pefabloc and 0.5M EDTA.)

His Purification Wash Buffer (for IRF-1-domain purification)

0.5M	NaCl
50mM	Tris pH8
20mM	Imidazole
1mM	Benzamidine

His Purification Wash Buffer (for IRF-1-domain purification) with Detergent

0.5M	NaCl
50mM	Tris pH8
20mM	Imidazole
1mM	Benzamidine
0.5%(v/v)	Triton X-100
0.5%(v/v)	Tween-20

His Purification Elution Buffer (for IRF-1-domain purification)

0.5M	NaCl
50mM	Tris pH8
250mM	Imidazole
1mM	Benzamidine

His-IRF-1 Purification (from pCold vector)

The bacterial cell pellet from 2L of culture was resuspended in 10ml of lysis buffer. The lysate was subjected to freeze-thaw in liquid nitrogen and sonicated followed by clarification by centrifugation at 12000RCF, 15mins, 4°C. Clarified lysate was filtered through a 0.45μm filter to remove debris, then passed over a 2ml Ni-NTA column twice at 0.4ml/min. The column was washed with 10CV Buffer I, 5CV Buffer I+ATP/$MgCl_2$ (to remove chaperones), 10CV Buffer I, 20CV Buffer II, 10CV Buffer III and eluted in 5CV elution buffer. Purified protein was buffer exchanged into storage buffer and stored at -80°C. The presence of purified IRF-1 was detected by SDS-PAGE followed by immunoblot or Coomassie Staining (see below).

His Purification Lysis Buffer (for IRF-1 purification)

50mM	Tris pH8
10%(w/v)	Sucrose
200mM	KCl
2.5mg/ml	Lysozyme
5mM	Benzamidine
2mM	Pefabloc
1X	Protease Inhibitor Mix (PIM)

(1X PIM: 20μg/ml leupeptin, 1μg/ml aprotinin, 2μg/ml pepstatin, 1mM benzamidine, 10μg/ml soybean trypsin inhibitor, 2M pefabloc and 0.5M EDTA.)

His Purification Wash Buffer I (for IRF-1 purification)

20mM	Tris pH8
300mM	NaCl
20mM	Imidazole
0.3%(v/v)	NP-40
0.5%(v/v)	TX-100
0.5%(v/v)	Tween

His Purification Wash Buffer I + ATP/$MgCl_2$ (for IRF-1 purification)

20mM	Tris pH8
300mM	NaCl
20mM	Imidazole
0.3%(v/v)	NP-40
0.5%(v/v)	TX-100
0.5%(v/v)	Tween
10mM	$MgCl_2$
5mM	ATP

His Purification Wash Buffer II (for IRF-1 purification)

20mM	Tris pH8
500mM	NaCl
40mM	Imidazole

His Purification Wash Buffer III (for IRF-1 purification)

20mM	Tris pH8
150mM	NaCl
40mM	Imidazole
5%	Glycerol

His Purification Elution Buffer (for IRF-1 purification)

20mM	Tris pH8
150mM	NaCl
200mM	Imidazole
5%	Glycerol

Protein Purification: GST-tagged proteins

The bacterial cell pellet from 2L of culture was resuspended in 10ml lysis buffer (see below). The lysate was subjected to freeze-thaw in liquid nitrogen and sonicated followed by clarification by centrifugation at 12000RCF, 15mins, 4°C. Clarified lysate was filtered through a 0.45μm filter to remove debris, then mixed with 1ml of pre-equililbrated glutathione-sepharose 4B bead slurry (GE Healthcare). Lysate and beads were incubated at 4°C for 1 hour on a rotating table. The beads were collected by centrifugation at 400RCF , 5mins, 4°C and the flowthrough was removed. The beads were washed with 5x10ml wash buffer then 3ml of elution buffer was then added to the beads and incubated for 30mins at 4°C on a rotating table. The beads were pelleted by centrifugation as above and the eluate collected. Purified domains were stored at -80 °C. The presence of purified IRF-1 domains was detected by SDS-PAGE followed by immunoblot or Coomassie Staining (see below).

GST Purification Lysis Buffer

20mM	Tris pH8
150mM	NaCl
1mM	EDTA
1%(v/v)	NP-40
1mg/ml	Lysozyme
2mM	DTT
1X	Protease Inhibitor Mix (PIM)

(1X PIM: 20μg/ml leupeptin, 1μg/ml aprotinin, 2μg/ml pepstatin, 1mM benzamidine, 10μg/ml soybean trypsin inhibitor, 2M pefabloc and 0.5M EDTA.)

GST Purification Wash Buffer

20mM	Tris pH8
150mM	NaCl
1mM	EDTA
1%(v/v)	NP-40
2mM	DTT
1mM	Benzamidine

GST Purification Elution Buffer

100mM	Tris pH8
120mM	NaCl
20mM	Reduced glutathione
1X	PIM

2.6 Protein Quantification

Protein concentration was quantified using either BCA Assay Kit (Pierce) or Bradford's Reagent (Bio-Rad) following the manufacturer's instructions. Abosrbance was measured

using a Victor 3 plate reader (Perkin Elmer).

2.7 SDS-PAGE

Polyacrylamide gels were prepared using the MiniProtean kit from Bio-Rad, following the manufacturer's instructions and using the reaction mixes detailed below. Acrylamide mix was from National Diagnostics. Sample concentrations were determined as described above, and the appropriate volume of sample was mixed 1:1 with 2X sample buffer then heated at 85°C for 2mins. Samples were loaded on the gel along with pre-stained protein ladder (Fermentas PageRuler) and gels were run in 1X Tris/Glycine running buffer at 120V until the dye front reached the bottom of the gel.

2X Sample Buffer	
4%	SDS
20%	Glycerol
0.24M	Tris pH 6.8
400mM	DTT

few grains bromophenol blue

10% Separating Gel	
10%(w/v)	Acrylamide mix
0.39M	Tris pH 8.8
0.1%(w/v)	SDS
0.1%(w/v)	Ammonium Persulphate
0.04%(v/v)	TEMED

Resolving Gel

5%(w/v)	Acrylamide mix
0.13M	Tris pH 6.8
0.1%(w/v)	SDS
0.1%(w/v)	Ammonium Persulphate
0.1%(v/v)	TEMED

1X Running Buffer

129mM	Glycine
25mM	Tris
0.1%(w/v)	SDS

2.8 Visualisation of Proteins

2.8.1 Coomassie staining

Gels were fixed and stained in Coomassie stain for 20mins at room temperature. Gels were destained in Coomassie stain until bands were visible.

Coomassie Stain

50%(v/v)	Methanol
10%(v/v)	Acetic Acid
0.2%(w/v)	Coomassie brilliant blue R-250

Coomassie Destain

50%(v/v)	Methanol
10%(v/v)	Acetic Acid

2.8.2 Western Blotting

Proteins in SDS-PAGE gels were transferred to nitrocellulose membrane (Protran) in 1X transfer buffer using Bio-Rad Mini TransBlot apparatus. Transfer was for 1 hour at 100V with cooling or 20mA overnight. Once the proteins had been transferred to the membrane, they were ink stained and then blocked for 0.5 hours using either 5% skimmed milk powder (Marvel) in PBS for conventional antibodies, or 3% BSA/PBS for phosphospecific antibodies. After blocking, membranes were probed with primary antibody diluted in blocking buffer for 1 hour at room temperature or overnight at 4°C. Phosphospecific antibodies were incubated for 24 hours at 4°C. The membranes were washed 3x 5mins in PBS-T (PBS with 0.1%(v/v) Tween-20) then incubated with secondary antibody for 1 hour at room temperature. Membranes were washed 3x5 mins in PBS-T before detecting peroxidase-conjugated secondary antibodies with enhanced chemiluminescence (ECL) reagent. ECL solutions I and II were mixed 1:1 and incubated with the membrane for 2mins. The solution was removed and X-Ray film (SLS) or Hyperfilm (Amersham) was exposed to the membrane. Film was developed using a Konica Medical Film Processor. For antibodies and dilutions, see Table 2.1.

1X Transfer Buffer

192mM	Glycine
25mM	Tris
20%(v/v)	Methanol

ECL Solution I

100mM	Tris pH8.5
2.5mM	Luminol
0.4mM	p-Coumaric acid

ECL Solution II

100mM	Tris pH 8.5
0.02%	H_2O_2

2.9 Cell lines and cell culture

Cell lines and maintenance conditions used are listed below (Table 2.2):

Cell Line	Source	Media*	Conditions
A375	malignant melanoma (human, skin)	DMEM	37°C, 10% CO_2
H1299	non-small cell lung carcinoma (human, lung)	RPMI	37°C, 5% CO_2
HeLa	epithelial adenocarcinoma (human, cervix)	DMEM	37°C, 5% CO_2
MDA-MB-231	epithelial adenocarcinoma (human, breast)	DMEM	37°C, 5% CO_2

Table 2.2: Cell lines and maintenance conditions

*All media were sourced from GIBCO and were supplemented with 10%(v/v) FBS (Autogen Bioclear) and 1% P/S (Invitrogen).

2.9.1 Sub-culturing

Cells were sub-cultured when they reached 100% confluence. Cells were rinsed in sterile PBS and detached using trypsin-EDTA (Invitrogen) (2ml/10cm plate). The trypsin was neutralised using complete medium and a 1:10 dilution was replated in fresh medium.

2.9.2 Long-term storage

For long-term storage, cells were frozen and kept in liquid nitrogen vapour phase. A confluent 10cm plate of cells was trypsinised and the cells collected by centrifugation at 1000RCF, 5mins, room temperature. The medium was discarded and cells were resuspended in 1ml of freezing medium. The cells were then placed in cryotubes (Nunc) and frozen slowly in a Nalgene cryo-freezing container for 1 day before being transferred to the liquid nitrogen vapour phase for long-term storage.

Freezing Medium

Complete culture medium

supplemented with 5% DMSO

2.9.3 Transient Transfection

Transient transfections of DNA were carried out using Attractene (Qiagen) according to manufacturer's instructions.

2.10 Cell Treatments

Cells were treated with the following activators of IRF-1 (Table 2.3):

Treatment	Concentration	Solvent	Length
Interferon-γ (GIBCO)	100U/ml	0.1% BSA, 40mM Tris pH 7.4	4 hours
Etoposide (Sigma)	10μM	50% DMSO	4 hours
p(I:C) (Invivogen)	50μg/ml	PBS	4 hours

Table 2.3: Concentrations and duration of IRF-1 activating treatments

Drugs were diluted in 1ml cell culture medium, then added to 9ml medium on cells.

2.10.1 Cell Lysis

0.5% Triton Mammalian Cell Lysis Buffer	
50mM	HEPES pH7.4
150mM	NaCl
0.1mM	EDTA
50mM	NaF
20mM	β-glycerophosphate
2mM	DTT
0.5%(v/v)	Triton X-100
1X	Protease Inhibitor Mix (PIM)

(1X PIM: 20μg/ml leupeptin, 1μg/ml aprotinin, 2μg/ml pepstatin, 1mM benzamidine,

10μg/ml soybean trypsin inhibitor, 2M pefabloc and 0.5M EDTA.)

Additional Phosphatase Inhibitors	
120nM	Okadaic Acid
2mM	Sodium Orthovanadate

Additional phosphatase inhibitors were added when the phosphorylation state of IRF-1 was particularly important.

1% NP-40 Mammalian Cell Lysis Buffer	
50mM	HEPES pH 7.4
100mM	NaCl
5mM	NaF
2mM	β-glycerophosphate
1mM	DTT
1%(v/v)	NP-40
1X	Protease Inhibitor Mix (PIM)

(1X PIM: 20μg/ml leupeptin, 1μg/ml aprotinin, 2μg/ml pepstatin, 1mM benzamidine, 10μg/ml soybean trypsin inhibitor, 2M pefabloc and 0.5M EDTA.)

2.11 Kinase Assay

In vitro phosphorylation of recombinant IRF-1 by cell lysate or purified kinases was performed by kinase assays.

2.11.1 Kinase assays using cell lysate

HeLa cells were lysed in 1% NP-40 mammalian cell lysis buffer and the protein concentration of the lysate was quantified using Bradford's Reagent. Cell lysate or purified kinase was incubated with substrate (GST-IRF-1 or His-IRF-1-domain) and ATP in reaction buffer (see below). The final volume was 9μl to which 1μl ATP/[$^{\gamma 32}$P]ATP mix was

added to initiate the reaction. Reactions were incubated at 30°C for 30mins in a water-bath and then terminated by addition of SDS-PAGE sample buffer. Samples were then resolved by SDS-PAGE, gels were fixed and stained by Coomassie, dried onto filter paper on a vacuum drier and the image transferred to a phosphorimager screen (Amersham Biosciences). Incorporation of ^{32}P labelled phosphate into IRF-1 was visualised using a Storm 840 phosphorimager (Amersham Biosciences) and ImageQuant software.

Kinase Assay Reaction Mix	
450ng/500ng/1μg as indicated	Substrate (GST-IRF-1 or His-IRF-1-domain)
4μl	1mg/ml Cell lysate
2μl	5x Kinase Assay Buffer
1μ	ATP mix (0.2mM)*
10μl	

*ATP mix: Added at end to initiate reaction
2mM ATP pH8 + 1:50 $^{\gamma}$[^{32}P]ATP. As [^{32}P]ATP decays, dilutions of up to 1:25 were used.

5x Kinase Assay Buffer	
125mM	HEPES
500mM	NaCl
50mM	$MgCl_2$
5mM	DTT

2.11.2 Kinase assays using purified kinase

Chk1

Reaction performed as above except cell lysate replaced with 0.25μl Chk1 (Kudos Pharmaceuticals).

AMPK

Reaction performed as above except AMPK kinase assay mix and AMPK assay buffer was used.

AMPK Kinase Assay Mix	
1μg	Substrate
40U	AMPK (Upstate)
1μl	ATP mix (0.1mM)*
xμl	AMPK buffer
10μl	

*ATP mix: Added at end to initiate reaction
1mM ATP pH8 + 1:50 $^{\gamma}[^{32}P]$ATP. As $[^{32}P]$ATP decays, dilutions of up to 1:25 were used.

AMPK Kinase Assay Buffer	
25mM	HEPES
25mM	KCl
1mM	$MgCl^2$
20μM	EDTA
0.1mM	DTT
300μM	AMP

2.12 Ammonium Sulphate Precipitation

Saturated ammonium sulphate solution (BDH) was added to cell lysate to a final concentration of 25% and equilibrated with stirring for 15mins. Supernatent was collected after spinning at 12000RCF, 15mins, 4°C and precipitate discarded. Saturated ammonium sulphate solution was added to supernatent to a final concentration of 40% and precipitate collected after spinning as before. Precipitate from 40% cut was resuspended in resuspension buffer and dialysed for 2h in dialysis buffer to reduce salt concentration.

Resuspension Buffer

50mM	HEPES
100mM	NaCl
10%	Glycerol
1mM	EDTA
10mM	NaF
10mM	β-glycerophosphate
0.1%	Triton X-100
2mM	DTT
1X	PIM

(1X PIM: 20μg/ml leupeptin, 1μg/ml aprotinin, 2μg/ml pepstatin, 1mM benzamidine, 10μg/ml soybean trypsin inhibitor, 2M pefabloc and 0.5M EDTA.)

Resuspension Buffer

1X PIM replaced with 1mM Benzamidine

2.13 Anion Exhange Chromatography

A375 cells were lysed in 0.5% Triton mammalian cell lysis buffer. 23mg of lysate was filtered through a 0.4μm syringe filter and loaded onto a HiTrap Q Sepharose HP column (GE Healthcare) pre equilibrated in Buffer A. Column was washed with Buffer A and protein eluted over a 20CV gradient to Buffer B (0.05-1.2M NaCl gradient) followed by a 5CV plateau (1.2M NaCl). 1ml elution fractions were collected.

Buffer A

50mM	Tris pH8
0.05mM	NaCl
1mM	DTT
1mM	EDTA
1mM	Benzamidine

Buffer B

As Buffer A except 1.2M NaCl

2.14 Acetone Precipitation

4X sample volume of ice cold (-20°C) acetone (300μl fraction, 1.2ml acetone) was added to the sample. Sample was vortexed and incubated for 1 hour at -20°C. After the incubation, the sample was centrifuged at 16000RCF, 10 mins, 4°C and supernatent was removed. Residual acetone was allowed to evaporate at room temperature for 30 mins, following which the sample was resuspended in 60μl 1X sample buffer.

2.15 2D Gel Electrophoresis

2.15.1 Sample Preparation

Cells were rinsed in 250mM sucrose/10mM Tris pH7.5 then lysed in 2D gel lysis buffer (500μl for a 10cm plate) with a 10min incubation on ice. DNA was sheared by passing lysate through a 0.6mm gauge needle until free flowing.

2D Gel Lysis Buffer	
8M	Urea
2%(v/v)	Triton X-100
40mM	Tris base
20mg/ml	DTT
1x	Protease Inhibitor Mix (PIM)

few grains bromophenol blue

2.15.2 First dimension: Isoelectric Focusing (IEF)

Sample was loaded onto 7cm pH4-7 IPG strips (GE Healthcare). 40μl of lysate was mixed with 90μl of rehydration buffer and incubated with the IPG strip overnight at room

temperature. IEF was carried out on a Multiphor II Electrophoresis system (GE Healthcare). Conditions were:

200V	0.01h
2500V	2800Vh (200V-3500V gradient)
3500V	4200Vh

Rehydration Buffer

8M	Urea
0.5%(v/v)	Triton X-100
2%(v/v)	IPG Buffer
10mM	DTT

few grains bromophenol blue

2.15.3 Second dimension: SDS-PAGE

The IPG strip was equilibrated first in equilibration buffer + DTT, then equilibration buffer + iodoacetamide. The IPG strip was then transferred to a single well 10% Tris/glycine minigel and run, transferred and immunoblotted as previously described for SDS-PAGE gels.

2D Gel Equilibration Buffer

6M	Urea
50mM	Tris pH 8.4
2%(w/v)	SDS
30%(v/v)	Glycerol

few grains bromophenol blue

either

10mg/ml DTT

or

4mg/ml Iodoacetamide

All reagents used in 2D gel protocol were from GE Healthcare. Chemicals were from the PlusOne range.

2.16 Phosphatase Treatment

Experiment carried out by Sarah Meek.
HCT116 cells were harvested and nuclear fraction was extracted: cells were rinsed in 250mM sucrose/10mM Tris pH 7.5 and lysed for 10mins on ice in hypotonic lysis buffer. Lysate was centrifuged 2500g, 5mins, 4°C and the pellet resuspended in nuclear lysis buffer. This was incubated on ice for 30 mins then spun 13000RCF, 10mins, 4°C. Supernatant is the nuclear fraction.

The nuclear fraction was treated with lambda phosphatase 400U, 30mins, 30°C then separated by 2D gel electrophoresis on a pH3-10NL IPG strip and immunoblotted using anti-IRF-1 (BD biosciences).

Hypotonic Lysis Buffer	
10mM	Tris pH 7.5
1.5mM	$MgCl_2$
10mM	NaCl
0.5%	NP-40
1mM	DTT
5mM	NaF
2mM	β-glycerophosphate
1X	Protease Inhibitor Mix (PIM)

(1X PIM: 20μg/ml leupeptin, 1μg/ml aprotinin, 2μg/ml pepstatin, 1mM benzamidine, 10μg/ml soybean trypsin inhibitor, 2M pefabloc and 0.5M EDTA.)

Nuclear Lysis Buffer	
50mM	Tris pH 7.5
10%	Glycerol
1.5mM	$MgCl_2$
0.4M	NaCl
0.2mM	EDTA
1mM	DTT
5mM	NaF
2mM	β-glycerophosphate
1X	Protease Inhibitor Mix (PIM)

(1X PIM: 20μg/ml leupeptin, 1μg/ml aprotinin, 2μg/ml pepstatin, 1mM benzamidine, 10μg/ml soybean trypsin inhibitor, 2M pefabloc and 0.5M EDTA.)

2.17 Dual Luciferase Reporter Assays

Cells were co-transfected with pcDNA3 IRF-1 or control (pcDNA3.1 empty vector (EV)), pCMV-Renilla/Luc vector as an internal control and either pIRF-E-, pTLR3, pIFNβ-, pCDK2- or -Firefly/Luc. Various ratios of p*x*-Firefly/Luc:pCMV-Renilla were used in order to get optimum signal to noise ratio (Table 2.4. DNA levels were normalised using empty vector. Reporter gene (luciferase) activity was measured 24 hours after transfection using the Dual Luciferase Assay system (Promega) according to manufacturer's instructions and using a Fluoroskan Ascent F1 luminometer (Labsystems).

p*x*-Firefly/Luc	Ratio p*x*-Firefly/Luc: pCMV- Renilla/Luc
pIRF-E	60:1
pTLR3	7:3
pIL7	6:1
pIFNβ	6:1
pCDK2	10:1
pMMP9	4:1

Table 2.4: Ratios of p*x*-Firefly/Luc:pCMV-Renilla used for different p*x*-Firefly constructs.

2.18 Geneticin Dose-Response Curves

The dose-response curves for geneticin were determined for cell lines to find the optimum concentration to be used to select for transfected cells containing geneticin-resistance elements in the protein expression vector. Cells were seeded in 6 well dishes and allowed to adhere overnight. A titration of geneticin (Invitrogen) was added to successive wells and the growth of the cells monitored at 3 and 5 days after treatment.

2.19 Clonogenic Assays

2.19.1 Anchorage-dependent Colony Formation Assay

Cells were grown in 6 well plates and transfected with IRF-1 WT or mutant. After 48 hours, cells were trypsinised and seeded into 10cm dishes in appropriate complete medium supplemented with 3% geneticin (Invitrogen) for A375 cells, or 1.5% geneticin for H1299 cells. Medium was changed after 4 days to maintain geneticin selective pressure, and after 10 days, assays were developed. Colonies were washed with PBS and fixed with 100% methanol (-20°C) for 30mins at room temperature. Colonies were then stained with 10% Giemsa stain (diluted in water) for 15mins at room temperature, washed thoroughly and allowed to air-dry. Colony counting and area measurement was performed using Image J software (NIH).

2.19.2 Anchorage-independent Colony Formation Assay

Cells were grown in 6 well plates and transfected with IRF-1 WT or mutant. After 48 hours, cells were trypsinised and $1x10^4$ cells were added to 2ml of methylcellulose (R&D systems) in complete MEM (GIBCO) with 3%(A375) or 1.5%(H1299) geneticin (Invitrogen). This was layered onto 2ml of 0.9% Agarose (Invitrogen) in complete MEM also with geneticin in 6 well tissue culture plates. Cells were incubated for 6-8 days to allow colonies to form. Colony counting and area measurement was performed using Image J

software (NIH).

2.20 Protein Half Life Determination

Cells were grown in 6 well plates and transfected with 1.2μg IRF-1 or mutant. After 24 hours, cells were treated with 30μg/ml cycloheximide and harvested after 0, 15, 30, 45, 60, 75 and 90mins of treatment. Cells were lysed using 0.5% Triton X-100 mammalian cell lysis buffer and half life of IRF-1 visualised by immunoblotting of SDS-PAGE gels using anti-IRF-1 (BD Biosciences). For fractionated half lives, the cells from each time point were harvested, fractionated using Calbiochem ProteoExtract subcellular fractionation kit according to manufacturer's instructions and visualised as above.

2.21 Inverse Invasion Assays

2.21.1 Setting up Transwells

Transwell inserts (Corning) in 24 well plates were filled with 100μl of ice cold Matrigel (BD) diluted 1:2 with ice cold PBS which was allowed to set for 30mins at 37°C. Transwells were then inverted and 5x10^4 cells in 100μl of complete medium were used to coat the bottom of the filter. Cells were left for 4 hours at 37°C to adhere to the inverted Transwell. Transwells were washed in 2x 1ml serum free medium and then a gradient was prepared by placing the transwell right way up in 1ml serum free medium and pipetting 100μl of complete medium on top of the Matrigel. Plates were incubated for 3 days to allow invasion. Experiment was performed in quadruplicate.

2.21.2 Staining Cells

Cells were stained with Calcein-AM (Invitrogen). 0.5ml of medium containing 4μM Calcein-AM was pippeted into a well, Transwells were placed in the wells and 0.5ml of

4μM Calcein-AM in medium was pipetted on top. Cells and stain were incubated for 1 hour at 37°C before being visualised using a confocal microscope.

2.21.3 Visualising and Quantifying Invasion

Z-sections were scanned at 15μM intervals from the base of the filter using a Leica TCS MP5 confocal microscope. Image J was used to quantify invasion. The total area of stained cells at the confluent monolayer on the filter was designated 100% and the area of stained cells at each z-section was normalised to this. Data was represented as percent of cells invaded through 45μm.

2.22 Cell Cycle Analysis

1x10^6 cells were resuspended in 300μl 50% FBS in PBS and fixed by adding 900μl ice cold 70% ethanol while vortexing then incubating at 4°C for 1 hour. Cells were then washed in 3ml PBS and pellet resuspended in 300μl propidium iodide staining solution and incubated in the dark for 1hour at 4°C. Samples were then analysed on a FACSAria II Flow Cytometer (BD Biosciences).

Propidium Iodide Staining Solution	
50μg/ml	Propidium Iodide
100μg/ml	RNAse
diluted in PBS	

2.23 Senescence Assay

A senescence-associated β-galactosidase staining kit (NEB) was used as per manufacturer's instructions.

2.24 Adhesion Assay

Cells were transfected with EV or pcDNA3-IRF-1 WT or T311D/S317D. After 24h, cells were harvested and counted and 100μl of a suspension of 8x10^5 cells/ml of A375 cells placed in wells of a 96 well plate. Cells were allowed to attach for 1h at 37°C, 10% CO_2 then washed twice with PBS, fixed for 15 mins with 50μl ice cold methanol and stained with 50μl 10% Giemsa stain for 1h. Cells were washed 5 times with PBS then lysed in 50μl 0.2% SDS in PBS to solubilise the stain. Absorbance at 595nm was detected as a measure of attached cells.

2.25 Polyclonal Antibody Production and Purification

Antibodies to phosphorylation sites in the C-terminus of IRF-1 were raised in rabbits by Eurogentec using their classic 87-day programme. Antigens were unlabelled phosphorylated peptides (Clonestar).

anti-p308S DATWLD(Sp)LLTPVR
anti-p311T WLDSLL(Tp)VRLPS
anti-p317S TPVRLP(Sp)IQAIPC

Upon receipt of final bleed, antisera was purified first against non-phosphorylated IRF-1 peptide to remove non-phosphospecific IRF-1 antibodies. The flowthrough from this step was then purified against either p308S, p311T or p317S phosphorylated IRF-1 peptide to isolate phosphospecific antibodies.

2.25.1 Purification against non-phosphorylated peptide

0.5μl of 5mg/ml biotinylated IRF-1 C-terminal peptide (aa301-325) (Chiron Mimotopes) in 200μl PBS was incubated with 100μl streptavidin agarose bead slurry (GE Healthcare) for 1 hour at room temperature on a rotating table. Beads were then washed with 3 x 1ml PBS, and 2ml of serum was added to beads. Beads and serum were incubated for 1 hour

at 4°C on a rotating table. Mix was poured into 1ml mobicol column with 90μm filter (MoBiTec) and the flowthrough was collected.

2.25.2 Purification against phosphorylated peptide

Coupling of peptide to beads

2.5mg of phosphorylated non-biotinylated IRF-1 peptide was added to 0.5ml of CDI-Agarose beads (Pierce) in 0.1M sodium borate buffer (pH9) and mixed overnight at room temperature on a rotating table. Beads were collected by centrifugation (500RCF, 5mins, room temperature), supernatent was removed and 1ml of 1M Tris pH8.8 was added to the beads for 8 hours at room temperature with mixing to quench non-reacted sites. Beads were then washed thoroughly to remove residual peptide (10x 1ml PBS+0.1% Tween-20 (PBS-T).

Sodium Borate Buffer

0.1M Boric Acid

45mM NaOH

adjust pH to 9

Purification of antibody

Phosphatase inhibitors (50mM NaF and 50mM β-glycerophosphate) and 50μ of phosphopeptide-coupled beads were added to 2ml of flowthrough from previous purification. Serum and beads were mixed overnight at 4°C, then beads were collected by centrifugation (500RCF, 5mins, 4°C), supernatant was removed and beads were washed 3x 0.5ml PBS-T + phosphatase inhibitors (50mM NaF and 50mM β-glycerophosphate). Phosphospecific antibody was eluted using low pH. Beads were placed in a 1ml mobicol column with 90μm filter (MoBiTec) and 6x 100μl 0.1M glycine pH2.5 was passed over the column. Antibody was collected in 6x low bind tubes (Eppendorf) containing 10μl 1.5M Tris pH8.8 to immediately neutralise the acid.

2.26 ELISA (Enzyme-linked immunosorbant assay)

ELISAs were used to test the specificity of phosphospecific antibodies. 96 well microtitre plates were coated with streptavidin (1μg/well) in 50μl PBS by overnight incubation at 37°C. Wells were washed 3x with 200μl PBS-T (PBS with 0.1%(v/v) Tween-20). Biotinylated peptides (phosphorylated or non-phosphorylated) (Chiron Mimotopes) were bound to streptavidin coated wells. Peptides (in DMSO) were diluted in 50μl PBS and incubated in the wells at the concentrations indicated in the figures for 1 hour at room temperature. Wells were washed again with 3x 200μl PBS-T and non-specific interactions blocked with 200μl 3% BSA/PBS for 1 hour. The peptides were detected with 50μl phosphospecific antibody diluted 1:2000 in 3% BSA/PBS for 1 hour at room temperature. The wells were washed again as above and incubated with 50μl HRP-conjugated secondary anitbody diluted 1:1000 in 3% BSA/PBS for 1 hour at room temperature. Wells were wased once more as above and antibody binding was detected using 50μl ECL mix (for recipe see Western Blotting protocol) on a Fluoroskan Ascent FL luminometer (Labsystems).

2.27 EMSA (electrophoretic mobility shift assay)

DNA binding to various probes was measured using EMSAs.

2.27.1 Probe Sequences

C1

GGGCATCGGTCGAAGTGAAAGTGAAAGTGAAAGTGAGACTCTAGAGGATCCGCT

ISG15

GATCCTCGGGAAAGGGAAACCGAAACTGAAGCC

Caspase 8

GATCGTTTTTGGTTTCTGTTTCACCTTGTG

TLR3

CTTAACAAGTACATTTACTTAACTAGTTGGA

2.27.2 Probe Labelling

Probe was labelled with [γ^{32}P] ATP by incubating in Labelling Buffer (see below) for 2 hours at 37°C, then adding 15.5μl TE buffer and 4.5μl KCl and heating to 95°C for 2min. Labelled probe was cooled slowly to room temperature, purified by passing through a Micro-Biospin 30 column (BioRad) and stored at 4°C.

Labelling Buffer	
0.6μl	1μg/μl probe (sense)
0.6μl	1μg/μl probe (antisense)
1μl	T4 DNA kinase buffer (NEB)
1μl	T4 DNA kinase (NEB)
0.4μl	10mCi/ml [γ^{32}P] ATP
10μl	

2.27.3 Binding and Visualisation

Protein (4-6μl protein-expressing reticulocyte lysate) and DNA were mixed and allowed to bind for 30mins at room temperature in EMSA Reaction Buffer (see below) along with non-specific DNA (see binding mix). After 30mins, DNA loading dye (NEB) was added and complexes were resolved by running on a 6% acrylamide gel (see below) at 35mA for 2.5 hours run in EMSA running buffer (see below). When the gel had finished running, it was dried onto filter paper (80°C, 1 hour) and the locations of probe or probe/protein complexes were visualised using a Storm 840 phosphorimager (Amersham Biosciences) and ImageQuant software. In order to verify IRF-1 binding to the probe, 1μl or as indicated of anti-IRF-1 antibody (BD Biosciences) was added to the reaction mix to supershift IRF-1 containing complexes. Peptide competition EMSAs were also carried out. Here, a titration of IRF-1 C-terminal peptide (Chiron Mimotopes) was added to the reaction mix.

1X Reaction Buffer

20mM	HEPES pH7.5
50mM	KCl
5%(v/v)	Glycerol
4mM	DTT
0.1mg/ml	BSA
0.5%	Triton X-100

Binding Mix

2μl	6x Reaction buffer
1μl	1μg/μl p[d(I:C)]
0.5μl	1μg/μl salmon sperm DNA
$x\mu$g	IRF-1
1μl	Labelled probe
12μl	

Acrylamide Gel Mix

1X	TBE*
6%(w/v)	Acrylamide Mix
0.1%(w/v)	APS
0.1%(v/v)	Triton X-100
0.1%(v/v)	TEMED

* TBE: 89mM Tris Base; 89mM Boric Acid; 2mM EDTA pH8.

EMSA Running Buffer

1X	TBE
0.1%(v/v)	Triton X-100

2.27.4 Acetylation Reaction

4μl IRF-1-expressing reticulocyte lysate was mixed with 3μl p300-expressing reticulocyte lysate and 2μM acetyl CoA. Mix was heated to 30°C for 10mins to allow acetylation

to occur, then incubated for 20mins at room temperature to allow DNA/protein interaction to continue. EMSA then continued as above.

2.27.5 Statistical Analysis

The tests indicated in the figure text were carried out using GraphPad or R statistical software.

Chapter 3

Development of Tools to Study the C-terminal Phosphorylation of IRF-1

3.1 Introduction

Interferon Regulatory Factor-1 (IRF-1) has many anti-oncogenic activities, targeting both tumours that are lacking IRF-1, and also non-related tumours. Thus, drugs that activate IRF-1 are clearly going to be useful, however, indiscrimately activating this protein would be illadvised since upregulation of IRF-1 has been linked to various autoimmune disorders including MS [89] and autoimmune manifestations in myelodysplasia [87]. Therefore, investigation into the selective activation of IRF-1 is important to allow development of anti-cancer drugs without auto-immune side-effects.

As a key post-translational modification, phosphorylation is likely to play a role in the regulation of IRF-1. Indeed there is some evidence that this is the case, but detailed investigations have never been pursued. In this chapter, various techniques were used to study the phosphorylation of IRF-1. Two lines of inquiry were pursued: a neutral approach and a targeted approach. The first involved setting up assays to identify IRF-1 kinases in cell lysate with the aim of determining the physiological phosphorylation sites of IRF-1 using mass spectrometry and classifying the kinases. The targeted approach

investigated candidate IRF-1 kinases, identified from binding partner screens or previous work in the laboratory, in an attempt to map phosphorylation sites and the function of such phosphorylations. In parallel, phosphospecific antibodies were raised and validated to study signal-specific, site-specific phosphorylation of IRF-1.

3.1.1 Purification of recombinant IRF-1

In order to study phosphorylation of IRF-1 *in vitro*, purified GST-IRF-1 and His-tagged domains of IRF-1 were used as substrates. In later experiments in this thesis, His-IRF-1 expressed from a pCold vector is used as this system yields undegraded IRF-1 at high levels of purity. The protocols for GST-IRF-1 and His-domain purifications can be found in the materials and methods, but, as an example, the purification of His-IRF-1 from the pCold vector (optimised by Dr. Vikram Narayan) is described here in more detail.

In this system, protein expression is under the control of a cold shock protein promoter containing a lac operator. Thus, the protein is efficiently expressed at low temperatures after induction by IPTG. The use of low temperature protein expression is thought to enhance protein yield by improving solubility. It has been suggested that a reduced translation rate at lower temperatures allows more time for correct folding and also that cold shock inhibits expression of most *E. Coli* proteins thus making more chaperones available for folding the recombinant protein. In addition, low temperatures reduce degradation of proteins by heat shock proteases [148].

As illustrated in Fig 3.1 ,the pCold-His-IRF-1 plasmid is transformed into BL21-DE3 *E. Coli* cells, and these are grown at 37°C with shaking until they are in the logarithmic phase of growth. This protocol involves a very short protein induction period so the bacteria are grown until they are at a higher density than usual. Therefore there are more bacteria present to produce protein, and in the short incubation, the bacteria do not have time to reach the end of the logarithmic phase.

Once the OD_{600} has reached 0.6, the bacteria are cooled to 15°C for 30 mins. This allows acclimitisation and ensures temperature equilibration throughout the cell suspen-

sion. After 30 mins, IPTG is added to induce protein expression. IRF-1 protein is targeted by a protease 15 mins after its induction (V. Narayan, unpublished observations). Therefore, an induction time of 15 mins is used, and all subsequent steps are performed on ice with chilled buffers/equipment to minimise protease activity.

After induction, bacteria are lysed and His-IRF-1 is purified on a nickel affinity column. Multiple wash steps with high and low salt concentrations, with and without detergents and with magnesium ions and ATP to remove chaperones result in a very clean product, as can be seen from the coomassie stained SDS-PAGE gel in Fig 3.1.

3.2 IRF-1 as a Kinase Substrate

3.2.1 Cellular Kinases

There is some evidence in the literature that phosporylation is important for IRF-1 activity and, as described in the introduction, previous work in the Ball laboratory has corroborated this.

At the start of this project, cell lysate was used to show that cellular kinases could phosphorylate IRF-1 directly. Kinase assays using $\gamma[^{32}P]$-ATP were set up where incorporation of the labelled phosphate into IRF-1 by phosphorylation is detected using a phosphorimager. GST-IRF-1 was used as a substrate, and phosphorylation of IRF-1 can be seen after incubation with HeLa cell lysate (Fig 3.2A). His-tagged subdomains of IRF-1 had previously been created in the laboratory and these were expected to be a useful tool in narrowing down the phosphorylation sites of specific kinases purified from cell lysate. In order to check that the domains would be substrates for phosphorylation, these were also included in the kinase assay. Interestingly, in cell lysate, the DNA binding domain (amino acids 1-124) in lane 2 is not efficiently phosphorylated whereas the central domain (118-256) in lane 3 (which contains a highly disordered, potentially regulatory, domain) is an excellent substrate (Fig 3.2A).

As a first step towards purification of kinases from cell lysate, an ammonium sulphate

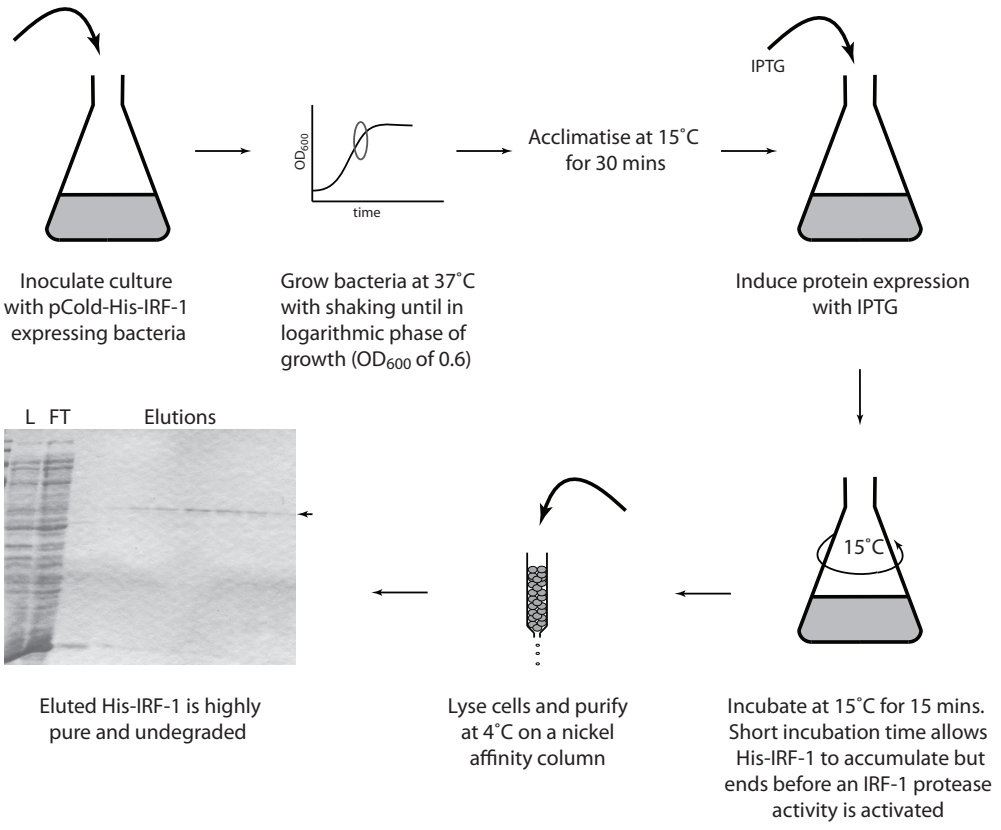

Figure 3.1: Purification scheme for His-IRF-1. Scheme is discussed in detail in the text.

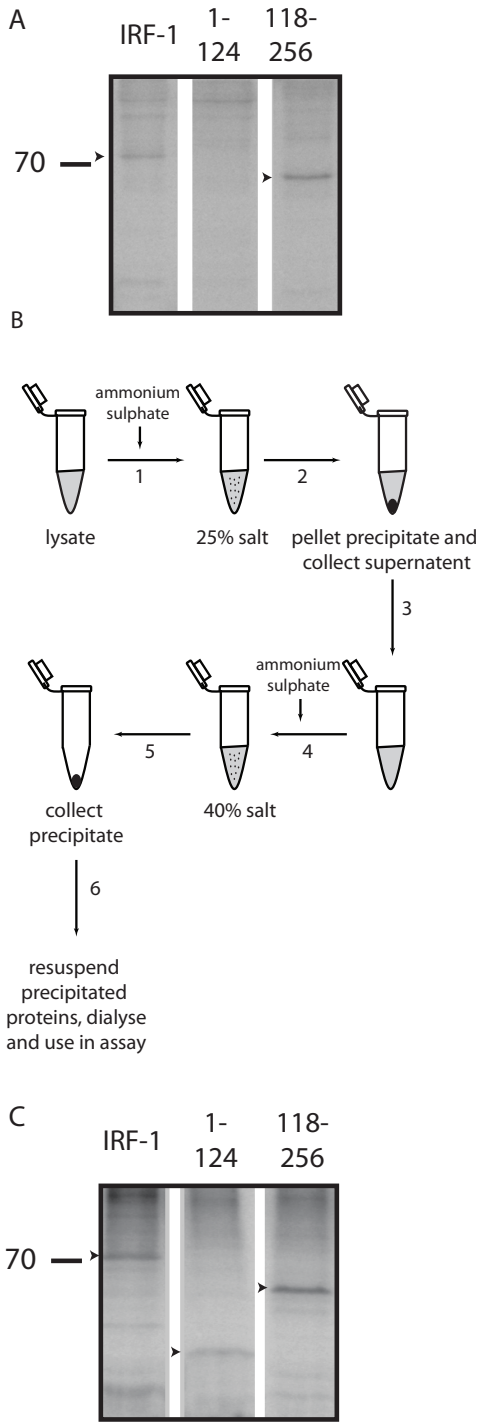

Figure 3.2: IRF-1 is phosphorylated by cellular kinases *in vitro*. Full length GST-IRF-1 and His-IRF-1 domains 1-124 and 118-256 were purified from E.Coli, then 450μg of each was incubated with 4μg of HeLa lysate and $\gamma[^{32}$P]ATP for 30 mins at 30°C. Phosphorylated GST-IRF-1 and His-118-256 are indicated by arrowheads. His-1-124 was not phosphorylated. (B) To concentrate kinases, an ammonium sulphate fractionation was carried out. Ammonium sulphate was added to lysate to a concentration of 25%, precipitated protein was pelleted and discarded. Additional ammonium sulphate was added to the supernatent up to a concentration of 40%. Precipitated proteins from the 40% cut were collected, resuspended and dialysed to remove salt. (C) The 40% ammonium sulphate cut was used to phosphorylate GST-IRF-1 and His-IRF-1 domains. After concentration of kinases by this method, phosphorylation of His-1-124 IRF-1 was visible in addition to phosphorylation of full length GST-IRF-1 and His-118-236. Data representative of two independent experiments.

precipitation was carried out. This removes denatured proteins and other contaminants, concentrating the native proteins. Preliminary experiments indicated that all IRF-1 kinases were concentrated in the 40% cut. A schematic of the ammonium sulphate precipitation is shown in Fig 3.2B. Briefly, ammonium sulphate is added to the lysate up to a final concentration of 25% (Step 1), after stirring to equilibrate the solution, precipitated denatured proteins/contaminants are collected by centrifugation (Step 2) and discarded (Step 3). The supernatent should contain properly folded, active proteins. These are concentrated by precipitation after addition of ammonium sulphate up to a concentration of 40% (Step 4) and collected by centrifugation (Step 5). These proteins are resuspended in buffer and, after dialysis to reduce salt concentration, are used in the kinase assay (Step 6). The concentration at which the "salting out" occurs depends on the physical characteristics of the proteins, and so no selection for particular attributes other than native conformation is taking place.

After ammonium sulphate precipitation, Fig 3.2C shows that phosphorylation of the DNA binding domain (amino acids 1-124, lane 2) occurs as well as phosphorylation of full length IRF-1 protein (lane 1) and the central domain (118-256, lane 3). Therefore, IRF-1 kinases have been enriched by the ammonium sulphate precipitation.

3.2.2 Purified Kinases

In parallel with setting up the assay to search for cellular kinases, the ability of purified kinases to phosphorylate IRF-1 was investigated. Chk1, previously identified in the laboratory as an IRF-1 kinase was used as a positive control to ensure the assay was working (Fig 3.3A). Chk1 autophosphorylation produces a strong signal which can be seen in the first lane in the absence of IRF-1, however, phosphorylation of IRF-1 by Chk1 can be seen just above the autophosphorylation band (lane 2). Chk1 preferentially phosphorylates sites in the central domain of IRF-1; N-terminal phosphorylation is very weak (lanes 4 & 5).

AMPK (AMP dependent protein kinase) was identified as a binding partner of IRF-1 in a phage display screen (Angeli Moeller, unpublished observations). In this technique,

IRF-1 domains were incubated with a peptide phage display library. The library consists of bacteriophage displaying randomly generated peptide sequences on their surfaces, fused to the N-terminus of a coat protein. After the incubation, unbound phage are then washed away and bound phage are eluted. These phage are amplified in *E. Coli* and again incubated with IRF-1 domains to select for high affinity interactions. The identity of the peptide is determined by sequencing of the peptide/coat protein fusion gene [149].

To determine if AMPK could phosphorylate IRF-1, a kinase assay was performed (Fig 3.3B). AMPK phosphorylates full length IRF-1 (lane 2), the phosphoryation site(s) appears to be in the N-terminal binding domain as there is no incorporation of ^{32}P into the central domain (lanes 5 & 6). Since the AMPK was only partially purified (manufacturers claim 15% purity), various controls were performed to ensure AMPK was responsible for the phosphorylation. First, AMP was omitted from the assay buffer (Fig 3.3B lane 4). In the absence of AMP, without which AMPK cannot function, no phosphorylation is seen. Furthermore, the AMPK inhibitor compound C titratably inhibits the phosphorylation of IRF-1 (Fig 3.3C). Next, 20 amino acid long peptides spanning the IRF-1 DNA binding domain were used to finely map the AMPK phosphorylation sites in IRF-1. *In vitro*, residues between 21-50, 91-110 and 106-124 are phosphorylated (Fig 3.3D). Thus, AMPK appears to be a kinase for IRF-1 *in vitro*.

As a first step towards determining if AMPK was an IRF-1 kinase in cells, A375 cell lysate was fractionated on an anion exchange column, and the fractions assayed for kinase activity against purified IRF-1. The same fractions were probed with an anti-AMPK antibody. As shown in (Fig 3.3E), AMPK co-elutes with cellular IRF-1 kinase activity (fraction 7) implying that it may have a role in IRF-1 regulation in cells.

In summary, in this section, assays were set up to search for kinases that could phosphorylate IRF-1. Using these assays, it was possible to show that cellular kinases can phosphorylate IRF-1 within its N-terminal and central domains, and that AMPK, a binding partner of IRF-1, could be one of these kinases.

At this stage, a decision had to be made about whether to focus on the search for IRF-1 kinases as described above, or on the study of site-specific phosphorylation of IRF-1

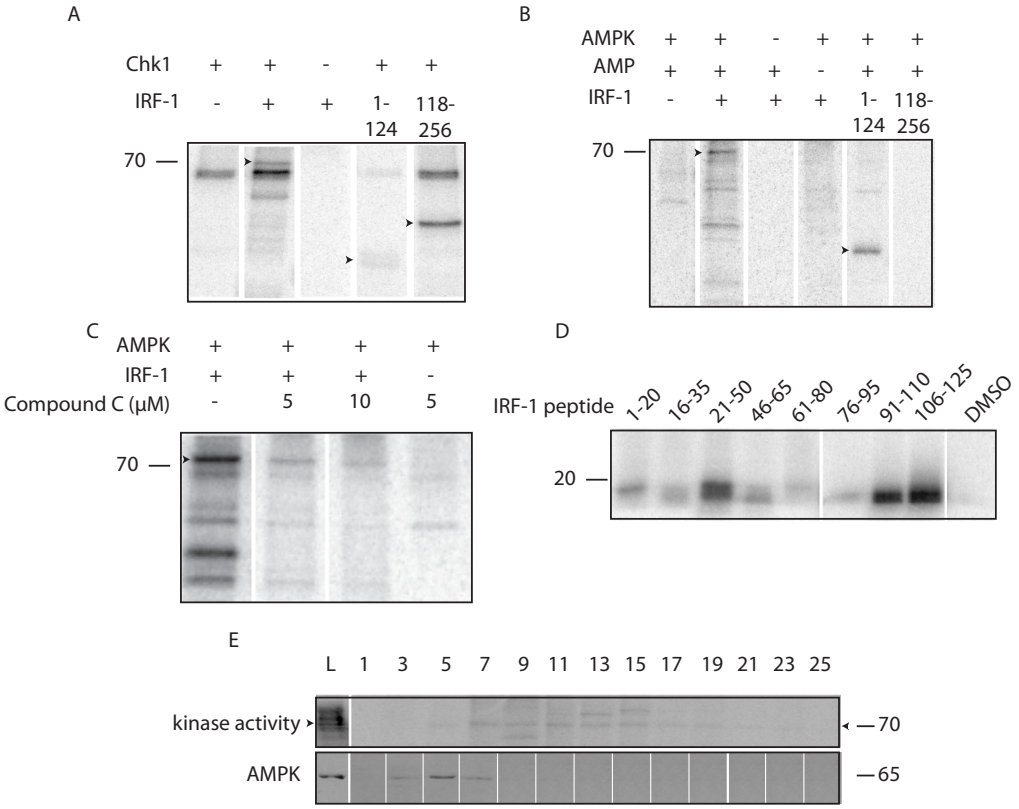

Figure 3.3: IRF-1 is a substrate for purified kinases Chk1 and AMPK. (A) Chk1 phosphorylates IRF-1. 500ng GST-IRF-1, His-IRF-1(1-124) or His-IRF-1(118-256) were incubated with Chk1 and $\gamma[^{32}P]$ATP for 30mins at 30°C. Phosphorylated substrate is indicated by arrowheads. (B) AMPK phosphorylates IRF-1. 1μg GST-IRF-1, His-IRF-1(1-124) or His-IRF-1(118-256) were incubated with 40U AMPK (Upstate) and $\gamma[^{32}P]$ATP for 30mins at 30°C. 300μM AMP (AMPK cofactor) was included in the reaction mix where indicated. Phosphorylated substrate is indicated by arrowheads. (C) Phosphorylation of IRF-1 by AMPK is inhibited by Compound C. As for (B) except that AMPK inhibitor Compound C was included at concentrations indicated. (D) Peptides spanning the IRF-1 DNA binding domain are selectively phosphorylated by AMPK. As for (B) except that 1μg peptide was used as substrate. (E) After anion exchange chromatography, AMPK co-elutes with IRF-1 kinase activity. A375 cell lysate was fractionated on an anion exchange column (HiTrap Q Sepharose HP, GE Healthcare). Alternate fractions were assayed for kinase activity against GST-IRF-1 (as in (A)) and also concentrated by acetone precipitation and probed with anti-AMPK (Millipore). Data representative of (A) one (B) one (C) two (D) two (E) one independent experiments.

described below, which was being pursued concomitantly. Both avenues would have entailed an interesting project, but it was decided that the investigation of site-specific phosphorylation was progressing more rapidly, and so this line of research was continued.

3.3 Phosphospecific Antibodies

3.3.1 Antibody design

IRF-1 is a multidomain protein with complex regulation (Fig 3.4). The Ball laboratory is particularly interested in the C-terminus of IRF-1 and, more specifically, a region within this - the Mf1 domain - which is involved in regulation of steady state levels and transcriptional activity. As described in the introduction, the Mf1 domain is vital to the regulation of IRF-1 activity and the aim of this work is to discover cellular mechanisms involving phosphorylation in the Mf1 domain that contribute to this regulation. To this end, phosphomimetic antibodies were raised to sites in the Mf1 domain. The sites chosen are highlighted in red in Fig 3.4. The LXXLL (cofactor binding) motif at residues 306-310 has been shown to be essential for IRF-1's growth inhibitory activity [70] and is involved in p300 binding [67]. Thus, the residues Ser308 and Thr311 are likely candidates for sites of phosphorylation that could control binding of factors to this motif. In addition, Thr311 is part of a TP motif, a substrate motif phosphorylated by many kinases including those of the MAPK family. Ser317 was also chosen as it had already been shown in the laboratory that Chk1 phosphorylated this site *in vitro*.

3.3.2 Antibody production and purification

Phosphospecific antibodies were raised to phosphorylated peptide antigens by Eurogentec using a 3 month immunisation protocol in rabbit. At the end of the protocol, serum was received for purification (Fig 3.5A). A two-step purification scheme was optimised for these antibodies. This is summarised in Fig 3.5B. First, IRF-1 specific but non-phosphospecific antibodies were removed from the antisera by capture on immobilised IRF-1 peptide. The

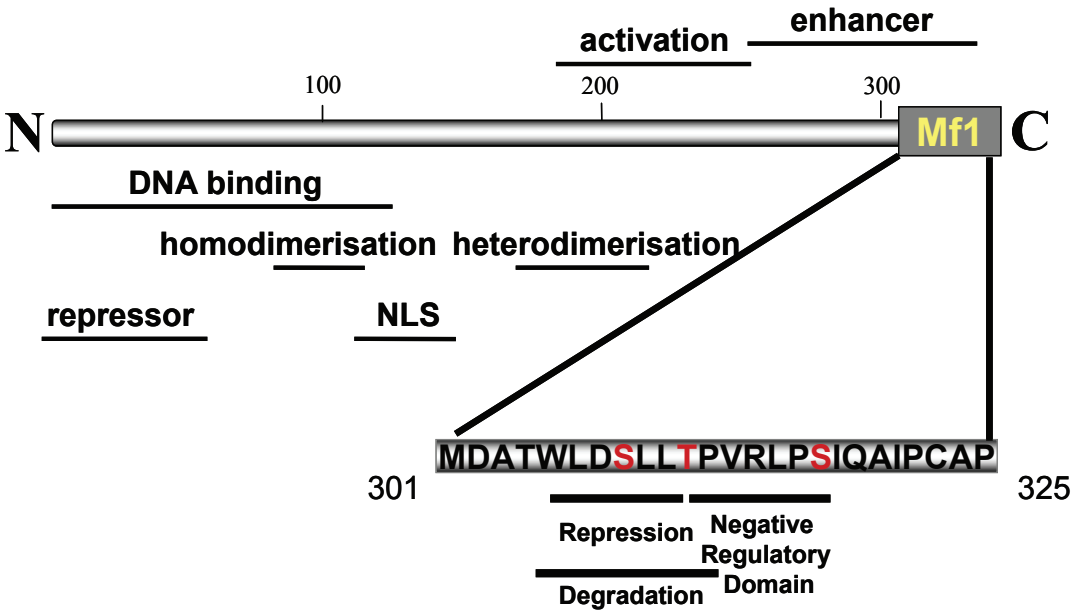

Figure 3.4: Modular structure of IRF-1. The IRF-1 protein is organised into many domains including a C-terminal multifunctional, multiprotein binding interface (Mf1) which has been shown to regulate both transcriptional activity and steady state levels. Antibodies have been raised to the speculative phosphorylation sites highlighted in red.

flowthrough from this step was then passed over untagged phosphorylated peptide, bound phosphoantibodies were washed and the purified antibody was eluted using low pH. The second step was repeated twice to ensure selection of the correct phosphospecific antibodies.

The success of the purification was tested in a number of ways. First the serum (load - L) which had been loaded on the phosphorylated peptide purification column, and flowthrough (FT), were compared to the elutions (E1-6) on a coomassie stained SDS-PAGE gel. BSA standards were also included to allow estimation of elution concentration. As seen in Fig 3.6A, most of the antibodies in the crude serum do not bind the phosphorylated peptide. Most other contaminants also do not bind the column, and a relatively pure product is collected. The major contaminant runs at the same size as BSA and is likely to be rabbit serum albumin which should not interfere with antibody function. Antibody concentration of E1-3 is an average of 0.4mg/ml.

The progression of the purification can be followed by comparing the specificity of the crude serum to serum after the first step of purification and the fully purified antibody. Fig 3.6B reveals that the first step of purification (removal of IRF-1 specific, non-phosphospecific antibodies) has little effect on the specificity of the serum for the cognate phosphopeptide, while purification of antibody against phosphopeptide greatly enhances specificity. The experiments in Fig 3.6 are useful as a proof of concept but were carried out using phosphoantibodies from a trial immunisation. These were able to recognise the native form of the protein in ELISAs but proved to be unable to detect denatured protein by immunoblot blot. Therefore, new antibodies were produced by the method described in Fig 3.5 and the validation of these will be described next.

3.3.3 Validation of Antibodies

After purification, the antibodies were validated. Phosphospecificity was verified by ELISA: biotinylated phosphorylated (either p308S, p311T or p317S) and non-phosphorylated peptide was immobilised on the plate, and the phosphospecific antibodies were added in the mobile phase. These experiments were only carried out two times as the activity of the

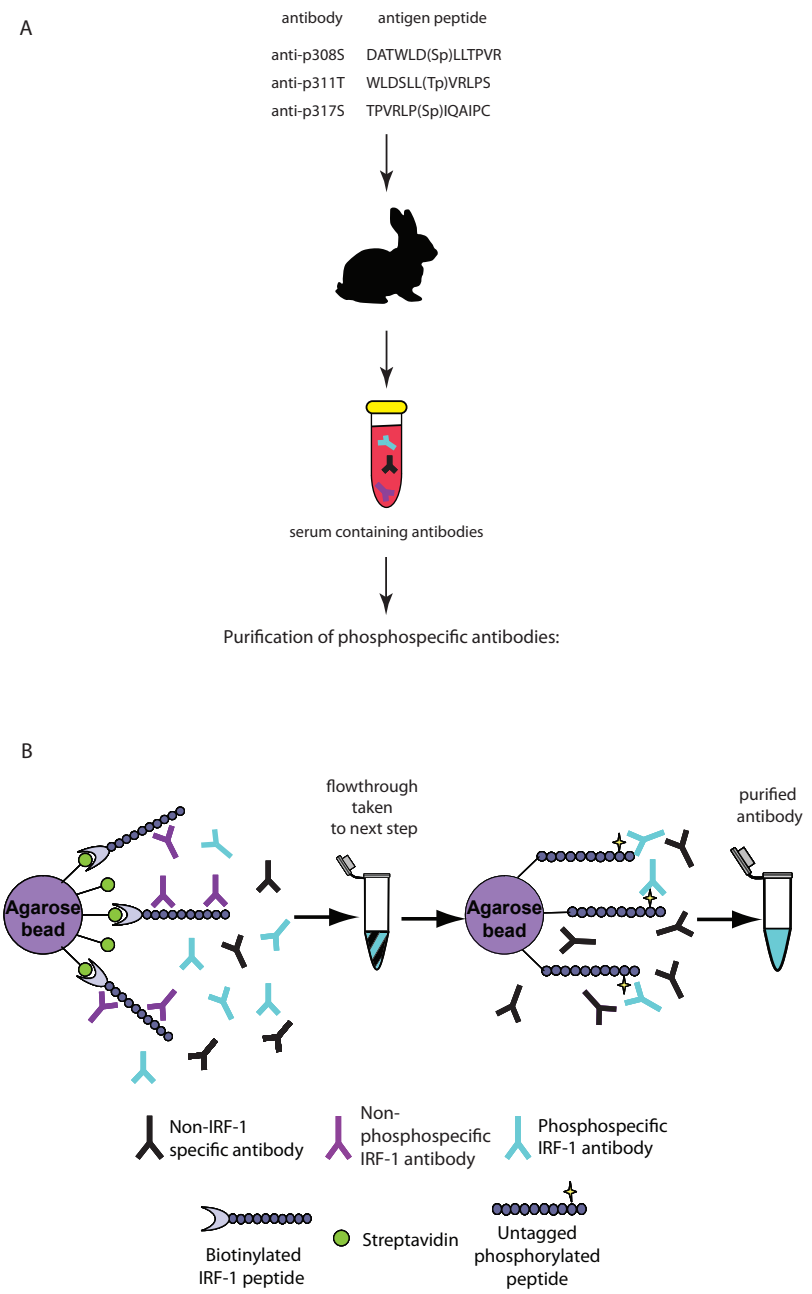

Figure 3.5: Phosphospecific antibody preparation. (A) Production of phosphospecific antibodies. Purified, unlabelled, phosphorylated IRF-1 C-terminal peptides (top panel) were used to induce an antibody response in rabbit. After 3 months and four immunisations, serum containing antibodies was collected. Upon receipt of serum, it was purified as in (B). (B) Crude anti-serum was passed over biotinylated IRF-1 WT peptide immobilised on streptavidin-agarose beads. Non-phosphospecific, IRF-1 specific antibodies were sequestered on the beads, and the flowthrough (containing non-IRF-1 specific and phosphospecific IRF-1 antibodies) was collected. Phosphatase inhibitors (50mM NaF and 50mM β-glycerophosphate) were added to the flowthrough and it was passed over phosphorylated (p308S, p311T or p317S) peptide immobilised on CDI-agarose beads. Bound phosphospecific antibody was washed thoroughly and then eluted using low pH which was immediately neutralised.

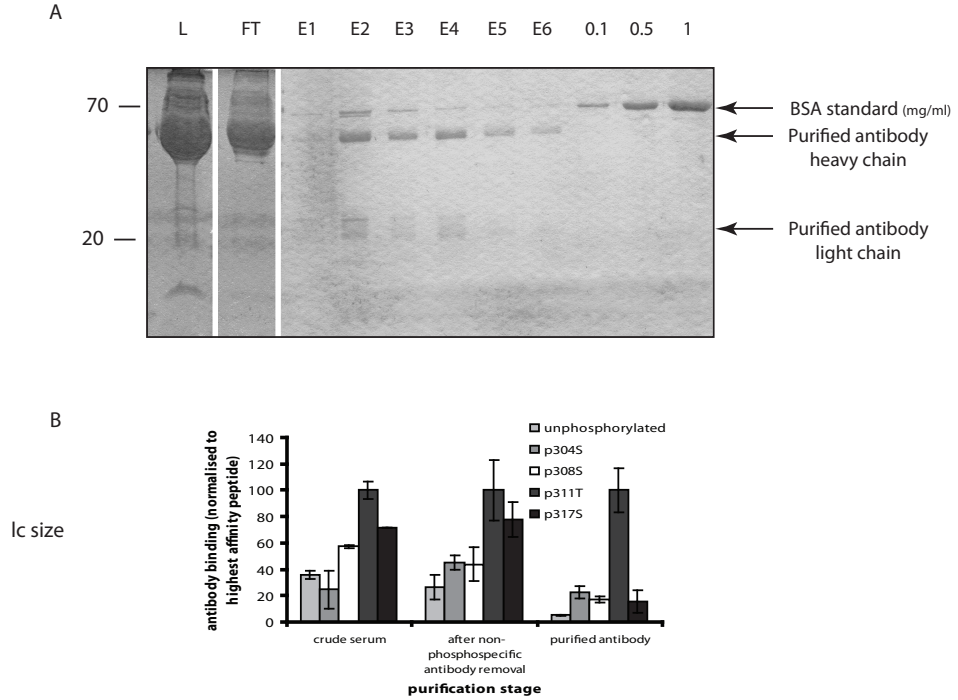

Figure 3.6: Antibody purification technique produces highly pure antibody and greatly enhances substrate specificity. (A) Commassie stained SDS-PAGE gel showing efficiency of purification of antibody from antibody serum. Crude antibody serum (L) and flowthrough from phosphorylated peptide purification column (FT) were compared to column elutions (E1-6). Most antibody proteins, and other serum proteins are removed by the purification. A contaminant suspected to be rabbit serum albumin remains. BSA standards are included to allow estimation of purified antibody concentration (B) ELISA was used to observe the progression of antibody purification. Unphosphorylated peptide, and peptides phosphorylated at the indicated site were coated in ELISA plate wells and detected by anti-p311T antibody followed by HRP-conjugated swine anti-rabbit secondary (Dako) and ECL. Detection was normalised to the recognition of the cognate phosphopeptide (p311T). Purification clearly enhances specificity for cognate phosphopeptide. These figures are included as an illustration of the efficiency of the purification process but the antibodies used were found to not be active on western blot and so subsequent figures (except fig 3.8 use a new batch of antibodies. Data representative of a single experiment. Error bars are standard deviation of three repeats.

anitbodies became undetectable before a third experiment oculd be carried out. See below for a discussion on the possible reasons for this. As seen in Fig 3.7A, anti-p308S cannot differentiate between p308S and non-phosphorylated peptide, indicating that phosphospecific antibodies were not present in the antisera. However, both anti-p311T and anti-p317S recognise only the phosphorylated peptide.

Next, the binding of the antibodies to each phosphopeptide was compared. Again, anti-p308S binds non-specifically to each peptide while anti-p311T and anti-p317S both recognise only their cognate phosphopeptide (Fig 3.7B). This confirms that anti-p311T and anti-p317S are each specific for their site of interest and do not simply recognise any phosphorylation in the context of the C-terminus.

Using an ELISA format, the ability of phosphospecific antibodies to detect *in vitro* phosphorylation of IRF-1 was measured. This experiment, like Fig 3.6 used the first batch of antibodies which were found to not be active on western blot and was only carried out once. Chk1 has previously been shown in the laboratory to phosphorylate the Ser317 site of IRF-1, so IRF-1 phosphorylated by Chk1, and unphosphorylated IRF-1 were coated on an ELISA plate. Protein was detected with anti-p311T, anti-p317S and, as a control, a commercial IRF-1 antibody raised to the C-terminus (Santa Cruz, C20) (Fig 3.8). Detection of phosphorylated IRF-1 compared to unphosphorylated by the commercial antibody is inhibited. This suggests that efficient phosphorylation has taken place, and partially blocks the epitope for this antibody. Detection of phosphorylated protein by anti-p317S exceeded that of the unphosphorylated protein, although there was some background recognition of unphosphorylated protein (according to the peptide ELISAs in Fig 3.7, the new batch of anti-p317S does not recognise unphosphorylated peptide). Anti-p311T antibody has very low recognition of both unphosphorylated and Chk1 phosphorylated protein, as would be expected as neither contain its epitope. However, it does recognise Chk1 phosphorylated protein to a greater extent than unphosphorylated, and in a titratable manner. This could be due to slight non-specificity of the antibody, or to a non-specificity of Chk1 under *in vitro* conditions resulting in some phosphorylation at the Thr311 site. It will be interesting to see if the recognition of its phosphorylated epitope in the context of the protein is significantly greater than the binding seen here to p317S,

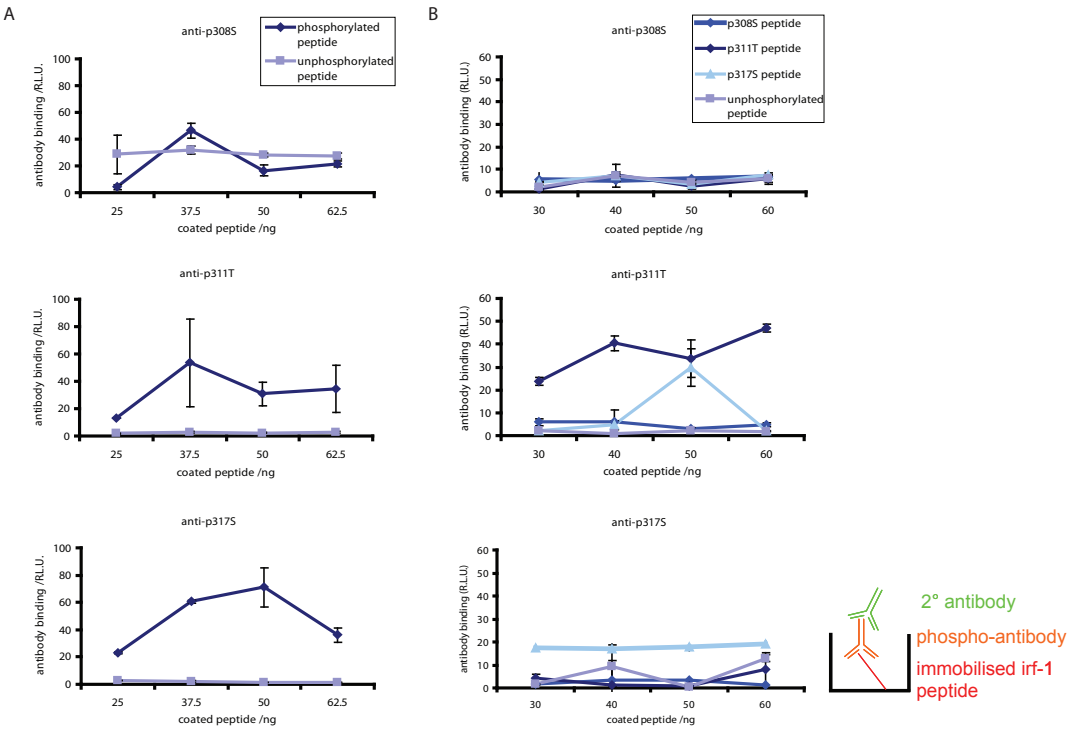

Figure 3.7: Anti-p311T and anti-p317S are specific for their cognate phosphopeptide. (A) To test specificity of antibodies for phosphorylated IRF-1 over non-phosphorylated, a titration of phosphorylated or unphosphorylated biotinylated peptide was bound to streptavidin coated ELISA plate wells. Binding of the phosphospecific antibody to the peptides was detected using HRP-conjugated anti-rabbit secondary antibody (Dako) and ECL. (B) To test specificity of antibodies for their cognate phosphorylation over other C-terminal phosphorylations, a titration of all three phosphopeptides were bound to streptavidin coated ELISA plate wells. Binding of phosphospecific antibody was detected as above. Data is representative of two independent experiments. Error bars are standard deviation of duplicates.

but at present, no Thr311 kinases have been validated.

3.3.4 Discovery of Stimulus-Specific Phosphorylation of IRF-1 Using Antibodies

With confidence in the specificity of the anti-p311T and anti-p317S antibodies, they were next used to identify signal specific phosphorylation of IRF-1 by immunoblot (Fig 3.9). Signals that are known to activate IRF-1 (Interferon-gamma (IFN-γ), pIpC and etoposide) were used to treat A375 cells, and the lysates were resolved by SDS-PAGE. After western blotting with the antibodies, a striking increase in phosphorylation can been seen at both the 311T and 317S sites after IFN-γ treatment. IFN-γ treatment also causes an increase in the protein levels of IRF-1 but it is clear that the bands are due to IFN-γ-induced phosphorylation, and not a non-specific signal resulting from the increased IRF-1 levels, as treatment with pIpC induces IRF-1 to a similar extent but no phospho-specific signal is detected by either the anti-p311T or -p317S antibodies. Etoposide (a DNA damage mimetic) treatment results in much lower levels of IRF-1 induction, but it does cause significant phosphorylation at the 317S site.

To confirm that IFN-γ induces phosphorylation of IRF-1, IFN-γ and control treated lysates were separated on a 2D gel and probed with pan-IRF-1 antibody. A 2D gel separates proteins based on charge in addition to the usual separation by weight observed in a 1D SDS-PAGE gel. The sequence of events is illustrated in Fig 3.10A. A sample, for example, cell lysate is first loaded onto an immobilised pH gradient (IPG) strip. After loading, proteins are arranged randomly on the strip (Fig 3.10A, Step 1). Next, an electric field is applied. Proteins have a net postive or negative charge depending on the balance of positively and negatively charged amino acids in their primary structure. At different pH, however, this charge will vary. At acidic pH, proteins carry a more positive charge whereas at basic pH, they carry a more negative charge. Therefore, at a certain pH, each protein will have no net charge - this is known as the pI of the protein. As the current passes through the IPG strip, it moves the protein towards the point on the pH gradient matching the pI. If the protein is, for example, holding a net positive charge, it is in a

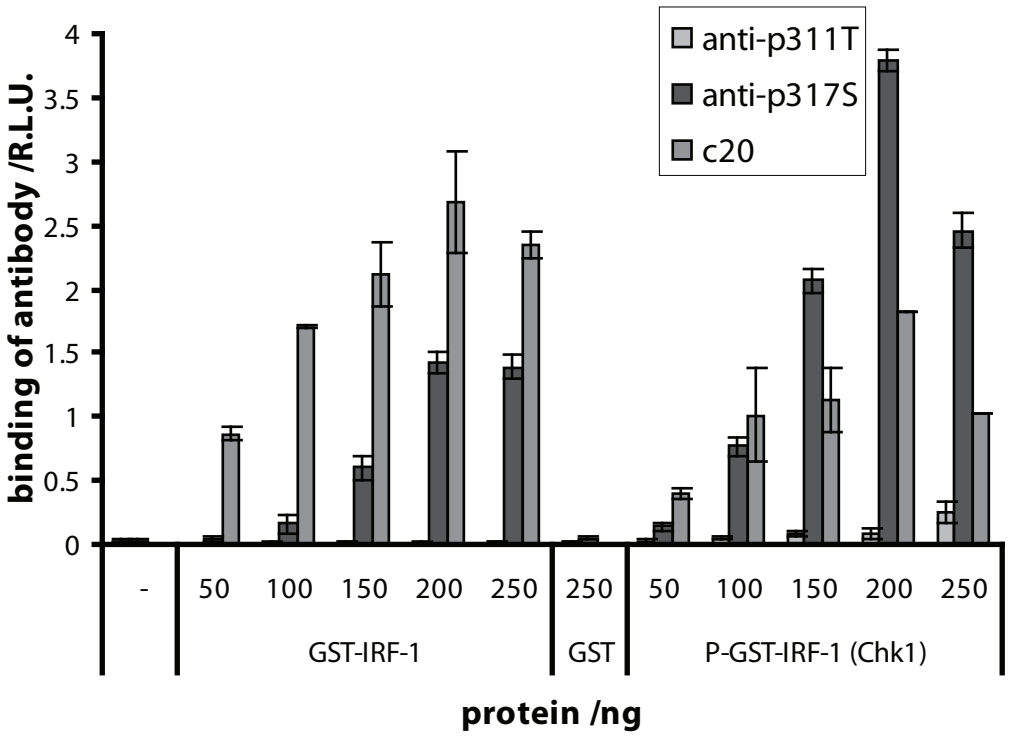

Figure 3.8: Recognition of Chk1 phosphorylated protein by phosphospecific antibodies. A titration (50-250ng) of GST-IRF-1 or P-GST-IRF-1 phosphorylated by Chk1 in a kinase assay and 250ng GST were coated onto ELISA plate wells. Protein was detected by commercial IRF-1 antibody (Santa Cruz, C20) (1:1000), anti-p311T and anti-p317S antibodies (1:50) followed by HRP-conjugated swine anti-rabbit antibody (Dako) and ECL. This data is from a single experiment. Error bars are standard deviation of three repeats.

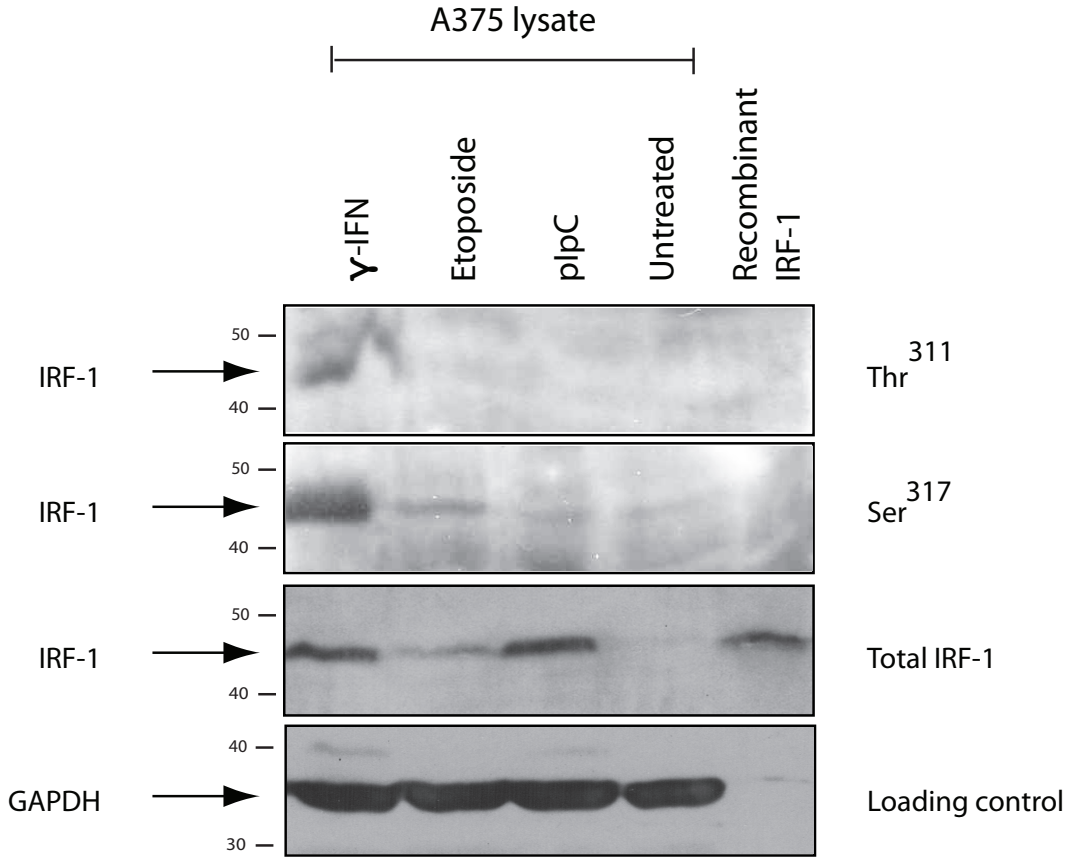

Figure 3.9: Signal specific phosphorylation of IRF-1. A375 cells were treated with the stimuli indicated, and the lysates subjected to SDS-PAGE. Purified recombinant IRF-1 expressed in the E. Coli-based cell free PURExpress system was also included on the gel as a non-phosphorylated control. No GAPDH exists in this system, so no loading control is possible, but total IRF-1 levels were normalised to IFN-γ/pIpC- treated levels. After western blotting, membranes were incubated with either anti-p311T IRF-1, anti-p317S IRF-1 or anti-IRF-1 (BD Biosciences). Membranes were also probed with anti-GAPDH (Abcam) as a loading control. Data representative of three independent experiments.

region more acidic than its pI, and the current carries it towards the cathode. The pH of the IPG strip becomes more basic towards the cathode, so eventually the protein reaches its pI and stops moving as it no longer holds a charge (Fig 3.10A, Step 2). Thus proteins are separated on the basis of their intrinsic charge. Phosphorylation of a protein confers a negative charge; as a result, phosphoisoforms of a protein appear nearer the acidic (anode) end of the IPG strip. After isoelectric focusing, proteins are denatured and the strip is loaded directly onto an SDS-PAGE gel for further separation by molecular weight (Fig 3.10A, Step 3).

Due to the induction of IRF-1 protein by IFN-γ, the signal is not comparable, so a much longer exposure of the control lysate, using ECL+ (Amersham) for enhanced signal was used. In the presence of IFN-γ, many phosphoisoforms of IRF-1 are apparent. There is a spread of spots of similar intensity across the immunoblot (Fig 3.9B). By comparison, in the absence of IFN-γ, IRF-1 appears to exist as a single phosphoisoform. Previous 2D gel analysis has shown around four isoforms (Fig 1.4), and perhaps if more lysate was loaded, the additional isoforms would also be seen. It is still clear, however, that IFN-γ treatment of IRF-1 causes a significant increase in the number of phosphoisoforms of IRF-1.

3.4 Creation and Expression of Phosphomimetic and Non-Phosphorylatable Mutants

On the basis of the findings in the previous section, a series of mutants were created by site directed mutagenesis to study the effects of phosphorylation at the relevant sites. The mutants comprised: T311A, T311D, S317A, S317D, T311D/S317D (Fig 3.11A). The S/T $\rightarrow$ D mutation constitutes a phosphomimetic mutation since the negative charge of the Asp sidechain mimics the effect of addition of a negatively charged phosphate group to the residue. The S/T $\rightarrow$ A mutation creates a non-phosphorylatable mutant as alanine has no hydroxyl group and hence cannot be phosphorylated.

Changes in the Mf1 domain have been shown to affect the steady state levels of IRF-

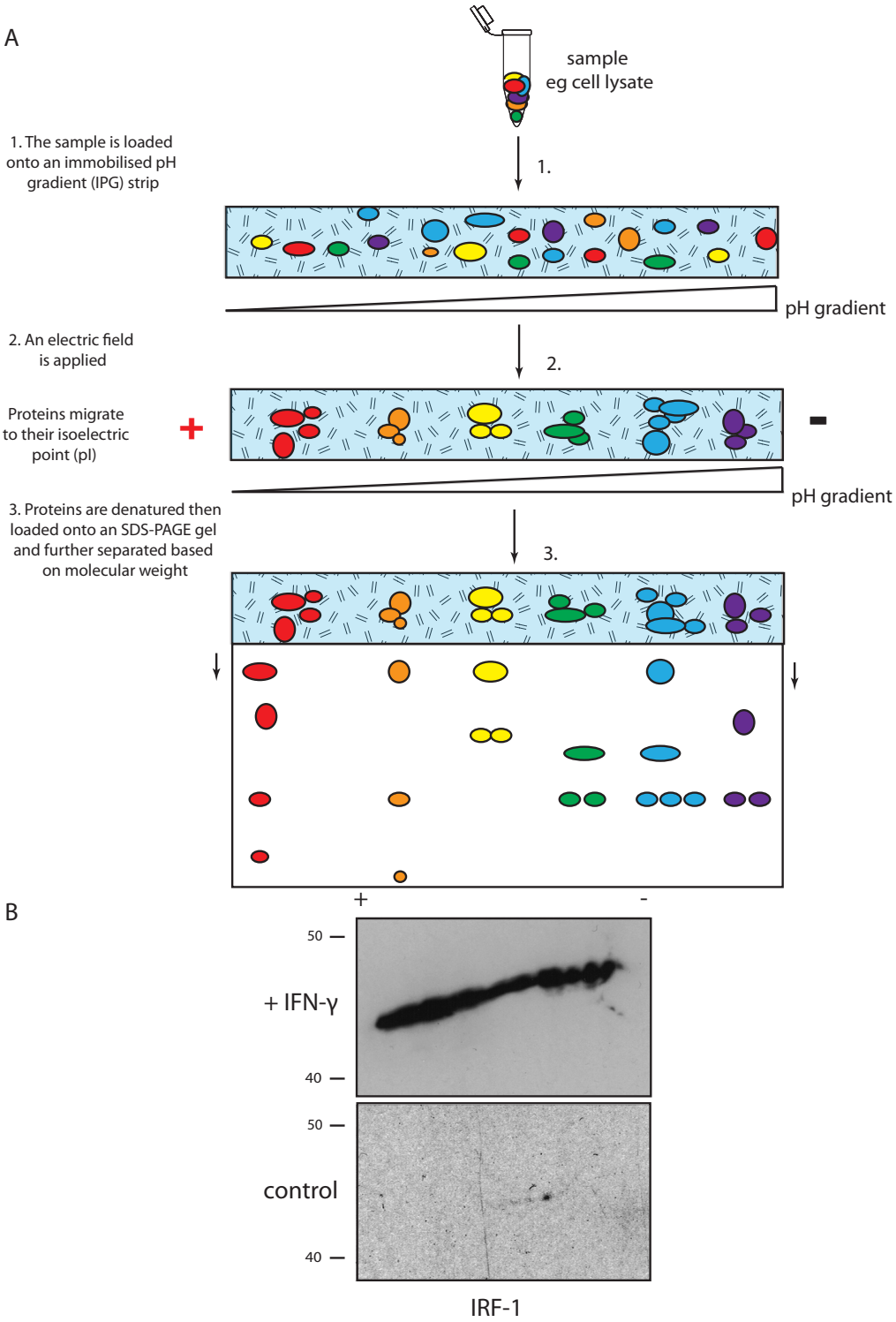

Figure 3.10: 2D gel analysis of IRF-1: Effect of IFN-γ treatment. (A) Schematic of 2D gel electrophoresis. Theory is described in detail in the text. Briefly, proteins are loaded onto an immobilised pH gradient (IPG) strip (Step 1) and separated by isoelectric point in the first dimension (Step 2). Phosphorylated proteins, having a more negative charge, have a more acidic pI and migrate further towards the acidic/cathode end of the IPG strip. After separation based on pI, the second dimension separates proteins by weight by conventional SDS-PAGE (Step 3). (B) HeLa cells were treated with IFN-γ or control (0.1% BSA, 40mM Tris pH 7.4). Whole cell lysate analysed by 2D gel electrophoresis followed by immunoblotting with anti-IRF-1 (BD Biosciences). IFN-γ blot exposed for 1 min with ECL, control blot exposed for 1h with ECL+ (Amersham). This data is representative of two independent experiments.

1. The Ball laboratory have previously shown that deletion of the Mf1 domain causes the half life of IRF-1 to more than double, although it is not itself ubiquitinated. It is suggested that the Mf1 domain contains binding sites for components of the ubiquitin pathway which facilitates polyubiquitination of IRF-1 elsewhere. [123]. Phosphorylation in the Mf1 domain could potentially occlude or create a binding site for components of the ubiquitin pathway and thus modulate IRF-1 degradation. For example, for IRF-3, phosphorylation in the C-terminus accelerates degradation [150]. The mutants were designed to study the effects of phosphorylation of IRF-1 on activity, however, differential rates of degradation would pose problems for comparing activity of mutants. Therefore, as a preliminary experiment, the mutants were expressed in the various expression systems expected to be used: mammalian cells, reticulocyte and wheatgerm lysates and bacterial cells, and the expression levels compared. As can be seen from (Fig 3.11B), expression levels are broadly similar.

3.4.1 Half Lives of Phosphomutants

To confirm that phosphorylation at the Thr311 and Ser317 sites does not impact on the stability of IRF-1, the half lives of the phosphomimetic mutants were determined. Initially the half life in whole cell lysate was assayed by cycloheximide chase (Fig 3.12A). As this showed only a small difference in half life between IRF-1 WT and mutants, subcellular fractionation was carried out to determine the half lives in different cellular compartments. An example of the half life of IRF-1 in the cytoplasm and nucleus is shown in Fig 3.12B left and right panels respectively. This experiment has been carried out a number of times, as it is technically challenging, and the half lives of the mutants have never been found to be reproducibly or significantly different (cytoplasm p=0.205, nucleus p=0.915 by one-way ANOVA). Therefore, it seems that although the C-terminus of IRF-1 regulates degradation, phosphorylation at the Thr311/Ser317 sites is not involved in modulation of this. This is advantageous from a practical point of view since expression levels in most systems are, as a result, comparable and minimal normalisation will be required before studying other aspects of IRF-1 activity.

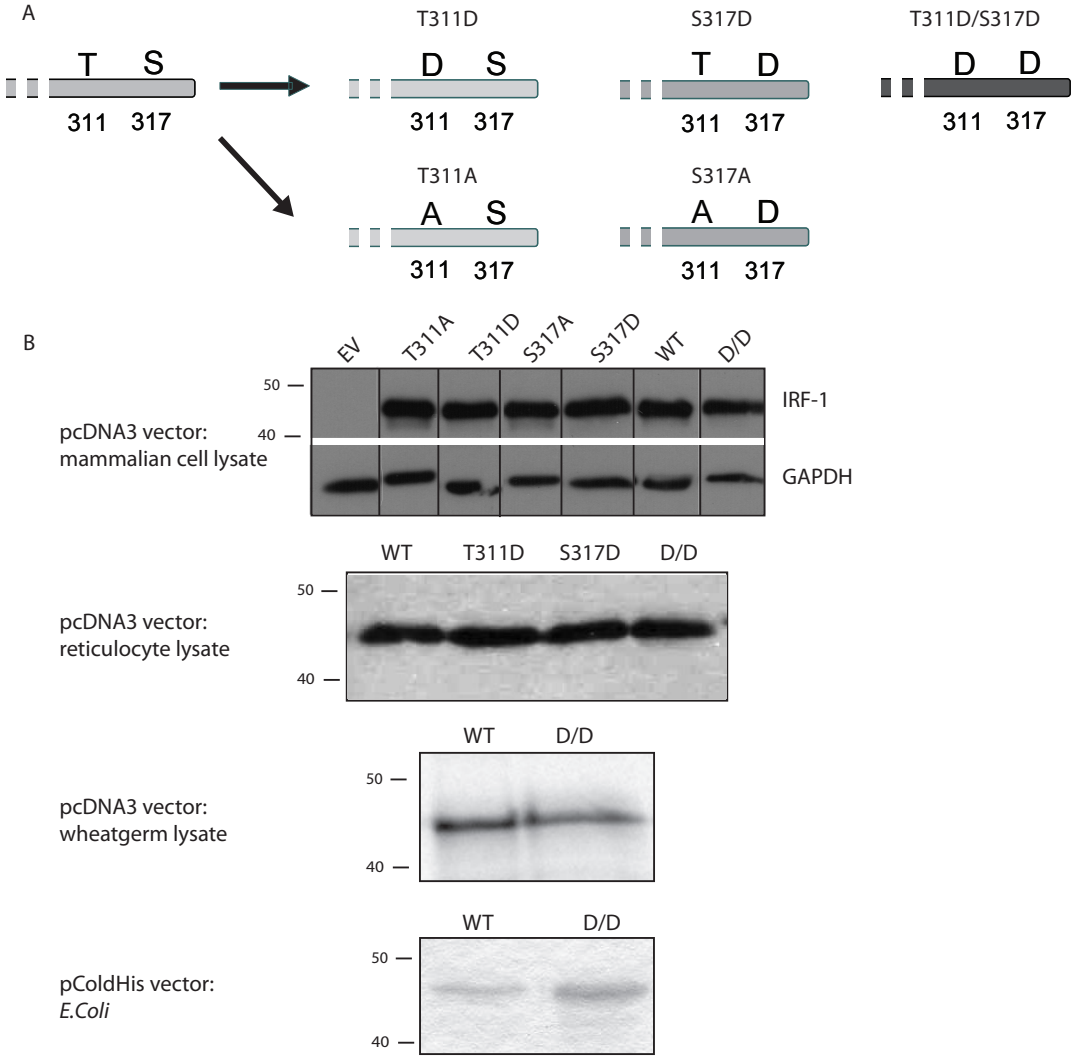

Figure 3.11: Phosphomimetic and non-phosphorylatable mutants of IRF-1. (A) Phosphomimetic (S/T $\rightarrow$ D) and non-phosphorylatable (S/T $\rightarrow$ A) mutants of IRF-1 were created by site directed mutagenesis. (B) *top panel* Expression of WT IRF-1 and all mutants from pcDNA3 vector in mammalian cells (H1299 cells) resulted in extremely similar expression levels. IRF-1 was detected using anti-IRF-1 (BD biosciences) and GAPDH was detected as a loading control by anti-GAPDH (Abcam). *middle panels* Expression of IRF-1 WT and phosphomimetic mutants in reticulocyte lysate and WT and T311D/S317D IRF-1 in wheatgerm lysate was also efficient and comparable. *lower panel* Expression of IRF-1 WT and T311D/S317D from pColdHis vector in *E. Coli* cells was efficient (as described in Fig 3.1), however, after elution of His-IRF-1 at the end of purification, levels were not so comparable. Protein concentrations were normalised before use in assays. Data representative of two (wheatgerm lysate) or more than three (mammalian cells, reticulocyte lysate and E. Coli) independent experiments.

In summary, in this section, C-terminal phosphorylation of IRF-1 in cells has been shown using phosphospecific antibodies. In response to this, reagents have been developed for mammalian and *E. Coli* expression. These have been used to demonstrate that the C-terminal phosphorylation has no effect on the half life of IRF-1. Thus, it will now be possible to investigate the effects of phosphorylation on IRF-1 transcriptional activity and tumour suppressor functions.

3.5 Discussion

Phosphospecific antibodies have been succesfully created to two sites in the C-terminus of IRF-1, namely p311T and p317S. 311T is a TP (common phosphorylation motif) site immediately adjacent to the LXXLL coactivator binding motif and 317S has previously been shown to be phosphorylated *in vitro*. Both sites are within the C-terminal Mf1 domain which is a key regulator of steady-state levels and transcriptional activity. The effect of phosphorylation on these attributes is discussed below and in the following chapter.

The phosphospecific antibodies have revealed for the first time that endogenous IRF-1 is a substrate for stimulus-specific phosphorylation at 311T and 317S. Interferon-gamma (IFN-γ) treatment results in phosphorylation at both sites, while etoposide (a DNA damage agent) induces phosphorylation at Ser317 (Fig 3.9).

Although few phosphorylation sites have been experimentally verified for IRF-1, web-based prediction programs suggest IRF-1 is a substrate for many kinases. Fig 3.13 indicates the Ser/Thr/Tyr residues predicted to be substrates for known kinases. Two prediction sites (KinasePhos2.0 and PPSP) even suggest kinases for every phosphorylatable residue within IRF-1.

IFN-γ is an efficient activator of IRF-1 expression and phosphorylation (Fig 3.9). The sequence of events leading to activation of IRF-1 by IFN-γ is shown in Fig 3.14A. Binding of IFN-γ (a homodimer) to two IFNGR1 (IFN-γ receptor 1) results in their dimerisation. This creates binding sites for IFNGR2 subunits, which bind IFNGR1, along with their associated JAK (Janus kinase). The resultant proximity of the JAKs allows auto- and

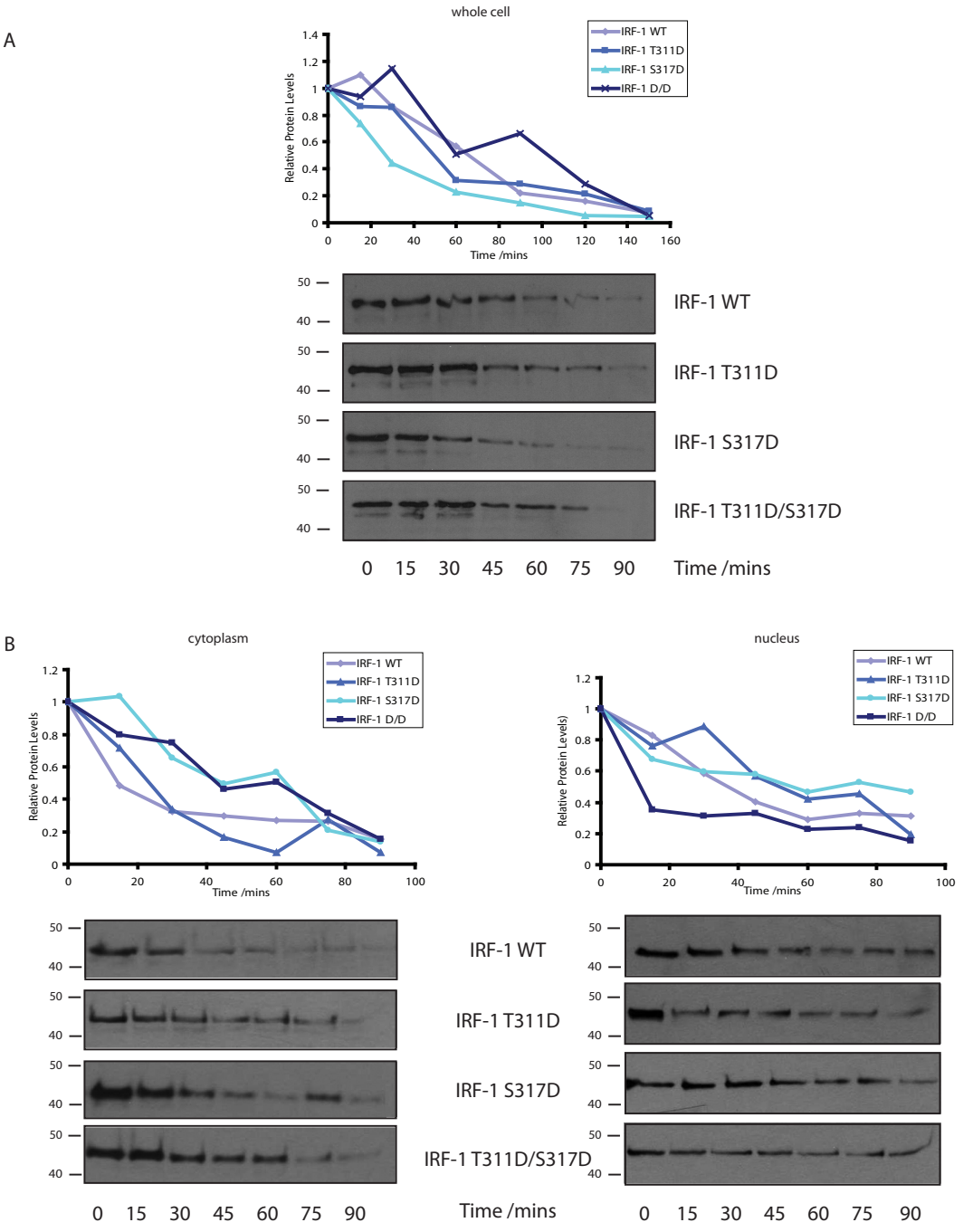

Figure 3.12: Effects of mutations on half life of IRF-1. (A) H1299 cells were transfected with pcDNA3 IRF-1 WT or mutant. After 24h, they were treated with 30μg/ml cycloheximide and harvested after the intervals indicated. Cells were lysed and lysates subjected to SDS-PAGE/immunoblot using anti-IRF-1 (BD Biosciences). Immunoblots were scanned and densitometry performed using Image J to give values for the intensity of each band which were then graphed. (B) Half life determined as for A except after harvesting, cell lysates were fractionated using Calbiochem ProteoExtract kit. Differences in half lives of mutants are not significantly different: cytoplasm p=0.205, nucleus p=0.915 by one-way ANOVA. Data representative of one experiment for whole cell half-life and three independent experiments for fractionated half-life.

Figure 3.13: Predicted phosphorylation sites of IRF-1. Phosphorylation sites were predicted for IRF-1 using the NetPhos2.0 [151], KinasePhos2.0 [152] and PPSP [153] web-based prediction programs. KinasePhos2.0 and PPSP predicted kinases for all phosphorylatable residues of IRF-1 (red) while NetPhos2.0 predicts phosphorylation of only a subset of these (orange).

trans-phosphorylation and activation of JAK1 and JAK2. (Fig 3.14A, Step 1). Activated JAK1 and JAK2 then proceed to phosphorylate the C-terminus of IFNGR1, creating a binding site for a STAT1 monomer. (Fig 3.14A, Step 2). A STAT1 monomer associates with each IFNGR1 and is phosphorylated by JAKs (Fig 3.14A, Step 3). After phosphorylation, STAT1 monomers dissociate from IFNGR2 and form a homodimer which translocates to the nucleus and activates transcription by binding to a GAS (gamma activated sequence) element in the *IRF-1* promoter (Fig 3.14A, Step 4). This is reviewed in [90].

A number of kinases are also activated after IFN-γ treatment (Fig 3.14B). The mechanism by which IFN-γ activates these kinase pathways is not known; Jak kinases could be responsible, or STAT1 activation could result in upregulation of kinase or activator expression. It would be interesting to investigate the effect of inhibition of these kinases during IFN-γ treatment in order to identify the kinases responsible for IRF-1 phosphorylation. As described in the thesis discussion, a literature search has been performed on the Thr311 and Ser317 kinases (predicted by the web-based tools) to find kinases that have been shown to be activated by IFN-γ (Table 6.1).

At this stage, the antibodies would have been used to determine if inhibition of the kinases mentioned above can inhibit IRF-1 phosphorylation at Thr311 or Ser317. Unfortunately, further experiments using the phosphospecific antibodies were not possible as specific binding was rapidly lost. Repurification from stored aliquotted crude anti-sera does not resolve the problem so it must be concluded that the phospho-specific antibodies were only a small subpopulation of the total antibodies in the serum, and that they lost their activity during storage. In keeping with this assumption, a large amount of lysate (80ug) was required to observe phosphorylation.

The antibodies were not isotyped, but it is likely that they were the fairly unstable IgM. Some antigens can only elicit an IgM response, particularly if they are highly conserved, due to lack of T-cell stimulation and so no isotype switching of B cells. Although this is a peptide antibody, the Mf1 domain is highly conserved between humans and rabbits, and as a regulatory region, it is likely to be exposed. Thus it is possible that the antigenic phosphopeptides are viewed as autoantigens and so only IgM antibodies are produced

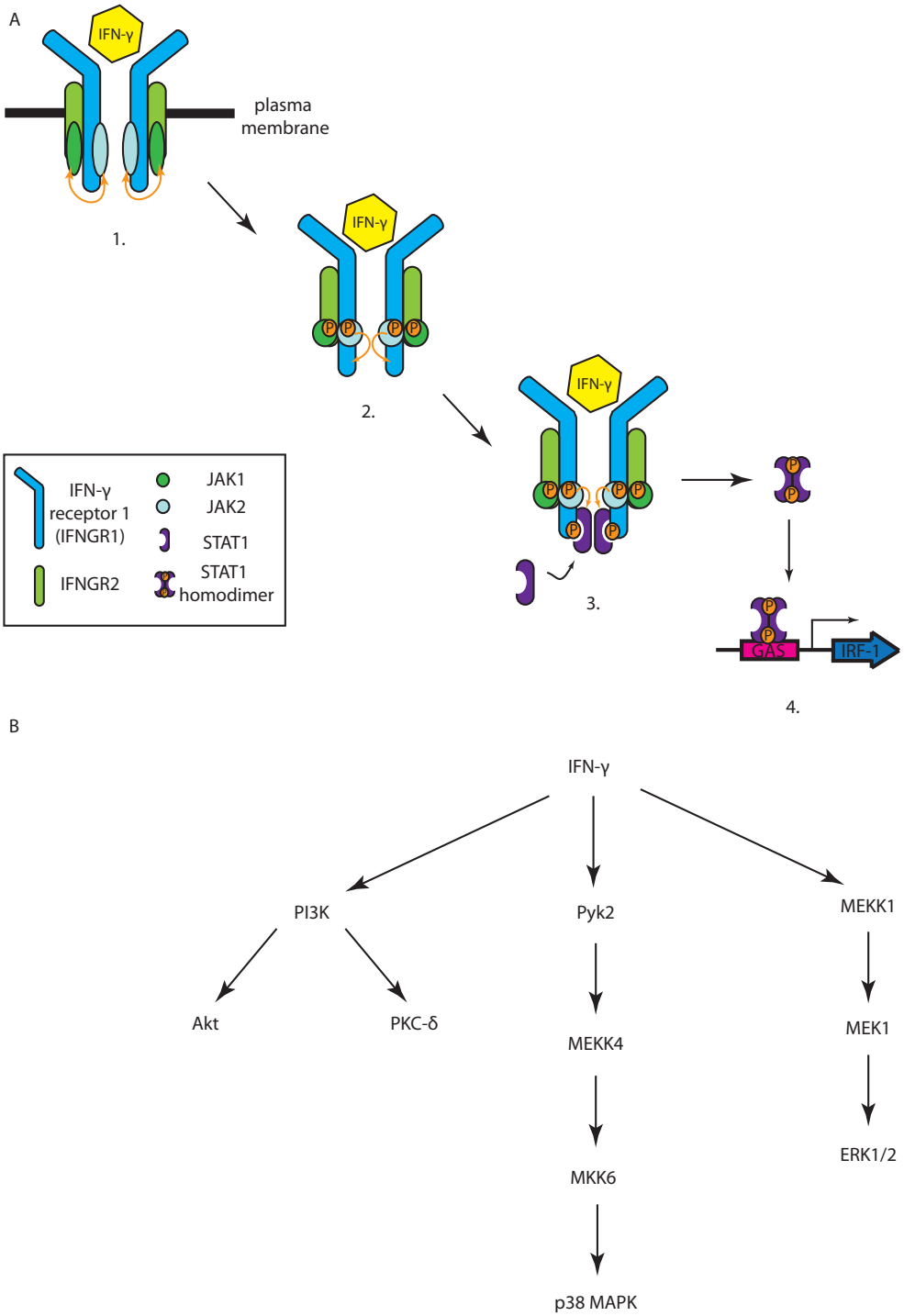

Figure 3.14: IFN-γ activates IRF-1 and protein kinases. (A) IFN-γ downstream signalling pathway. 1) Binding of IFN-γ to the IFNGR1 (Interferon-gamma receptor 1) causes multimerisation of receptor subunits resulting in auto- and trans-activation of JAKs (Janus kinases) as a result of their proximity. 2) Activated JAKs phosphorylate IFNGR1 creating a binding site for STAT1 monomers. 3) STAT1 monomers bind phosphorylated IFNGR1 and are phosphorylated by JAKs. 4) Phosphorylated STAT1s form homodimers, translocate the to nucleus and activate transcription by binding GAS (gamma activated sequence) elements, for example in the *IRF-1* promoter [90]. (B) IFN-γ is known to activate kinase signalling pathways. IFN-γ treatment has been shown to activate PI3K and Akt [154]. PI3K has also been shown to activate PKCδ in response to IFN-γ treatment [155]. IFN-γ activates Pyk2 which initiates a MEKK4, MKK6, p38 MAPK cascade [156] and IFN-γ activated MEKK1 activates ERK1/2 via MEK1 [157]. These kinases could be involved in the phosphorylation of IRF-1 in response to IFN-γ treatment.

[158]. Antibodies can lose activity and stability during storage by a number of processes including deamidation, oxidation and fragmentation [159]. It is possible that some or all of these mechanisms contributed to the loss of activity or stability of the phosphospecific antibodies.

It would also have been very interesting to determine if both the phosphorylation events at 311T and 317S which occur after IFN-γ treatment are to be found on one molecule of IRF-1. To do this, IRF-1 phosphorylated at one site could be extracted from cell lysate using an immobilised phosphospecific antibody, the selected IRF-1 could then be probed with the second antibody and a pan-IRF-1 antibody to see if both sites are simultaneously phosphorylated. If that were the case, a time course of IFN-γ treatment could reveal if one phosphorylation primed for another.

Despite the lack of phosphospecific antibodies, the effects of kinase inhibitors on IRF-1 activity could be assayed in future. In fact, recently, work by Khaldoon Al-Samman in the Ball laboratory using a kinase inhibitor library has found that a number of kinase inhibitors impact on IRF-1's transactivatory activity. The top hits were a CK2 inhibitor and an EGFR kinase inhibitor. These leads are promising as CK2 has already been shown to phosphorylate IRF-1 [119] and activation of EGFRs activate IRF-1 [110]. Furthermore, CK2 has been shown to be activated by IFN-γ, although it is not predicted to phosphorylate IRF-1 at Thr311 or Ser317. If other kinases implicated have been shown to be activated by IFN-γ treatment, kinase assays using WT protein and non-phosphorylatable mutants could be carried out to interrogate their importance at the IFN-γ induced phosphorylation sites.

Further work could then investigate the effects of the kinases/kinase inhibitors on the cellular activity of IRF-1. A little work has been done looking at the effect of inhibitors on protein levels of IRF-1 downstream targets likely to be affected by IFN-γ such as PKR and Cdk2. So far, no effects have been seen, but optimisation of inhibitor concentrations may yield results.

A more effective approach could be to use a focused microarray to look at the effects of specific kinase inhibitors on the mRNA transcript levels of a large number of genes in

IRF-1 associated pathways. It would be important in this case to be able to verify that the effects were due to altered IRF-1 activity and not effects on other transcription factors.

Although the phosphomimetic mutations at the IFN-γ-stimulated phosphorylation sites did not have any effect on half life on the protein, it may have effects on the activity of the protein, without changing steady state levels. This would agree with the nanobody data that indicates that the C-terminus of IRF-1 is rate-limiting for activity and imposes a negative regulation that can be released by interventions such as antibody binding or potentially phosphorylation. This is investigated in the following chapter.

In conclusion, this chapter has described the development of a number of tools to study the role of phosphorylation in regulating IRF-1 activity. Kinase assays were set up to allow identification of cellular kinases with activity against IRF-1, and to allow validation of kinases found as binding partners of IRF-1. Phosphospecific antibodies were produced and were used to discover stimulus-specific phosphorylation of endogenous IRF-1 at Thr311 and Ser317. IFN-γ and DNA damage response pathways were identified as physiological signalling pathways upstream of these phosphorylation sites. Following this, phosphomimetic and non-phosphorylatable mutants of IRF-1 were created by site-directed mutagenesis. Expression of the mutants has been tested in various environments, and their comparable stability confirmed. These will be used in subsequent chapters to investigate the effect of phosphorylation of IRF-1 on activity.

Chapter 4

Effects of C-terminal phosphorylation of IRF-1 on transcriptional activity

4.1 Activity of Phosphomimetic Mutants in Reporter Assays

4.1.1 Introduction

As a transcription factor, IRF-1 regulates the expression of many downstream genes involved in a wide variety of pathways such as immune response, cell cycle control and tumour suppression. To ensure these genes are only switched on/off under the appropriate conditions, IRF-1 must be strictly regulated, however, it is not known what form this regulation takes.

On the basis of the stimulus-specific phosphorylation discussed in the previous chapter, the series of mutants described were used to study the effects of phosphorylation at these sites. The results below indicate that phosphorylation could be one form of post-translational regulation affecting IRF-1 activity.

4.1.2 Comparison of Transactivatory Potential of Phosphomimetic Mutants

The transactivatory potential of IRF-1 phosphomimetic mutants was measured using the dual luciferase reporter assay system. As this system uses live cells to provide the necessary transcriptional machinery, there is the potential for other trancription factors to interact with the promoter being studied. To minimise the possiblity of this happening, a very specific synthetic minimal IRF-1 promoter was used (IRF-E). To test the specificity of the minimal promoter, IRF-3, another member of the IRF family was used as a control since the IRF family all have highly conserved DNA binding domains and thus very similar recognition sequences [160]. As shown in Fig 4.1A, when H1299 cells were transfected with the IRF-E-luciferase construct, and a titration of IRF-1 or IRF-3, there is no activity at the promoter in the absence of transfected IRF-1 and IRF-3 cannot activate the promoter but IRF-1 gives a titratable response.

Having established the specificity of the promoter construct, it was initially used to check that the activity was a product of DNA binding. H1299 cells were again transfected with IRF-E-luciferase and a titration of IRF-1 WT or IRF-1 W11R. IRF-1 W11R has previously been shown to lack DNA binding ability [161]. No activity was seen with the W11R mutant, but again, IRF-1 gives a titratable response (Fig 4.1B).

Next, the IRF-E promoter was used to compare the activity of IRF-1 WT to the phosphomimetic mutants described in the previous chapter. When the three mutants were titrated into H1299 cells, IRF-1 WT and IRF-1 T311D activities were similar while all mutants showed higher activity than IRF-1 WT (Fig 4.2A), with the dual phosphomimetic mutant IRF-1 T311D/S317D having the highest activity; on average 5x greater than WT when 400ng protein is transfected. Under these conditions, it seems that the S317D mutation is dominant as this mutant's activity is most similar to IRF-1 T311D/S317D (10x greater than WT activity at 400ng protein transfected), although the T311D mutation still contributes some activity.

Transcription factors can work both by binding directly to DNA and modulating transcription, or by affecting another transcription factor bound to the promoter. To confirm

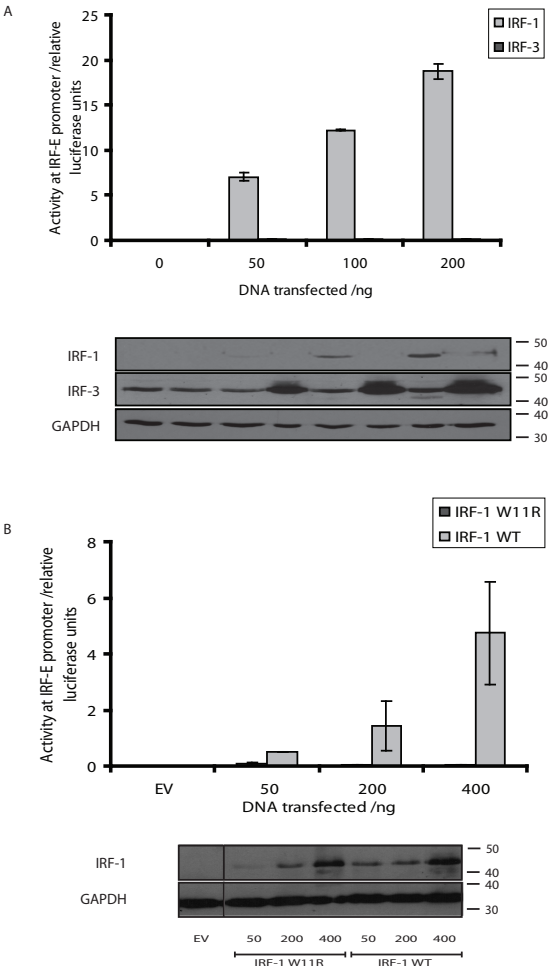

Figure 4.1: Verification of IRF-E promoter. (A) H1299 cells were transfected with pcDNA3 EV (200ng) or a titration of pcDNA3-IRF-3 or IRF-1 WT (as indicated). 50ng IRF-E-luc reporter plasmid and 0.833ng control CMV-Renilla-luc was co-transfected. After 24h, reporter gene activity was measured in relative light units (RLU) and normalised to CMV-Renilla-luc activity. Results are expressed as mean +/- half the range for duplicate experiments. Expressed proteins were detected by SDS-PAGE/immunoblot using anti IRF-1 (BD Biosciences), anti-IRF-3 (NEB) and anti-GAPDH (Abcam) as a loading control. (B) H1299 cells were transfected with 400ng pcDNA3 EV or a titration of pcDNA3-IRF-W11R or IRF-1 WT (as indicated). Luciferase reporter transfection, measurement of activity and detection of protein were as in (A). Black line indicates lanes run at same time but not adjacent. Data representative of (A) a single experiment (B) two independent experiments

that this assay was looking at DNA binding to the IFR-E and therefore the direct effects of IRF-1, a reporter assay was set up using the DNA-binding-dead W11R mutant in both IRF- WT and T311D/S317D backgrounds. Fig 4.2B clearly demonstrates that the DNA binding ability of IRF-1 is absolutely required for activity of both IRF-1s at this promoter and the enhanced activity of the mutant requires DNA binding.

The activities of the phosphomimetic mutants (T311D, S317D, T311D/S317D) were compared across cell lines and with a set of non-phosphorylatable mutants where Ser or Thr was replaced with Ala (T311A, S317A) (Fig 4.3A&B). It is interesting to note that there may be a difference in relative activities between cell lines. In H1299 cells (Fig 4.3A), IRF-1 T311D/S317D has the highest activity, followed by IRF-1 S317D then IRF-1 T311D and WT which have the lowest activity. In contrast, in A375 cells (Fig 4.3B), IRF-1 WT and T311D/S317D activities appear to be more similar, while the single mutants have higher activities. The comparison has only been performed once for the single mutants and twice for IRF-1 WT and T311D/S317D but differences in relative activities between cell lines are perhaps not surprising, as different cell lines will have different co-factor expression, and will be preferentially expressing a different subset of genes.

The non-phosphorylatable mutants (T/S-A) were included to give more insight into how the phosphomimetic mutations enhance the activity of IRF-1. For example, in H1299 cells (Fig 4.3A), T311D activity is the same as T311A. An explanation for this is that phosphorylation could block a binding site for repressor proteins that requires the presence of the Thr residue, so substituting T311A has a similar blocking effect. Conversely, S317D has higher activity than S317A (S317A is similar to WT). This suggests that phosphorylation creates a binding site, or causes a conformational change specific to the phosphorylation, and S317A cannot substitute.

4.1.3 Activity at naturally occurring promoters

As the previous experiments were all performed using the minimal promoter (IRF-E), the next step was to confirm if the same effects are seen at naturally occurring IRF-

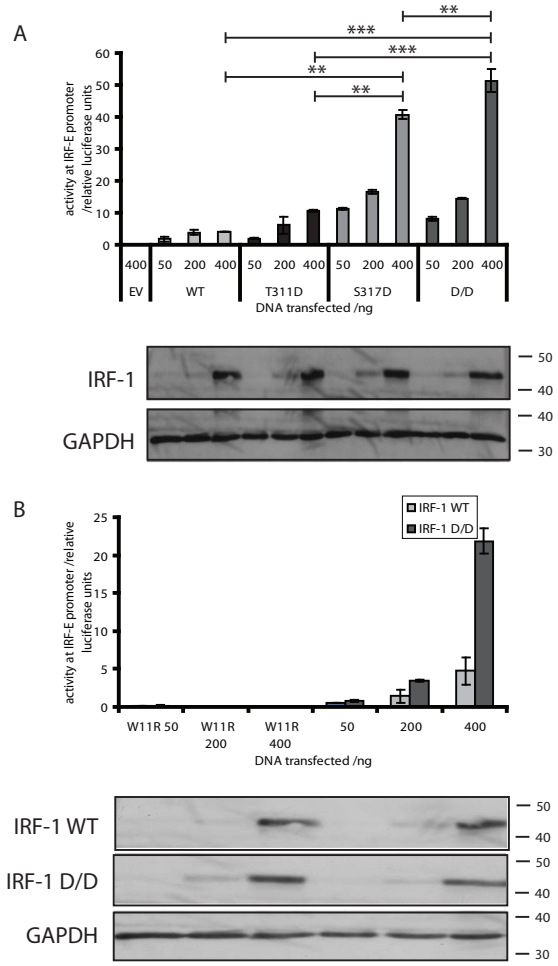

Figure 4.2: Phosphomimetic mutations of IRF-1 enhance transcriptional activity at the IRF-E promoter in a DNA-binding-dependent manner. (A) H1299 cells were transfected with pcDNA3 EV or a titration of pcDNA3-IRF-1 WT, T311D, S317D or T311D/S317D. 50ng IRF-E-luc reporter plasmid and 0.833ng control CMV-Renilla-luc was co-transfected. After 24h, reporter gene activity was measured in relative light units (RLU) and normalised to CMV-Renilla-luc activity. Results are expressed as mean +/- half the range for duplicate experiments. Expressed proteins were detected by SDS-PAGE/immunoblot using anti IRF-1 (BD Biosciences), and anti-GAPDH (Abcam) as a loading control. Significant differences between activities by randomised block ANOVA followed by Tukey's test are indiciated. (** $p=<0.01$, *** $p=<0.001$) (B) As for (A) except that pcDNA3 EV or IRF-1 W11R-WT or IRF-1 W11R D/D was transfected. Data representative of two independent experiments for (A) and (B).

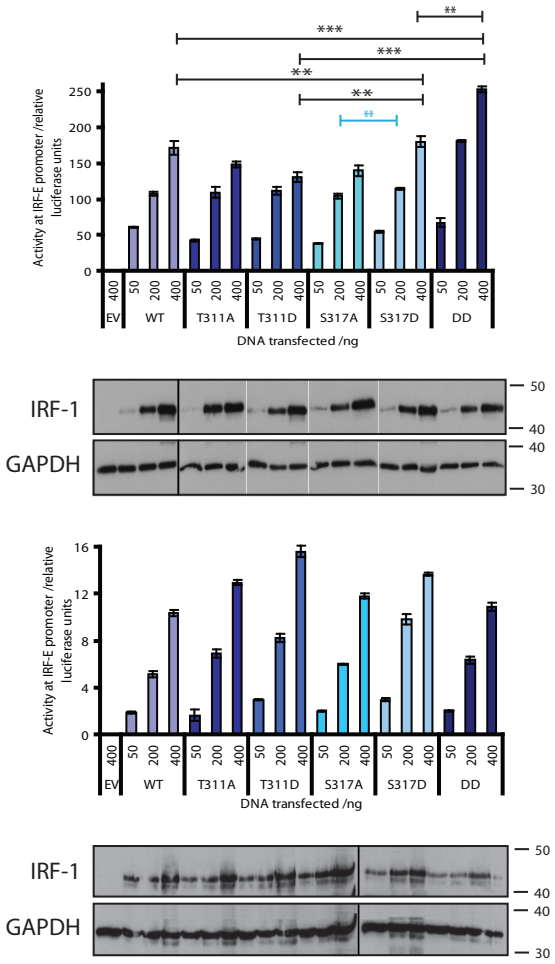

Figure 4.3: Activity of phosphomimetic and non-phosphorylatable mutants may be cell line dependent. (A) H1299 cells were transfected with pcDNA3 EV or a titration of pcDNA3-IRF-1 WT, T311A, T311D, S317A, S317D or T311D/S317D. 50ng IRF-E-luc reporter plasmid and 0.833ng control CMV-Renilla-luc was co-transfected. After 24h, reporter gene activity was measured in relative light units (RLU) and normalised to CMV-Renilla-luc activity. Results are expressed as mean +/- half the range for duplicate experiments. Expressed proteins were detected by SDS-PAGE/immunoblot using anti IRF-1 (BD Biosciences), and anti-GAPDH (Abcam) as a loading control. Significant differences between activities by randomised block ANOVA followed by Tukey's test are indiciated. (** p=<0.01, *** p=<0.001). (B) as for (A) using A375 cells. Data are representative of (A) five independent experiments for phosphomimetic mutants and three independent experiments for non-phosphorylatable mutants (B) data from a single experiment for single mutants and representative of two independent experiments for IRF-1 WT and T311D/S317D. Black line indicates lanes run at same time but not adjacent.

1-responsive promoters. *TLR3* is a well characterised target for IRF-1 with an IRF-1 responsive element located at -97 $\rightarrow$ -89, very close to the transcription start site [95]. When the *hTLR3* promoter was transfected into H1299 cells, it showed a much higher background activity than the artificial promoter, possibly due to background activity of other transcription factors. The construct comprises -588 $\rightarrow$ +12 and contains potential binding sites for other transcription factors such as Sox, STAT1, Ets etc., but has been shown to be highly inducible by IRF-1 [95]. However, the general pattern of activity in H1299 cells was the same as for the IRF-E, with IRF-1 WT having the lowest, and T311D/S317D having the highest activity (Fig 4.4A). As a result of this, for simplicity, IRF-1 WT and T311D/S317D were chosen to examine the effects at other promoters.

IL7 is a cytokine functioning within the intestinal mucosa, involved in immune regulation. The *IL7* promoter contains an IRF-E which is required for constitiutive activity, regulated by IRF-2, and inducible activity in response to IFN-γ-induced IRF-1 [147]. IFN-β is involved in regulating immune responses to virus infection. The *IFN-β* promoter was, in fact, the first promoter shown to be IRF-1-responsive [1].

Titration of IRF-1 WT and T311D/S317D into H1299 cells co-expressing the *IL7* and *IFN-β* promoter reporter constructs again reveals enhanced activity of T311D/S317D IRF-1 at these promoters, although this is less striking that at the IRF-E promoter. At the *IL7* promoter, mutant IRF-1 is, on average, 1.6x more active, while at the *IFN-β* promoter, 1.8x more active. In both cases, this activity is dependent on DNA binding as the activity of the W11R mutants is similar to background. There is more obvious background activity at each of these promoters than at the IRF-E promoter. For the *IL7* promoter, this is probably due to endogenous IRF-2 [147] and at the *IFN-β* promoter, NF-κB or ATF-2/c-jun whose binding sites are also within the promoter construct [130] (Fig 4.4B&C).

The promoters described above are all from immune related genes, and as IRF-1 activity is increased by the phosphomimetic mutation at all these promoters, it appears that immune related stimuli could act as a signal to upregulate IRF-1 activity by its C-terminal phosphorylation. This is particularly relevant as IFN-γ originally induced the phosphorylation at these sites, prompting further investigation using phosphomimetic mutants.

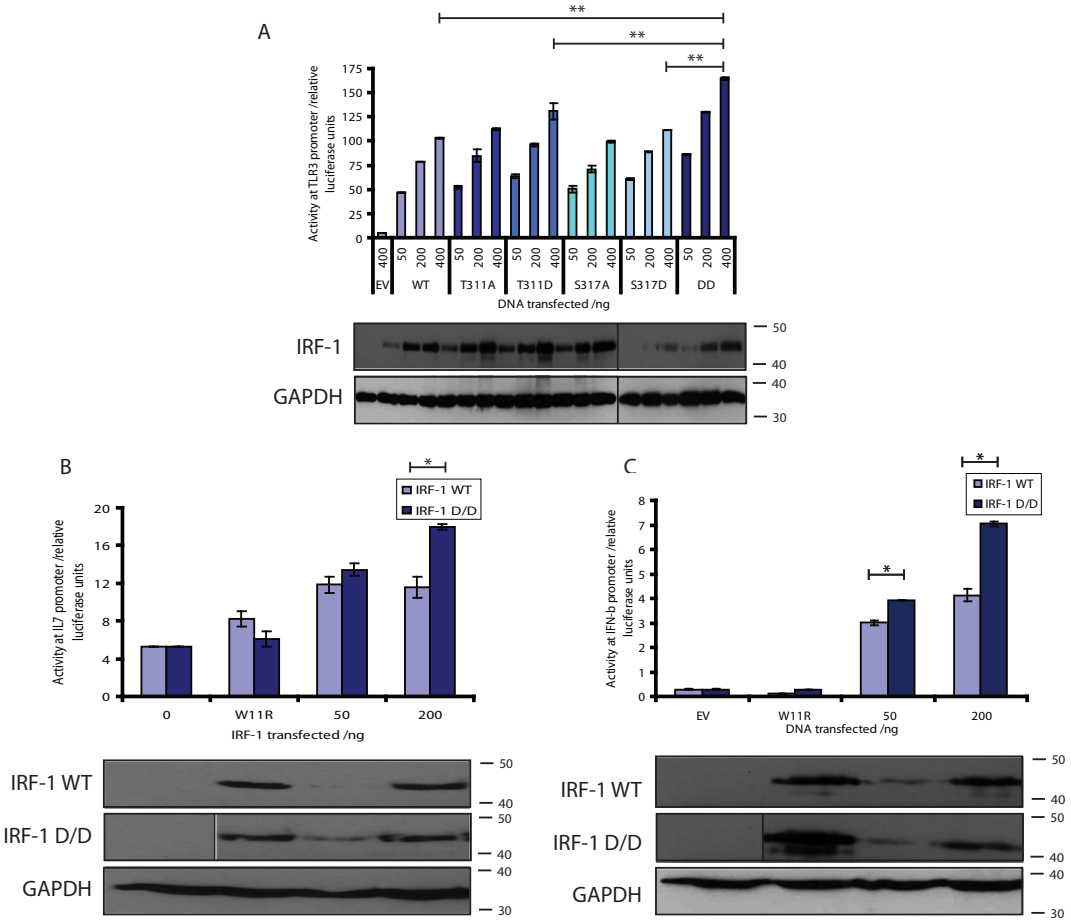

Figure 4.4: Activity at naturally occurring IRF-1 activated promoters. (A) H1299 cells were transfected with a titration of pcDNA3-IRF-1 WT or mutant. 70ng *TLR3*-luc reporter plasmid and 30ng control CMV-Renilla-luc was co-transfected. Data representative of three independent experiments.(B and C) H1299 cells were transfected with a titration of pcDNA3-IRF-1-WT or -T311D/S317D. 100ng *IL7*-luc (B) or *IFN-*β-luc (C) and 50ng control CMV-Renilla-luc was co-transfected After 24h, reporter gene activity was measured in relative light units (RLU) and normalised to CMV-Renilla-luc activity. Results are expressed as mean +/- half the range for duplicate experiments. Expressed proteins were visualised by SDS-PAGE/immunoblot using anti IRF-1 (BD Biosciences) and anti-GAPDH (Abcam) as a loading control. Data representative of three independent experiments for (A), (B) and (C). Significant differences between activities by randomised block ANOVA followed by Tukey's test are indiciated. (* p=$<$0.05, ** p=$<$0.01).

To be sure that the enhanced activity at the immune related promoters is not due to a non-specific enhanced activity of the IRF-1 T311D/S317D mutant, unrelated promoters were assayed. *Cdk2* and *MMP9* promoter constructs were chosen as IRF-1 represses these promoters, so the effects of MF-1 domain phosphorylation on IRF-1 repressor activity could be studied. Cdk2 is a cyclin dependent kinase which has previously been shown to be repressed by IRF-1. The mechanism of repression has been shown to be through inhibition of Sp1 activation of this promoter [32]. This study implied that the inhibition of *Cdk2* is not through direct promoter binding of IRF-1, however, studies from our lab have shown that repression of *Cdk2* requires DNA binding of IRF-1 since a DNA-binding refractive mutant IRF-1-YLP/A cannot repress the *Cdk2* promoter [70]. EMSAs using a *Cdk2* promoter probe would constitute a simple experiment to directly assess the binding of IRF-1 to the *Cdk2* promoter, and the effect of IRF-1 on Sp1 binding.

MMP9 is a martix metalloprotease involved in extracellular matrix degradation; it is overexpressed in many human cancers. IRF-1 mediates interferon-induced inhibition of MMP9 expression through competition with NF-κB for promoter binding [45].

When IRF-1 was titrated into H1299 cells co-expressing the *Cdk2* or *MMP9* promoters, activity at these promoters is inhibited. Interestingly IRF-1 WT and T311D/S317D both inhibit the promoters to the same extent - around a 4 fold inhibition at 200ng of protein for the *Cdk2* promoter, and 2 fold inhibition at 200ng for the *MMP9* promoter (Fig 4.5A&B). Amino acids 301-314 of IRF-1 have been shown to be required for inhibition of *Cdk2*. Thus, it would be interesting to determine the effect of the T311D mutation alone on repression.

These data indicate that the effect of phosphorylation on IRF-1 activity is a promoter specific, and therefore likely regulatory effect. It seems unlikely, therefore, that the mutations could be causing a gross, non-physiological change that indiscriminately affects IRF-1 activity.

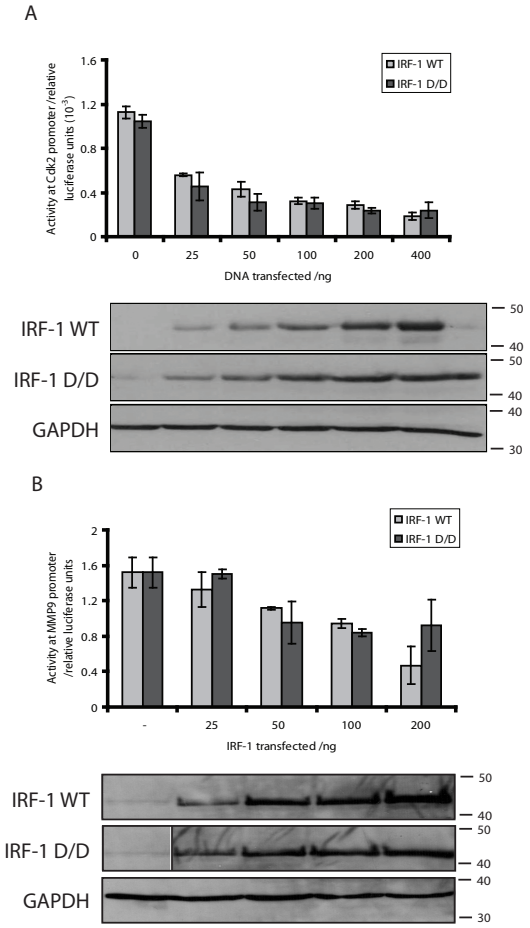

Figure 4.5: Activity at naturally occurring IRF-1 repressed promoters. (A) H1299 cells were transfected with a titration of pcDNA3-IRF-1 WT or mutant. 100ng *Cdk2*-luc reporter plasmid and 10ng control CMV-Renilla-luc was co-transfected. (B) H1299 cells were transfected with a titration of pcDNA3-IRF-1-WT or mutant. 100ng *MMP9*-luc and 25ng control CMV-Renilla-luc was co-transfected After 24h, reporter gene activity was measured in relative light units (RLU) and normalised to CMV-Renilla-luc activity. Results are expressed as mean +/- half the range for duplicate experiments. Expressed proteins were visualised by SDS-PAGE/immunoblot using anti IRF-1 (BD Biosciences) and anti-GAPDH (Abcam) as a loading control. No significant difference between IRF-1 WT and T311D/S317D was found at any DNA concentration for either promoter by randomised block ANOVA. Data representative of three independent experiments for (A) and (B).

4.1.4 Repression of IRF-1 WT and T311D/S317D by IRF-2

The activity of IRF-1 is repressed by IRF-2 [2]. The enhanced activity of IRF-1 T311D/S317D may be linked to an ability to escape this repression, therefore, the effect of IRF-2 co-expression on IRF-1 WT and T311D/S317D activity was investigated.

A titration of IRF-2 was co-transfected with constant (200ng) IRF-1 WT and T311D/S317D. The effect was compared in H1299 and HeLa cells and at the IRF-E and *TLR3* promoters. In these cells, at these promoters, there was no significant dirference between IRF-1 WT and T311D/S317D. When using the *TLR3* promoter, the amount of IRF-1 T311D/S317D transfected was reduced in an attempt to normalise the IRF-1 WT and T311D/S317D activities in case the higher activity of T311D/S317D made it less susceptible to inhibition by IRF-1. Despite this, no significant difference in activity was observed. The data is shown as a bar graph of activity to represent absolute inhibition, and also as a line graph of activity normalised to -IRF-2. This more clearly visualises the inhibition (Fig 4.6A&B).

Since the activity of IRF-1 T311D/S317D is significantly higher than that of WT, the amount of IRF-1 T311D/S317D transfected was reduced in an attempt to normalise IRF-1 WT and T311D/S317D promoter activities to see if this might accentuate the effect. The *TLR3* promoter was also used, as previous lab members had seen inhibition of IRF-1 activity by IRF-2 at this promoter. These changes enhance the difference between IRF-1 WT and T311D/S317D inhibition by IRF-2 in both HeLa and H1299 cells (Fig 4.6C&D).

4.2 Effect of phosphomimetic mutations on the DNA-binding capacity of IRF-1

4.2.1 Introduction

The enhanced transactivatory potential of the IRF-1 phosphomimetic mutants may be a result of improved DNA binding caused by the mutation. To determine if this is the

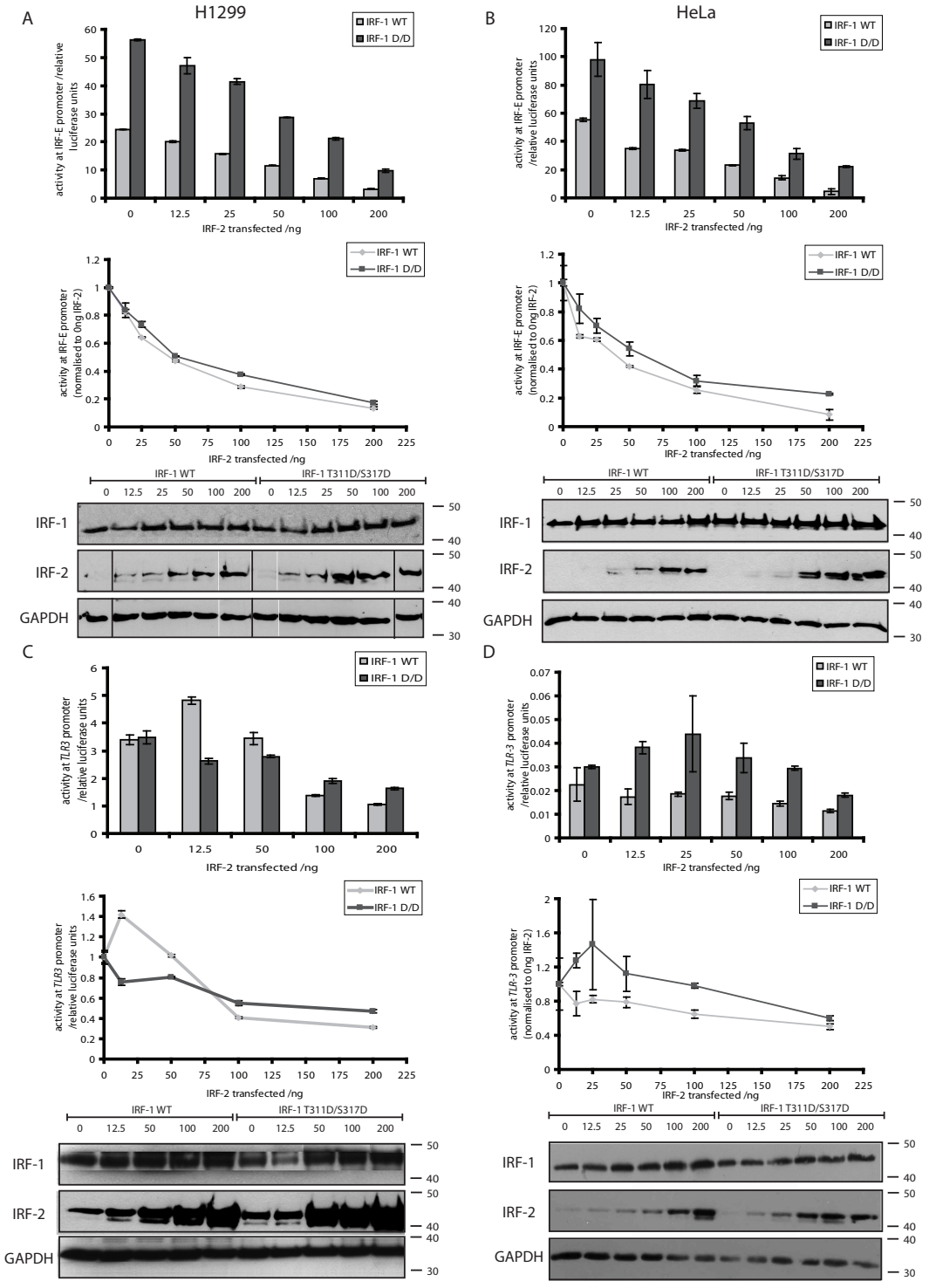

Figure 4.6: Inhibition of IRF-1 WT and T311D/S317D by IRF-2. H1299 (A)&(C) and HeLa (B)&(D) cells were transfected with 200ng pcDNA3-IRF-1 WT or 200 ng (A)&(B) or 100ng (C)&(D) IRF-1 T311D/S317D. (A)&(B) 50ng IRF-E-luc reporter plasmid, 0.835ng control CMV-Renilla-luc and a titration of pcDNA3-IRF-2 was co-transfected. (C)&(D) 70ng *TLR3*-luc, 30ng control CMV-Renilla-luc and a titration of pcDNA3-IRF-2 was co-transfected. After 24h, reporter gene activity was measured in relative light units (RLU) and normalised to CMV-Renilla-luc activity. Results are expressed as mean +/- half the range for duplicate experiments. Lower graph displays activity normalised to activity in absence of IRF-2. Expressed proteins were visualised by SDS-PAGE/immunoblot using anti IRF-1 (BD Biosciences), anti-IRF-2 (Abcam) and anti-GAPDH (Abcam) as a loading control. No significant difference between inhibition of IRF-1 WT and IRF-1 T311D/S317D was observed by randomised block ANOVA. Data representative of three independent experiments for (A), (B), (C) and (D).

case, gel shift assays were carried out using IRF-1 expressed in reticulocyte lysate. In a gel shift assay, protein is incubated with ^{32}P-labelled DNA probe, and protein/DNA complexes are allowed to form. As a control, antibody can be included in the mix. The protein/DNA(/antibody) mix is then run on a native gel to maintain complexes. Separation occurs based on weight so the free probe runs furthest, then the probe with protein bound higher up the gel (it is "shifted") and finally the DNA/protein/antibody complex runs near the top of the gel (it is "supershifted"). The presence of these three complexes is detected by phosphorimager analysis of the gel allowing detection of the ^{32}P-labelled DNA probe.

4.2.2 Relative binding affinities

Initially, binding of IRF-1 WT and phosphomimetic mutants IRF-1 T311D/S317D, T311D and S317D at the optimised C1 probe [162] (Fig 4.7A) was compared. The assays were optimised and carried out in an excess of free probe, however, only the top portion of the phosphorimage is shown. From Fig 4.7B (left panel), it appears that all the mutants bind DNA with higher affinity than IRF-1 WT, however, the difference is quite subtle, especially after supershift. Due to the presence of a non-specific band running with the non-supershifted IRF-1/DNA complex (see control, lane 1), it is easier in this instance to compare the binding of the supershifted complexes. Using densitometry, the difference in binding between IRF-1 WT and IRF-1 T311D and S317D was found to be reproducible but not significant across three experiments. The enhanced binding of IRF-1 T311D/S317D compared to IRF-1 WT, is however, significant (data from nine experiments), reflecting enhanced affinity or stability of the DNA/protein complex. Further experiments have shown a larger difference in the binding of IRF-1 WT and T311D/S317D (for example Fig 4.7B right panel) and, on average, the binding of IRF-1 T311D/S317D is 1.7x more stable than IRF-1 WT.

The difference in IRF-1 WT and T311D/S317D DNA binding is titratable (Fig 4.7B (right panel)). In this case, IRF-1 T311D/S317D binds with an average of 2.3 times more affinity/stability across the three points of the titration.

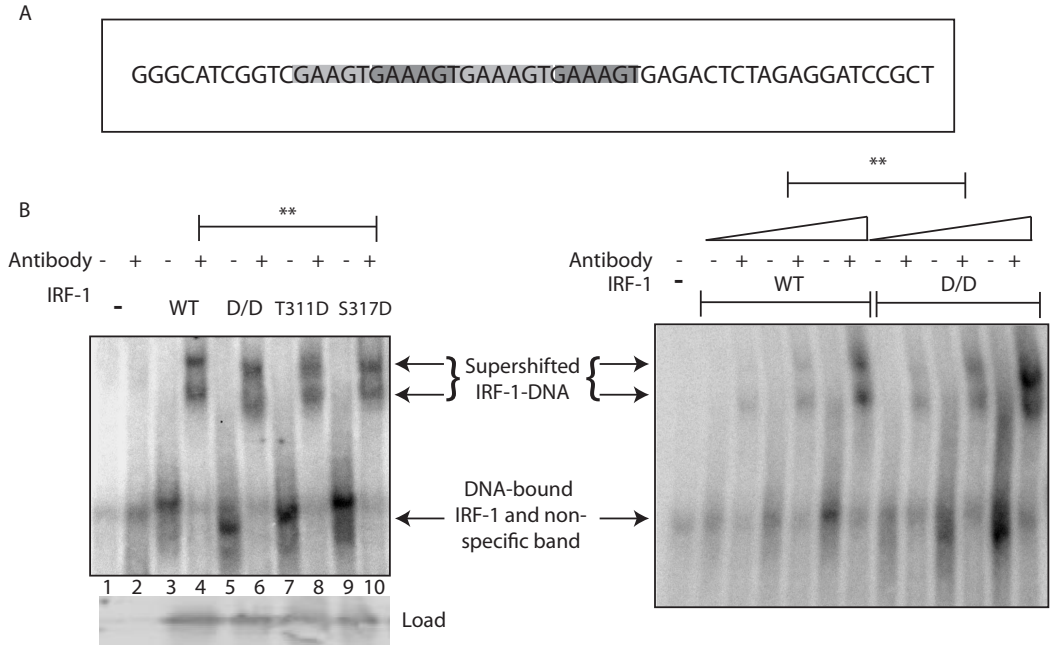

Figure 4.7: Comparison of IRF-1 mutants binding to C1 promoter. (A) Sequence of C1 promoter with the 4 tandemly arranged hexamer repeats highlighted. (B) *Left panel*: Binding of IRF-1 and mutants to C1 probe. IRF-1 WT, T311D/S317D, T311D and S317D were expressed in reticulocyte lysate and ^{32}P-labelled C1 probe binding to 6μl of lysate was determined by EMSA (Lanes 3,5,7 and 9). IRF-1-DNA complex is supershifted by anti-IRF-1 antibody (BD Biosciences) (Lanes 4,6,8 and 10). Expression levels of all four IRF-1 constructs was visualised by immunoblotting using anti-IRF-1 (Santa Cruz, C20). Difference between IRF-1 WT and IRF-1 T311D/S317D binding is significant (** p=$<$0.01 by paired t-test). *Right panel*: DNA binding of IRF-1 WT and T311D/S317D is titratable. 2, 6 and 12μl of reticulocyte lysate expressing indicated IRF-1 construct was incubated with ^{32}P-labelled C1 probe. IRF-1-DNA complex is supershifted by anti-IRF-1 (Santa Cruz). Expression levels of proteins as for left panel. Data representative of: (B) *left panel* three experiments for all mutants and nine experiments for IRF-1 WT/ IRF-1-T311D/S317D comparison and (B) *right panel* one experiment.

4.2.3 Mechanism of DNA Binding

To investigate the mechanism of the enhanced DNA binding of IRF-1 T311D/S317D further, an IRF-1 WT C-terminal peptide (last 20 amino acids of IRF-1) was titrated into the EMSA as a competitor. It was hoped that this would help distinguish between different mechanisms.

Four potential mechanisms of enhanced DNA binding were considered. These mechanisms are illustrated in Fig 4.8, along with the effects of addition of the peptide

One possibility is that a negative charge in the C-terminus could enhance a conformational regulation that has a positive effect on DNA binding (Fig 4.8A). IRF-1 could exist in an equilibrium between a less favourable DNA binding conformation (for example, with the C-terminus free) (light blue), and a more favourable DNA binding conformation (for example, with the C-terminus bound to an acceptor site elsewhere in the protein) (dark blue). If this was mediated by an intramolecular interaction between the C-terminus (black line) and a C-terminus binding site (purple spot), phosphorylation could enhance this interaction by increasing its affinity. Thus the equilibrium would change such that almost all the protein is in the favourable DNA binding conformation. If this was the case, addition of WT C-terminal peptide (green line) to the mix would inhibit DNA binding of WT IRF-1. The peptide is identical to the IRF-1 WT C-terminus and thus has similar affinity for the acceptor site. Therefore, the peptide will compete with the C-terminus for binding to the acceptor site, and shift the equilibrium further to the side of the less favourable DNA binding conformation.

For IRF-1 T311D/S317D, the equilibrium is far to the side of the favourable DNA binding conformation (due to the proposed high affinity interaction between the negatively charged C-terminus and the acceptor site). When the peptide is added, little protein is in the less favourable DNA binding conformation with the acceptor site exposed for binding to the peptide, and the peptide also has a lower affinity for the acceptor site than does the phosphoprotein's C-terminus, so will be less likely to bind. In this case, there will be some inhibiton of DNA binding as a small proportion of the protein is held in the less favourable DNA binding conformation by binding of the peptide; however, it will be

Figure 4.8 *(following page)*: Four potential mechanisms of enhanced IRF-1 T311D/S317D DNA binding compared to IRF-1 WT and effect of peptide competition with on DNA binding.
(A) Negative charge in the C-terminus enhances a conformational positive regulation. Favourable (dark blue) and less favourable (light blue) DNA binding conformations for IRF-1 exist in equilibrium. This is mediated by a **positive** regulatory intramolecular interaction between the C-terminus (black line) and a C-terminus binding site (purple spot). Negative charge in the C-terminus (phosphorylation or S/T→D mutation) increases the affinity of the interaction, stabilising the favourable DNA binding conformation (dark blue), thus enhancing DNA binding of IRF-1 T311D/S317D. *Effect of addition of IRF-1 C-terminal peptide*: For IRF-1 WT, peptide and protein C-terminus have the same affinity for the C-terminus binding site. Peptide competes for binding to this site, and more protein adopts the unbound, less favourable DNA binding (light blue), resulting in inhibition of DNA binding. For IRF-1 D/D, peptide cannot compete as effectively with the high affinity intramolecular interaction, and IRF-1 D/D DNA binding is less affected.
(B) Negative charge in the C-terminus releases a conformational negative regulation. Favourable (dark blue) and less favourable (light blue) DNA binding conformations for IRF-1 exist in equilibrium. This is controlled by a **negative** regulatory interaction between the C-terminus (black line) and a C-terminus binding site (purple spot). A negative charge in the C-terminus interferes with the negative regulatory interaction, thus enhancing the DNA binding of IRF-1 T311D/S317D. *Effect of addition of IRF-1 C-terminal peptide*: The peptide will have different effects, depending on whether the favourable DNA conformation results from the C-terminus binding site (purple spot) being free (1) or the C-terminus (black line) being free (2). For IRF-1 WT, if free C-terminus binding site induces the favourable DNA binding conformation (1), peptide occupies the C-terminus binding site and maintains the less favourable DNA binding conformation, resulting in inhibited DNA binding. In contrast, if free C-terminus is required for favourable DNA binding (2), peptide binds the C-terminus binding site, resulting in more free C-terminus and therefore enhanced DNA binding. For IRF-1 T311D/S317D, the effects are very similar except that for situation (2), since the negatively charged C-terminus already interacts less with the binding site, peptide competition results in a smaller increase in DNA binding.
(C) Negative charge in the C-terminus enhances binding of a positive cofactor. Binding of a positive cofactor at the C-terminus of IRF-1 enhances DNA binding. In the absence of C-terminal phosphorylation, little co-factor (navy circle) binds and IRF-1 is in a less favourable DNA binding conformation (light blue). Negative charge creates a superior co-factor binding site, and enhanced co-factor interaction results in more IRF-1 in a favourable DNA binding conformation (dark blue). *Effect of addition of IRF-1 C-terminal peptide*: For IRF-1 WT, peptide and real C-terminus have the same affinity for the cofactor so peptide competes with IRF-1 and DNA binding is inhibited. For IRF-1 T311D/S317D, the negatively charged IRF-1 C-terminus has a higher affinity for the co-factor and so peptide competes less efficiently resulting in less inhibition of DNA binding.
(D) Negative charge in the C-terminus inhibits binding of a negative cofactor. Binding of a negative cofactor (purple circle) at the C-terminus of IRF-1 inhibits DNA binding. In the absence of phosphorylation, co-factor binds tightly so IRF-1 maintains a less favourable DNA binding conformation (light blue). Negative charge repels the negative cofactor, resulting in more IRF-1 in a favourable DNA binding conformation (dark blue). *Effect of addition of IRF-1 C-terminal peptide*: For IRF-1 WT, peptide and IRF-1 C-terminus have the same affinity for the negative co-factor; peptide competes with IRF-1 for co-factor binding resulting in more IRF-1 in the favourable DNA binding conformation. For IRF-1 T311D/S317D, less co-factor binds already, so although the peptide competes with IRF-1 for co-factor binding, the increase in DNA binding is less obvious.

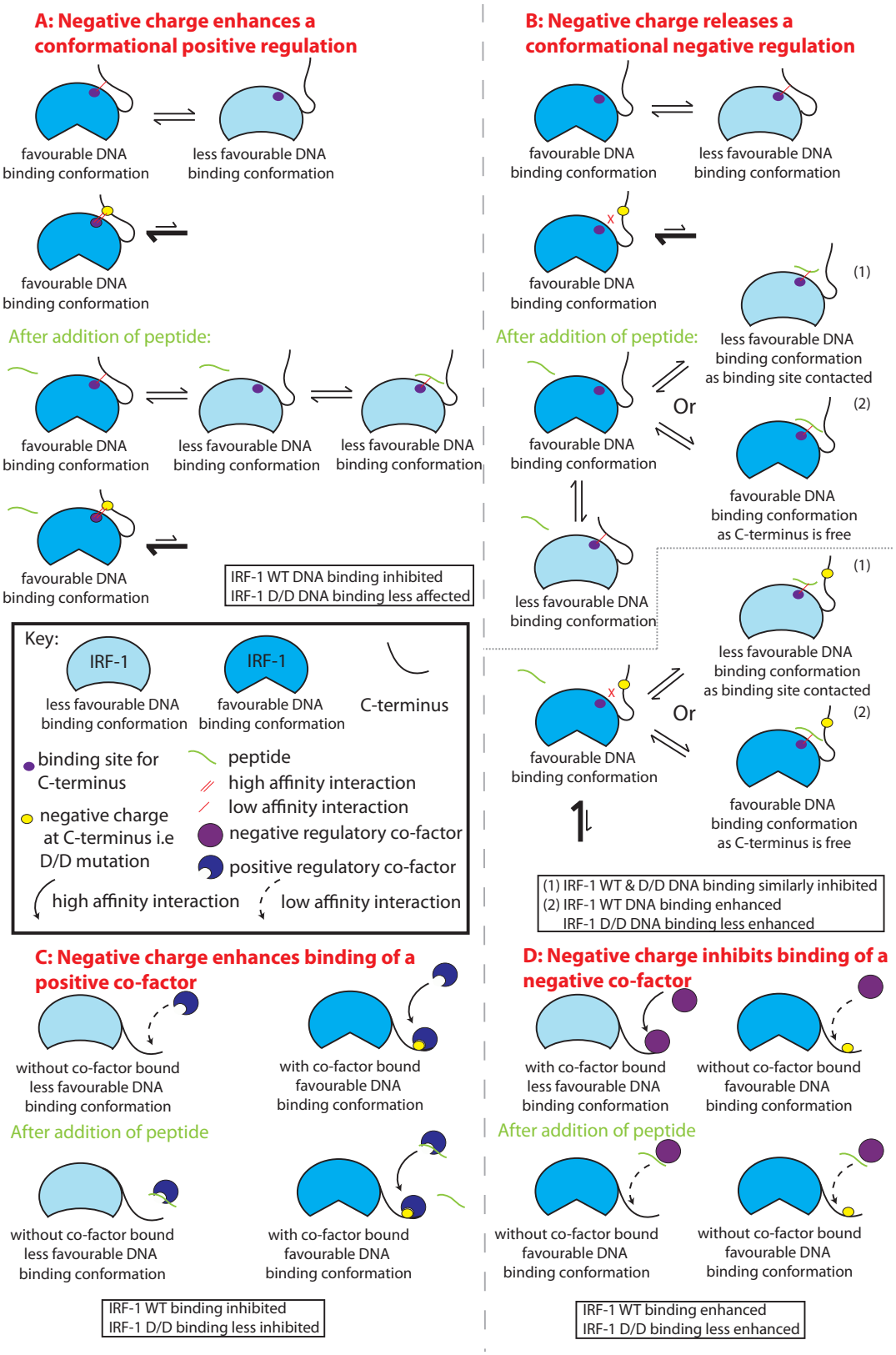
A: Negative charge enhances a conformational positive regulation
favourable DNA binding conformation
less favourable DNA binding conformation
favourable DNA binding conformation
After addition of peptide:
favourable DNA binding conformation
less favourable DNA binding conformation
less favourable DNA binding conformation
favourable DNA binding conformation
IRF-1 WT DNA binding inhibited
IRF-1 D/D DNA binding less affected
Key:
IRF-1
less favourable DNA binding conformation
IRF-1
favourable DNA binding conformation
C-terminus
binding site for C-terminus
negative charge at C-terminus i.e D/D mutation
peptide
high affinity interaction
low affinity interaction
negative regulatory co-factor
positive regulatory co-factor
high affinity interaction
low affinity interaction
B: Negative charge releases a conformational negative regulation
favourable DNA binding conformation
less favourable DNA binding conformation
favourable DNA binding conformation
(1)
less favourable DNA binding conformation as binding site contacted
After addition of peptide:
favourable DNA binding conformation
Or
(2)
favourable DNA binding conformation as C-terminus is free
less favourable DNA binding conformation
(1)
less favourable DNA binding conformation as binding site contacted
favourable DNA binding conformation
Or
(2)
favourable DNA binding conformation as C-terminus is free
(1) IRF-1 WT & D/D DNA binding similarly inhibited
(2) IRF-1 WT DNA binding enhanced
IRF-1 D/D DNA binding less enhanced
C: Negative charge enhances binding of a positive co-factor
without co-factor bound less favourable DNA binding conformation
with co-factor bound favourable DNA binding conformation
After addition of peptide
without co-factor bound less favourable DNA binding conformation
with co-factor bound favourable DNA binding conformation
IRF-1 WT binding inhibited
IRF-1 D/D binding less inhibited
D: Negative charge inhibits binding of a negative co-factor
with co-factor bound less favourable DNA binding conformation
without co-factor bound favourable DNA binding conformation
After addition of peptide
without co-factor bound favourable DNA binding conformation
without co-factor bound favourable DNA binding conformation
IRF-1 WT binding enhanced
IRF-1 D/D binding less enhanced

less than seen for the WT protein (Fig 4.8A lower panel)

Alternatively, the negative charge in the C-terminus could inhibit a conformational regulation that has a negative effect on DNA binding (Fig 4.8B). In this hypothesis, instead of the interaction between the C-terminal binding site and the C-terminus maintaining a favourable DNA binding conformation, it favours the less favourable DNA binding conformation. Addition of peptide to this system would have different effects on both types of IRF-1, depending on the exact mechanism of the negative regulation. If, for example, release of the interaction between binding site and C-terminus promotes the more favourable DNA binding conformation because the C-terminal binding site is unoccupied (Fig 4.8B(1)), addition of the peptide to IRF-1 WT will have an inhibitory effect on DNA binding since the peptide will occupy the binding site. Exactly the same inhibition will occur if the peptide is added to IRF-1 T311D/S317D since phosphorylation cannot affect peptide binding to the C-terminus binding site.

On the other hand, if release of the interaction between binding site and C-terminus promotes the more favourable DNA binding conformation because the C-terminus is free to adopt any position it choses, (Fig 4.8B(2)), addition of the peptide to WT IRF-1 will enhance DNA binding as it competes with the protein C-terminus for the binding site. For IRF-1 T311D/S317D, the same competition will occur, but since less protein exists in the less favourable DNA binding state to begin with (due to the negative charge in the C-terminus), the increase in DNA binding will be less pronounced.

The protein used in the EMSAs was prepared in reticulocyte lysate as this was found to produce the least degraded IRF-1, and will have all post-translational modifications required for DNA binding. As a result, co-factors may be present as contaminants. These were taken into consideration when suggesting mechanisms for the enhanced DNA binding of T311D/S317D IRF-1.

Phosphorylation in the C-terminus could create a high affinity binding site for a positive cofactor (Fig 4.8C). In the absence of this co-factor, IRF-1 could adopt a less favourable DNA binding conformation (light blue). As IRF-1 WT binds to the co-factor with lower affinity, it spends more time in this state. Positive co-factor (navy circle) bind-

ing (enhanced by phosphorylation) could stimulate transition to, or stabilise occupation of the favourable DNA binding conformation (dark blue). Addition of peptide (green line) to IRF-1 WT would inhibit DNA binding by inhibiting the low affinity interaction between IRF-1 and co-factor. For IRF-1 T311D/S317D, however, addition of peptide would inhibit DNA binding to a lesser degree as the WT peptide is less able to compete with the high affinity phospho-C-terminus-co-factor interaction (Fig 4.8C lower panel).

Finally, phosphorylation in the C-terminus could inhibit binding site of a negative cofactor (Fig 4.8D). For IRF-1 WT, the negative co-factor (purple circle) binds tightly so IRF-1 maintains a less favourable DNA binding conformation (light blue). The negative charge in the C-terminus resulting from phosphorylation could repel the negative cofactor, allowing more IRF-1 to take the favourable DNA binding conformation (dark blue). If peptide is added to IRF-1 WT, peptide and protein C-terminus have the same affinity for the negative co-factor so peptide competes with IRF-1 for co-factor binding resulting in more IRF-1 in the favourable DNA binding conformation. For IRF-1 T311D/S317D, less co-factor binds already, so although the peptide competes with IRF-1 for co-factor binding, the increase in DNA binding is less striking.

The peptide competition EMSA was performed by including a titration of WT IRF-1 C-terminal peptide in the binding mix for IRF-1 WT and IRF-1 T311D/S317D. In the assay (repeated twice), the C-terminal WT IRF-1 peptide titratably reduced binding of both IRF-1 WT and T311D/S317D to C1 probe (Fig 4.9 upper panel), but it was a more effective inhibitor of IRF-1 WT binding. Due to the increased initial binding of IRF-1 T311D/S317D, this is most clearly seen after densitometry when the densities are normalised to “no peptide” values (Fig 4.9 lower panel). In this experiment, as one of the supershifts did not work (due to a pipetting error), the densities of the non-supershifted bands were compared, and the background non-specific intensity was assumed to be equal for all lanes.

The overall inhibitory effect of the peptide, and enhanced inhibition of IRF-1 WT binding indicate that the mutation/phosphorylation could enhance a conformational positive regulation as shown in Fig 4.8A, or create a binding site for a positive regulator whose binding subsequently causes a favourable conformational change in IRF-1 (Fig 4.8C).

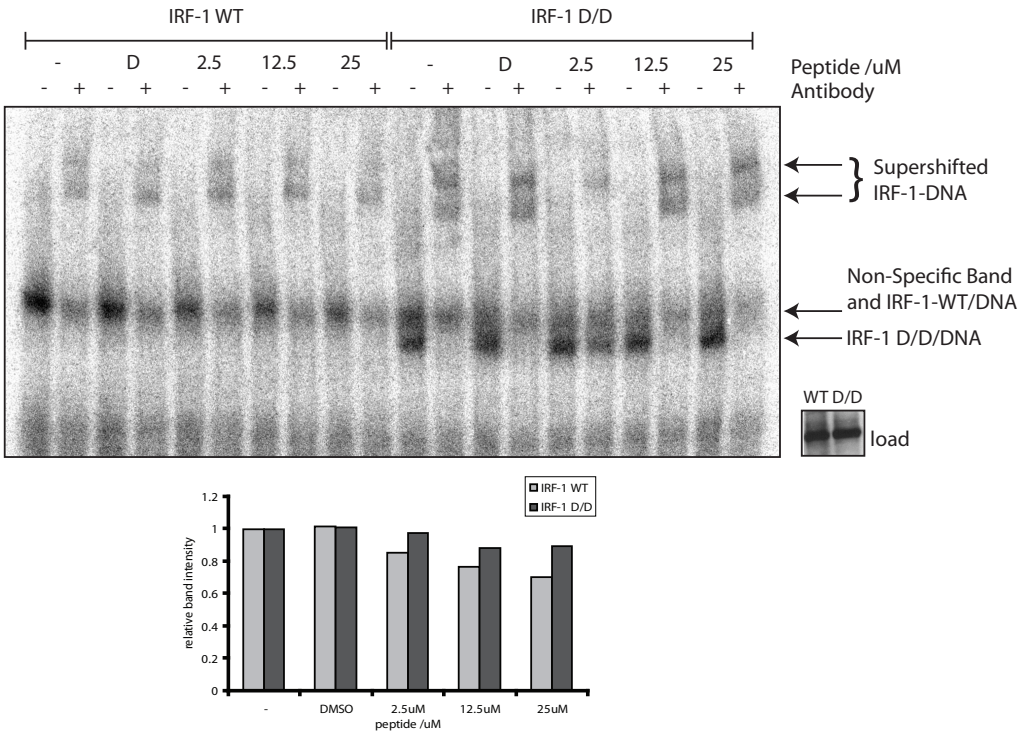

Figure 4.9: Mechanism of IRF-1 T311D/S317D enhanced DNA binding: Peptide competition EMSA. *Upper panel*: 6μl of reticulocyte lysate expressed IRF-1 was pre-incubated for 10 mins at room temperature with a titration of 2.5-25μM of C-terminal IRF-1 peptide (20aa), water [-] or DMSO control [D] before EMSA was carried out to assess binding to ^{32}P-labelled C1 probe. IRF-1-DNA complex could be supershifted with anti-IRF-1 (BD Biosciences). Normalisation of IRF-1 WT and T311D/S317D protein was visualised by immunoblot using anti-IRF-1 (Santa Cruz, C20). *Lower panel*: Intensity of IRF-1-DNA complexes was determined by densitometry using Image J, normalised to [-] contol and plotted on a graph. Data representative of two independent experiments.

It should be noted that the differences in DNA binding between the IRF-1 WT and T311D/S317D proteins may be slightly less pronounced than expected as some of the T311D and S317D sites in the WT protein may have been phosphorylated in the reticulocyte lysate, causing it to act like the mutant protein. Making a non-phosphorylatable mutant might solve this problem, but these mutations could have their own effects such as destroying a binding site that required the Ser or Thr residues.

To differentiate between the two mechanisms indicated above, further EMSAs were performed: If the DNA binding ability of IRF-1 was being modulated by co-factors from the reticulocyte lysate, IRF-1 from sources other than reticulocyte lysate should not show a difference in binding. Although plants do have orthologues of the transcriptional regulatory proteins p300/PCAF [163], it was hoped that these would be different enough to their mammalian counterparts to not be able to interact with IRF-1. This seems to have been the case (see below).

IRF-1 from wheatgerm extract, and His-tagged IRF-1 purified from E.Coli were assayed. The purification of His-IRF-1 was described in Chapter 3. When His-IRF-1 is allowed to bind to DNA, similar IRF-1 WT and IRF-1 T311D/S317D DNA binding is seen. The relative density of IRF-1WT-probe complex:IRF-1 D/D-probe complex is, on average, 1:0.98. (Fig 4.10 left panel). With untagged IRF-1 expressed in wheatgerm extract, both proteins bind DNA with very similar affinity (Fig 4.10 right panel). This time the relative densities are 1:0.9, although this comparison has only been performed once. Taken together, these results suggest that a factor in the rabbit reticulocyte lysate is contributing to the enhanced DNA binding activity of IRF-1 T311D/S317D.

The wheatgerm EMSA used ^{35}S labelled protein rather than ^{32}P-probe and, although this did not affect the enhanced IRF-1 T311D/S317D binding with reticulocyte lysate protein (data not shown), it would still be helpful to repeat the wheatgerm assay using ^{32}P-probe.

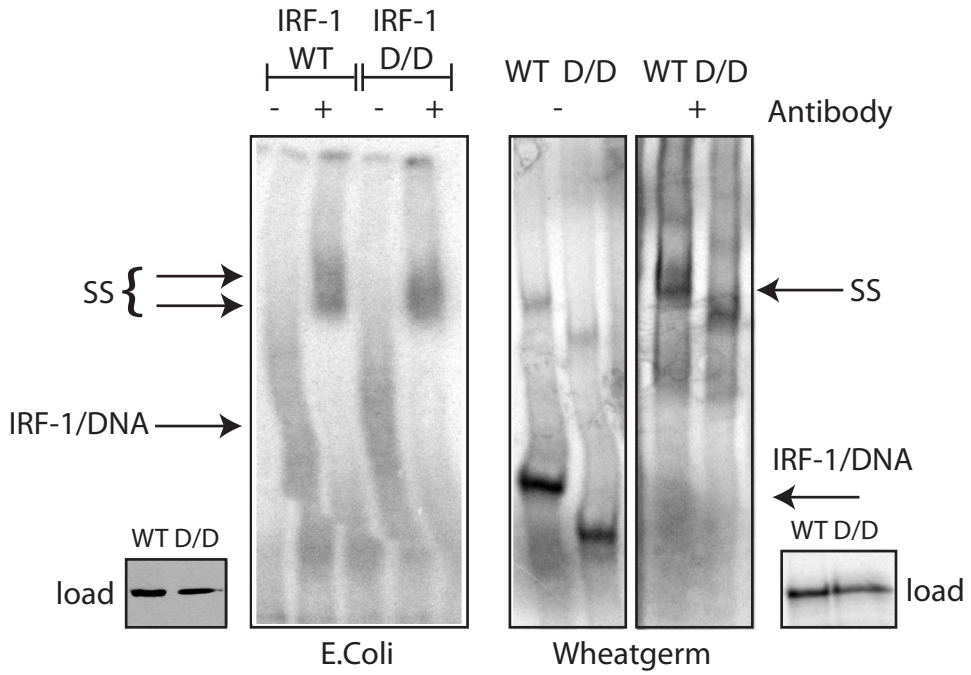

Figure 4.10: Mechanism of IRF-1 T311D/S317D enhanced DNA binding: Direct or indirect conformational change. IRF-1 WT and T311D/S317D were expressed in *E.Coli* (left panel) and wheatgerm lysate (right panel) and binding to ^{32}P-C1 probe observed by EMSA. IRF-1 DNA complexes could be supershifted by anti-IRF-1 (BD Biosciences) (ss= supershifted complexes). No significant difference between IRF-1 binding for *E. Coli* expressed protein was observed across three experiments. DNA binding of IRF-1 expressed in wheatgerm extract was only compared once; in this experiment no difference in binding was observed.

4.2.4 Effect of p300 on IRF-1 DNA binding

IRF-1 has previously been shown to interact with the co-factor p300 [67], [130] although the effect of this interaction on IRF-1 DNA binding has never been investigated. p300 is a histone acetylase, and so the effect of addition of acetyl coA to the binding mixture to allow p300 to acetylate IRF-1 was also studied.

In this experiment, p300, expressed in reticulocyte lysate, was incubated with IRF-1 WT and IRF-1 D/D and C1 probe. Acetyl CoA was also included in the mix in some tubes. The results of this experiment are shown in Fig 4.11. Addition of p300 to IRF-1 modestly enhanced its DNA binding ability. For IRF-1 WT, the increase in binding was 1.2 fold, for IRF-1 D/D, 1.4 fold. Further addition of the p300 substrate acetyl CoA resulted in another moderate increase in DNA binding. For IRF-1 WT, the binding was 1.3x binding in the absence of p300, for IRF-1 D/D, 1.5x. Enhanced DNA binding is more evident for IRF-1 T311D/S317D (illustrated in Fig 4.11 lower panel). This could argue in favour of the negative charge improving binding of positive co-factors; as described in Fig 4.8C. As addition of acetyl CoA further enhances DNA binding, it is possible that acetylation of IRF-1 stabilises the favourable DNA binding conformation. This experiment does, however, need to be repeated to confirm these findings; enhanced binding as a result of p300 addition, and the increased susceptibility of IRF-1 T311D/S317D to this effect has been observed in two independent experiments, while the effect of inclusion of acetyl CoA has only been performed once. In this experiment, no HDAC inhibitors were used. If they were included in future experiments, the results might be more obvious

4.2.5 Comparison of IRF-1 Binding at Naturally Occurring Promoters

Next, probes using the IRF-1 binding element of other naturally occuring promoters were compared to see if the effects of IRF-1 phosphorylation are similar at all promoters. Probes comprising the *ISG15*, *caspase 8* and *TLR3* promoters had already been created in the lab and their binding of IRF-1 confirmed. Therefore, these probes were used here.

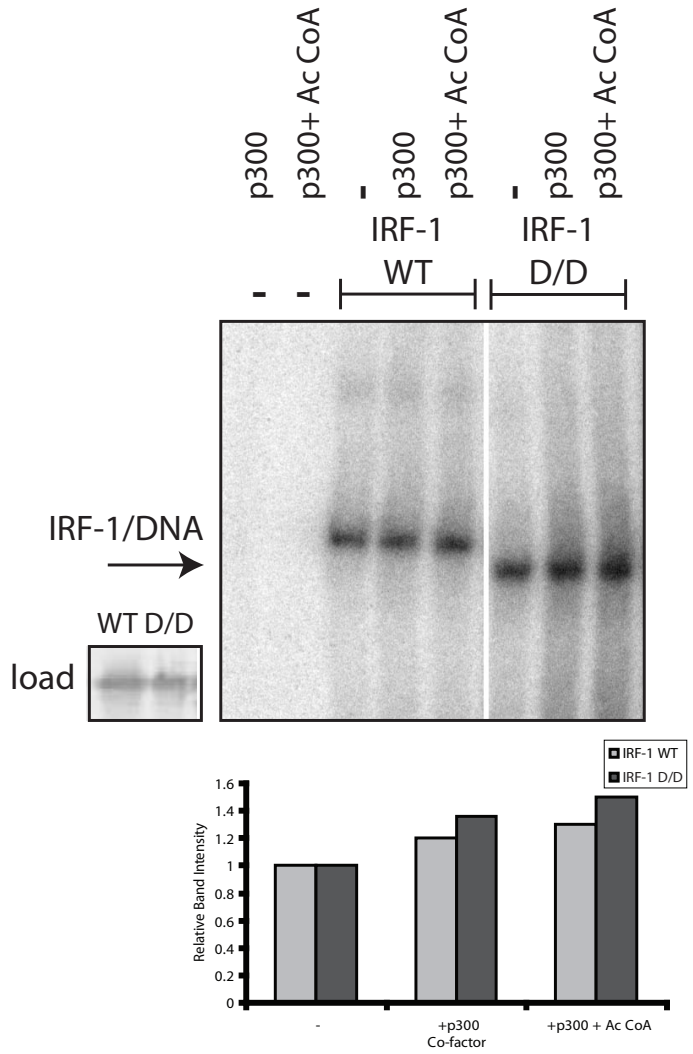

Figure 4.11: Effect of p300 on IRF-1 DNA binding. *Upper panel*: Cofactor p300 was included in EMSA. 4μl rabbit reticulocyte lysate expressing EV, IRF-1 WT or T311D/S317D was incubated with 3μl EV (lanes 3,6) or p300-expressing reticulocyte lysate (lanes 1,4,7) while binding probe (30mins, room temp). For acetylation reaction (lanes 2,5,8), EV/IRF-1 WT/IRF-1 T311D/S317D and p300 reticulocyte lysate were mixed with 2μM acetyl CoA and incubated at 30°C, 10mins for acetylation and binding then 20mins, room temp, to complete binding. *Lower panel*: Intensity of IRF-1-DNA complexes was determined by densitometry using Image J, normalised to binding in the absence of p300 and plotted on a graph. Enhanced binding of IRF-1 WT and further enhanced binding of IRF-1 T311D/S317D as a result of addition of p300 has been observed in two independent experiments. The effects of inclusion of acetyl CoA have only been analysed once.

For *ISG15* and *caspase 8* promoters, binding of IRF-1 T311D/S317D was significantly more stable (1.7x and 1.8x respectively). At the *TLR3* promoter, it seems that IRF-1 WT binds with more stability, however this was only performed once (Fig 4.12).

More stable binding of IRF-1 WT than IRF-1 T311D/S317D at the *TLR3* promoter would imply the regulation is through co-factor binding (as discussed above and in Fig 4.8C), and not simply through the negative charge causing a direct conformational change in the protein (Fig 4.8A). This is because despite IRF-1 T311D/S317D's lower affinity for the *TLR3* promoter sequence, its transactivatory activity at this promoter is higher than IRF-1 WT (Fig 4.2A). An explanation for this discrepancy would be the absence of the necessary co-factors in the reticulocyte lysate. Even if the result at the *TLR3* promoter is not reproducible, earlier results where transactivatory activity at the same promoters in different cell lines is differentially affected by the mutation (Fig 4.1), also suggest the regulation is at the level of co-factor binding.

4.2.6 Insights into IRF-1 DNA Binding from Antibody Supershift

It has been very noticible in these EMSAs that after supershift with anti-IRF-1 antibody, a DNA-IRF-1 doublet appears, for example see Fig 4.7A. The simplest explanation is that IRF-1 binds DNA as a dimer, and that the lighter band is dimer with one antibody bound; the heavier band is dimer with one antibody bound to each IRF-1 molecule.

To test this theory, a titration of anti-IRF-1 antibody was added to IRF-1 and DNA. It was expected that at lower concentrations of antibody, any supershifted complexes would have one antibody bound, i.e. would be in the lower position, and as the concentration increased, more complexes would bind two antibodies until all complexes were in the upper position.

As shown in Fig 4.13, this is not the case. At the lowest antibody concentrations, only the higher (heavier/larger) band is present. Then, with increasing antibody concentration, the lower (lighter/more compact) band apppears, and eventually an equilibrium of about 50:50 is reached.

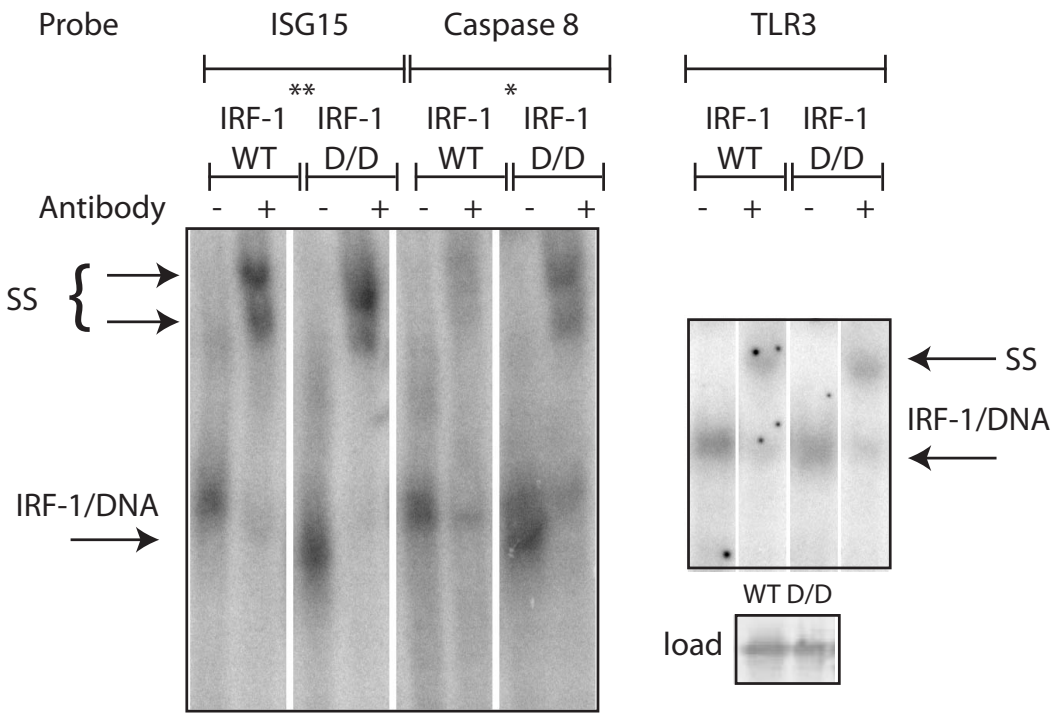

Figure 4.12: Comparison of IRF-1 binding at naturally occuring promoters. IRF-1 WT and T311D/S317D was expressed in rabbit reticulocyte lysate. Binding of IRF-1 to ^{32}P-labelled probe based on naturally occuring *ISG15*, *caspase 8* and *TLR3* promoters was observed by EMSA. IRF-1-DNA complexes could be supershifted by anti-IRF-1 antibody (BD Biosciences) (ss = supershifted complexes). Load was detected by western blotting of reticulocyte lysate using anti-IRF-1 (Santa-Cruz, C20). Binding of IRF-1 T311D/S317D to the *ISG15* and *caspase 8* promoters was significantly more stable across three experiments (* p=$<$0.05, ** p=$<$0.01 by paried t test). The comparison of binding to the *TLR3* promoter has only been performed once.

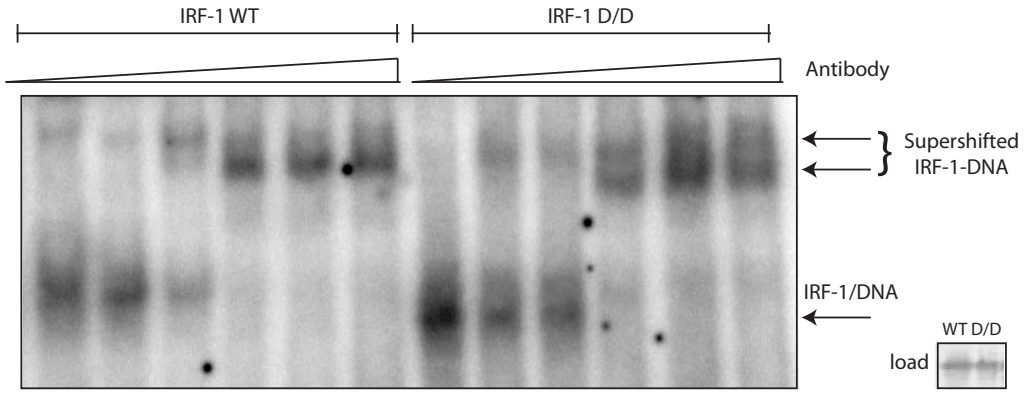

Figure 4.13: Investigating the doublet of DNA-bound IRF-1 appearing after supershift. Rabbit reticulocyte lysate-expressed IRF-1 WT or T311D/S317D was incubated with ^{32}P-labelled C1 probe in an EMSA reaction along with a titration of anti-IRF-1 antibody (BD Biosciences). Titration was: 6.25, 12.5, 25, 62.5, 250, 500 μg of antibody per reaction. This experiment has only been performed once.

There are various explanations for these observations, depending on whether IRF-1 binds DNA as a monomer or dimer. Both are observed in the literature [3], [164], although for different lengths of promoters. For a dimer, anti-IRF-1 could initially bind to only one molecule in the complex creating the single supershifted band observed. Subsequently, when the antibody concentration is high enough (at 0.25ul per reaction in this case), it could bind to the second IRF-1 molecule. Instead of producing a slower migrating band, if the antibody caused a conformational change in the complex, a higher motility band would be formed. For example, binding of antibody to IRF-1 could cause IRF-1 to adopt a conformation that forces the DNA to bend further. As this kind of conformation is likely to be fairly unstable, the equilibrium would never reach 100%; indeed, from the EMSA, it seems that a 50:50 state is optimal.

Alternatively, if IRF-1 binds monomerically to the DNA, the doublet could be produced if two different states of IRF-1-DNA exist. One state could be more compact, but less favourable, and thus is not clearly seen before supershifting. However, the binding of antibody could stabilise this state and so, after supershift, and above a certain concentration of antibody, this higher motility DNA-IRF-1-antibody complex could appear along with the more stable complex.

4.3 Discussion

In this chapter, the effects of the C-terminal phosphorylation of IRF-1 induced by IFN-γ have been investigated using phosphomimetic mutants. Phosphomimetic mutants generally have enhanced transactivatory potential at various promoters compared to IRF-1 WT, although this is cell line dependent and promoter. Moreover, IRF-1 T311D/S317D is also more resistant to inhibition by IRF-2.

IRF-2 is a repressor of IRF-1 activity, although there is some debate about its mechanism of action. An intriguing theory, put forward by Senger *et. al.* (2000) ([165]), is that IRF-2 prevents recruitment of the CBP/p300 co-activator and subsequently RNA Pol II to the promoter. They propose IRF-2 is present along with IRF-1 in the *IFN-β*

enhanceosome and that positively charged residues in the "repression domain" of IRF-2 repulse CBP. Furthermore, they show that IRF-3(5D), a more transcriptionally active form of IRF-3 known to have higher affinity for CBP/ p300, is only weakly inhibited by IRF-2. IRF-3(5D) contains 5 S→D mutations in the C-terminus and it was suggested that the increased negative charge created a favourable microenvironment for CBP/p300 binding [165]. The inhibition of IRF-2 repression for IRF-1 T311D/S317D is less obvious than for IRF-3(5D) but perhaps this is due to the presence of only two phosphomimetic mutations compared to IRF-3(5D). It would be useful to repeat the competition experiments for IRF1/2 at the *IFN-*β promoter rather than at the IRF-E/TLR3 promoters. It may be that in the context of the enhanceosome formed at *IFN-*β promoter, the relaxation of repression is most clearly seen.

The discovery that phosphorylation enhanced transcriptional activity prompted an investigation into the mechanism underlying this effect. EMSAs were used to study the DNA binding of IRF-1 WT and mutants. the dual T311D/S317D phosphomimetic mutants has enhanced DNA binding and, with repeated experiments, it may be possible to show that T311D and S317D mutations also have a positive effect on DNA binding (Fig 4.7). When naturally occuring promoters were assayed, promoter specific differences in relative affinities for IRF-1 WT and T311D/S317D were observed, although at this stage, these cannot be said to be statistically significant, despite being reproducible. ChIP studies in cells transfected with IRF-1 WT and T311D/S317D would allow comparison of relative promoter occupation. This would give some insight into the spectrum of promoters preferentially bound by IRF-1 T311D/S317D and so predictions could be made about which genes would be upregulated by this species after IFN-γ treatment. Looking to the future, this could inform us about likely side effects of activating IRF-1 by phosphorylation at this site.

It is also obvious from Fig 4.7 that IRF-1 T311D/S317D has a higher motility than IRF-1 WT. This could be an indication of a conformational change in the mutant that makes the protein more compact and allows it to move faster through the native EMSA gel. An alternative explanation would be that the two extra negative charges introduced by the mutation cause the protein to move faster towards the positive electode. This is less

likely as a very precise jump is observed. If all phosphorylation events caused such large jumps, phosphorylated protein from reticulocyte lysate would appear as a large smear on the gel rather than as a fairly resolved band. In addition, if the charge was the major factor causing the shift, IRF-1 S317D and T311D would be expected to be the same, and intermediate, in motility. This is not the case.

There are a number of mechanisms by which phosphorylation could cause enhanced DNA binding. If purified IRF-1 were being used, these would be limited to intrinsic conformational changes (Fig 4.8A&B). However, since rabbit reticulocyte lysate was being used to make the protein, other factors were present. This opened the possibility that interaction with a positive or negative cofactor could be modulating DNA binding activity (Fig 4.8C&D). A peptide competition EMSA suggested that enhanced interaction with a positive cofactor was responsible for the enhanced DNA binding of IRF-1 T311D/S317D (Fig 4.9 and 4.8C). Consistent with this, expression of IRF-1 in two different systems, *E.Coli* (His-purified IRF-1) and wheatgerm lysate (untagged IRF-1, unpurified) (both lacking the factors present in reticulocyte lysate) resulted in binding of IRF-1 WT and T311D/S317D that was more similar than in reticulocyte lysate (Fig 4.10A).

Since IRF-1 T311D/S317D was less susceptible to inhibition by IRF-2, which, as described above, may involve enhanced cofactor p300/CBP interaction, p300 was included in the DNA binding reaction. Addition of p300 enhanced the binding of IRF-1 to DNA, and this was more pronounced for IRF-1 T311D/S317D. DNA binding could be further augmented by the addition of acetyl CoA to the reaction (Fig 4.10B). Thus, p300 may bind to, and acetylate IRF-1 in order to enhance its DNA binding and transcriptional activity.

In support of this, it has previously been shown that, not only does p300 bind to the IRF-1 enhancer *in vitro* [67], but phosphorylation of IRF-1 at 317S and 308S enhances p300 binding to peptides from the Mf1 domain (as suggested by peptide competition EMSA) (Fig 4.14). Further, IRF-1 is a substrate for p300 acetylation *in vitro* [126]. This is similar to the situation for p53 where phosphorylation of Thr18 and 20 (close to the LXXLL motif) enhances p300 binding, resulting in sequence specific DNA dependent acetylation and stabilisation of the p53-DNA-p300 complex [166]. Thus, the interaction

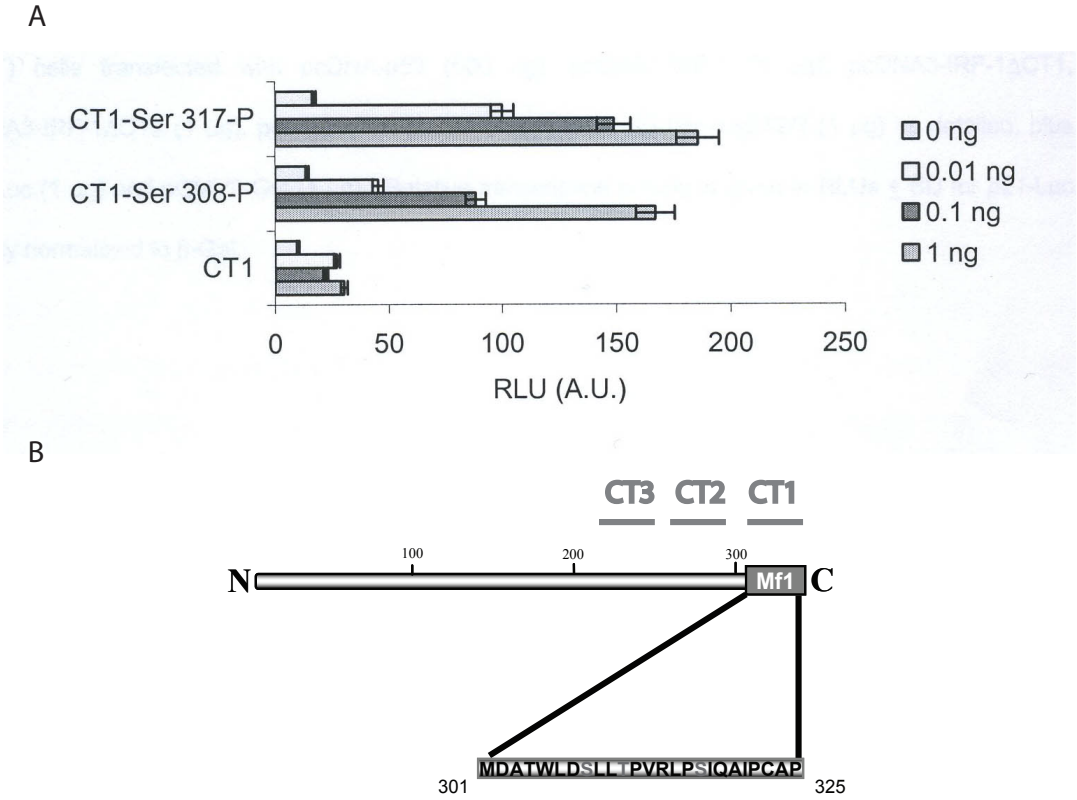

Figure 4.14: C-terminal phosphorylation of IRF-1 enhances p300 binding *in vitro*. (A) Biotinylated IRF-1 C-terminal 20aa peptide (CT1), or phosphorylated C-terminal 20 aa peptide (CT1-Ser317-P/-Ser309-P) was bound to streptavidin coated ELISA wells. A titration of p300 protein (0-1ng) was incubated in the wells, and binding of p300 to IRF-1 peptide was detected by anti-p300 antibody (Santa-Cruz) and quantified by chemiluminescence (R.L.U. +/- SD). (Experiment performed by David Dornan). (B) Diagram of IRF-1 showing location of the three p300 interagtion sites CT1, 2 and 3 determined by David Dornan [67].

of IRF-1 with p300 warrants further investigation.

Interestingly the Mf1 domain is not the highest affinity interaction site in IRF-1 for p300. Two motifs within IRF-1 (CT2 and CT3) (Fig 4.14B) were shown to have higher affinity binding to p300; these domains were shown to be required for p300 to stimulate IRF-1 activity at the IFN-β promoter. [67]. Our current hypothesis is that binding of p300 to the C-terminus (Mf1/CT1 domain) regulates its binding to the higher affinity CT2 and CT3 domains, perhaps by causing conformational change that exposes these p300-binding sites. This would allow the interaction of p300 and IRF-1 to be tightly controlled, for example, C-terminal phosphorylation of IRF-1 in response to an activatory signal (e.g. IFN-γ) could create a binding site for p300. Binding of p300 to IRF-1, and potentially acetylation of IRF-1 by p300, could cause a conformational change in IRF-1, exposing the previously occluded CT2 and CT3 sites. Binding of p300 to these sites may then enhance IRF-1 DNA binding and transactivatory activity.

CBP/p300 is a broad-spectrum transcriptional cofactor which is thought to act through a variety of mechanisms: It can bridge transcription factors and basal transcription machinery; provide a scaffold for assembly of multiprotein initiation complexes or acetylate chromatin and transcription factors to enhance transcriptional activity [167]. Such effects could be promoter specific and are not necessarily mutually exclusive. In the IFN-β enhanceosome, IRF-1, along with other factors, recruits p300 to the promoter where it bridges the enhanceosome and RNA Pol II [130]. Such a process could be responsible for the enhanced transactivatory activity of IRF-1 T311D/S317D, but since acetylation is important, and DNA-binding activity is directly affected, it is likely that p300 has additional roles here. The repressor activity of IRF-1 is not affected by T311/S317 phosphorylation suggesting that co-repressor binding to IRF-1 is regulated by different means.

In order to more clearly define the IRF-1-p300 interaction, the effects of p300 on IRF-1 DNA binding should first be repeated with purified proteins in the EMSA. Then, the interaction of p300 with IRF-1 WT, IRF-1 T311D/S317D, IRF-1 T311D and IRF-1 S317D full length proteins should be investigated by immunoprecipitation and ELISA to confirm that C-terminal phosphorylation does enhance the interaction. Next, the effect of acetylation on DNA binding should be more thoroughly defined using *in vitro*

acetylation assays and the location of the acetylation determined using IRF-1 peptides and domains or mass-spectrometry. The relative importance/role of p300 binding and acetylation of IRF-1 in cells could be assessed by modulation of p300 expression (transient p300 expression and siRNA knock down) and inhibition of HAT (acetyl transferase) activity (ΔHAT-p300 expression and p300 inhibitor treatment). Finally, mutants of IRF-1 that cannot bind p300 (perhaps T311A/S317A) and non-acetylatable mutants K$\rightarrow$R should exhibit reduced DNA-binding activity.

Acetylation could cause direct conformational change in IRF-1 which stabilises it in a DNA-binding conformation, or it could modulate binding of other factors which could affect IRF-1 activity. It should be possible to use biophysical techniques such as intrinsic fluorescence or thermal denaturation to determine if conformational change in IRF-1 results from the phosphomimetic mutation/phosphorylation or acetylation. Unfortunately these techniques require substantial amounts of purified protein which is not compatible with expression in reticulocyte lysate. Purifying protein from *E. Coli* is the obvious solution, however, the results will need to be carefully considered as *E. Coli* lack the protein phosphorylation machinery of mammalian cells, and thus IRF-1 may not be in its native conformation, especially if important intramolecular interactions are missing. In addition, *E. Coli* contain proteases which rapidly degrade IRF-1 as quickly as 30 mins after induction (Dr. Vikram Narayan, unpublished observations) and any purified protein is a mixture of full length IRF-1 and different degradation products which may have different conformations if important interactions are lost.

It is likely that other factors apart from p300 are differentially bound to WT and phosphorylated IRF-1. In fact, Hsp70 has recently been shown to bind more strongly to the WT Mf1 peptide (Dr. Vikram Narayan, unpublished observations). This observation is considered in more detail in the discussion.

Conventionally, screening for binding partners would involve expression of exogenous tagged protein in cells and purification of protein-binding partner complexes by, for example, tandem affinity purification. For IRF-1, this technique is not possible as studies in the lab have determined that the expression levels in cells are not high enough. For this study, stable cell lines were created in an attempt to create a population of efficient IRF-1

expressing cells, but these lost IRF-1 expression very quickly, despite maintainence in selective medium. Therefore, an alternative screening technique has been developed for IRF-1 [144]. IRF-1 peptide aptamers are immobilised on a suppport to create an affinity purification column, and cell lysate is passed over the column to find interacting proteins. Proteins eluted from the column are identified by mass spectrometry. This technique could be used to identify phosphospecific binding partners for IRF-1. For p53, acetylation by p300 affects cofactor binding[168]. If the acetylation site of IRF-1 can be mapped, the binding partners of acetylated peptide could be identified.

In conclusion, IFN-γ-induced phosphorylation of the IRF-1 Mf1 domain has been shown to enhance its transcriptional activatory activity. This is most likely through creation of a binding site for p300 which enhances DNA binding of IRF-1, perhaps through acetylation, and might, by analogy to events in the IFN-β enhanceosome [130], recruit RNA Pol II.

Chapter 5

Effects of C-terminal phosphorylation of IRF-1 on tumour suppressor activity

Since IRF-1 is an effective tumour suppresssor through its regulation of downstream genes, and phosphorylation of IRF-1 impacts on its transactivatory activity [119], [120], Chapter 4, the effect of C-terminal phosphorylation of IRF-1 on its tumour suppressor activity was investigated.

5.1 Anchorage-dependent Colony Formation Assays and Cell Adhesion Assays

Anchorage-dependent colony formation assays measure the ability of cells to establish and grow colonies in the presence of a substrate. They are effectively a measure of cell survival and long-term cell proliferation. Cells are transfected with empty vector control (EV) or IRF-1 WT or T311D/S317D and seeded at a low density in the presence of geneticin to select for cells containing the expression plasmid. The expression plasmid contains a neomycin gene which confers resistance to geneticin. The concentration of geneticin that will kill untransfected cells varies depending on cell line. Therefore, before carrying out the colony formation assays, kill curves were constructed for A375

and H1299 cells to determine the optimum geneticin concentration. Untransfected cells were plated at low density and incubated in medium containing various concentrations of geneticin. At a number of time points, the survival of the cells is estimated. The optimum concentration of geneticin for colony formation assays is the lowest concentration required to kill all untransfected within 5 days. For H1299 cells, this is 600-800μg/ml whereas for A375 cells, 1200-1500μg/ml (Fig 5.1).

Once the optimum geneticin concentration had been established, cells were transfected for 24 hours with pcDNA3 EV, IRF-1 WT or IRF-1 T311D/S317D, then seeded at low density in the appropriate concentration of antibiotic. The medium was changed after four days and the geneticin refreshed. After 10 days, colonies were fixed and stained with Giemsa for counting. For both H1299 (Fig 5.2) and A375 (Fig 5.3) cells, IRF-1 is an efficient suppressor of anchorage-dependent colony formation. In both cases, IRF-1 T311D/S317D appears slightly more effective than IRF-1 WT, but this difference is not significant. Transfection of A375 cells with IRF-1 WT resulted in a average 3.4 fold decrease in the number of colonies and transfection with IRF-1 T311D/S317D a 5.7 fold decrease (Fig 5.3A). For H1299 cells, IRF-1 T311D/S317D was even more effective as its transfection resulted in a 14 fold decrease compared to a 3.7 fold decrease with IRF-1 WT(Fig 5.2A). However, when the sizes of the colonies are measured, in H1299 cells, both IRF-1 WT and IRF-1-T311D/S317D transfected cells show a reduction in colony sizes, although only the reduction for IRF-1 T311D/S317D is significant (Fig 5.2B), whereas in A375 cells, there is no significant difference in colony size (Fig 5.3B). Representative images of colonies obtained are shown in Fig 5.2C and 5.3C.

For H1299 cells, this implies that the ability of IRF-1 to suppress anchorage dependent-colony formation is dependent on its ability to inhibit cell proliferation (because IRF-1 treated cells produce smaller colonies). IRF-1 T311D/S317D is consistently, but not significantly, more effective at colony formation suppression in both cell lines. Further experiments using larger numbers of cells could be appropriate to clarify this since, in some cases, no colonies were established on IRF-1 T311D/S317D-transfected plates, and therefore, the difference in relative numbers of colonies may be underestimated. If the difference between IRF-1 WT and T311D/S317D colony formation suppression was sig-

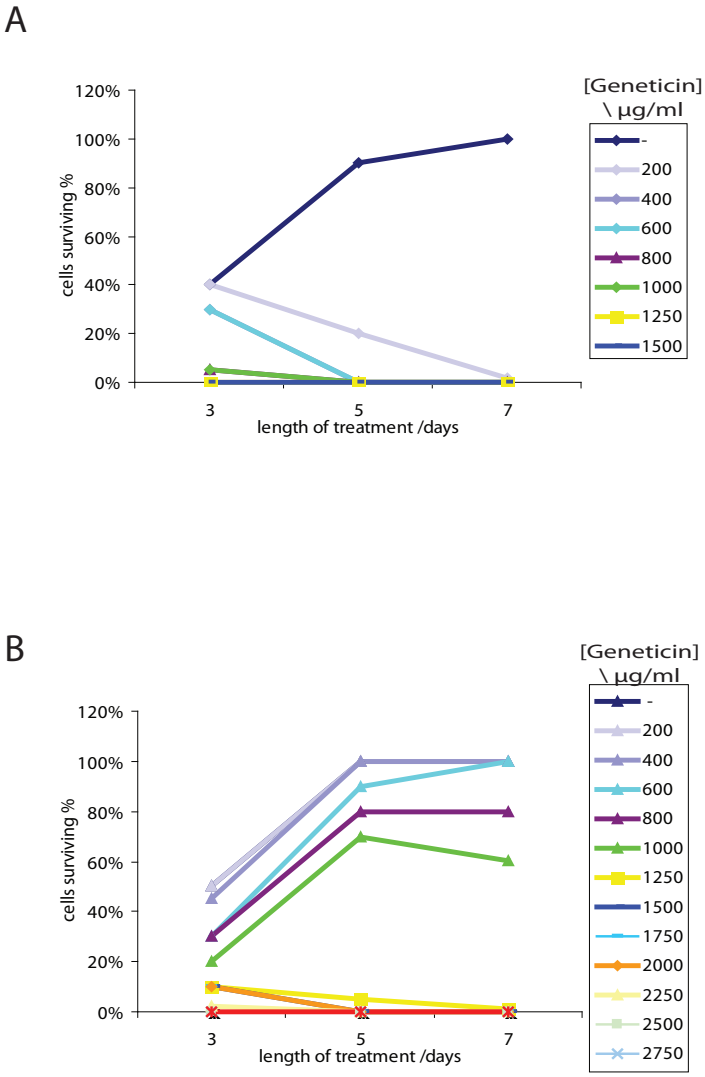

Figure 5.1: Kill curves to determine optimum geneticin concentration for H1299 and A375 cell colony formation assays. (A) H1299 cells or (B) A375 cells were plated at low density and incubated with a titration of geneticin. Cells surviving were estimated after 3, 5 and 7 days.

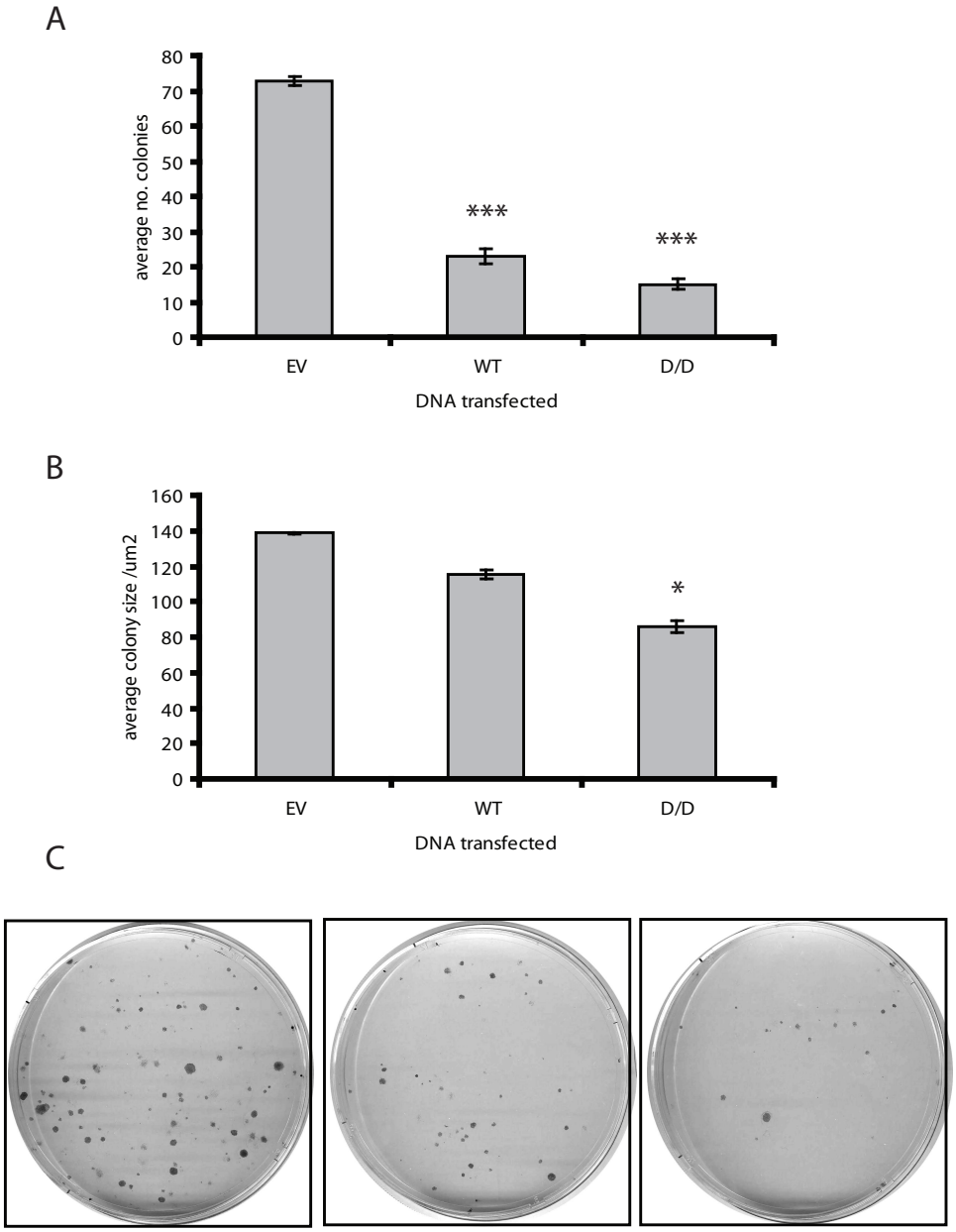

Figure 5.2: Effect of IRF-1 on anchorage dependent colony formation for H1299 cells. Cells transfected with pcDNA3-EV, -IRF-1 WT or -IRF-1 T311D/SD317D were seeded in geneticin (750μg/ml) and grown for 10 days before methanol fixation and staining with Giemsa stain. (A) Cells were counted using Image J. (B) Average size of colonies was estimated using Image J. Significant differences between colony numbers/sizes compared to EV by randomised block ANOVA followed by Tukey's test are indiciated. (* p=<0.05, *** p=<0.001). Results expressed as mean +/- standard deviation for duplicates. (C) Representative images of colonies from EV, IRF-1 WT and IRF-1 T311D/S317D-transfected cells. Data representative of three independent experiments.

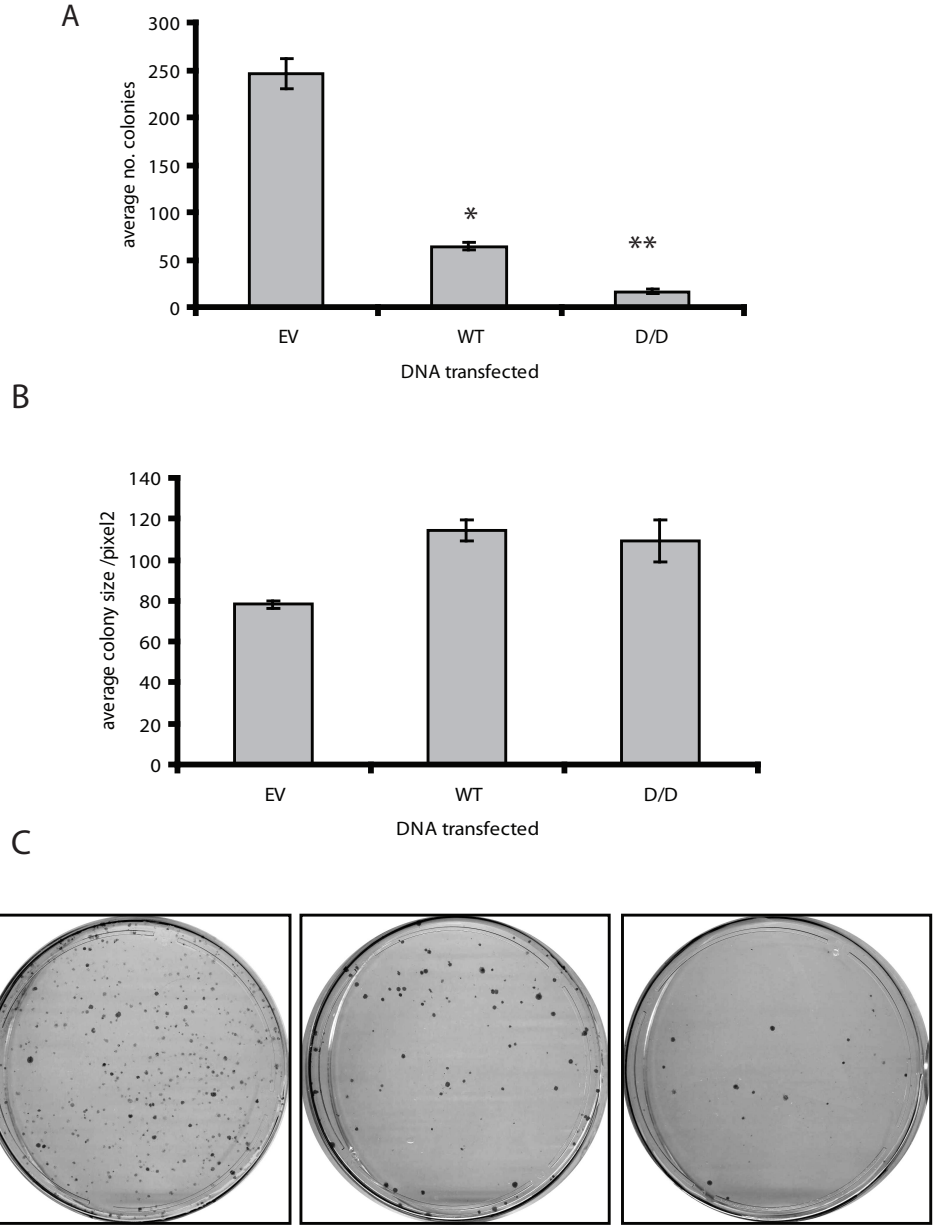

Figure 5.3: Effect of IRF-1 on anchorage dependent colony formation for A375 cells. Cells transfected with pcDNA3-EV, -IRF-1 WT or -IRF-1 T311D/SD317D were seeded in geneticin (1500μg/ml) and grown for 10 days before methanol fixation and staining with Giemsa stain. (A) Cells were counted using Image J. (B) Average size of colonies was estimated using Image J. Significant differences between colony numbers/sizes compared to EV by randomised block ANOVA followed by Tukey's test are indiciated. (* p=<0.05, ** p=<0.01). Results expressed as mean +/- standard deviation for duplicates. (C) Representative images of colonies from EV, IRF-1 WT and IRF-1 T311D/S317D-transfected cells. Data representative of three independent experiments.

nificant, the enhanced activity of IRF-1 T311D/S317D could be due to either its effects on cell growth (demonstrated by its effects on colony size), or due to an additional activity, for example, affecting the initial stages of establishing a colony. For A375 cells, since the colonies on IRF-1 WT and T311D/S317D-transfected plates have fewer colonies (with IRF-1 T311D/S317D-transfected cells having the fewest), but similar-to-control sized colonies, it seems that in these cells, IRF-1 affects the initial survival, and not the rate of growth, of cells. Factors influencing the establishment of colonies could include apoptosis of cells, or reduced adhesion to substrate as a result of IRF-1 expression. To address this, a time course looking at rates of apoptosis at various points after IRF-1 transfection should be carried out.

As a tumour suppressor, IRF-1 should, if anything, enhance cell-substrate contacts, but, as fewer colonies are established by IRF-1 expressing cells, an adhesion assays was carried out to assess the effects of IRF-1 on cell-substrate adhesion. Preliminary results indicated that neither IRF-1 WT nor IRF-1 T311D/S317D have any effect on cell adherance to plastic (Fig 5.4), although a positive and negative control that enhance and reduce cell adhesion need to be sourced. Sialomucin complex (SMC) which reduces A375 cell adhesion to plastic could be used as a control. Its overexpression reduces adhesion and inhibition restores adhesion[169].

5.2 Anchorage-independent Colony Formation Assays

Anchorage-independent colony formation assays measure the ability of cells to establish and grow colonies in the absence of a substrate i.e. without attachment. This is a hallmark of transformed cells. Again cells are seeded at a low density and maintained in geneticin to select transformed cells. In these assays, however, the bottom of the well is covered with a layer of agar to provide a solid support that cells cannot adhere to. Cells are seeded in a methylcellulose mixture which is layered onto the agar. The viscosity of the methylcellulose prevents the cells moving and clumping together, but cannot be used by the cells as a substrate to attach to.

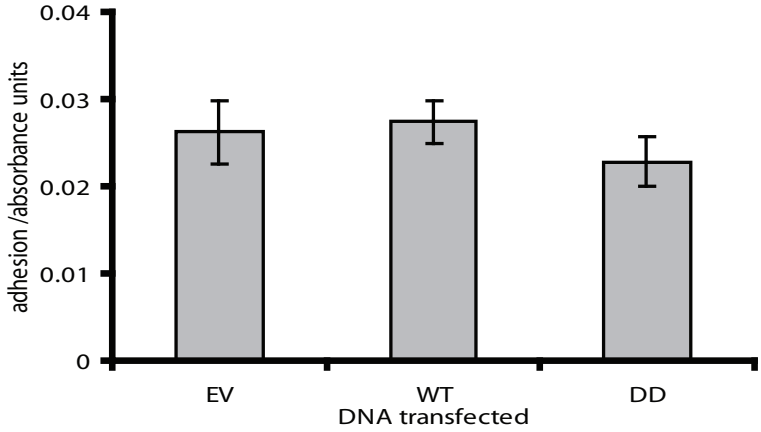

Figure 5.4: Effect of IRF-1 on cell-substrate adhesion. A375 cells were transfected with pcDNA3-EV, -IRF-1 WT or -T311D/S317D. After 24h, cells were harvested and allowed to readhere to plastic for 1h then washed and stained. Cells were lysed and absorbance of solubilised stain was measured to determine the level of adherance. Data from a single experiment. Results expressed as mean +/- standard deviation for duplicates.

HeLa and A375 cells were transfected for 24 hours with pcDNA3 EV, IRF-1 WT or IRF-1 T311D/S317D, then seeded at low density in methylcellulose containing the appropriate concentration of antibiotic. After 24 hours, to allow the cells to settle, images were taken to determine the average cell size. Minimum colony size was extrapolated from these data as a colony is taken to be at least 3 cells in area. After around 6 days, the colonies were photographed and the number of colonies per number of events (cells+colonies) was calculated. In A375 cells, IRF-1 reduces the frequency of single cells growing into colonies (>3 cells) in methylcellulose, and C-terminal phosphorylation of IRF-1 (T311D/S317D) may enhance this effect (although after three repeats, the difference between IRF-1 WT and IRF-1 T311D/S317D activity is not significant (Fig 5.6A). In HeLa cells, IRF-1 WT reproducibly but not significantly reduces the formation of colonies whereas IRF-1 T311D/S317D significantly reduces the number of colonies (Fig 5.5A). (HeLa cells were selected to compare to A375 as, unlike H1299 cells, these produce good colonies, and they respond to IRF-1 T311D/S317D in the same way as H1299 cells for luciferase reporter assays.) In both cell lines, IRF-1 reduces the proliferation of the cells, resulting in smaller colonies (Fig 5.5B, Fig 5.6B), but phosphorylation seems to have no further effect on this activity. Representative images of colonies are shown in Fig 5.5C and Fig 5.6C.

The reduction in the number of colonies in methylcellulose could be due to (1) the mitigated proliferation rate reducing the number of cells that have divided sufficiently to form colonies, (2) an initial barrier to colony formation imposed by IRF-1, (3) a reinstatement of the anchorage-dependence exhibited by non-transformed cells, or indeed, a combination of all three. Since the colony size of both IRF-1 WT- and T311D/S317D-transfected cells is similar, yet IRF-1 T311D/S317D-transfected cells appear to produce fewer colonies (although for A375 cells, further experiments need to be done to confirm a difference between IRF-1 WT and T311D/S317D as discussed for the anchorage-dependent assays), it would seem that proliferation control is important but not the only mechanism by which IRF-1 inhibits colony formation, and phosphorylation of IRF-1 enhances the unknown activity. Again, apoptosis and sensecence should be investigated.

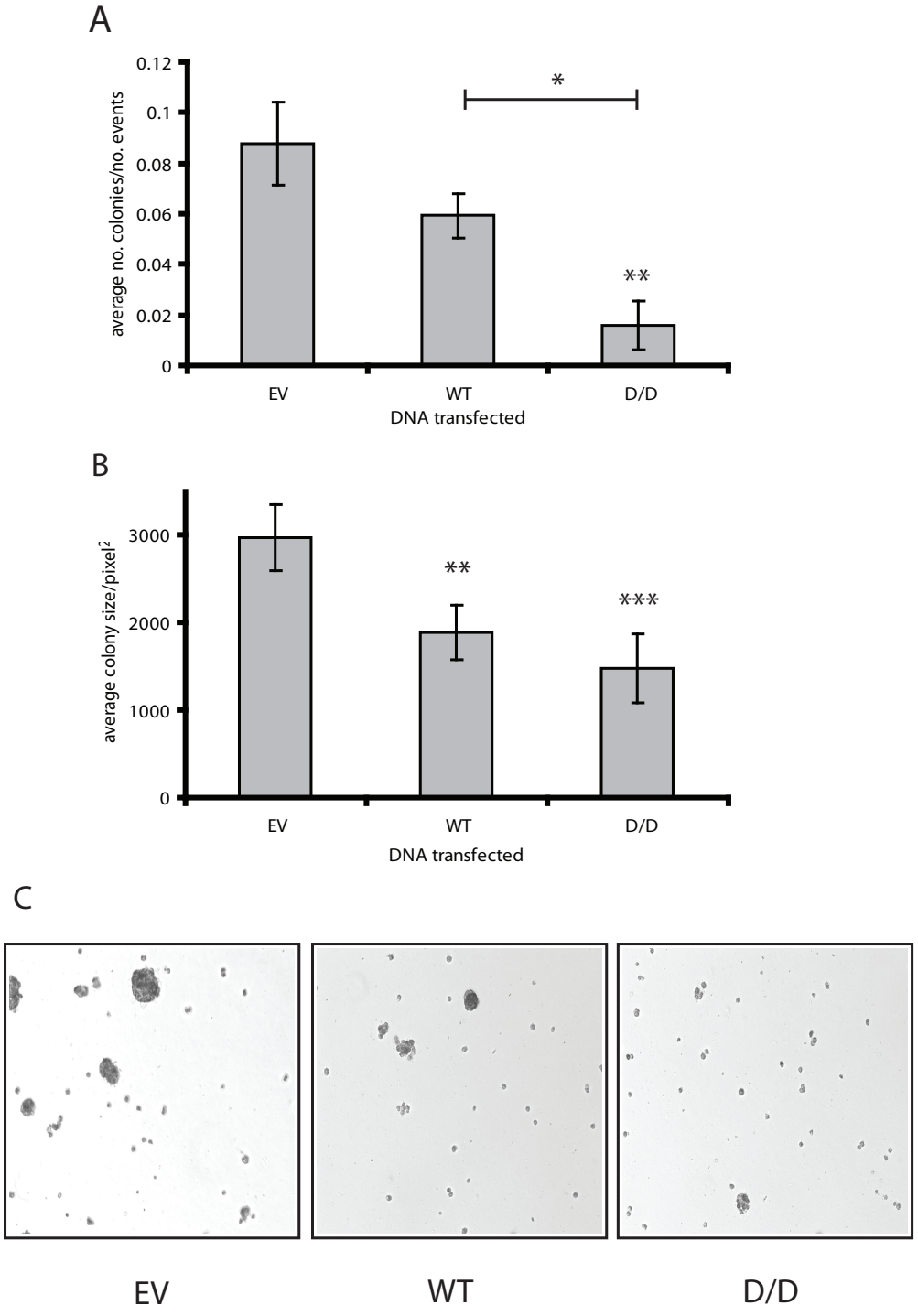

Figure 5.5: Effect of IRF-1 on anchorage independent colony formation in HeLa cells. (A) Anchorage independent colony formation assays were performed using pcDNA3-EV, -IRF-1 WT and -IRF-1 T311D/S317D-transfected cells seeded in 1.4% methylcellulose containing 1500μg/ml geneticin. Colonies were counted after 5-7 days using Image J. (B) Average size of colonies was estimated using Image J. Significant differences between colony numbers/sizes compared to EV by randomised block ANOVA followed by Tukey's test are indiciated. (* p=<0.05, ** p=<0.01, *** p=<0.001). Line indicates a significant difference between IRF-1 WT and DD-transfected cell colony size. Results expressed as mean +/- standard deviation for duplicates. (C) Representative images of colonies from EV, IRF-1 WT and IRF-1 T311D/S317D-transfected cells. Data representative of three independent experiments.

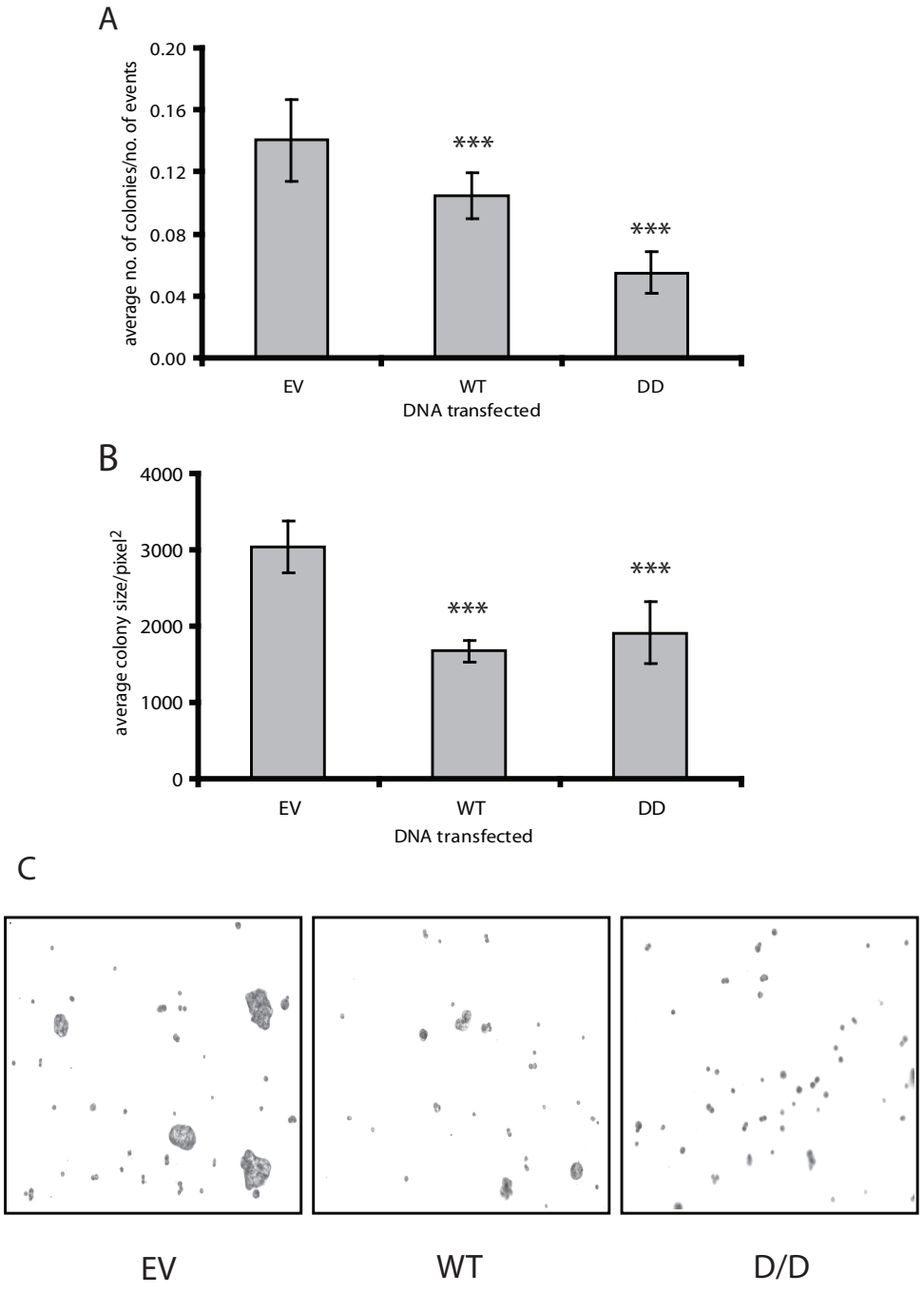

Figure 5.6: Effect of IRF-1 on anchorage independent colony formation in A375 cells. (A) Anchorage independent colony formation assays were performed using pcDNA3-EV, -IRF-1 WT and -IRF-1 T311D/S317D-transfected cells seeded in 1.4% methylcellulose containing 1500μg/ml geneticin. Colonies were counted after 5-7 days using Image J. (B) Average size of colonies was estimated using Image J. Significant differences between colony numbers/sizes compared to EV by randomised block ANOVA followed by Tukey's test are indiciated. (*** p=$<$0.001). Results expressed as mean +/- standard deviation for duplicates. (C) Representative images of colonies from EV, IRF-1 WT and IRF-1 T311D/S317D-transfected cells. Data representative of three independent experiments.

5.3 Proliferation, Cell Cycle Arrest and Senescence

5.3.1 Proliferation

Inhibition of proliferation of cells by IRF-1 was also examined in a proliferation assay. The colony size measured in the anchorage dependent colony formation assay suggested that the proliferation of H1299 cells was inhibited by IRF-1 WT and further inhibited by IRF-1 T311D/S317D, whereas, for A375 cells, proliferation might actually increase. To address this more directly, cells were transfected for 24 hours, then seeded at low density. After 1, 2 and 3 days growth, cells were stained, solubilised and the absorbance of stain in the solution was used as a measure of cell numbers. The experiment was only performed once once; in HeLa cells, IRF-1 may inhibit cell proliferation, but IRF-1 WT was more effective than IRF-1 T311D/S317D, suggesting that IRF-1 T311D/S317D could have an additional mechanism by which it inhibits colony formation (Fig 5.7A). For A375 cells, the proliferation of EV, IRF-1 WT and IRF-1 T311D/S317D cells was very similar, although a slight increase in proliferation caused by IRF-1 WT and T311D/S317D transfection is in agreement with the anchorage-dependent colony formation assay (Fig 5.7B). Selecting only IRF-1 expressing cells by geneticin treatment might give clearer results.

5.3.2 Cell Cycle Arrest

The inhibition of proliferation seen above could be a result of IRF-1 induced cell cycle arrest. Since IRF-1 upregulates the CDK inhibitors p21 [30] and p27[31], and down-regulates cyclins D and E and CDKs 2 and 4 [68], this seemed very plausible. To address this, HeLa and H1299 cells were transfected with pcDNA3 EV, IRF-1 WT or IRF-1 T311D/S317D. After 24 hours cells were fixed and cell cycle anaylsis by propidium iodide staining was carried out. However, only very subtle differences in profile between EV, IRF-1 WT and IRF-1 T311D/S317D transfections were observed. In both cell lines, IRF-1 WT causes a very modest arrest in G0/G1 phase and IRF-1 T311D/S317D a slightly more pronounced effect (Fig 5.8). It is not clear whether this effect is significant, and

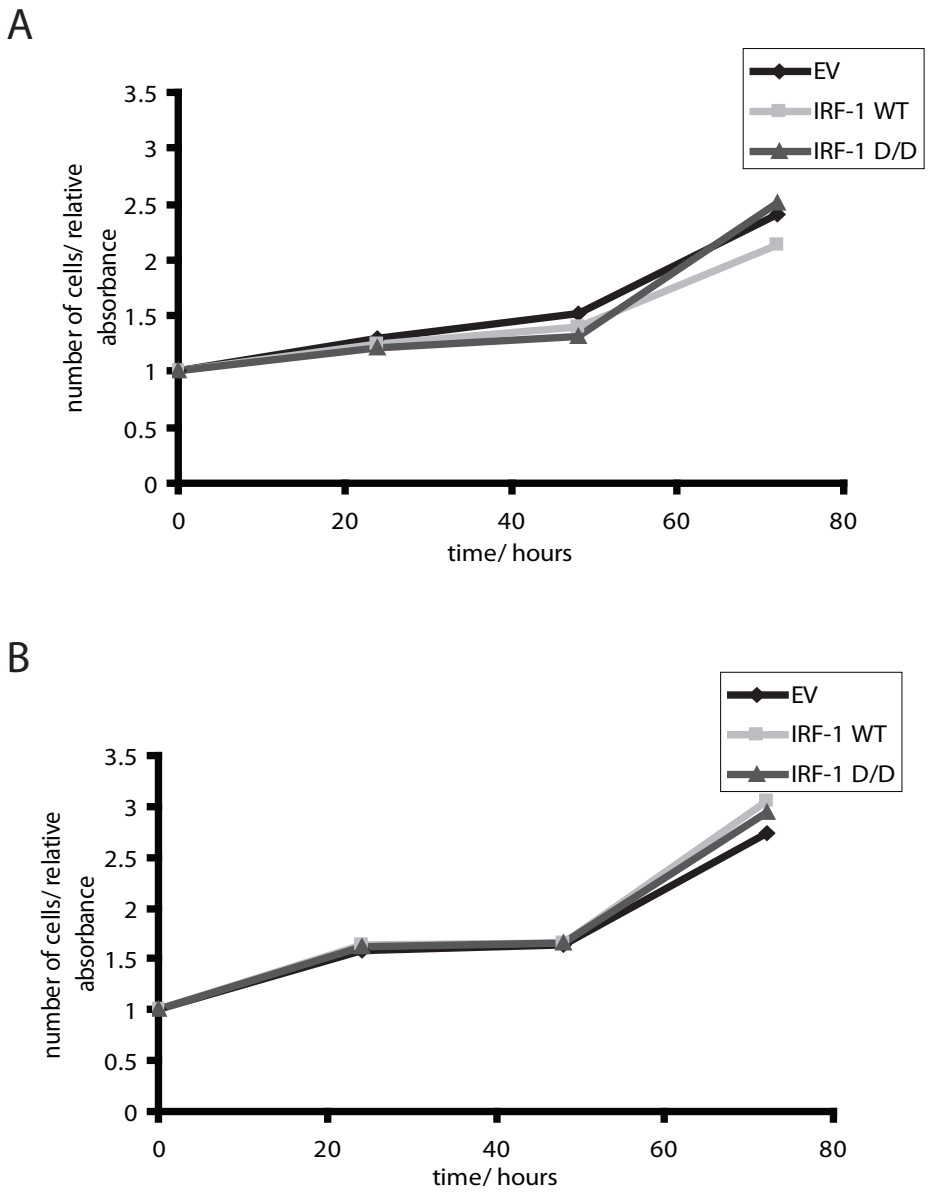

Figure 5.7: Effect of IRF-1 WT and T311D/S317D on cell proliferation. (A) HeLa cells (B) A375 cells. Proliferation of pcDNA3-EV, -IRF-1 WT and T311D/S317D-transfected cells was measured by fixing and staining cells after 1, 2 and 3 days of growth, then lysing cells and measuring the absorbance of the solubilised stain. Data representative of a single experiment.

since the experiment was only carried out once, repeats are needed.

5.3.3 Senescence

A candidate for the alternative mechanism by which IRF-1 also inhibits colony formation is senescence. Senescent cells have exited the cell cycle i.e. have undergone irreversible G1 arrest and so do not proliferate, but remain as viable cells. In endothelial cells, IRF-1 has been shown to mediate IFN-α induced senescence [60]. In the anchorage-independent colony formation assays, IRF-1 caused there to be fewer colonies per total cells without affecting the total number of cells. Therefore, if IRF-1 T311D/S317D causes greater initiation of senescence compared to IRF-1 WT, this would agree with the data from the methylcellulose assay. It would not, however, be in keeping with the conflicting data from the proliferation assay, which showed that IRF-1 WT reduced proliferation rates to a greater extent than T311D/S317D (Fig 5.8A).

Senescence was measured in A375 cells using a senescence-associated β-galactosidase staining kit. When the numbers of senescent cells were counted manually, the effect of IRF-1 WT transfection was variable but IRF-1 T311D/S317D caused an increase in the number of sensecent cells (Fig 5.9). This may mean that IRF-1 T311D/S317D enhances senescence but the assay is not reliably quantatative and was not repeated. Manual counting requires an arbitrary definition of a staining threshold above which a cell is considered senescent. Greater confidence could be achieved using fluorometric senescence assay where cleavage of a senescence-associated β-galactosidase substrate renders it fluorescent.

5.4 Inverse Invasion Assays

IRF-1 suppresses the *MMP9 promoter* [45], and inhibits metastasis *in vivo* [42], [23], [46], but its effects on the invasive potential of cells in *in vitro* assays have not yet been investigated. Here, MDA-MB-231 cells were transfected with IRF-1 WT and T311D/S317D

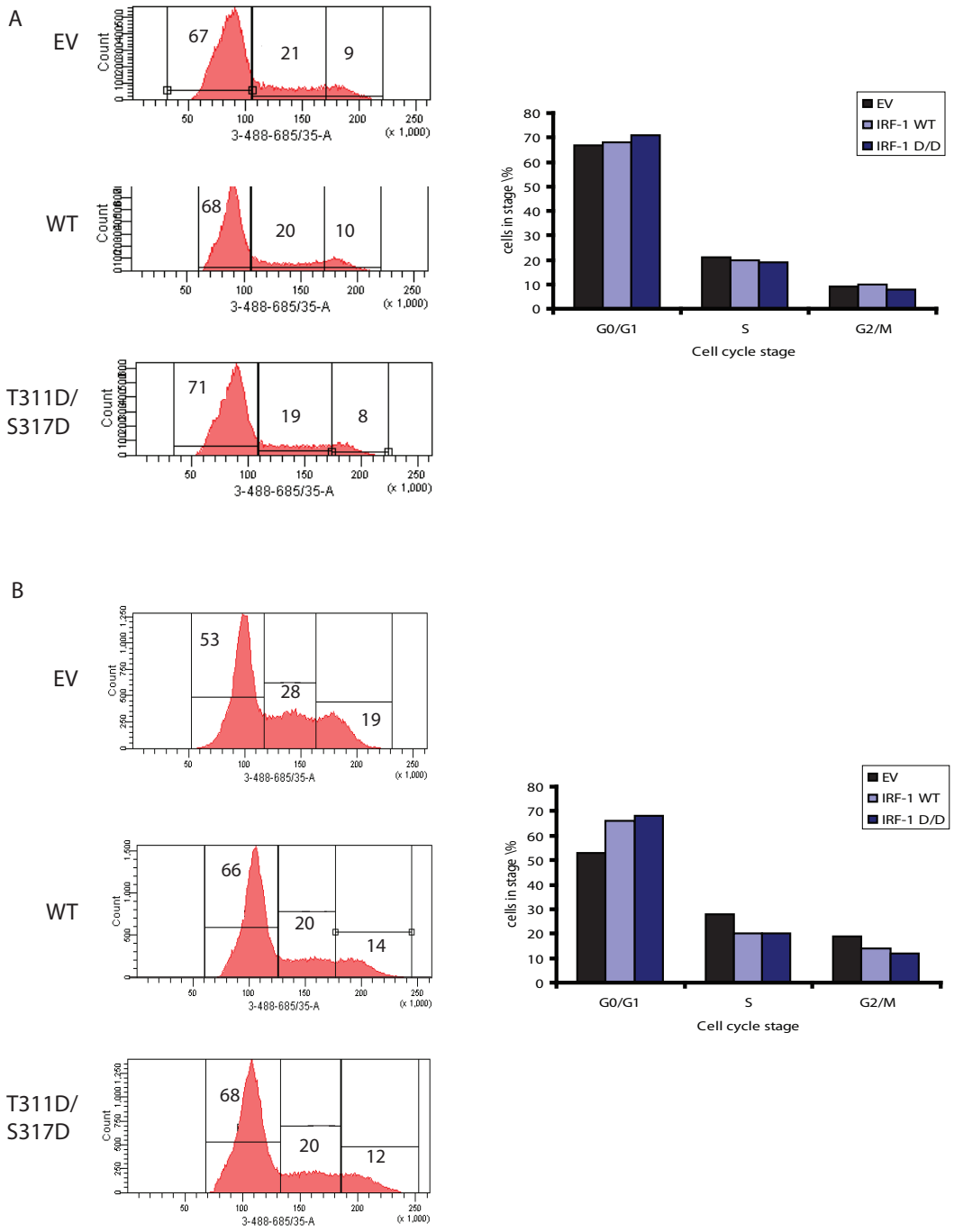

Figure 5.8: Effect of IRF-1 WT and T311D/S317D on cell cycle arrest. (A) HeLa and (B) H1299 cells were transfected with pcDNA3-EV, -IRF-1 WT or T311D/S317D. After 24h, cells were fixed and stained with propidium iodide then anaylsed by flow cytometry. Left panel displays cell cycle profile data, right panel shows a comparison of the percentage of cells at each cycle cycle stage for EV, IRF-1 WT and IRF-1 T311D/S317D. Data representative of a single experiment.

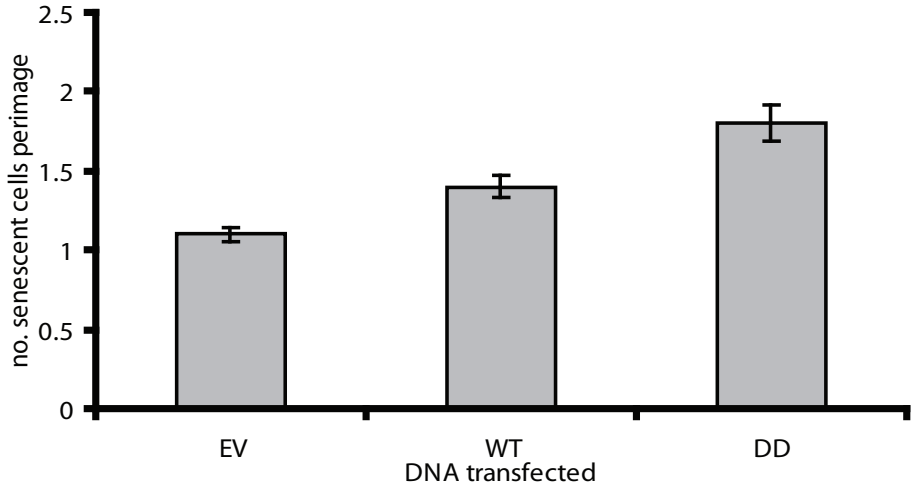

Figure 5.9: Effect of IRF-1 WT and T311D/S317D on senescence. Senescence levels in pcDNA3-EV, -IRF-1 WT and T311D/S317D-transfected A375 cells were estimated using a senescence-associated β-galactosidase staining kit (NEB). Results expressed as mean +/- standard deviation for duplicates. Data representative of a single experiment.

and the extent of their invasion through matrigel-filled transwells was measured. MDA-MB-231 cells are highly metastatic and so are very suitable for this assays. Lack of IRF-1 expression has been linked to metastatic phenotype, and IRF-1 is expressed at very low levels in MDA-MB-231 cells [23]. Therefore, transfection of IRF-1 into these cells should give a measurable response in this assay.

In the inverse invasion assay (Fig 5.10A), a matrix (matrigel) is placed in a transwell insert on top of a filter. The transwell is inverted and cells are seeded on the base of the filter. Once the cells have attached, the transwell is placed right-way-up in a tissue culture well containing medium without growth factors. Medium containing growth factors is pipetted on top of the matrigel to create a gradient which encourages the cells to invade upwards across the filter and into the matrix. After 3 days, the extent of invasion is measured by staining the cells and visualising them using a confocal microscope, taking images at 15μm intervals. Invasion of cells at each interval was expressed as a percent of the staining at the confluent monolayer on the filter.

The preliminary results indicate that IRF-1 inhibits invasion of MDA-MB-231 cells, and that IRF-1 T311D/S317D might be more effective than IRF-1 WT (Fig 5.10B&C). While it is possible to be confident in the findings of each individual assay, this assay will need repeated many times to have a statistically relevant data set. Before setting up multiple repeats, however, the time of the assay needs to be reduced as IRF-1's activity as a growth suppressor makes normalisation difficult; after a few days, the number of cells present on the monolayer is less for the IRF-1-transfected cells than the control. Since the amount of invasion is expressed as a percentage of the monolayer, the results are still relevant, however, it would be a more direct comparison to have confluent monolayers for each condition.

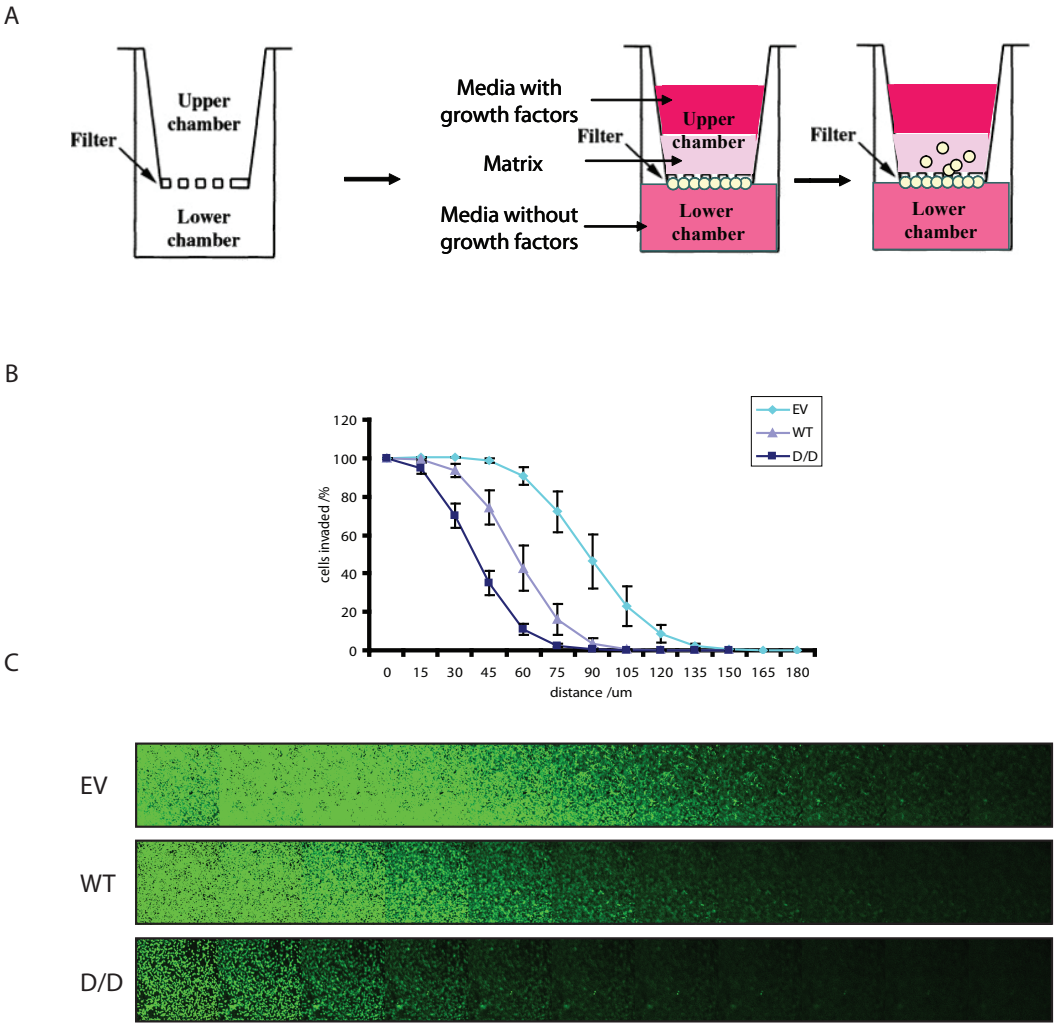

Figure 5.10: Effect of IRF-1 on invasion through matrigel. (A) Schematic representation of inverse invasion assay. *left panel* An insert with a permeable membrane is inserted into a tissue culture dish well. The well consitutes the lower chamber and the insert the upper chamber. /em centre panel A matrix (in this case 50% matrigel) is placed in the insert to simulate the extracellular matrix. Cells are seeded on the base of the membrane, then a gradient of growth factors is created by filling the lower chamber with serum free medium, and the upper chamber with medium containing FBS. *right panel* The gradient encourages migration of the cells across the membrance and invasion into the matrigel. (B) Inverse invasion of pcDNA3-EV, -IRF-1 WT and T311D/S317D-transfected MDA-MB-231 cells. 24h after transfection, cells were seeded on matrigel-containing transwell inserts and allowed to migrate for 3 days through a FBS gradient. Cells were stained using calcein-AM and images were taken every 15μm from the base of the transwell. Staining at each level was normalised to the staining at the base of the stack. Results expressed as mean +/- standard error for four pictures from four different positions in each well.(C) Representative images of invasion of pcDNA3-EV, -IRF-1 WT and T311D/S317D-transfected MDA-MB-231 cells. Data from a single experiment.

5.5 Discussion

IFN-γ is known to elicit anti-tumoural effects by both directly affecting the tumour cell and enhancing immune recognition of tumour cells [170]. IRF-1 is involved in mediating many of these activities. More recently, however, evidence has emerged that constitutive activation of the STAT1 pathway (downstream of IFN-γ) may be oncogenic. It has been suggested that radioresistance and chemoresistance are caused by the upregulation of some Interferon Stimulated Genes (ISGs) (not including IRF-1) that promote survival. This is speculated to be the result of activity by unphosphorylated STAT1 which upregulates a different subset of promoters to phosphorylated STAT1, some of which control prosurvival genes. Upregulation of STAT1 has been observed in radioresistant and chemoresistant tumour cells [171]. Despite the anti-tumour activities of IFN-γ, its upregulation of STAT1 may limit its theraputic value.

Consequently, IRF-1 artificially activated to mimic IFN-γ-mediated activation has the potential be a useful tool. Although not all of the promoters targeted by IFN-γ are activated by IRF-1, it is the downstream effector of many antitumour activities, and furthermore, has been shown to demonstrate antioncogenic effects *in vivo* [41], [23], [61], enhance the activity of chemotherapeutics [58], [59], [60] and mediate the apoptotic activity of antiestrogens [57].

As summarised below, in this chapter the effects of mutations in IRF-1 mimicing IFN-γ-induced phosphorylation have been examined in clonogenic and invasion assays.

IRF-1 has previously been shown to inhibit anchorage dependent [70] and independent colony formation [5]. The data in this chapter build on those findings and shows that C-terminal phosphorylation might enhance the activity of IRF-1 in such assays, altough further experiments with more cells are required to confirm this as discussed above.

It has not been possible so far to fully elucidate the mechanism by which IRF-1 inhibits colony formation. The data presented here suggest that a dual mechanism is operating with proliferation being inhibited by IRF-1 in most cell lines for anchorage dependent and independent growth, but a further, unknown mechanism might effect the greater inhi-

bition seen with IRF-1 T311D/S317D. The effect of IRF-1 T311D/S317D on senescence and apoptosis will be studied in more detail to determine if either of these could be responsible.

It would also be interesting to try and isolate cells from large and small colonies and cells which did not produce colonies, and compare IRF-1 expression levels in each. It is tempting to suspect that the size/presence of a colony is related to the level of IRF-1 expression in each cell. Related to this, an attempt was made to create stable, IRF-1 expressing, cell lines. Over time (a few weeks), the cells downregulated the forced expression of IRF-1, even in the presence of a selection agent. Therefore the presence of IRF-1 exerts a strong negative selection pressure and the extent of IRF-1 expression could determine the rate of cell growth/colony initiation.

IRF-1 has here, for the first time, been shown to inhibit invasion in an *in vitro* metastasis assay. IRF-1 has been shown to inhibit metastasis *in vivo* through its effects on immune-mediated clearance of tumour cells [46], however, clearly in an *in vitro* assay, another activity is responsible. Matrix Metalloproteases (MMPs) are involved in the invasion and metastasis of tumour cells [172]. IRF-1 downregulates the *MMP9* promoter through competition with NF-κB [45]. Therefore, it would be useful to determine if the effects of IRF-1 on invasion in the transwell invasion assays are linked to MMP9 inhibition. MMP9 activity of transfected cells could be measured using a gelatinase assay. Of note, IRF-1 WT and T311D/S317D show similar efficiency of inhibition at the *MMP9* promoter in reporter assays (Fig 4.2), but IRF-1 T311D/S317D might be more effective in inhibiting invasion. Thus, inhibition of MMP9 at the promoter level may not be the only mechanism operating. Perhaps other *MMP*s are regulated by IRF-1 or perhaps, as discussed above, the optimisation of the *in vitro* assay will reveal that IRF-1 WT and T311D/S317D have similar effects.

In conclusion, the results in this chapter demonstrate that *in vitro* IRF-1 T311D/S317D might be a more effective tumour suppressor than IRF-1 WT. It follows that delivery of IRF-1 T311D/S317D could be an effective cancer treatment, and a logical development of this project would be to carry out *in vivo* experiments to determine the efficacy of IRF-1 T311D/S317D in inhibiting tumour growth, and augmenting the activity of pre-existing

treatments such as antiestrogens.

An alternative to directly administering IRF-1 T311D/S317D through gene therapy would be to activate the kinases responsible for phosphorylation of IRF-1 at these sites. Small molecule activation of protein kinases is still in its infancy, but drugs employing this mechanism are under investigation for diseases such as Alzheimers, (PKC activators) [173], diabetes (GK activators) [174] and neurological diseases (Akt activators) [175]. Interestingly, both PKC and Akt are IFN-γ activated kinases and have been predicted to phosphorylate IRF-1 Thr311 and Ser317 (see discussion). Kinase activators are commercially available, and could be useful tools in identifying the kinases upstream of IRF-1 and further characterising the effects of phosphorylation at these sites on IRF-1 activity.

Chapter 6

Discussion and Future Directions

The aims of this thesis have been to identify regulatory phosphorylation events for IRF-1 and to try to study the mechanisms by which these phosphorylations modulate IRF-1 activity. Using phosphospecific antibodies, phosphorylation at T311, and S317 sites was observed in response to IFN-γ treatment, and at S317 in response to the DNA damage mimetic etoposide. Phosphomimetic (S/T$\rightarrow$D) mutants of each phosphorylation site, and a dual phosphomimetic mutant where both sites were changed, were created. Since the dual phosphomimetic mutant showed the highest activity in transcriptional reporter assays, this mutant was used to study the mechanism of the enhanced transcriptional activity and to examine the effect of IFN-γ-induced phosphorylation on IRF-1 activity in cell-based assays. Although the presence of dual phosphorylation at these sites in cells could not be confirmed due to the deterioration of the phosphospecific antibodies, multi-site phosphorylation is well-recognised and it is postulated that a requirement for multiple phosphorylations imposes a threshold for activation [176].

Phosphorylation is well recognised as a crucial post-translatory modification of transcription factors which can regulate transcription factor activity at a number of levels, namely: localisation; stability; DNA binding and protein-protein interaction [177]. The impact of phosphorylation on the regulation of IRF-1 through these mechanisms, and the contributions of the findings reported in this thesis to the understanding of such regulation, is discussed below.

Localisation

Upon IFN-γ treatment, IRF-1 translocates to the nucleus [138]. Although preliminary studies suggest that neither 311T nor 317S phosphorylation affects nuclear transport, (subcellular fractionation of cells transfected with IRF-1 containing phosphomimetic mutations at the above sites indicates no difference in localisation compared to WT-IRF-1) evidence from the literature implies that phosphorylation is important in this process, as described below.

Inhibition of PKC by minocycline reduces IRF-1 nuclear translocation after IFN-γ treatment without affecting total IRF-1 protein levels. PKC is upregulated by IFN-γ treatment, therefore, it is plausible that phosphorylation of IRF-1 by PKC is required for nuclear transport of IRF-1 [178].

After TLR9 stimulation by CpG DNA, IKKα is required for IRF-1 nuclear translocation. Moreover, IKKα coimmunoprecipitates with IRF-1 and phosphorylates it *in vitro* [179]. IRF-1 interacts with the TLR adaptor protein MyD88 after TLR9 stimulation, resulting in its "licensing" (probably phosphorylation), and nuclear translocation [96]. Therefore, it is likely that, by analogy with IRF-7 [180], TLR9 engagement recruits MyD88 which binds IRF-1. IRF-1 is then phosphorylated by IKKα which has been activated by IRAK1 as a result of TLR9 engagement. Phosphorylated IRF-1 then translocates to the nucleus where it can upregulate immune-related promoters. This is illustrated in Fig 6.1.

IRF-1 contains a bipartite NLS. The NLS is contacted by importin-α1, which mediates its nuclear translocation after IFNγ treatment [138]. Since there are phosphorylation sites in and around the NLS, phosphorylation could regulate the interaction with importins. As mentioned by Whitmarsh & Davies, phosphorylation could unmask a binding site for an importin or block a binding site for another factor which occludes the importin binding site [177]. In keeping with this, it has been shown that although the NLS is critical for binding of the importin, the surrounding structure of the protein is also important for selective importin binding [181].

Stability

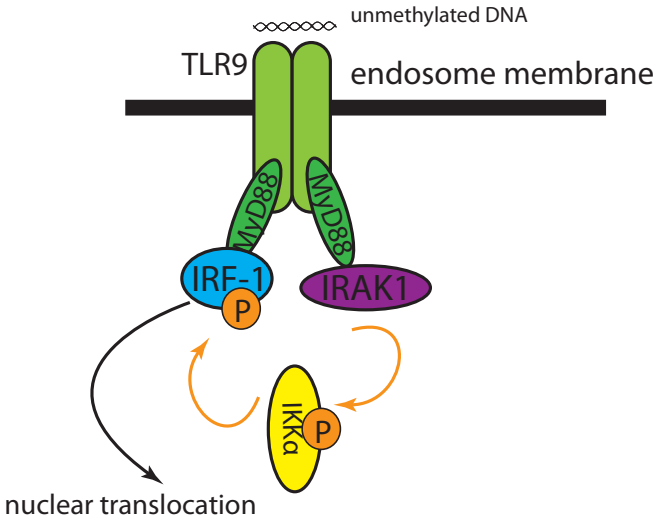

Figure 6.1: Predicted phosphorylation of IRF-1 in response to TLR9 activation (Adapted from[180]). Unmethylated DNA activates TLR9. By analogy to IRF-7, the adaptor protein MyD88 could contact IRF-1 and bring it into proximity with IRAK1-activated IKKα [180]. IKKα phosphorylates IRF-1 [179]. Phosphorylation of IRF-1 after Myd88 interaction results in nuclear translocation [96].

Proteins with regulatory functions often have short half lives to allow rapid regulation by changes in rates of synthesis [182]. The protein levels of IRF-1 are upregulated in response to many stimuli. This involves enhanced mRNA production and, in the case of genotoxic stress (but not viral mimetics), it has been shown that reduced degradation of the protein also contributes to the increased steady state protein levels. ATM kinase has been shown to be required for the induction of IRF-1 in response to genotoxic stress, however, it is not known if direct or indirect kinase activity is involved [76].

IRF-1 is degraded by the 26S proteasome in response to its polyubiquitination. The C-terminal portion of the protein was found to determine its stability but is not itself ubiquitinated [123]. It is suggested that, as for IRF-3 [150], a phosphorylation-dependent degradation signal could be located in the C-terminus of IRF-1 [122]. Pion *et. al.* have defined the region 301-311 as comprising a degradation signal which most likely recruits factors to deliver ubiquitinated IRF-1 to the proteasome [123]. Phosphorylation within this region (most likely at Ser308 since Thr311 phosphorylation has been shown not to affect stability) could regulate binding of the proteasome-delivery proteins. Interestingly, work by Dr Sarah Meek indicated that a S $\rightarrow$ D mutation at the Ser308 site stabilises IRF-1 protein (Dr Sarah Meek, unpublished observations).

Interestingly, in response to DNA damage (as a result of MNNG treatment), IRF-1 is acetylated within the DNA binding domain by CBP (a protein closely related to p300). Acetylation stabilises the IRF-1 protein, increasing its half-life without affecting mRNA synthesis [44]. The mechanism of recruitment of CBP to IRF-1 upon DNA damage is not known, however, since phosphorylation can modulate the recruitment of CBP/p300 to p53 [183], [184], and C-terminal phosphorylation of IRF-1 may enhance p300 binding (Chapter 4), it is possible that phosphorylation directs p300 to IRF-1 in response to DNA damage.

Although phosphorylation may be important for IRF-1 stability, the sites 311T and 317S do not appear to be involved in this regulation. Cycloheximide chase experiments of IRF-1 phosphomimetic mutants show that in whole cell lysate, and in nuclear and cytoplasmic compartments, the half lives of WT, T311D, S317D and T311D/S317D IRF-1 are very similar. It would, however, be interesting to perform cycloheximide chase after

IFN-γ treatment, as activated transcription factors are often targeted for rapid degradation [185]. Phosphorylation at another site in response to IFN-γ treatment may enhance degradation of IRF-1 in the nucleus. For example, phosphorylation of AML1c on specific residues controls both transcriptional activity and degradation [186]. Similarly, activated (non-RB bound) E2F-1 is phosphorylated by TFIIH (a component of the basal transcription machinery) and is subsequently degraded [187]. IRF-1 and TFIIB physically interact and cooperatively stimulate transcription in an *in vitro* transcription assay [188]. It would be interesting to determine if the half life of IRF-1 is affected by this interaction, and if IRF-1 can be targeted for degradation by TFIIH-mediated phosphorylation.

Protein-protein interaction

IRF-1 has previously been shown to interact with the co-activator p300 and enhance its acetylation of p53 [67]. Evidence from this thesis, and from others in the Ball lab indicates that phosphorylation of IRF-1 at 311T and 317S enhances its interaction with the co-activator p300 (Chapter 4). This appears to enhance the transcriptional activity of IRF-1 in response to IFN-γ treatment and correlates with the observations that a more transcriptionally active form of IRF-3, IRF-3(5D), has a higher affinity for CBP/ p300 [165].

Several mechanisms have been suggested for the transcription-regulatory properties of p300/CBP. One or a number of these may affect the activity of IRF-1. p300/CBP can contact both sequence-specific transcription factors, and the basal transcription machinery, thus, it can act as a bridge to couple recognition of a specific promoter to transcription of the downstream gene. The varied substrates of p300/CBP allow it to act as a scaffold for construction of a transcriptional regulatory complex. In addition, the HAT activity of p300/CBP can alter chromatin structure through histone acetylation, or transcription factor activity, for example, through altering DNA binding capacity, or modulating other protein-protein interactions [167].

So far, p300-IRF-1 interaction has been shown in preliminary experiments to enhance the DNA binding of IRF-1 (see below), however, further activities may be uncovered in the future. IRF-1-p300 complex interaction with the transcription apparatus *in vivo* and

with other cofactors should be investigated. A ChIP assay could be employed to discover the effect of co-transfection with p300 on IRF-1 association with components of the transcriptional machinery at promoters, and a ChIP assay coupled with mass-spectrometry could identify binding partners recruited to IRF-1 through p300 activity. The acetylation of IRF-1 after p300 binding should also be investigated.

The LXXLL motif within the IRF-1 Mf1 domain binds the Hsp70 chaperone protein, which recruits Hsp90 to IRF-1. Hsp70 and Hsp90 cooperate to regulate the stability, localisation and activity of IRF-1 [121]. It has been shown recently in the Ball laboratory that phosphorylation of an IRF-1 C-terminal peptide at Ser308 inhibits Hsp70 binding (Dr Vikram Narayan, unpublished observations). To extend this, an ELISA was performed to examine the effect of phosphorylation at Thr311 and Ser317 on Hsp70, Hsc70 and Hsp90 binding to full length IRF-1. It can be seen that endogenous Hsp70, Hsc70 and Hsp90 bind less well to immobilised IRF-1 T311D/S317D than IRF-1 WT (Fig 6.2A). Since Hsp90 increases IRF-1 transcriptional activity, and enhances its nuclear accumulation [121], and IRF-1 T311D/S317D is more transcriptionally active at IRF-1 transactivated promoters (Chapter 4), it seems counterintuitive that IRF-1 T311D/S317D does not bind as strongly to Hsp70/90. However, for IRF-3, it has been observed that Hsp90 forms a complex with IRF-3 and the kinase TBK1, bringing them into close proximity to allow phosphorylation of IRF-3 by TBK1. After phosphorylation, IRF-3 dissociates from Hsp90 and the IRF-3(5D) phosphomimetic mutant cannot bind Hsp90 [189]. Therefore, a similar pathway could regulate IRF-1 where Hsp90 recruits an activatory kinase to IRF-1, and after phosphorylation at 311T/317S sites the complex could dissociate, resulting in a low affinity of IRF-1 T311D/S317D for Hsp70 and 90. The binding site for Hsp70 on IRF-1 spans both 311T and 317S (Fig 6.2B from [121]). The residues on either side of both phosphorylation sites are all critical for the interaction [121], therefore, it is possible that phosphorylation directly blocks binding of Hsp70 and Hsp90.

A pull-down assay with Hsp90/control transfected cells (or Hsp90 inhibitor (17AAG)/control treated cells) followed by a kinase assay using eluted IRF-1 binding proteins (as depicted in Fig 6.3) would reveal if Hsp90 couples IRF-1 with a kinase. If an IRF-1 kinase is found associated with Hsp90, it could be purified from the complex and identified by

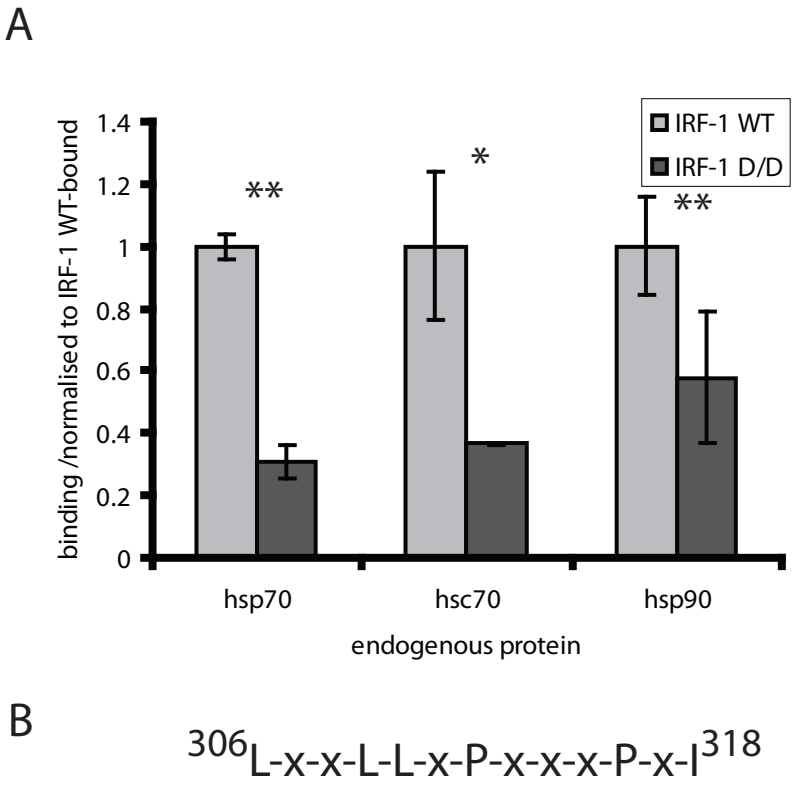

Figure 6.2: IRF-1 phosphorylation inhibits Hsp70, Hsc70 and Hsp90 binding. (A) 100ng purified His-IRF-1 WT or T311D/S317D was immobilised on an ELISA plate and incubated with 300ng A375 lysate for 1 hour. Binding of proteins from lysate was detected by anti-hsp70 (Stressgen), anti-hsc70 (Stressgen) and anti-hsp90 (Stressgen) antibodies followed by HRP-swine anti-rabbit antibody (Dako). Binding was normalised to IRF-1 WT-binding levels for each protein. Results expressed as mean +/- standard deviation for triplicates. (B) Hsp70 binding motif [121] x is any amino acid. Data representative of three independent experiments. Significant differences in cofactor binding by paired t test are indiciated (* p=<0.05, ** p=<0.01).

mass-spectrometry. Then, the effect of the kinase on IRF-1 activity, localisation and DNA binding could be investigated. It is possible that a kinase is only recruited to the complex after stimulation of cells, or that different kinases are recruited after different signals, therefore, various cell stimuli should be incorporated into the experiment.

It is likely that there are other proteins differentially binding to IRF-1 WT and IRF-1 T311D/S317D, which could be identified using SILAC mass-spectrometry. An example of how this technique was successfully used to identify phospho-dependent binding partners is given in reference [190]. Briefly, phosphorylated or non-phosphorylated peptide is immobilised on a column, and incubated with cell lysate to pull out binding partners. Phosphorylated peptide is incubated with lysate labelled by growing in media supplemented with, for example, heavy (^{13}C lysine and arginine) amino acids, and non-phosphorylated peptide is incubated with lysate labelled with, for example light (^{12}C lysine and arginine) amino acids. The binding partners can be eluted and separated by SDS-PAGE, then identified using mass-spectrometry. The labelled amino acids allow quantification of the relative amounts of each protein bound to the phosphorylated and unphosphorylated peptides by comparing the ^{12}C/^{13}C isotope ratios [190].

It was interesting to note that IRF-1 T311D/S317D repressed the *Cdk2* and *MMP9* promoters to the same extent as IRF-1 WT. Therefore, phosphorylation at these sites appears to have no effect on the interaction of IRF-1 with co-repressors.

DNA-binding

This thesis has demonstrated that phosphomimetic IRF-1 T311D/S317D shows enhanced DNA binding compared to IRF-1 WT in EMSAs. This is likely to be mediated by enhanced binding of IRF-1 T311D/S317D to a cofactor, the histone acetylase p300, and acetylation of IRF-1 appears to further stabilise the interaction with DNA (see Fig 4.10). A model for this pathway has been suggested in Fig 6.4. This phenomenon has previously been observed for p53, where phosphorylation of p53 increases its affinity for p300 and PCAF, promoting acetylation elsewhere in p53 which, in turn, enhances DNA binding [191] [192] and coactivator recruitment [168]. RelA also shows phosphorylation-induced p300-dependent acetylation resulting in enhanced DNA binding [193] and many other

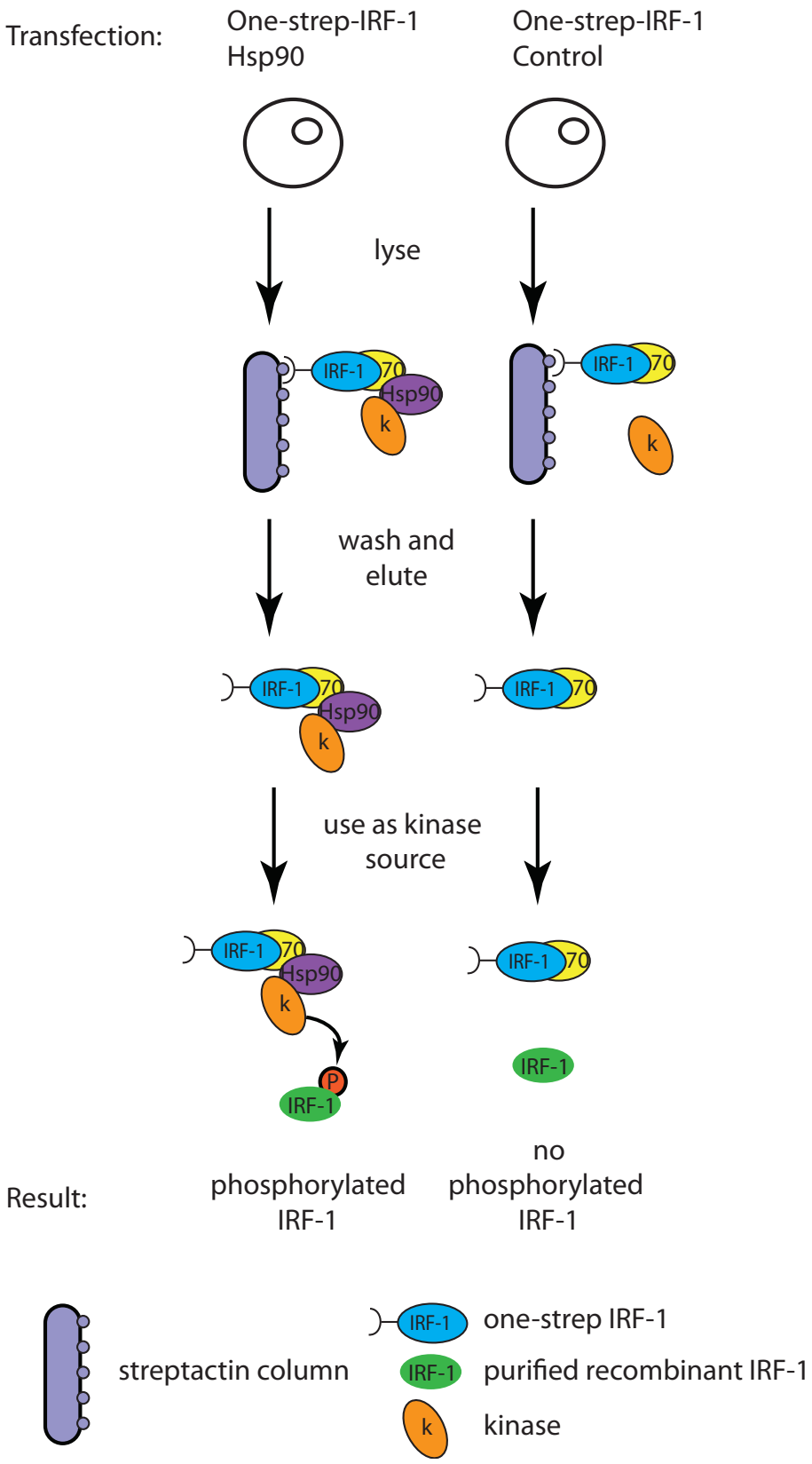

Figure 6.3: Experimental design for determining if Hsp90 recruits a kinase to IRF-1. Lysate from cells transfected with one-strep-IRF-1 +/- Hsp90 is passed over a streptactin column to isolate one-strep-IRF-1 complexes. The complexes are gently washed and eluted using biotin. The eluted complexes are used as a kinase source to phosphorylate purified, recombinant IRF-1. Phosphorylation could be visualised using a phosphorimager.

transcription factors show enhanced DNA binding activity after p300-dependent acetylation including MEF2 [194], GATA4 [195], and Nrf2 [196]. IRF-1 has previously been shown to interact with p300 and stimulate acetylation of promoter-bound p53 [67], but this is the first time p300 has been shown to directly regulate IRF-1 activity.

Phosphorylation by Protein Kinase R (PKR) or a PKR-activated kinase modulates IRF-1 DNA binding. PKR has been shown to be activated upon IFN-γ treatment [94]. In the absence of PKR, IRF-1 protein is expressed normally, but DNA binding activity in response to various stresses is lost [197]. Further, inhibition of PKR by a hepatitis C virus protein results in inhibition of DNA binding [198]. As yet, however, direct phosphorylation of IRF-1 by PKR has not been demonstrated, although, interestingly, 311T matches the PKR consensus phosphorylation site [153].

Enhanced DNA binding of IRF-1 in response to IFN-γ treatment has been shown indirectly by the large increase in the variety of promoters bound by IRF-1 after IFN-γ treatment [43].

All of the mechanisms of regulation discussed above combine to dictate the transcriptional activity of IRF-1. The reporter assays recorded in Chapter 4 show that for IRF-1-activated promoters, phosphorylation in response to IFN-γ enhances transcriptional activity, however, IRF-1-repressed promoters are not affected by phosphorylation at T311D or S317D. Since IFN-γ triggers inhibition of both of the IRF-1-repressed promoters studied - the *MMP9* [45] and *Cdk2* [199] promoters, it is clear that other signals modulating IRF-1 activity in response to IFN-γ treatment remain to be elucidated. Phosphorylation at other sites, or other post-translational modifications could recruit co-repressors to co-operate with IRF-1 at these promoters. It is clear that there is much work to be done to fully characterise the regulation of IRF-1, even by a single signal.

One approach to better characterising the effect of, for example, IFN-γ treatment on IRF-1 is to determine all the stimulus-specific phosphorylation sites using mass-spectrometry, and then identify the kinases responsible. Since this is a large undertaking, a first step could be the identification of kinases responsible for phosphorylation at the 311T and 317S sites. Using the online phosphorylation site prediction programmes NetPhosK2.0

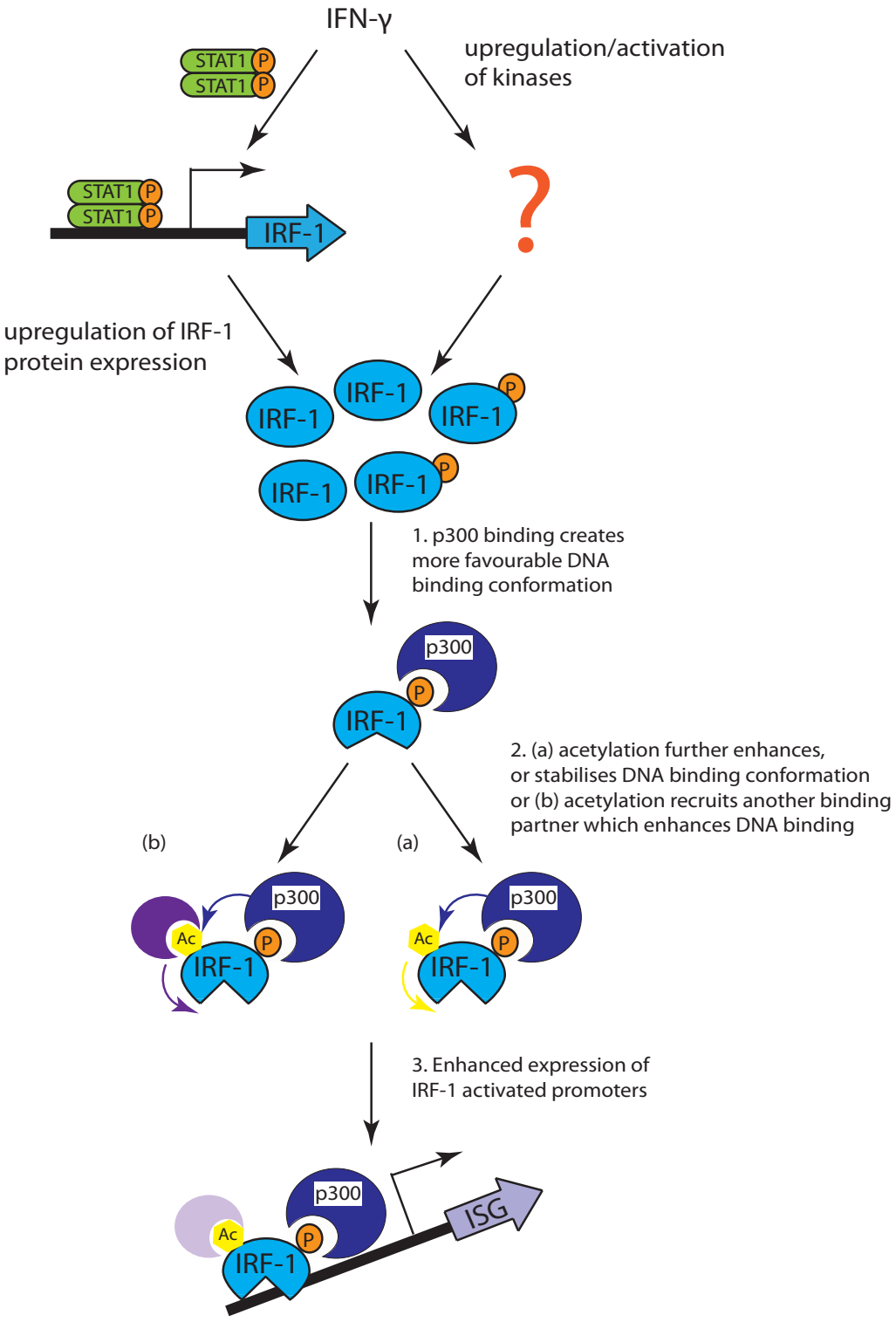

Figure 6.4: Model for mechanism of enhanced transcriptional activity of IRF-1 after IFN-γ treatment. IFN-γ causes upregulation of IRF-1 protein expression through STAT1. IFN-γ signalling also activates/upregulates IRF-1 kinases. Phosphorylation of IRF-1 creates a binding site for p300. p300 binding enhances the affinity of IRF-1 for DNA, and acetylation of IRF-1 by p300 further enhances DNA binding. This could be due either to (a) acetylation causing conformational change of IRF-1 which further enhances or stabilises a favourable DNA binding conformation, or (b) acetylation creating a binding site for another cofactor whose interaction stabilises or enhances a favourable DNA binding conformation. As a result of the enhanced DNA binding, and potentially the improved recruitment of other components of the transcriptional machinery by the cofactors, there is enhanced expression of IRF-1 activated promoters.

[151], KinasePhos2.0 [152] and PPSP [153], a list of kinases whose phosphorylation motifs matched 311T and 317S was generated. To narrow down the list, a literature search was performed to identify kinases that were known to be activated upon IFN-γ treatment. The resulting set of kinases is shown in Table 6.1. Inhibitors/siRNA studies could be used to determine if these kinases can modulate IRF-1 activity, and 2D gels and *in vitro* kinase assays could be used to assess if they can phosphorylate IRF-1. If S/T $\rightarrow$ A mutation at the appropriate site abrogates phosphorylation of IRF-1 by the kinase, it is likely that the kinase could be part of a signalling pathway controlling IRF-1.

311T	317S	
p38MAPK	**AKT1**	CHK1/2
CDK5	**PKB/AKT**	IPL1
GRK	ATM	MAPKAPK2
PKB/AKT	**PKC**	PAK
CDC2	Aurora	PHK
CK2	PKG	**PKA**
PDK	**MAPK**	S6K
CAK	RSK	AMPK
CDK5	**PKA**	CAK
GSK3	STK4	CAM I/IV
MAPK	CHK1	CAM II
MAPKK		
MTOR		
p34CDC2		
PKR		

Table 6.1: Kinases predicted to phosphorylate IRF-1 311T or 317S. Kinases reported to be activated by IFN-γ treatment are highlighted in bold.

An as yet unexplored aspect of IRF-1 regulation is role of dephosphorylation. No phosphatases have been reported to act on IRF-1 and the impact of negative-regulatory phosphorylations has not been studied. If a picture of the phosphorylated sites of "resting" IRF-1 was known, this could be compared to the phosphorylation of activated IRF-1, and inhibitory phosphorylation sites identified. If such phosphorylation events were identified, inhibitors of the phosphatases responsible could also be useful drug targets.

Acetylation of IRF-1 also deserves more attention. As well as the acetylation by p300 identified here, IRF-1 is known to bind PCAF and GCN5 at promoters and this interaction enhances the activity of IRF-1 [127]. Thus, acetylation is likely to be a major player in the regulation of IRF-1.

Cell based assays investigating the effect of phosphorylation on the tumour suppressor activities of IRF-1 have shown that T311D/S317D IRF-1 may be more efficient at suppressing anchorage dependent and independent colony formation, although this does not appear to be due to effects on cell cycle progression, but could be triggering of senescence. IRF-1 was also shown, for the first time, to be able to inhibit invasion in an *in vitro* assay of invasion. Again phosphomimetic IRF-1 appears to enhance this activity.

On the basis of this enhanced tumour suppressor activity *in vitro*, it would be useful to study the effects *in vivo*. What is the effect on tumour growth/metastasis of transfecting cells with IRF-1 T311D/S317D before xenografting? Can administration of IRF-1 T311D/S317D slow/reverse the progression of tumours?

If the identitiy of the kinases catalysing the activatory phosphorylations was known, it might be possible to manipulate these to enhance the effects of IRF-1 on tumours *in vivo*. However, this might be a treatment doomed to rapid resistance, as many tumours escape the control of IRF-1 by causing its downregulation [200], and the effects could be non-specific. Therefore, administration of artificial IRF-1 seems like a better option. Ectopic expression of IRF-1 by an adenoviral vector in mice has been shown to inhibit tumour growth [41], [34], thus expression of activated IRF-1 (T311D/S317D) could be even more effective.

As well as activating the transcriptional activity of IRF-1, ectopically expressed protein could be made more effective as a therapeutic by prolonging its half life. IRF-1 is degraded through the ubiquitin-proteasome pathway [122], [123]. Perhaps mutation of the lysine residues which accept the polyubiquitin could further enhance the activity of IRF-1. It seems that this is a mechanism used *in vivo* to modulate IRF-1 activity since acetylation of IRF-1 lysine residues (which protects them from ubiquitination) stabilises the protein [44].

It is important, however, to properly characterise the effects of the activatory mutations. IRF-1 upregulation has been linked with autoimmune disease [87] [88] [89] *in vivo*, therefore, the effect of T311D/S317D on inflammatory and immune-related promoters should be studied (for example, by ChIP-seq). *MHC I*, *iNOS* and *caspase 1* overexpression have all been linked to MS [201] [88] [202] and since their promoters are all regulated by IRF-1 [28] [35] [40], they could form an initial panel of genes to monitor. *In vivo* studies should monitor for autoimmune side effects as well as considering tumour suppression.

In conclusion, this thesis has firmly established phosphorylation as a post-translational method of control of IRF-1. Two stimulus-specific phosphorylation sites have been identified and a model for the mechanism by which they selectively enhance the transcriptional activity of IRF-1 has been suggested. Furthermore, the activity of a mutant mimicing phosphorylation at the two sites (IRF-1 T311D/S317D) has been characterised in *in vitro* assays and found to be an effective tumour suppressor and metastatic inhibitor.

Bibliography

[1] Takashi Fujita, Jun Sakakibara, Sudo Yoshiaki, Masaaki Miyamoto, Yoko Kimura, and Tadatsugu Taniguchi. Evidence for a nuclear factor(s), IRF-1, mediating induction and silencing properties to IFN-beta gene regulatory elements. *EMBO Journal*, 7(11):3397 – 3405, 1988.

[2] Hisashi Harada, Takashi Fujita, Masaaki Miyamoto, Yoko Kimura, Mitsuo Maruyama, Adriana Furia, Takashi Miyata, and Tadatsugu Taniguchi. Structurally Similar but Functionally Distinct Factors, IRF-1 and IRF2, Bind to the Same Regulatory Elements of IFN and IFN-Inducible. *Cell*, 58:729–739, 1989.

[3] Nobuyuki Tanaka, Takatoshi Kawakami, and Tadatsugu Taniguchi. Recognition DNA Sequences of Interferon Regulatory Factor 1 (IRF-1) and IRF-2 , Regulators of Cell Growth and the Interferon System. *Molecular and Cellular Biology*, 13(8):4531–4538, 1993.

[4] Cheryl L Willman, Cordelia E Sever, Maria G Pallavicini, Hisashi Harada, Nobuyuki Tanaka, Marilyn L Slovak, Hitomi Yamamoto, Kenji Harada, Timothy C Meeker, Alan F List, and Tadatsugu Taniguchi. Deletion of IRF-1 , Mapping to Chromosome 5q31.1, in Human Leukemia and Preleukemic Myelodysplasia. *Science*, 259:968–971, 1993.

[5] Hisashi Harada, Motoo Kitagawa, Nobuyuki Tanaka, Hitomi Yamamoto, Kenji Harada, Masahiko Ishihara, and Tadatsugu Taniguchi. Anti-Oncogenic and Oncogenic Potentials of Interferon Regulatory Factors-1 and -2. *Science*, 259:971–974, 1993.

[6] Abbas Abdollahi, Kenneth A Lord, and Dan A Liebermann. Interferon Regulatory Factor 1 Is a Myeloid Differentiation Primary Response Gene Induced by Inter-

leukin 6 and Leukemia Inhibitory Factor : Role in Growth Inhibition . *Cell Growth & Differentiation*, 2(August):401–407, 1991.

[7] Gen Yamada, Minetaro Ogawa, Kiwamu Akagi, Hajime Miyamoto, Naoko Nakano, Susumu Itoh, Jun-Ichi Miyazaki, Shin-Ichi Nishizuka, Ken-Ichi Yamamura, and Tadatsugu Taniguchi. Specific depletion of the B-cell population induced by aberrant expression of human interferon regulatory factor 1 gene in transgenic mice. *PNAS*, 88:532–536, 1991.

[8] G Tamura, S Ogasawara, S Nishizuka, K Sakata, C Maesawa, Y Suzuki, Masanon Terashima, Kazuyoshi Saito, and Ryoichi Satodate. Two distinct regions of deletion on the long arm of chromosome 5 in differentiated adenocarcinomas of the stomach. *Cancer Research*, 56:612–615, 1996.

[9] Satoshi Ogasawara, Gen Tamura, Chihaya Maesawa, Yasushi Suzuki, Kaoru Ishida, Nobuhiro Satoh, Noriyuki Uesugi, Kazuyoshi Saito, and Ryoichi Satodate. Common deleted region on the long arm of chromosome 5 in esophageal carcinoma. *Gastroenterology*, 110:52–57, 1996.

[10] P Mendes-da Silva, A Moreira, J Duro-da Costa, D Matias, and C Monteiro. Papers Frequent loss of heterozygosity on chromosome 5 in non-small cell lung carcinoma. *J Clin Pathol: Mol Pathol*, 53:184–187, 2000.

[11] Ju Hye Shin, Shin Myung Kang, Young Sam Kim, and Dong Hwan Shin. Identification of Tumor Suppressor Loci on the Long Arm of Chromosome 5 in Pulmonary Large Cell Neuroendocrine Carcinoma * Identification of Tumor Suppressor Loci on the Long Arm of Chromosome 5 in Pulmonary Large Cell Neuroendocrine Carcinoma *. *Chest*, 2005.

[12] Hrefna K Johannsdottir, Goran Jonsson, Gudrun Johannesdottir, Bjarni A Agnarsson, Hannaleena Eerola, Paivi Heikkila, Valgardur Egilsson, Hakan Olsson, Oskar Th Johannsson, and Heli Nevanlinna. Chromosome 5 imbalance mapping in breast tumors from BRCA1 and BRCA2 mutation carriers and sporadic breast tumors. *Gene*, 1060:1052–1060, 2006.

[13] Luciane Cavalli, Rebecca Biggins, Antai Wang, Robert Clarke, and Bassem R Haddad. Frequent loss of heterozygosity at the interferon regulatory factor-1 gene locus in breast cancer. *Breast Cancer Research T*, 121(1):227–31, 2010.

[14] Hiroaki Nozawa, Eri Oda, Ueda Seiji, Gen Tamura, Chihaya Maesawa, Tetsuichiro Muto, Tadatsugu Taniguchi, and Nobuyuki Tanaka. Functionally Inactivating Point Mutation in the Tumor-Suppressor IRF-1 Gene Identified in Human Gastric Cancer. *International Journal of Cancer*, 77:522–527, 1998.

[15] Takeshi Kondo, Naoto Minamino, Tokiko Nagamura-inoue, and Masahito Matsumoto. Identifcation and characterization of nucleophosmin/B23/numatrin which binds the anti-oncogenic transcription factor IRF-1 and manifests oncogenic activity. *Oncogene*, 15:1275–1281, 1997.

[16] Jong-sup Park, Eun-joo Kim, Ho-jeong Kwon, Eun-seong Hwang, Sung-eun Namkoong, and Soo-jong Um. Inactivation of Interferon Regulatory Factor-1 Tumor Suppressor Protein by HPV E7 Oncoprotein. *Biochemistry*, 275(10):6764 –6769, 2000.

[17] H Harada, T Kondo, S Ogawa, T Tamura, M Kitagawa, N Tanaka, M S Lamphier, H Hirai, and T Taniguchi. Accelerated exon skipping of IRF-1 mRNA in human myelodysplasia/leukemia; a possible mechanism of tumor suppressor inactivation. *Oncogene*, 9(11):3313–20, 1994.

[18] Christos I Maratheftis, Pelagia E Bolaraki, Stavroula Giannouli, Efstathia K Kapsogeorgou, Haralampos M Moutsopoulos, and Michael Voulgarelis. Aberrant alternative splicing of interferon regulatory factor-1 (IRF-1) in myelodysplastic hematopoietic progenitor cells. *Leukemia Research*, 30:1177–1186, 2006.

[19] Eun-ju Lee, Minwha Jo, Junsoo Park, Wei Zhang, and Je-ho Lee. Alternative splicing variants of IRF-1 lacking exons 7, 8 and 9 in cervical cancer. *Biochemical and Biophysical Research Communications*, 347:882–888, 2006.

[20] Nobuyuki Tanaka, Masahiko Ishihara, and Tadatsugu Taniguchi. Suppression of c-myc or fosB-induced cell transformation by the transcription factor IRF-1. *Cancer Letters*, 83:191–196, 1994.

[21] Nobuyuki Tanaka, Masahiko Ishihara, Shinichi Aizawa, and Tak W Mak. Cellular Commitment to Oncogene-Induced Transformation or Apoptosis Is Dependent on the Transcription Factor IRF-1. *Cell*, 77:829–839, 1994.

[22] Hiroaki Nozawa, Eri Oda, Kazuki Nakao, Hiroaki Nozawa, Eri Oda, Kazuki Nakao, Masahiko Ishihara, Seiji Ueda, Taeko Yokochi, Kouetsu Ogasawara, Yoko

Nakatsuru, Seiichiro Shimizu, Yoshikazu Ohira, Kyoji Hioki, Shinichi Aizawa, Takatoshi Ishikawa, Motoya Katsuki, Tetsuichiro Muto, Tadatsugu Taniguchi, and Nobuyuki Tanaka. Loss of transcription factor IRF-1 affects tumor susceptibility in mice carrying the Ha- ras transgene or nullizygosity for p53 service Loss of transcription factor IRF-1 affects tumor susceptibility in mice carrying the Ha-ras transgene or nullizygosity for p53. *Genes & Development*, pages 1240–1245, 1999.

[23] Kerrie B Bouker, Todd C Skaar, Rebecca B Riggins, David S Harburger, David R Fernandez, Alan Zwart, Antai Wang, and Robert Clarke. Interferon regulatory factor-1 (IRF-1) exhibits tumor suppressor activities in breast cancer associated with caspase activation and induction of apoptosis. *Carcinogenesis*, 26(9):1527–1535, 2005.

[24] Jianguo Liu, Zhaoying Xiang, and Xiaojing Ma. Role of IFN Regulatory Factor-1 and IL-12 in Immunological Resistance to Pathogenesis of N -Methyl- N -Nitrosourea-Induced T Lymphoma. *J Immunol*, 173:1184–1193, 2004.

[25] Moitreyee Chatterjee-kishore, Raj Kishore, Daniel J Hicklin, Francesco M Marincola, and Soldano Ferrone. Different Requirements for Signal Transducer and Activator of Transcription 1alpha and Interferon Regulatory Factor 1 in the Regulation of Low Molecular Mass Polypeptide 2 and Transporter Associated with Antigen Processing 1 Gene Expression. *Journal of Biological Chemistry*, 273(26):16177–16183, 1998.

[26] Grethe S Foss and Hans Prydz. Interferon Regulatory Factor 1 Mediates the Interferon-gamma Induction of the Human Immunoproteasome Subunit Multicatalytic Endopeptidase Complex-like 1. *Journal of Biological Chemistry*, 274(49):35196 –35202, 1999.

[27] John H Yim, Susan J Wu, Matthew J Casey, Jeffrey A Norton, and Gerard M Doherty. IFN Regulatory Factor-1 Gene Transfer into an Aggressive, Nonimmunogenic Sarcoma Suppresses the Malignant Phenotype and Enhnaces Immunogenicity in Syngenic Mice. *The Journal of Immunology*, 158:1284–1292, 1997.

[28] Michael Hobart, Vido Ramassar, Nelson Goes, Joan Urmson, and Philip F Halloran. IRF-1 plays a central role in the regulation of the expression of class I and II

MHC genes in vivo. *The Journal of Immunology*, 158:4260–4269, 1997.

[29] Tomohiko Tamura, Hideyuki Yanai, David Savitsky, and Tadatsugu Taniguchi. The IRF Family Transcription Factors in Immunity and Oncogenesis. *Annual Review of Immunology*, 2008.

[30] Nobuyuki Tanaka, Masahiko Ishihara, Marc Lamphier, Hiroaki Nozawa, Toshifumi Matsuyama, Tak W Mak, Shinichi Aizawa, Tokino Takashi, Moshe Oren, and Tadatsugu Taniguchi. Cooperation of the tumour suppressors IRF-1 and p53 in response to DNA damage. *Nature*, 382:816–818, 1996.

[31] Seung-hoon Lee, Jung-whan Kim, Sun-hee Oh, Yong-jin Kim, Seung-bae Rho, Kyungsook Park, Kui-lea Park, and Je-ho Lee. IFN-gamma IRF-1- induced p27 downregulates telomerase activity and human telomerase reverse transcriptase expression in human cervical cancer. *FEBS Letters*, 579:1027–1033, 2005.

[32] Rong-lin Xie, Sunita Gupta, Angela Miele, Dov Shiffman, Janet L Stein, Gary S Stein, and Andre J Van Wijnen. The Tumor Suppressor Interferon Regulatory Factor 1 Interferes with SP1 Activation to Repress the Human CDK2 Promoter. *Journal of Biological Chemistry*, 278(29):26589 –26596, 2003.

[33] Andrea Kröger, Anja Stirnweiss, Julia Elisabeth Pulverer, Katjana Klages, Martina Grashoff, Jörg Reimann, and Hansjörg Hauser. Tumor Suppression by IFN Regulatory Factor-1 Is Mediated by Transcriptional Down-regulation of Cyclin D1. *Cancer Research*, 67:2972–2981, 2007.

[34] Peter K M Kim, Michaele Armstrong, Ye Liu, Peng Yan, Brian Bucher, Brian S Zuckerbraun, Andrea Gambotto, Timothy R Billiar, and John H Yim. IRF-1 expression induces apoptosis and inhibits tumor growth in mouse mammary cancer cells in vitro and in vivo. *Oncogene*, 23:1125–1135, 2004.

[35] R Kamijo, H Harada, T Matsuyama, M Bosland, J Gerecitano, D Shapiro, J Le, I Koh, T Kimura, S J Green, T W Mak, T Taniguchi, and J Vilček. Requirement for Transcription Factor IRF-1 in NO Synthase Induction in Macrophages. *Science*, 263(5153):1612–1615, 1994.

[36] Jide Wang, Wenjing Zhang, Yusheng Zhang, Bing Zou, Bo Jiang, Roberta Pang, Qing Gu, Liang Qiao, Huiyao Lan, Hsiang-fu Kung, and Benjamin C Y Wong. c-Jun-terminal kinase (JNK1) upregulates XIAP-associated factor 1 (XAF1) through

interferon regulatory factor 1 (IRF-1) in gastrointestinal cancer. *Carcinogenesis*, 30(2):222–229, 2009.

[37] Angela Papageorgiou, Colin P N Dinney, and David J McConkey. Interferon-α Induces TRAIL Expression and Cell Death Via an IRF-1-Dependent Mechanism in Human Bladder Cancer Cells. *Cancer Biology and Therapy*, 6(6):872–879, 2007.

[38] J Gao, M Senthil, B Ren, J Yan, Q Xing, J Yu, L Zhang, and J H Yim. IRF-1 transcriptionally upregulates PUMA which mediates the mitochondrial apoptotic pathway in IRF-1-induced apoptosis in cancer cells. *Cell Death and Differentiation*, 17:699–709, 2010.

[39] Warren A Chow, Jing Jing Fang, and Jiing-kuan Yee. The IFN Regulatory Factor Family Participates in Regulation of Fas Ligand Gene Expression in T Cells. *The Journal of Immunology*, 164:3512–3518, 2000.

[40] Tomohiko Tamura, Masahiko Ishihara, Marc Lamphier, Nobuyuki Tanaka, Isao Oishi, Shinichi Aizawa, Toshifumi Matsuyama, Tak W Mak, Shinsuke Taki, and Tadatsugu Taniguchi. An IRF-1-dependent pathway of DNA damage-induced apoptosis in mitogen-activated T lymphocytes. *Nature*, 376:596–599, 1995.

[41] Eva Pizzoferrato, Ye Liu, Andrea Gambotto, Michaele J Armstrong, Michael T Stang, William E Gooding, Sean M Alber, Stuart H Shand, Simon C Watkins, Walter J Storkus, and John H Yim. Ectopic Expression of Interferon Regulatory Factor-1 Promotes Human Breast Cancer Cell Death and Results in Reduced Expression of Survivin. *Cancer Research*, 64:8381– 8388, 2004.

[42] Yan Wang, Dong-ping Liu, Ping-ping Chen, H Phillip Koeffler, Xiang-jun Tong, and Dong Xie. Involvement of IFN Regulatory Factor (IRF) -1 and IRF-2 in the Formation and Progression of Human Esophageal Cancers. *Cancer Research*, 67:2535–2543, 2007.

[43] Mattia Frontini, Meeraa Vijayakumar, Alexander Garvin, and Nicole Clarke. A ChIP chip approach reveals a novel role for transcription factor IRF1 in the DNA damage response. *Nucleic Acids Research*, 37(4):1073–1085, 2009.

[44] Hongyan Qi, Huifang Zhu, Meng Lou, Yanfeng Fan, Hong Liu, Jing Shen, Zhongjie Li, Xue Lv, Jianzhen Shan, Lijun Zhu, Y Eugene Chin, and Jimin Shao.

Interferon Regulatory Factor 1 Transactivates Expression of Human DNA Polymerase n in Response to Carcinogen N-Methyl-N'-nitro-N-nitrosoguanidine. *Journal of Biological Chemistry*, 287(16):12622–12633, 2012.

[45] Josiane Sanceau, Douglas D Boyd, Motoharu Seiki, and Brigitte Bauvois. Interferons Inhibit Tumor Necrosis Factor-alpha-mediated Matrix Metalloproteinase-9 Activation via Interferon Regulatory Factor-1 Binding Competition with NF-kB. *Journal of Biological Chemistry*, 277(38):35766 –35775, 2002.

[46] Antje Ksienzyk, Berit Neumann, Ramya Nandakumar, Katija Finsterbusch, Martina Grashoff, Rainer Zawatzky, Gunter Bernhardt, Hansjörg Hauser, and Andrea Kroger. IRF-1 Expression Is Essential for Natural Killer Cells to Suppress Metastasis. *Cancer Research*, 71(20):6410–6418, 2011.

[47] Susan Elmore. Aopotosis: A Review Of Programmed Cell Death. *Toxicologic Pathology*, 35:495–516, 2007.

[48] Sujan Shresta, Christine T N Pham, Dori A Thomas, Timothy A Graubert, and Timothy J Ley. How do cytotoxic lymphocytes kill their targets? *Current Opinion in Immunology*, 10:581–587, 1998.

[49] Nobuhiko Kayagaki, Noriko Yamaguchi, Akemi Kawasaki, Hisaya Akiba, Ko Okumura, and Hideo Yagita. Involvement of TNF-Related Apoptosis-Inducing Ligand in Human CD4+ T Cell-Mediated Cytotoxicity. *Journal of Immunology*, 162:2639–2647, 1999.

[50] Nicole Clarke, Ana M Jimenez-lara, Emilie Voltz, and Hinrich Gronemeyer. Tumor suppressor IRF-1 mediates retinoid and interferon anticancer signaling to death ligand TRAIL. *EMBO Journal*, 23(15):3051–3060, 2004.

[51] S P Garrison, D C Phillips, J R Jeffers, J E Chipuk, M J Parsons, J E Rehg, J T Opferman, and G P Zambetti. Genetically defining the mechanism of Puma- and Bim-induced apoptosis. *Cell Death and Differentiation*, 19:642–649, 2012.

[52] Shui Ping Tu, Yun Wei Sun, Jian Tao Cui, Bing Zou, and Marie C M Lin. Tumor Suppressor XIAP-Associated Factor 1 (XAF1) Cooperates With Tumor Necrosis Factor-Related Apoptosis-Inducing Ligand to Suppress Colon Cancer Growth and Trigger Tumor Regression. *Analysis*, 1:1252–1263, 2010.

[53] VE Velculescu, SL Madden, L Zhang, AE Lash, J Yu, C Rago, A Lal, CJ Wang,

GA Beaudry, KM Ciriello, BP Cook, MR Dufault, AT Ferguson, Y Gao, TC He, H Hermeking, SK Hiraldo, PM Hwang, MA Lopez, HF Luderer, B Mathews, JM Petroziello, K Polyak, L Zawel, and KW Kinzler. Analysis of human transcriptomes. *Nature Genetics*, 23(december):387–388, 1999.

[54] M T Stang, M J Armstrong, G A Watson, K Y Sung, Y Liu, B Ren, and J H Yim. Interferon regulatory factor-1-induced apoptosis mediated by a ligand- independent fas-associated death domain pathway in breast cancer cells. *Oncogene*, 26:6420–6430, 2007.

[55] Eun-joo Kim, Joon-mo Lee, Sung-eun Namkoong, Soo-jong Um, and Jong-sup Park. Interferon Regulatory Factor-1 Mediates Interferon- Gamma-Induced Apoptosis in Ovarian Carcinoma Cells. *Journal of Cellular Biochemistry*, 85:369–380, 2002.

[56] Robert Clarke, Fabio Leonessa, James N Welch, and Todd C Skaar. Cellular and Molecular Pharmacology of Antiestrogen Action and Resistance. *Pharmacological Reviews*, 53(1):25–71, 2001.

[57] Kerrie B Bouker, Todd C Skaar, David R Fernandez, Kerry A O Brien, Rebecca B Riggins, Donghua Cao, and Robert Clarke. Interferon Regulatory Factor-1 Mediates the Proapoptotic but Not Cell Cycle Arrest Effects of the Steroidal Antiestrogen ICI 182 , 780 (Faslodex , Fulvestrant). *Cancer Letters*, 64:4030 – 4039, 2004.

[58] Yanxia Ning, Rebecca B Riggins, Jennifer E Mulla, Haniee Chung, Alan Zwart, and Robert Clarke. Interferon Gamma Restores Breast Cancer Sensitivity to Fulvestrant by Regulating STAT1, IRF-1, NFkB, BCL2 Family Members, and Signaling to Caspase-dependent Apoptosis. *Molecular Cancer Therapeutics*, 9(5):1274–1285, 2010.

[59] Jinbo Gao, Yuan Tian, and Jinghui Zhang. Overexpression of interferon regulatory factor 1 enhances chemosensitivity to 5-fl uorouracil in gastric cancer cells. *Journal of Cancer Research and Therapeutics*, 8(1):57–61, 2012.

[60] M Upreti, N A Koonce, L Hennings, T C Chambers, and R J Griffin. Pegylated IFN-a sensitizes melanoma cells to chemotherapy and causes premature senescence in endothelial cells by IRF-1-mediated signaling. *Cell Death and Disease*,

1(8):e67–9, 2010.

[61] Gregory A Watson, Pierre E Queiroz De Oliveira, Michael T Stang, Michaele J Armstrong, William E Gooding, Shih-fan Kuan, John H Yim, and Steven J Hughes. Ad-IRF-1 Induces Apoptosis in Esophageal Adenocarcinoma. *Neoplasia*, 8(1):31 – 37, 2006.

[62] Sabine Kirchhoff and Hansjörg Hauser. Cooperative activity between HER oncogenes and the tumor suppressor IRF-1 results in apoptosis. *Oncogene*, 18:3725–3736, 1999.

[63] Peiyuan Li, Qiang Du, Zongxian Cao, Zhong Guo, John Evankovich, Wei Yan, Ying Chang, Lifang Shao, Donna Beer, Allan Tsung, and David A Geller. Interferon-gamma induces autophagy with growth inhibition and cell death in human hepatocellular carcinoma (HCC) cells through IRF-1. *Cancer Letters*, 314(2):213–222, 2012.

[64] Damian E Berardi, Paola B Campod, Maria Ines D, Alejandro J Urtreger, and Laura B Todaro. Autophagy: Friend or Foe in Breast Cancer Development, Progression, and Treatment. *International Journal of Breast Cancer*, 2011:ID595092, 2011.

[65] Lemeng Zhang, Jon S Cardinal, Runalia Bahar, John Evankovich, Hai Huang, Gary Nace, Timothy R Billiar, Matthew R Rosengart, Pinhua Pan, and Allan Tsung. Interferon Regulatory Factor-1 Regulates the Autophagic Response in LPS-Stimulated Macrophages through Nitric Oxide. *Molecular Medicine*, 16:201–208, 2012.

[66] Giorgio Senaldi, Christine L Shaklee, Jane Guo, Laura Martin, Thomas Boone, Tak W Mak, and Thomas R Ulich. Protection Against the Mortality Associated with Disease Models Mediated by TNF and IFN-gamma in Mice Lacking IFN Regulatory Factor-1. *The Journal of Immunology*, 163:6820–6826, 1999.

[67] David Dornan, Mirjam Eckert, Maura Wallace, Harumi Shimizu, Eleanor Ramsay, Ted R Hupp, and Kathryn L Ball. Interferon Regulatory Factor 1 Binding to p300 Stimulates DNA-Dependent Acetylation of p53. *Molecular and Cellular Biochemistry*, 24(22):10083–10098, 2004.

[68] Michaele J Armstrong, Michael T Stang, Ye Liu, Jinbo Gao, Baoguo Ren, Brian S

Zuckerbraun, Raja S Mahidhara, Quanhua Xing, Eva Pizzoferrato, and John H Yim. Interferon Regulatory Factor 1 (IRF-1) induces p21 WAF1 / CIP1 dependent cell cycle arrest and p21 WAF1 / CIP1 independent modulation of survivin in cancer cells. *Cancer Letters*, 319:56–65, 2012.

[69] Renald A. Blundell. The Biology of p21 Waf1/Cip1. *American Journal of Biochemistry and Biotechnology*, 2(1):33–40, 2006.

[70] Mirjam Eckert, Sarah E M Meek, and Kathryn L Ball. A Novel Repressor Domain Is Required for Maximal Growth Inhibition by the IRF-1 Tumor Suppressor. *Journal of Biological Chemistry*, 281(32):23092–23102, 2006.

[71] Charles J Sherr and James M Roberts. CDK inhibitors: positive and negative regulators of G1-phase progression. *Genes & Development*, 13:1501–1512, 1999.

[72] Nam W Kim, Mieczyslaw A Piatyszek, Karen R Prowse, Calvin B Harley, Michael D West, Peter L C Ho, Gina M Coviello, Woodring E Wright, Scott L Weinrich, and Jerry W Shay. Specific Association of Human Telomerase Activity with Immortal Cells and Cancer. *Science*, 266(5193):2011–2015, 1994.

[73] K M Detjen, K Farwig, M Welzel, B Wiedenmann, and S Rosewicz. Interferon-gamma inhibits growth of human pancreatic carcinoma cells via caspase-1 dependent induction of apoptosis. *Gut*, 49:251–262, 2001.

[74] Sabine Kirchhoff, Fred Schaper, and Hansjorg Hauser. Interferon regulatory factor 1 (IRF-1) mediates cell growth inhibition by transactivation of downstream target genes. *Nucleic Acids Research*, 21(12):2881–2889, 1993.

[75] Andrea Kroger, Andreas Dallugge, and Sabine Kirchhoff. IRF-1 reverts the transformed phenotype of oncogenically transformed cells in vitro and in vivo. *Oncogene*, 22:1045–1056, 2003.

[76] Jessica Pamment, Eleanor Ramsay, Michael Kelleher, David Dornan, and Kathryn L Ball. Regulation of the IRF-1 tumour modifier during the response to genotoxic stress involves an ATM-dependent signalling pathway. *Oncogene*, 21:7776 – 7785, 2002.

[77] S Prost, C Bellamy, D Cunningham, and D Harrison. Altered DNA repair and dysregulation of p53 in IRF-1 null hepatocytes. *The FASEB Journal*, 12:181–188, 1998.

[78] Rafael Carretero, Ena Wang, Ana I Rodriguez, Jennifer Reinboth, Maria L Ascierto, Alyson M Engle, Hui Liu, Francisco M Camacho, Francesco M Marincola, Federico Garrido, and Teresa Cabrera. Regression of melanoma metastases after immunotherapy is associated with activation of antigen presentation and interferon-mediated rejection genes. *International Journal of Cancer*, 131:387–395, 2012.

[79] Juliette Nguyen, Perrine Knapnougel, Philippe Lesavre, and Brigitte Bauvois. Inhibition of matrix metalloproteinase-9 by interferons and TGF-b1 through distinct signalings accounts for reduced monocyte invasiveness. *FEBS Letters*, 579:5487–5493, 2005.

[80] Frederique Lindenmeyer, Yves Legrand, and Suzanne Menashi. Upregulation of MMP-9 expression in MDA-MB231 tumor cells by platelet granular membrane. *Cell*, 418:19–22, 1997.

[81] Thorsten Hagemann, Stephen C Robinson, Lorenz Tr, Frances R Balkwill, and Claudia Binder. Enhanced invasiveness of breast cancer cell lines upon cocultivation with macrophages is due to TNF-a dependent up-regulation of matrix metalloproteases. *Carcinogenesis*, 25(8), 2004.

[82] A Ben-Baruch. Host microenvironment in breast cancer development. Inflammatory cells cytokines and chemokines in breast cancer progression : reciprocal tumor microenvironment interactions. *Breast Cancer Research*, 5:31–36, 2003.

[83] Jennifer K Lowney, Leslie D Boucher, Paul E Swanson, and Gerard M Doherty. Interferon Regulatory Factor-1 and -2 Expression in Human Melanoma Specimens. *Annals of Surgery*, 6(6):604 – 608, 1999.

[84] By Katia Boggio, Giordano Nicoletti, Emma Di Carlo, Federica Cavallo, Lorena Landuzzi, Cecilia Melani, Mirella Giovarelli, Ilaria Rossi, Patrizia Nanni, Carla De Giovanni, Page Bouchard, Stanley Wolf, Andrea Modesti, Piero Musiani, Pier Luigi Lollini, Mario P Colombo, and Guido Forni. Interleukin 12mediated Prevention of Spontaneous Mammary Adenocarcinomas in Two Lines of Her-2/neu Transgenic Mice. *J Exp Med*, 188(3):589–596, 1998.

[85] Aristides Moschonas, Maria Kouraki, Pauline G Knox, Efstathia Thymiakou, Dimitris Kardassis, and Aristides G Eliopoulos. CD40 Induces Antigen Transporter

and Immunoproteasome Gene Expression in Carcinomas via the Coordinated Action of NF- kB and of NF-kB-Mediated De Novo Synthesis of IRF-1. *Molecular and Cellular Biology*, 28(20):6208–6222, 2008.

[86] Andrea Kröger, Dörte Ortmann, Tim U Krohne, Leonhardt Mohr, Hubert Blum, Hansjörg Hauser, and Michael Geissler. Growth Suppression of the Hepatocellular Carcinoma Cell Line Hepa1-6 by an Activatable Interferon Regulatory Factor-1 in Mice. *Cancer Research*, 61:2609–2617, 2001.

[87] Ronald Feitosa, Konradin Metze, Maria Regina, Régis Silva, Maria De Lourdes, and Lopes Ferrari. The ambiguous role of IRF-1 immunoexpression in myelodysplastic syndrome. *Leukemia Research*, 33:1308–12, 2009.

[88] By Yoshifumi Tada, Alexandra Ho, Toshifumi Matsuyama, and Tak W Mak. Reduced Incidence and Severity of Antigen-induced Autoimmune Diseases in Mice Lacking Interferon Regulatory Factor-1. *J Exp Med*, 185(2):231–238, 1997.

[89] Zhihua Ren, Yan Wang, David Liebenson, Thomas Liggett, Rajendra Goswami, Dusan Stefoski, and Roumen Balabanov. IRF-1 signaling in central nervous system glial cells regulates inflammatory demyelination. *Journal of Neuroimmunology*, 233(1-2):147–159, 2011.

[90] George R Stark, Ian M Kerr, Bryan R G Williams, Robert H Silverman, and Robert D Schreiber. How cells respond to interferons. *Annual Review of Biochemistry*, 67:227–64, 1998.

[91] Naoko Kanda and Shinichi Watanabe. Prolactin Enhances Interferon-gamma-Induced Production of CXC Ligand 9 (CXCL9), CXCL10, and CXCL11 in Human Keratinocytes. *Endocrinology*, 148(5):2317–2325, 2007.

[92] Takashi Fujita, Luiz Reis, Nobumasa Watanabe, Yoko Kimura, Tadatsugu Taniguchi, and J Vilček. Induction of the transcription factor IRF-1 and ifn-b mrnas by cytokines and activators of second-messenger pathways. *PNAS*, 86(December):9936–9940, 1989.

[93] N. Beretta, L; Gabbay, M; Berger, R; Hanash, SM; Sonenberg. Expression of the protein kinase PKR in modulated by IRF-1 and is reduced in 5q- associated leukemias. *Oncogene*, 12:1593–6, 1996.

[94] Aseem Kumar, Yi-li Yang, Vincenzo Flati, Sandy Der, Suzanne Kadereit,

Amitabha Deb, Jaharul Haque, Luiz Reis, Charles Weissmann, and Bryan R G Williams. Deficient cytokine signaling in mouse embryo fibroblasts with a targeted deletion in the PKR gene : role of IRF-1 and NF-κB. *EMBO Journal*, 16(2):406–416, 1997.

[95] Sven Heinz, Viola Haehnel, Marina Karaghiosoff, Lucia Schwarzfischer, Mathias Mu, Stefan W Krause, and Michael Rehli. Species-specific Regulation of Toll-like Receptor 3 Genes in Men and Mice. *Journal of Biological Chemistry*, 278(24):21502–21509, 2003.

[96] Hideo Negishi, Yasuyuki Fujita, Hideyuki Yanai, Shinya Sakaguchi, Xinshou Ouyang, Masahiro Shinohara, Hiroshi Takayanagi, Yusuke Ohba, Tadatsugu Taniguchi, and Kenya Honda. Evidence for licensing of IFN- gamma -induced IFN regulatory factor 1 transcription factor by MyD88 in Toll-like receptor-dependent gene induction program. *PNAS*, 103:15136–15141, 2006.

[97] Frank Schmitz, Antje Heit, Simone Guggemoos, Anne Krug, Jörg Mages, Matthias Schiemann, Heiko Adler, Ingo Drexler, Tobias Haas, Roland Lang, and Hermann Wagner. Interferon-regulatory-factor 1 controls Toll-like receptor 9-mediated IFN-b production in myeloid dendritic cells. *Eur J Immunol*, 37:315–327, 2007.

[98] Zhu Guo, Sanjay Garg, Karen M Hill, Lakshmi Jayashankar, Myesha R Mooney, Mary Hoelscher, Jacqueline M Katz, Jeremy M Boss, and Suryaprakash Sambhara. A Distal Regulatory Region is Requitred for Constitutive and IFN-beta-Induced Expression of Murine TLR9 Gene. *J Immunol*, 175:7407–18, 2005.

[99] Sheila A Barber, Marion J Fultz, Cindy A Salkowski, and Stefanie N Vogel. Differential expression of interferon regulatory factor 1 (IRF-1), IRF-2 , and interferon consensus sequence binding protein genes in lipopolysaccharide (LPS)-responsive and LPS-hyporesponsive macrophages. *Infect. Immun*, 63(2):601–8, 1995.

[100] Virginia Vila-del Sol, Carmen Punzón, and Manuel Fresno. Regulatory Factors 1 and 8 in Mouse Macrophages 1. *J Immunol*, 181:4461–70, 2008.

[101] Zulema A Percario, Valeria Giandomenico, Gianna Fiorucci, Maria V Chiantore, Serena Vannucchi, John Hiscott, Elisabetta Affabris, and Giovanna Romeo. Retinoic Acid Is Able to Induce Interferon Regulatory Factor 1 in Squamous Carcinoma Cells via a STAT-1 Independent Signalling Pathway 1. *Cell Growth &*

Differentiation, 10:263–270, 1999.

[102] Andreas H Wagner, Matthias Gebauer, Beatrix Pollok-kopp, and Markus Hecker. Cytokine-inducible CD40 expression in human endothelial cells is mediated by interferon regulatory factor-1. *Blood*, 99:520–525, 2002.

[103] Chris M Bacon, Daniel W McVicar, John R Ortaldo, Robert C Rees, John J O'Shea, and James A Johnston. Interleukin 12 (IL-12) Induces Tyrosine Phosphorylation of JAK2 and TYK2: Differential Use of Janus Family Tyrosine Kinases by IL-2 and IL-12. *Journal of Experimental Medicine*, 181:399–404, 1995.

[104] Jérôme Galon, Chitra Sudarshan, Satochi Ito, David Finbloom, and John J O Shea. IL-12 Induces IFN Regulating Factor-1 (IRF-1) Gene Expression in Human NK and T Cells. *The Journal of Immunology*, 162:7256–7262, 1999.

[105] Suxing Liu, W Robert Bishop, and Ming Liu. Differential effects of cell cycle regulatory protein p21 WAF1 / Cip1 on apoptosis and sensitivity to cancer chemotherapy. *Drug Resistance Updates*, 6:183–195, 2003.

[106] Sheila Harroch, Yael Gothelf, Nobumasa Watanabe, Michel Revel, and Judith Chebath. Interleukin-6 Activates and Regulates Transcription Factors of the Interferon Regulatory Factor Family in M1 Cells. *Journal of Biological Chemistry*, 268(12):9092–9097, 1993.

[107] Peter C Heinrich, Iris Behrmann, Gerhard Muller-Newen, Fred Schaper, and Lutz Graeve. Interleukin-6-type cytokine signalling through the gp130/Jak/STAT pathway. *Biochem. J.*, 334:297–314, 1998.

[108] Hodaka Fujii, Yoko Nakagawa, Ulrike Schindleri, Atsuo Kawahara, Hisashi Mori, Fabrice Gouilleux, Bernd Groner, James N Ihlei, Yasuhiro Minami, and Tadaaki Miyazaki Ii. Activation of Stat5 by interleukin 2 requires a carboxyl-terminal region of the interleukin 2 receptor 1B chain but is not essential for the proliferative signal transmission. *Cell*, 92(June):5482–5486, 1995.

[109] Lee H Wong, Helena Sim, Moitreyee Chatterjee-kishore, Irene Hatzinisiriou, Rodney J Devenish, George Stark, and Stephen J Ralph. Isolation and Characterization of a Human STAT1 Gene. *Journal of Biological Chemistry*, 277(22):19408 –19417, 2002.

[110] Peter Andersen, Mikkel Wandahl Pedersen, Anders Woetmann, Mette Villingshø j,

Marie-Therese Stockhausen, Niels Odum, and Hans Skovgaard Poulsen. EGFR induces expression of IRF-1 via STAT1 and STAT3 activation leading to growth arrest of human cancer cells. *International Journal of Cancer*, 122:342–349, 2008.

[111] Masaaki Miyamoto, Takashi Fujita, Yoko Kimura, Mitsuo Maruyama, Hisashi Harada, Yoshiaki Sudo, Takashi Miyata, Tadatsugu Taniguchi, and Cellular Biology. Regulated Expression of a Gene Encoding a Nuclear Factor, IRF-1, That Specifically Binds to IFN-b Gene Regulatory Elements. *Cell*, 54:903–913, 1988.

[112] Nobumasa Watanabe, Jun Sakakibara, Ara G Hovanessian, and Tadatsugu Taniguchi. Activation of IFN-beta element by IRF-1 requires a post- translational event in addition to IRF-1 synthesis. *Nucleic Acids Research*, 19(16):4421–4428, 1991.

[113] Richard Pine, Antony Canova, and Chris Schindler. Tyrosine phosphorylated p91 binds to a single element in the ISGF2/IRF-1 promoter to mediate induction by IFNcx and IFNy , and is likely to autoregulate the p91 gene. *EMBO Journal*, 13(1):158–167, 1994.

[114] Xiaoxia Li, Stewart Leung, Sajjad Qureshi, James E Darnell, and George R Stark. Formation of STAT1-STAT2 Heterodimers and Their Role in the Activation of IRF-1 Gene Transcription by Interferon- *. *Journal of Biological Chemistry*, 271(10):5790 –5794, 1996.

[115] Yu-fen Wang, Kevin D O Neal, and Li-yuan Yu-Lee. Multiple Prolactin (PRL) Receptor Cytoplasmic Residues and Stat1 Mediate PRL Signaling to the Interferon Regulatory Factor-1 Promoter. *Molecular Endocrinology*, 11:1353–1364, 1997.

[116] Daisuke Imanishi, Kazuo Yamamoto, Hideki Tsushima, Yasushi Miyazaki, Kazutaka Kuriyama, Masao Tomonaga, and Toshifumi Matsuyama. Identification of a Novel Cytokine Response Element in the Human IFN Regulatory Factor-1 Gene Promoter. *Journal of Immunology*, 165:3907–3916, 2000.

[117] Istvan Arany, William E Whitehead, Kenneth J Grattendick, Istvan A Ember, and Stephen K Tyring. Suppression of Growth by All-trans Retinoic Acid Requires Prolonged Induction of Interferon Regulatory Factor 1 in Cervical Squamous Carcinoma (SiHa) Cells. *Clinical and Diagnostic Laboratory Immunology*, 9(5):1102–1106, 2002.

[118] Richard Pine. Convergence of TNFα and IFNγ signalling pathways through synergistic induction of IRF-1 / ISGF-2 is mediated by a composite GAS / κB promoter element. *Cell*, 25(21), 1997.

[119] Rongtuan Lin and John Hiscott. A role for casein kinase II phosphorylation in the regulation of IRF-1 transcriptional activity. *Molecular and Cellular Biochemistry*, 191:169–180, 1999.

[120] Melanie Giroux, Manuel Schmidt, and Albert Descoteaux. IFN-γ-Induced MHC Class II Expression: Transactivation of Class II Transactivator Promoter IV by IFN Regulatory Factor-1 is Regulated by Protein Kinase C-α. *Journal of Immunology*, 171:4187–4194, 2003.

[121] Vikram Narayan, Mirjam Eckert, Alicja Zylicz, Maciej Zylicz, and Kathryn L Ball. Cooperative Regulation of the Interferon Regulatory Factor-1 Tumor Suppressor Protein by Core Components of the Molecular Chaperone Machinery. *Journal of Biological Chemistry*, 284(38):25889 –25899, 2009.

[122] Koji Nakagawa and Hideyoshi Yokosawa. Degradation of transcription factor IRF-1 by the ubiquitin-proteasome pathway. *Eur J Biochem*, 267:1680–1686, 2000.

[123] Emmanuelle Pion, Vikram Narayan, Mirjam Eckert, and Kathryn L Ball. Role of the IRF-1 enhancer domain in signalling polyubiquitination and degradation. *Cellular Signalling*, 21(10):1479–87, 2009.

[124] Koji Nakagawa and Hideyoshi Yokosawa. PIAS3 induces SUMO-1 modification and transcriptional repression of IRF-1. *Cell*, 530:204–208, 2002.

[125] Junsoo Park, Kwangsoo Kim, Eun-ju Lee, Yun-jee Seo, Si-nae Lim, Kyoungsook Park, Seung Bae Rho, Seung-hoon Lee, and Je-ho Lee. Elevated level of SUMOylated IRF-1 in tumor cells interferes with IRF-1-mediated apoptosis. *PNAS*, 104(43):17028–17033, 2007.

[126] Atsuko Masumi and Keiko Ozato. Coactivator p300 Acetylates the Interferon Regulatory Factor-2 in U937 Cells following Phorbol Ester Treatment. *Journal of Biological Chemistry*, 276(24):20973–20980, 2001.

[127] Atsuko Masumi, I-ming Wang, Bruno Lefebvre, Xing-jiao Yang, Yoshihiro Nakatani, and Keiko Ozato. The Histone Acetylase PCAF Is a Phorbol-Ester-Inducible Coactivator of the IRF Family That Confers Enhanced Interferon Re-

sponsiveness. *Molecular and Cellular Biology*, 19(3):1810–1820, 1999.

[128] Patrick A Grant. Review A tale of histone modifications. *Science*, pages 1–6, 2001.

[129] Giulia Marsili, Anna Lisa Remoli, Marco Sgarbanti, and Angela Battistini. Role of Acetylases and Deacetylase Inhibitors in IRF-1-Mediated HIV-1 Long Terminal Repeat Transcription. *Annals New York Academy of Sciences*, 1030:636–643, 2004.

[130] Menie Merika, Amy J Williams, Guoying Chen, Tucker Collins, and Dimitris Thanos. Recruitment of CBP/p300 by the IFN-beta Enhanceosome Is Required for Synergistic Activation of Transcription. *Molecular Cell*, 1:277–287, 1998.

[131] Wu-guo Deng and Kenneth K Wu. Regulation of Inducible Nitric Oxide Synthase Expression by p300 and p50 Acetylation. *The Journal of Immunology*, 171:6581–6588, 2003.

[132] Marta Saura, Carlos Zaragoza, Clare Bao, Audrey Mcmillan, and Charles J Lowenstein. Interaction of Interferon Regulatory Factor-1 and Nuclear Factor k B During Activation of Inducible Nitric Oxide Synthase Transcription. *Journal of Molecular Biology*, 289:459–471, 1999.

[133] Katrin Ramsauer, Matthias Farlik, Gordin Zupkovitz, Christian Seiser, Andrea Kroger, Hansjörg Hauser, and Thomas Decker. Distinct modes of action applied by transcription factors STAT1 and IRF1 to initiate transcription of the IFN-gamma-inducible gbp2 gene. *PNAS*, 104(8):2849–2854, 2007.

[134] Moitreyee Chatterjee-kishore, Kenneth L Wright, Jenny P Ting, and George R Stark. How Stat1 mediates constitutive gene expression : a complex of unphosphorylated Stat1 and IRF1 supports transcription of the LMP2 gene. *EMBO Journal*, 19(15):4111–4122, 2000.

[135] Atsushi Kumatori, Dan Yang, Shoichi Suzuki, and Michio Nakamura. Cooperation of STAT-1 and IRF-1 in Interferon- -induced Transcription of the gp91 phox Gene *. *Biochemistry*, 277(11):9103–9111, 2002.

[136] Yaxin Wang, Bo Gao, Wei Xu, and Sidong Xiong. BRG1 is indispensable for IFN-gamma -induced TRIM22 expression , which is dependent on the recruitment of IRF-1. *BIOCHEMICAL AND BIOPHYSICAL RESEARCH COMMUNICATIONS*, 2011.

[137] Shinichi Matsuzaki, Tamotsu Ishizuka, Takeshi Hisada, Haruka Aoki, Mayumi Komachi, Isao Ichimonji, Akihiro Ono, Yasuhiko Koga, Kunio Dobashi, Hitoshi Kurose, Hideaki Tomura, Masatomo Mori, and Fumikazu Okajima. Lysophosphatidic Acid Inhibits CC Chemokine Ligand 5/RANTES Production by Blocking IRF-1-Mediated Gene Transcription in Human Bronchial Epithelial Cells. *Journal of Immunology*, 185:4863–4872, 2010.

[138] Noriko Umegaki, Katsuto Tamai, Hajime Nakano, Ryuta Moritsugu, Takehiko Yamazaki, Ichiro Katayama, and Yasufumi Kaneda. Differential Regulation of Karyopherin a 2 Expression by TGF-b 1 and IFN-c in Normal Human Epidermal Keratinocytes : Evident Contribution of KPNA2 for Nuclear Translocation of IRF-1. *Journal of Investigative Dermatology*, 127, 2007.

[139] Rongtuan Lin, Amir Mustafa, Hannah Nguyen, Dirk Gewert, and John Hiscott. Mutational Analysis of Interferon (IFN) Regulatory Factors 1 and 2. *Journal of Biological Chemistry*, 269(26):17542–17549, 1994.

[140] Carlos R Escalante, Junming Yie, Dimitris Thanos, and Aneel K Aggarwal. Structure of IRF-1 with bound DNA reveals determinants of interferon regulation. *Nature*, 391:103–106, 1998.

[141] Sabine Kirchhoff, Andre Oumard, Mahtab Nourbakhsh, Ben-zion Levi, and Hansjörg Hauser. Interplay between repressing and activating domains defines the transcriptional activity of IRF-1. *Eur J Biochem*, 267:6753–6761, 2000.

[142] Fred Schaper, Sabine Kirchhoff, Guido Posern, Mario Ko, Andre Oumard, Rakefet Sharf, Ben-zion Levi, and Hansjörg Hauser. Functional domains of interferon regulatory factor I (IRF-1). *Biochem. J.*, 335:147–157, 1998.

[143] Sabine Kirchhoff, Fred Schaper, Andre Oumard, and Hansjörg Hauser. In vivo formation of IRF-I homodimers. *Biochimie*, 80:659–664, 1998.

[144] Vikram Narayan, Petr Halada, Lenka Hernychova, Yuh Ping Chong, Jitka Z, Ted R Hupp, Borivoj Vojtesek, and Kathryn L Ball. A Multiprotein Binding Interface in an Intrinsically Disordered Region of the Tumor Suppressor Protein Interferon Regulatory Factor-1 * . *Journal of Biological Chemistry*, 286(16):14291–14303, 2011.

[145] Vikram Narayan, Emmanuelle Pion, Vivien Landre, Petr Mu, and Kathryn L Ball.

Docking-dependent Ubiquitination of the Interferon Regulatory Factor-1 Tumor Suppressor Protein by the Ubiquitin Ligase CHIP. *Journal of Biological Chemistry*, 286(1):607–619, 2011.

[146] A. Moeller, E Pion, V Narayan, and K Ball. intracellular activation of interferon regulatory factor-1 by nanobodies to the multi-functional (Mf1) domain. *Journal of Biological Chemistry*, 2010.

[147] Shigeru Oshima, Tetsuya Nakamura, Shin Namiki, Eriko Okada, Kiichiro Tsuchiya, Ryuichi Okamoto, Motomi Yamazaki, Takanori Yokota, Masatoshi Aida, Yuki Yamaguchi, Takanori Kanai, Hiroshi Handa, and Mamoru Watanabe. Interferon Regulatory Factor 1 (IRF-1) and IRF-2 Distinctively Up-Regulate Gene Expression and Production of Interleukin-7 in Human Intestinal Epithelial Cells. *Society*, 24(14):6298–6310, 2004.

[148] Hans Peter Sø rensen and Kim Kusk Mortensen. Soluble expression of recombinant proteins in the cytoplasm of Escherichia coli. *Microbial Cell Factories*, 8:1–8, 2005.

[149] Brian K Kay, Jeremy Kasanov, and Montarop Yamabhai. Screening Phage-Displayed Combinatorial Peptide Libraries. *Methods*, 24:240–246, 2001.

[150] Rongtuan Lin, Christophe Heylbroeck, Paula M Pitha, and John Hiscott. Virus-Dependent Phosphorylation of the IRF-3 Transcription Factor Regulates Nuclear Translocation, Transactivation Potential, and Proteasome-Mediated Degradation. *Molecular and Cellular Biology*, 18(5):2986–2996, 1998.

[151] N Blom, T Sicheritz-Ponten, R Gupta, S Gammeltoft, and S Brunak. Prediction of post-translational glycosylation and phosphorylation of proteins from the amino acid sequence. *Proteomics*, 4(6):1633–1649, 2004.

[152] Y.H. Wong, T.Y. Lee, H.K. Liang, C.M Uang, Y.H. Yang, C.H. Chu, H.D. Huang, M.T. Ko, and J.K. Hwang. KinasePhos 2.0: a web server for identifying protein kinase-specific phosphorylation sites based on sequences and coupling patterns. *Nucleic Acids Research*, 35:W588–594, 2007.

[153] Yu Xue, Jian Ren, Xinjiao Gao, Changjiang Jin, Longping Wen, and Xuebiao Yao. GPS 2.0: Prediction of Kinase-Specific Phosphorylation Sites in Hierarchy. *Mol Cell Proteomics*, 7:1598–1608, 2008.

[154] Hannah Nguyen, Chilakamarti V Ramana, Joshua Bayes, and George R Stark. Roles of Phosphatidylinositol 3-Kinase in Interferon-gamma-dependent Phosphorylation of STAT1 on Serine 727 and Activation of Gene Expression. *Biochemistry*, 276(36):33361–33368, 2001.

[155] Dilip K Deb, Antonella Sassano, Fatima Lekmine, Beata Majchrzak, Amit Verma, Suman Kambhampati, Shahab Uddin, Arshad Rahman, Eleanor N Fish, and Leonidas C Platanias. Activation of Protein Kinase C δ by IFN- γ. *The Journal of Immunology*, 171:267–273, 2003.

[156] Ursula M Halfter, Zachary E Derbyshire, and Richard R Vaillancourt. Interferon-γ -dependent tyrosine phosphorylation of MEKK4 via Pyk2 is regulated by annexin II and SHP2 in keratinocytes. *Society*, 28:17–28, 2005.

[157] Sanjit K Roy, Junbo Hu, Qingjun Meng, Ying Xia, Paul S Shapiro, Sekhar P M Reddy, Leonidas C Platanias, Daniel J Lindner, Peter F Johnson, Catrin Pritchard, Gilles Page, Jacques Pouyssegur, and Dhananjaya Kalakolanu. MEKK1 plays a critical role in activating the transcription factor C /EBP-beta-dependent gene expression in response to IFN-gamma. *PNAS*, 99(12):7945–50, 2002.

[158] James Goding. *Monocolonal Antibodies: Principles and Practice*. Academic Press, London, 3rd edition, 1996.

[159] W E I Wang, Satish Singh, David L Zeng, Kevin King, Sandeep Nema, and Wang E T Al. Antibody Structure, Instability, and Formulation. *Journal of Pharmaceutical Sciences*, 96(1):1–26, 2007.

[160] Tadatsugu Taniguchi, Kouetsu Ogasawara, Akinori Takaoka, and Nobuyuki Tanaka. IRF FAMILY OF TRANSCRIPTION FACTORS AS REGULATORS OF HOST DEFENSE. *Annual Review of Immunology*, 19:623–55, 2001.

[161] Donna D Eason, Alexander T Shepherd, and George Blanck. Interferon regulatory factor 1 tryptophan 11 to arginine point mutation abolishes DNA binding. *In Vitro*, 1446:140–144, 1999.

[162] Takashi Fujita, Hiroshi Shibuya, and Haku Hotta. Interferon-beta Gene Regulation: Tandemly Repeated Sequences of a Synthetic 6 bp Oligomer Function As a Virus-Inducible Enhancer. *Cell*, 49(1983):357–367, 1987.

[163] Lorenza Bordoli, Marco Netsch, Urs Lüthi, Werner Lutz, and Richard Eck-

ner. Plant orthologs of p300/CBP: conservation of a core domain in metazoan p300/CBP acetyltransferase- related proteins. *Nucleic Acids Research*, 29(3):589–597, 2001.

[164] Jayne Spink and Tom Evans. Binding of the Transcription Factor Interferon Regulatory Factor-1 to the Inducible Nitric-oxide Synthase Promoter. *Journal of Biological Chemistry*, 272(39):24417–24425, 1997.

[165] Kate Senger, Menie Merika, Theodora Agalioti, Junming Yie, Carlos R Escalante, Guoying Chen, Aneel K Aggarwal, and Dimitris Thanos. Gene Repression by Coactivator Repulsion. *Molecular Cell*, 6:931–937, 2000.

[166] David Dornan, Harumi Shimizu, Neil D Perkins, and Ted R Hupp. DNA-dependent Acetylation of p53 by the Transcription Coactivator p300. *Journal of Biological Chemistry*, 278(15):13431–13441, 2003.

[167] Ho Man Chan and Nicholas B La Thangue. p300/CBP proteins: HATs for transcriptional bridges and scaffolds. *Journal of Cell Science*, 114:2363–2373, 2001.

[168] Nickolai A Barlev, Lin Liu, Nabil H Chehab, Kyle Mansfield, Kimberly G Harris, Thanos D Halazonetis, and Shelley L Berger. Acetylation of p53 Activates Transcription through Recruitment of Coactivators/Histone Acetyltransferases. *Molecular Cell*, 8:1243–1254, 2001.

[169] Masanobu Komatsu, Coralie A Carothers Carraway, Nevis L Fregien, and Kermit L Carraway. Reversible Disruption of Cell-Matrix and Cell-Cell Interactions by Overexpression of Sialomucin Complex *. *Biochemistry*, 272(52):33245–33254, 1997.

[170] Hiroaki Ikeda, Lloyd J Old, and Robert D Schreiber. The roles of IFN-gamma in protection against tumor development and cancer immunoediting. *Cytokine & Growth Factor Reviews*, 13:95–109, 2002.

[171] Nikolai N Khodarev, Bernard Roizman, and Ralph R Weichselbaum. Molecular Pathways : Interferon/Stat1 Pathway : Role in the Tumor Resistance to Genotoxic Stress and Aggressive Growth. *Clinical Cancer Research*, 18:3015–3021, 2012.

[172] Lisa J Mccawley and Lynn M Matrisian. Matrix metalloproteinases: multifunctional contributors to tumor progression. *Molecular Medicine Tday*, 6(4):149–156, 2000.

[173] Tapan Khan, Thomas Nelson, Vishal Verma, Paul Wender, and Daniel Alkon. A cellular model of Alzheimer's disease therapeutic efficacy: PKC activation reverses Abeta-induced biomarker abnormality on cultured fibroblasts. *Neurobiol Dis*, 34(2):332–339, 2009.

[174] Ana Castro. Kinase activators as a novel class of antidiabetic agents. *Drug Discovery Today*, 17(9/10):528–529, 2012.

[175] Hakryul Jo, Subhanjan Mondal, Dewar Tan, Eiichiro Nagata, Shunya Takizawa, Alok K Sharma, Quingming Hou, Kumaran Shanmugasundaram, Amit Prasad, Joe Tung, Alexander Tejeda, Hengye Man, Alan Rigby, and Hongbo Luo. Small molecule-induced cytosolic activation of protein kinase Akt rescues ischemia-elicited neuronal death. *PNAS*, 109(26):10581–10586, 2012.

[176] Carina I Holmberg, Stefanie E F Tran, John E Eriksson, and Lea Sistonen. Multisite phosphorylation provides sophisticated regulation of transcription factors. *Trends in biochemical sciences*, 27(12):619–627, 2002.

[177] A J Whitmarsh and R J Davis. Regulation of transcription factor function by phosphorylation. *Cellular and Molecular Life Sciences*, 57:1172–1183, 2000.

[178] Maria Nikodemova, Jyoti J Watters, Samuel J Jackson, Shaun K Yang, and Ian D Duncan. Minocycline Down-regulates MHC II Expression in Microglia and Macrophages through Inhibition of IRF-1 and Protein Kinase C (PKC). *Journal of Biological Chemistry*, 282(20):15208 –15216, 2007.

[179] Katsuaki Hoshino, Izumi Sasaki, Takahiro Sugiyama, Takahiro Yano, Chihiro Yamazaki, Teruhito Yasui, Hitoshi Kikutani, and Tsuneyasu Kaisho. Critical Role of IκB Kinase α in TLR7/9-Induced Type I IFN Production by Conventional Dendritic Cells. *J Immunol*, 184:3341–3345, 2010.

[180] Kenya Honda and Tadatsugu Taniguchi. IRFs: master regulators of signalling by Toll-like receptors and cytosolic pattern-recognition receptors. *Nature Reviews Immunology*, 6(September):644–658, 2006.

[181] Beate Friedrich, Christina Quensel, Thomas Sommer, Enno Hartmann, and Matthias Kohler. Nuclear Localization Signal and Protein Context both Mediate Importin α Specificity of Nuclear Import Substrates Nuclear Localization Signal and Protein Context both Mediate Importin Specificity of Nuclear Import Sub-

strates . *Molecular and Cellular Biology*, 26(23):8697–8709, 2006.

[182] B Alberts, D Bray, J Lewis, M Raff, K Roberts, and J Watson. *General Principles of Cell Signalling*, chapter 1. Garland Science, New York, 3rd edition, 1994.

[183] Smarajit Polley, Soumi Guha, Neeladri Sekhar Roy, Sanchari Kar, Kazuyasu Sakaguchi, Yoshiro Chuman, V Swaminathan, Tapas Kundu, Siddhartha Roy, and Siddhartha Roy. Differential Recognition of Phosphorylated Transactivation Domains of p53 by Different p300 Domains. *Journal of Molecular Biology*, 376:8–12, 2008.

[184] Paul F Lambert, Fatah Kashanchi, Michael F Radonovich, Ramin Shiekhattar, and John N Brady. Phosphorylation of p53 Serine 15 Increases Interaction with CBP. *Journal of Biological Chemistry*, 273(49):33048 –33053, 1998.

[185] Masafumi Muratani and William P Tansey. HOW THE UBIQUITIN PROTEASOME SYSTEM CONTROLS TRANSCRIPTION. *Nature Reviews Molecular Cell Biology*, 4(March):192–201, 2003.

[186] Joseph R Biggs, Youhong Zhang, Luke F Peterson, Marileila Garcia, Donger Zhang, and Andrew S Kraft. Phosphorylation of AML1/RUNX1 Regulates Its Degradation and Nuclear Matrix Association. *Molecular Cancer Research*, 3(7):391–401, 2005.

[187] Laurence Vandel and Tony Kouzarides. Residues phosphorylated by TFIIH are required for E2F-1 degradation during S-phase. *EMBO Journal*, 18(15):4280–4291, 1999.

[188] I M Wang, J C Blanco, S Y Tsai, M J Tsai, and K Ozato. Interferon regulatory factors and TFIIB cooperatively regulate interferon-responsive promoter activity in vivo and in vitro. *Molecular and Cellular Biology*, 16(11):6313–6324, 1996.

[189] Kai Yang, Hexin Shi, Rong Qi, Shaogang Sun, Yujie Tang, Bianhong Zhang, and Chen Wang. Hsp90 Regulates Activation of Interferon Regulatory Factor 3 and TBK-1 Stabilization in Sendai Virus-infected Cells. *Molecular Biology of the Cell*, 17(March):1461–1471, 2006.

[190] Marc Sylvester, Stefanie Kliche, Sabine Lange, Sabine Geithner, Clementine Klemm, Andreas Schlosser, Arndt Groß mann, Ulrich Stelzl, Burkhart Schraven, Eberhard Krause, and Christian Freund. Adhesion and Degranulation Promoting Adapter Protein (ADAP) Is a Central Hub for Phosphotyrosine-Mediated Interac-

tions in T Cells. *PLoS ONE*, 5(7):e11708, 2010.

[191] Kazuyasu Sakaguchi, Julio E Herrera, Shin'ichi Saito, Toru Miki, Michael Bustin, Alex Vassilev, Carl W Anderson, and Ettore Appella. DNA damage activates p53 through a phosphorylationacetylation cascade. *Genes & Development*, 12:2831–2841, 1998.

[192] Wei Gu and Robert G Roeder. Activation of p53 Sequence-Specific DNA Binding by Acetylation of the p53 C-Terminal Domain. *Cell*, 90:595–606, 1997.

[193] Lin-feng Chen, Samuel A Williams, Yajun Mu, Hiroyasu Nakano, James M Duerr, Leonard Buckbinder, and Warner C Greene. NF-kB RelA Phosphorylation Regulates RelA Acetylation. *Molecular and Cellular Biology*, 25(18):7966–7975, 2005.

[194] Kewei Ma, Jonathan K L Chan, Guang Zhu, and Zhenguo Wu. Myocyte Enhancer Factor 2 Acetylation by p300 Enhances Its DNA Binding Activity, Transcriptional Activity, and Myogenic Differentiation. *Molecular and Cellular Biology*, 25(9):3575–3582, 2005.

[195] Tomohide Takaya, Teruhisa Kawamura, Tatsuya Morimoto, Koh Ono, Toru Kita, Akira Shimatsu, and Koji Hasegawa. Identification of p300-targeted Acetylated Residues in GATA4 during Hypertrophic Responses in Cardiac Myocytes. *Journal of Biological Chemistry*, 283(15):9828 –9835, 2008.

[196] Zheng Sun, Y Eugene Chin, and Donna D Zhang. Acetylation of Nrf2 by p300/CBP Augments Promoter-Specific DNA Binding of Nrf2 during the Antioxidant Response. *Molecular and Cellular Biology*, 29(10):2658–2672, 2009.

[197] Sandy Der, Yi-li Yang, Charles Weissmann, and Bryan R G Williams. A double-stranded RNA-activated protein kinase-dependent pathway mediating stress-induced apoptosis. *PNAS*, 94(April):3279–3283, 1997.

[198] Jill Pflugheber, Brenda Fredericksen, Rhea Sumpter, Chunfu Wang, Felecia Ware, Donald L Sodora, and Michael Gale. Regulation of PKR and IRF-1 during hepatitis C virus RNA replication. *PNAS*, 99(7):1–6, 2002.

[199] Miki Hiroi, Kazumasa Mori, Keisuke Sekine, Yoshiichi Sakaeda, Jun Shimada, and Yoshihiro Ohmori. Mechanisms of Resistance to Interferon-gamma-mediated Cell Growth Arrest in Human Oral Squamous Carcinoma Cells. *Journal of Biological Chemistry*, 284(37):24869 –24880, 2009.

[200] J L Schwartz, A N Shajahan, and R Clarke. The Role of Interferon Regulatory Factor-1 (IRF1) in Overcoming Antiestrogen Resistance in the Treatment of Breast Cancer. *International Journal of Breast Cancer*, 2011:912102, 2011.

[201] R Höftberger, W Brueck, C Lucchinetti, M Rodriguez, M Schmidbauer, K Jellinger, and H Lassmann. Expression of Major Histocompatibility Complex Class I Molecules on the Different Cell Types in Multiple Sclerosis Lesions. *Brain Pathology*, 14(1):43–50, 2004.

[202] Roberto Furlan, Gianvito Martino, Francesca Galbiati, Pietro L Poliani, Simona Smiroldo, Alessendra Bergami, Gaetano Desina, Giancarlo Comi, Richard Flavell, Michael S Su, and Luciano Adorini. Caspase-1 Regulates the Inflammatory Process Leading to Autoimmune Demyelination. *Journal of Immunology*, 163:2403–2409, 1999.